CHEMISTRY AND BIOACTIVITY STUDIES OF AFRICAN MEDICINAL PLANTS *XIMENIA CAFFRA*, *HIBISCUS SABDARIFFA* AND *COMBRETUM MICRANTHUM*

By

JING ZHEN

A dissertation submitted to the

Graduate School-New Brunswick

Rutgers, The State University of New Jersey

In partial fulfillment of the requirements

For the degree of

Doctor of Philosophy

Graduate Program in Medicinal Chemistry

Written under the direction of

Dr. James E. Simon

And approved by

_____

_____

_____

_____

New Brunswick, New Jersey

October 2016

ABSTRACT OF THE DISSERTATION

Chemistry and bioactivity studies of African medicinal plants *Ximenia caffra*, *Hibiscus sabdariffa* and *Combretum micranthum*

Jing Zhen

Dissertation Director: Professor James E Simon

Africa has been and continues to be an important source of medicinal plants yet only a relative few have been extensively studied. Three different traditional African medicinal plants *Ximenia caffra*, *Hibiscus sabdariffa* and *Combretum micranthum,* were selected for phytochemical investigations and potential pharmacological activities. For *Ximenia caffra,* more than ten polyphenol compounds were identified in the leaf sample using LC/UV/MS profiling, including gallic acid, catechin, quercetin, kaempferol and their derivatives. The antioxidant capacities of leaf extract were determined by Folin-Ciocalteu assay as 261.87 ± 7.11 mg GAE/g and ABTS free radical scavenging assay as 1.46 ± 0.01 mmol TE/g. The anti-proliferative effect of *Ximenia caffra* leaf extract was measured by MTS assay with IC_{50} value of 239.0 ± 44.5 μg/ml. Cell-based assays show that the leaf extract inhibits the mRNA expression of pro-inflammatory genes (iL-6, iNOS, and TNF-α) by using RT-qPCR, indicating its anti-inflammatory effects. Further studies suggest that the underlying therapeutic mechanism may involve the suppression of NF-κB, a shared pathway between cell death and inflammation. For *Hibiscus sabdariffa,* which is originally native to Africa, the phytochemical profile of leaves from 25 different populations from worldwide accessions were determined by LC/MS and compared with each other. Ten polyphenols including neochlorogenic acid, chlorogenic acid, cryptochlorogenic acid, quercetin, kaempferol and their glycosides were identified together with 5-(hydroxymethyl)furfural, some of which were quantified with

commercially available standards. The leaves have shown anti-oxidant activities as measured by Folin-Ciocalteu assay and ABTS free radical scavenging assay. Leaves extracts reduced LPS-induced NO production in RAW 264.7 cell in a dose-dependent manner indicating the extract's potential anti-inflammatory activity. The compound 5-HMF was identified in dried samples and later investigated as a biomarker of the freshness of the leaf samples. For plant *Combretum micranthum*, in prior phytochemical investigations, our lab identified a group of new skeleton compounds named kinkéloids. As a continuation of this project, two total synthetic methods for these novel compounds kinkéloids A group and B were developed, which were then applied for regioisomers determination, scale-up synthesis and potential analogues synthesis. The key and final step was achieved by Mannich reaction, through which the piperidine moiety coupled to the flavan moiety. One method goes through the synthesis of intermediate compound eriodictyol followed by further de-oxygenation using $NaBH_3CN$, while the second scheme involves the formation of *o*-quinone methide and the inverse electron-demand Diels-Alder reaction. The identities of synthesized kinkéloids were further confirmed through the comparison with the ones in the plant leaves extract using LC/MS. The enantiomers of each previous identified flavan molecules in the leaf samples were successfully separated on AD-RH column. A series of novel kinkéloids analogues were synthesized with different flavonoid aglycones and the attached nitrogen-containing moieties. The synthesized analogues were screened for the inhibitory activity of α-glucosidase, in which compound **23** has the lowest IC_{50} of 4.1 μM. Kinetic analysis indicates synthesized compounds **15** and **23** inhibit enzyme in a non-competitive model with *Ki* value of 37.8 ± 0.8 and 13.2 ± 0.6 μM. Further docking study suggests that the preferred binding pocket is close to the catalytic center, correlating to the experimental results very well. Structure activity relationship study indicates that 4'-hyroxyl group and the 4-position carbonyl group are important for the inhibitory activity. Addition of extra hydrogen bonding and hydrophobic groups on ring A may increase the inhibitory activity.

ACKNOWLEDGEMENTS

First and foremost, I would like to express my sincere gratitude to my advisors, Professor Qingli Wu and Professor James Simon. It would not be possible for me to finish my research projects without their training, guidance, encouragement and continuous support. Professor Wu was always very patient to listen to my opinions on each research project and shared his precious knowledge and experiences. He also spent countless hours in the lab working along side me as needed showing new techniques and helping me solve experimental problems faced in such complex chemistry. Professor Simon had also given me numerous important advice and guidance, which has been helpful during my graduate studies and research, and also for my future career. Both Wu and Simon have always trusted in me and as a consequence assigned me to an increasing number of important and relevant projects some of which appear here in my dissertation and others were introduced to me to simply round out my natural products chemistry training. In the hard times of my graduate study, both of them stood solidly behind me, giving me needed encouragement and strong support and assistance in scientific writing as well as performing the lab studies. I thank them for all they have done and provided to me, for accepting me into their lab and supporting me in all the research in which I've been involved during my graduate studies at Rutgers University.

I also would like to thank Professor Edmond J. LaVoie, for his sharing of knowledge and advices on my seminars and thesis projects. His encouraging comments made me more determined to continue my graduate study. I also would like to thank my committee member, Professor Qingrong Huang, for his valuable advices and precious time on my proposal and thesis project.

I would like to express my sincere thanks to all people in our department of Medicinal Chemistry and the members of the New Use Agriculture and Natural Plant Products Program. Working with all of you is one of the most beautiful pages in my life. Special thanks are given to Tom Villani, Daniel Giurleo, Herve Aloysius, who I was lucky to work with in the past five years.

Finally, I would like to give my deepest thanks to my wife, my father, my mother, my uncle and my parents-in-law, for their love and selfless support in my life. In the past five years, my wife is always there to support my graduate study and share the joy of every piece of my success. Her encouragement is an efficient painkiller when I am in trouble. Her love makes my life full of happiness. My father and mother taught me the importance of knowledge when I was a kid, which lead to my graduate study today. Their love and dedication support me to continue school study, from primary school to high school, from college to graduate school. I feel proud of them and blessed to be their child. I also would like to thank my uncle Jixue, who spent a lot effort on my middle school education and gave me numerous good advices on further education. I also would like to thank my parents-in-law for being supportive in my graduate study.

DEDICATION

To My Beloved Mom

TABLE OF CONTENTS

LIST OF TABLES

LIST OF FIGURES

ABBREVIATIONS

ABTS	2,2'-Azino-Bis(3-Ethylbenzothiazoline-6-Sulphonic Acid)
COSY	Correlation Spectroscopy
DIPEA	N,N-Diisopropylethylamine
DMSO	Dimethyl Sulfoxide
ESI	Electrospray Ionization
GAE	Gallic Acid Equivalent
HCl	Hydrochloric Acid
HMBC	Heteronuclear Multiple Bond Correlation
HMDS	Hexamethyldisilazane
HMF	Hydroxymethylfurfural
HMQC	Heteronuclear Multiple Quantum Correlation
HPLC	High Performance Liquid Chromatography
iL-6	Interleukin 6
LC	Liquid Chromatography
LPS	Lipopolysaccharide
MOM-Cl	Chloromethyl Methyl Ether
MS	Mass Spectrometry
NCS	N-Chlorosuccinimide
NF-κB	Nuclear Factor Kappa-Light-Chain-Enhancer Of Activated B Cells
NMR	Nuclear Magnetic Resonance Spectroscopy
NO	Nitric Oxide
NOS	Nitric Oxide Synthase
RT-qPCR	Reverse Transcription Quantitative Polymerase Reaction
TEAC	Trolox Equivalent Antioxidant Capacity
THF	Tetrahydrofuran
TMS	Trimethylsilyl
TNF	Tumor Necrosis Factor
UV	Ultraviolet

CHAPTER ONE

Introduction

1.1 Medicinal Plants and Traditional Uses

1.1.1 *Ximenia caffra*

Ximenia caffra (Family Olacaceae), commonly known as large sourplum or ximenia, is a native species of sub-Sahara African tropical areas, including Kenya, South Africa, Zambia, and Zimbabwe (Ben-Erik Van Wyk, 2000). Ximenia can reach up to 6 meters in height under favorable conditions. The sourplum has rough and dark grey bark, leathery and dark green leaves. Leaves are elliptic to lanceolate and around 60 mm long and 25 mm wide. The fruit is in ellipsoidal shape and its skin color ranges from green to red orange (Orwa et al., 2012). *Ximenia caffra* has been playing an important role in local food and traditional medicine. The fruit is rich in vitamin C, protein and potassium, can be eaten raw, or processed into jam (Van Wyk, 2011). The seed oil is locally used to soften leather, skin and for some cosmetic applications (Chivandi et al., 2008). As a medicinal plant, the root and leaf of *X. caffra* has been used for the treatment of infertility, indigestion, gonorrhea and more (Cheikhyoussef et al., 2011; Mulaudzi et al., 2011). Modern pharmacological researches have further confirmed or explored new biological

activities of the leaf and root of *X. caffra*, such as antigonococcal, antibacterial and antifungal activities (Nair et al., 2013; Mulaudzi et al., 2011).

Most prior studies with *X. caffra* focused on the fruit and seed, as these represent the products of current commerce and traditional use, rather than the leaf. In this study, we purposefully investigate the phytochemical profile of *X.caffra* leaf using LC/UV/MS, which had not been previously examined. Interestingly though not unexpectedly, a number of polyphenol compounds were identified in the leaf. Polyphenols are a class of compounds characterized by the presence of large multiples of phenol structural units, and abundantly exist in food products, including crops, fruit, vegetables, tea, and wine (Erlund, 2004; Vauzour et al., 2010; Xia et al., 2010). These compounds have shown a wide range of biological activities including anti-inflammation, prevention of cancer and cardiovascular diseases (Hamalainen et al., 2007; Scalbert et al., 2005).

1.1.2 *Hibiscus sabdariffa*

Hibiscus sabdariffa (Family Malvaceae), commonly known as Roselle or Bissap, is an original native species to West Africa, while a naturalized non-native species to the United States (Ross, 2003). The calyx also known as a sepal (and in this species appears as the outer ring of the flower under the ovary) is commonly used in beverages and foods such as teas, jams, and jellies (Mahadevan et al., 2009). *Hibiscus* tea, a popular herbal tea around the world, from Mexico and the Americas, the Middle East, to North and sub-Sahara Africa to southeast Asia is thus found in international commerce as a sole

ingredient in herbal infusions or blend imparting a characteristic red color and unique flavor to such beverages (Villani et al., 2013). While the focus has been on the calyx, the leaves are also consumed in many countries in sub-Sahara Africa as a leafy green vegetable. Research has shown *Hibiscus sabdariffa* to exhibit nutraceutical properties, and this plant has been recognized in traditional medicines where it has been used as medicine for the treatment of hypertension, inflammation, and liver disorders (Lans, 2006; Lin et al., 2007). Anti-hypertensive activity was also demonstrated in both experimental animals and humans clinically, in which the underlying therapeutic mechanism was explained by a vasodilator effect in the aortic rings (Ajay et al., 2007; Herrera-Arellano et al., 2004; Onyenekwe et al., 1999). Extracts from the calyces were observed to inhibit enzymes cyclooxygenase COX-1 and COX-2 and down regulate the expression of COX-2 expression in lipopolysaccharide (LPS) treated RAW 264.7 cells, indicating anti-inflammatory activity (Christian et al., 2006; Kao et al., 2009). Other biological activities such as cancer prevention and liver protection activities have also been reported (Chang et al., 2014; Lin et al., 2007). Researchers hypothesize that many of these biological properties were due to the high content of anthocyanins, colored pigments found in many fruits and flowers. The major anthocyanin compounds identified in calyx include delphinidin-3-sambubioside and cyanidin-3-sambubioside (Juliani et al., 2009b).

Compared with the calyx, the leaf of *H. sabdariffa*, the most abundant portion of roselle foliage, is underutilized and as a consequence under-investigated. When the calyx is used, the leaf is usually discarded. Interestingly, in some regions of sub-Sahara Africa where leaves of hibiscus are considered as a leafy vegetable and the leaf is consumed as a

vegetable in soups and sauces, the calyces are generally discarded or not collected, except to save seeds to grow for the following season. Hibiscus leaf also has been reported to exhibit various bioactivities both *in vitro* and *in vivo* including anti-oxidant, antihyperlipidemic, anti-atherosclerotic, and anti-proliferation (Chen et al., 2013; Gosain et al., 2010; Lin et al., 2012; Ochani and D'Mello, 2009). After four weeks' treatment of *H. sabdariffa* leaf extract in rats, significant reductions of serum cholesterol, serum triglyceride, serum LDL (low-density lipoprotein) and serum VLDL (very-low-density lipoprotein) levels were observed in cholesterol-induced hyperlipidemic rats, suggesting antihyperlipidemic effects (Gosain et al., 2010). The anti-atherosclerotic activity is explained by the inhibition of LDL oxidation and foam cell formation via LXRα /ABCA1 pathway (Chen et al., 2013; Ochani and D'Mello, 2009)). The anti-proliferation effects of *H. sabdariffa* leaf extract on LNCaP cells (human prostate cancer cells) may involve both intrinsic (Bax/cytochrome c-mediated caspase 9) and extrinsic (Fas-mediated caspase 8/t-Bid) apoptotic pathways (Lin et al., 2012).

Figure 1. Picture of *Hibicus sabdariffa* (provided by Kit Chin)

1.1.3 *Combretum micranthum*

Kinkéliba (*Combretum micranthum*), belongs to the family Combretaceae (Iwu, 2014). The plant is a small shrub of about 4 meters height, but could grow up to 10 meters under favorable conditions. Kinkéliba has grey and fibrous bark, reddish brown branches, and oblong-elliptic leaves (Sacandé et al., 2007). The leaves are 5 to 10 cm long and 2.5 to 5 cm wide. Kinkéliba is native to western African, ranging from Senegal and Mauritania to Nigeria and Niger. As a savannah plant, it grows where annual rainfall is between 300 to 1500 mm, and altitudes ranges from 0 to 1000 meters (Sacandé et al., 2007).

Kinkéliba has been playing an important role in local food and medicine. The kinkéliba tea made from steeping leaves in boiling water is a traditional drink in local areas including Senegal, Mali (Juliani et al., 2009a). As an African traditional medicine, the kinkéliba tea can be used for the treatment of fever, cough, bronchitis, and for diuretic purposes; the leaves could also be used as plasters to cover and treat the wounds; the bark decoction can be used for stomachache and diarrhea (Muhammad, 2005).

Modern scientific research indicates that leaf extracts exhibit a number of pharmacological activities. For example, a kinkéliba decoction was shown to inhibit both chloroquine-sensitive and chloroquine-resistant strains of *Plasmodium falciparum in vitro*, indicating its potential for the treatment of malaria disease (Benoit et al., 1996). Methanol leaf extracts was reported to significantly inhibit the production of carrageenan induced

oedema in rats, suggesting its potential use for anti-inflammatory applications (Olajide et al., 2003). Udoh et al., reported that the methanol and water extract of kinkéliba leaves have effective anti-microbial activities against both Gram-positive and Gram-negative isolates including *Pseudomonas aeruginosa* and *Staphylococcus aureaus* (Udoh et al., 2012). Previous research in our lab found that the leaves' ethyl acetate extract and *n*-butanol extract have glucose-lowering effect *in vitro* on H4IIE hepatoma cell line through the suppression of phosphoenolpyruvate carboxykinase (PEPCK) mRNA expression. The extract would also increase the glucose tolerance *in vivo* on C57BL/6*J* mice (Welch, 2010; Simon et al. 2014)

Previous phytochemical studies in our lab revealed that the leaf extract contains a number of biological active flavan molecules including (-)-epicatechin, (-)-epigallocatechin, 3', 4', 5', 5, 7-pentahydroxyflavan, 3', 4', 5, 7-tetrahydroxyflavan, and confirmed the existence of various *C*-glycosylflavone compounds, including vitexin, isovitexin, orientin, homoorientin, 2"-*O*-galloylvitexin, 2"-*O*-galloylisovitexin, 2"-*O*-galloylorientin and 2"-*O*-galloylhomoorientin. These flavonoids in kinkéliba, especially (-)-epigallocatechin, showed potent bioactivity toward the inhibition of glucose production *in vitro* and increased glucose tolerance *in vivo* (Welch, 2010; Simon et al. 2014). Apart from these flavonoid compounds, other phytochemicals have also been reported in kinkéliba, such as alkaloids including stachydrine, choline, hydroxyl-stachydrine (Bassene, 1986); and sugar alcohols including *m*-inositol and sorbitol (Bassène et al., 1981). One of the most unique phytochemicals discovered from kinkéliba is a series of novel flavan alkaloids,

named kinkéloids in honor of this plant species. Kinkéloids belong to a small family of natural products named flavonoid alkaloids (Welch, 2010) (Simon et al. 2014).

1.2 Flavonoids

1.2.1 Chemistry

Flavonoids are ubiquitously present in plants and are a very important class of organic chemicals related to plants, food, nutrition, drug discovery and public health (Andersen and Markham, 2005). Flavonoids traditionally refer to a group of compounds that share a core structure of 2-phenyl-benzo-γ-pyrane. However, with the increasing discoveries of a lot similar phytochemicals in plants, flavonoids can be generally referred as a wide range of compounds that have two phenol rings connected by three carbon atoms. The basic structures of flavonoids are shown as Figure 2. According to the oxidation status of carbon 3, 4, the position of ring B (position 2, or 3) and the cyclization status of ring C, flavonoids would be further subdivided into a series of subclasses including flavone, flavonol, flavanone, flavanonol, anthocyanidin, flavan, flavanol isoflavone, isoflavanone, chalcones, and dihydrochalcones (Andersen and Markham, 2005).

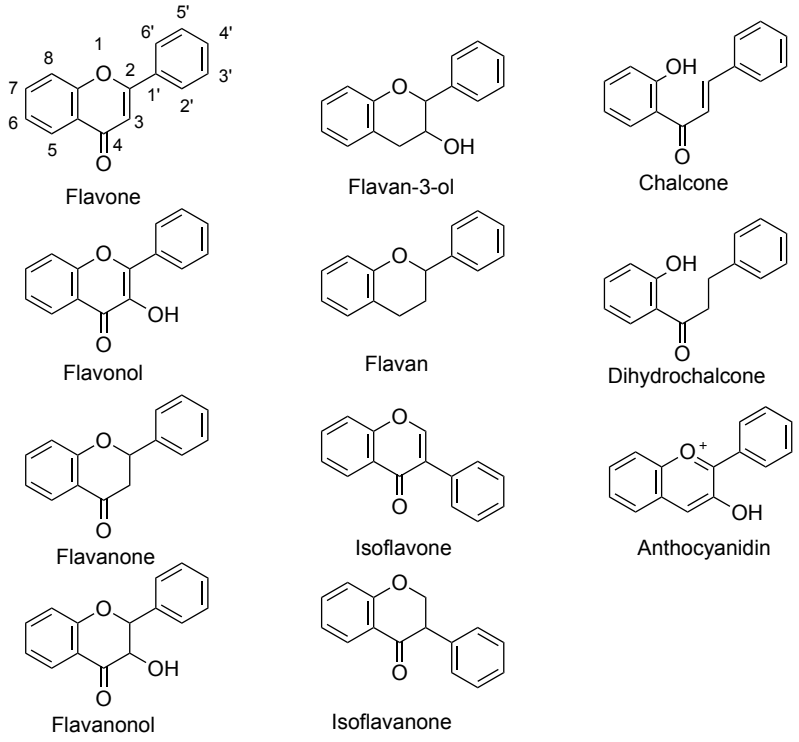

Figure 2. The basic structure of flavonoids and representative subclasses

1.2.2 Biological Activities

1.2.2.1 Anti-oxidant Activity

Flavonoids, universally found in a wide range of fruits and vegetables, have come to be associated with improving human health by numerous epidemiological studies, including the prevention of cancer, cardiovascular disease, allergies, atherosclerosis, Alzheimer disease and the treatment of bacterial infection, virus infection and some inflammatory diseases (Yao et al., 2011; Hollman and Katan, 1999; Kawai et al., 2007; Geleijnse et al., 1999; Engelhart et al., 2002; Cushnie and Lamb, 2005; Saw et al., 2014; Nagai et al., 1995). Some of these activities may be due, at least in part, to the antioxidant activities of

flavonoids, which could quench free reactive radicals inside the body and prevent potential tissue damage caused peroxidation (Robak and Gryglewski, 1995) .

During the process of oxygen metabolism, reactive oxygen species (ROS) will be produced and potentially damage the cells and tissues inside the body. One of the most well-known damages caused by ROS is lipid oxidation, which may contribute to the dysfunction of cellular membranes, cell death and inflammatory responses (Heim et al., 2002) (Nijveldt et al., 2001). Excessive ROS can induce a wide range of diseases including cellular aging, mutagenesis, carcinogenesis and coronary heart disease. ROS and other free radical species could be terminated by enzymatic reactions or by free radical scavengers, such as flavonoids. Even if flavonoids have been proven to interact a variety of enzymes such as xanthine oxidase, or metal ions to prevent the generation of free radicals, its best-known property is the direct radical scavenging activity. Flavonoids with phenol groups can donate one electron and one hydrogen to the ROS, while transforming itself into a flavonoid radical. The formed flavonoid radical is much less reactive compared with ROS due to the delocalization of radical electron around its conjugated rings. As a consequence, the relatively stable radical will cause less harm to the body than the ROS. Among these flavonoids, quercetin and catechin are the most potent radical scavengers (Fujisawa et al., 2002). Because after the removal of one electron and one hydrogen, the catechol moiety of catechin and quercetin will form *ortho*-semiquinone radicals as shown in Figure 3, which are relatively more stable compared with other flavonoid radicals (Amic et al., 2007). The double bond at position 2-3 and the carbonyl group at position 4 will contribute to an increased radical

scavenging activity (Hollman and Katan, 1999; Nijveldt et al., 2001; Harleen Kaur Sandhar, 2011).

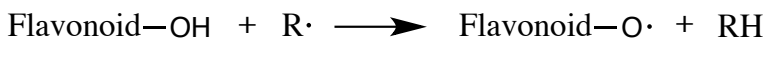

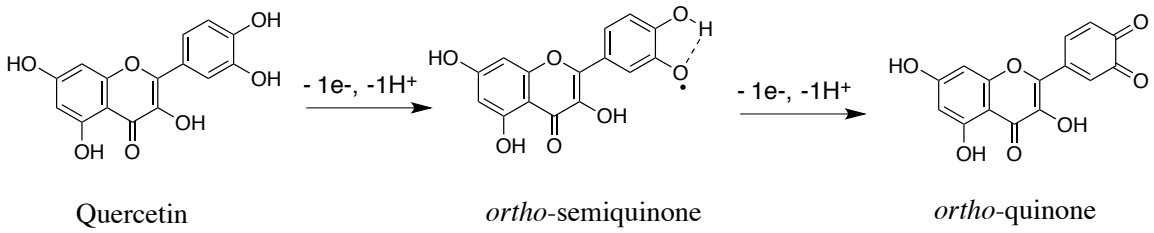

Figure 3. (A) The radical scavenge mechanism of flavonoid molecules; (B) The radical scavenge mechanism of quercetin and the formation of *ortho*-semiquinone intermediate

1.2.2.2 Anti-inflammatory Activity

Inflammation is an integrated response to microbial pathogen invasion, tissue injury, chemical irritation, and more. Inflammation involves pathogenesis of a number of diseases, such as arthritis, asthma, multiple sclerosis, colitis and atherosclerosis. This protective response involves immune cells, blood vessels and a wide range of molecular mediators, such as prostaglandin E_2 (PGE_2) and nitric oxide (NO) (Serhan et al., 2010). PGE_2 are generated by arachidonic acid under the catalysis of cyclooxygenase (COX), and NO is synthesized by three isoforms of nitric oxide synthase (NOS). Except these mediators, a number of pro-inflammatory cytokines are also involved in the inflammation process, such as interleukin 6 (iL-6) and tumor necrosis factor α (TNF- α). Eukaryotic transcription factor nuclear factor-kappa B (NF-κB) also plays an important role in the

inflammation process as it regulates expression of iNOS, COX-2 and other pro-inflammatory genes (Baeuerle and Baltimore, 1996; Kim et al., 2007).

Phospholipase A_2 (PLA_2) can catalyze the removal of arachidonic acid from phospholipids in cells. After its removal, arachidonic acid can be oxygenated and further transformed into a number of signal products that mediate the inflammatory reactions. For example, arachidonic acid can be catalyzed by cyclooxygenase (COX) to prostaglandins G_2, which could be further transformed into other prostaglandins (PGs) and thromboxanes (TX). Both PGs and TX play key roles in the generation of inflammatory responses (Tilley et al., 2001). The production of prostanoids depends on the activity of COX-1 and COX-2 enzymes within cells. The expression of COX-1 is generally constitutive and present in most cells. But the expression of COX-2 is low in most cells but increases dramatically upon stimulation. So the induction of COX-2 expression by inflammatory stimuli is more likely accounting for the much increased of prostanoids and subsequent chronic inflammatory responses. Arachidonic acid could also be oxidized by 5-lipoxygenase (5-LO) and forms compound 5-HPET (5-hydroperoxyeicosatetraenoic acid). 5-HPETE is an intermediate in the production of a number of leukotrienes, which are also very closely involved in the inflammatory responses.

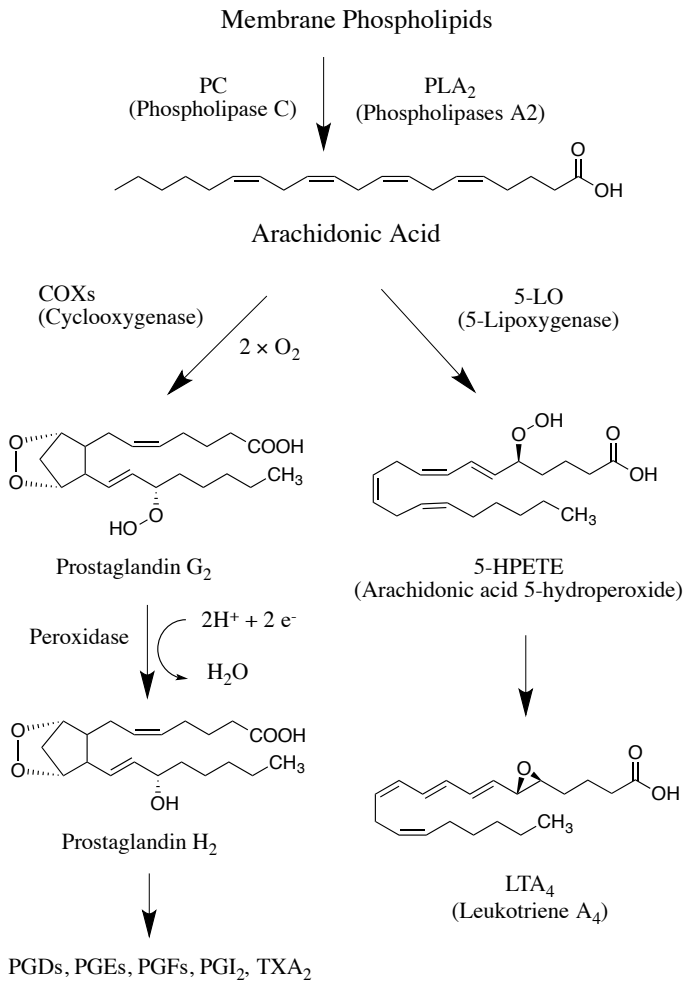

Figure 4. The biosynthesis of eicosanoids

Nitric oxide (NO) is an important cellular signaling molecule in pathogenesis of diverse inflammatory and infectious diseases (MacMicking et al., 1997). It can diffuse rapidly across cell membranes and modulate a wide range of physiological responses including gene regulation, neurotransmission, immune stimulation, apoptosis and more. Nitric oxide can regulate most stages of the development of inflammation. It is synthesized enzymatically by nitric oxide synthases (NOS), which coverts L-arginine to nitric oxide (NO) and L-citrulline. There are three isoforms of nitric oxide synthases: neuronal

(nNOS), endothelial NOS (eNOS) and inducible NOS (iNOS). nNOS and eNOS continuously synthesize low physiological levels of NO in neurons and endothelial cells respectively and controlled by the intracellular calcium/calmodulin levels. In contrast, iNOS is calcium-independent and produces prolonged high levels of NO, when initiated by immunological stimuli in macrophages, monocytes and some other cells (Guzik et al., 2003). In the course of an inflammatory response, large amount of NO will be synthesized by iNOS, much more than the physiological amounts synthesized by nNOS and eNOS. Some studies that NO would have pro-inflammatory effects; while equally others suggest the NO also own anti-inflammatory activities (Grisham et al., 1999).

Cytokines is a broad category of small proteins with molecular weights of 8 to 40 kDa, which regulate host responses to infection, immune responses and inflammation (Dinarello, 2000). Some cytokines can reduce the inflammation and promote healing, as anti-inflammatory cytokines, while others would accelerate a disease state, as pro-inflammatory cytokines. Blocking the functions of pro-inflammatory cytokines may yield therapeutic effects. For example, blocking pro-inflammatory cytokines interleukin (IL)-1 and tumor necrosis factor (TNF-α) has been highly successful in the treatment of inflammatory disease rheumatoid arthritis (So et al., 2007; Aaltonen et al., 2012).

Interleukin 6 (IL-6) is a secreted protein that mediates fever and can transport across blood-brain barrier and initiate the synthesis of PGE_2 in the hypothalamus, resulting in the increasing of body temperature. Human IL-6 binds with two cell surface receptors, IL-6Rα and gp130 to exert its biological activities. Its receptor antagonist tocilizumab has

been marketed for the treatment of rheumatoid arthritis, systemic juvenile idiopathic arthritis and etc. Monoclonal antibody siltuximab that directly targets iL-6 has been approved by FDA for the treatment of Castleman's disease (MCD) in 2014.

Tumor necrosis factor α (TNF-α) is a cell signaling protein involved in systematic inflammation. The expression level of TNF-α in serum and tissue is very low in healthy people, but increases in inflammatory and infectious conditions. Its concentration correlates well with the severity of infectious disease (Bradley, 2008). Five drugs based on blocking TNF have been approved for the treatment of inflammatory diseases. Four of them including infliximab, adalimumab, golimumab and certolizumab pegol are monoclonal antibodies against TNF-α. While another molecule etanercept is a soluble TNF-α receptor through the fusion between TNF-α receptor and the constant end of an IgG1 antibody. The expressions of IL-6 and TNF-α are both increased in most inflammatory states and they have been seen as important biomarkers for pharmacological researches (Aaltonen et al., 2012).

NF-κB (nuclear factor kappa-light-chain-enhancer of activated B cells) is a protein complex that regulates the transcription of DNA and is involved in cellular responses to stress. The activation of NF-κB is generally considered to up-regulate a range of genes encoding growth factors, cytokines, apoptosis, and immunomodulatory molecules (Lawrence, 2009). In cytosol, NF-κB nuclear localization sequence (NLS) is masked by inhibitor molecule IκB. Certain stimuli such as cytokines, lipopolysaccharide (LPS), virus, could lead to the phosphorylation of IκB at two serine residues (Ser 32 and Ser 36) by

IκB kinase (IKK) signalosome complex (Müller and Harrison, 1995). Phosphorylated IκB will under go ubiquitination and subsequent proteolytic degradation. Then NF- κB will be directed to the nucleus and bind to the promoter region of the target gene, then induces the transcription of pro-inflammatory mediators and cytokines, such as iNOS, COX-2, TNF-α, IL-1, 6, 8 (Baeuerle and Baltimore, 1996; Surh et al., 2001). The process is shown in Figure 5. Besides, NF-κB does play an important role in the control of cell proliferation, oncogenesis and cell transformation (Luque and Gélinas, 1997).

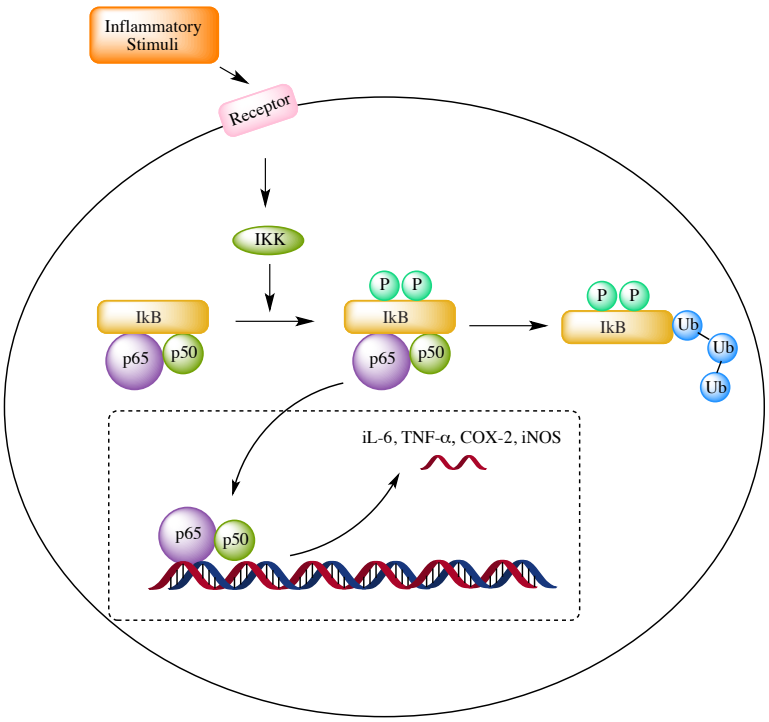

Figure 5. The canonical NF-κB pathway. NF-κB dimers: composed of p65 and p50 subunits; IκBs: NF-κB inhibitors; IKK: IκB kinase.

The anti-inflammatory activities from flavonoid compounds have been proven both *in vitro* and *in vivo*. While therapeutic mechanism from flavonoids are not completely

understood, several important cellular action mechanisms have been proposed, including the inhibition of enzymes phospholipase A_2 (PLA_2), cyclooxygenase (COX) and lipoxygenase (LOX); suppression of the expression of iNOS, cyclooxygenase (COX), tumor necrosis factor α (TNF-α) and interleukin (iL-6). Details are discussed below.

Flavonoids can inhibit a number of enzymes that regulate the activity of arachidonic acid (AA). These enzymes include phospholipase A_2 (PLA_2), cyclooxygenase (COX), lipoxygenase (LOX). (Gabor, 1986; Garcia-Mediavilla et al., 2007; Guardia et al., 2001; Kim et al., 2004; Pan et al., 2010; Read, 1995). Quercetin was the first flavonoid identified to have inhibition effect on PLA_2 from human neutrophils (Lee et al., 1982). The IC_{50} value of quercetin on PLA_2 from rabbit peritoneal neutrophil is around 57-100 μM (Lanni and Becker, 1985). Later, other flavonols including kaempferol and myricetin were found to also be able to inhibit PLA_2 considerably. Comparatively, the flavanone molecules including naringenin, hesperetin and eriodictyol have less inhibition activity, suggesting that the double bond at position 2-3 is critical for the binding between flavonoid molecules and PLA_2 enzyme (Kim et al., 2004). Flavone molecules luteolin, 3'4'-dihydroxyflavone, and flavanol molecules including galangin and morin were reported to inhibit enzyme COX (Raso et al., 2001). The prenylated flavonoids such as morusin and kuwanon C can increase the inhibition activity. Amentoflavone has IC_{50} of 3 uM on COX-1 from guinea-pig epidermis; while control compound indomethacin has IC_{50} of 1uM. The expression of COX-2 in LPS induced RAW 264.7 cell line could be inhibited by flavonoids apigenin, genistein and kaempferol with IC_{50} less than 15 uM (Liang et al., 1999).

While flavonoids generally don't inhibit the enzyme NOS, but it was discovered that they could down-regulate the expression in iNOS which in turn results in lower NO production in inflammation. Quercetin was tested for inhibitory activity of NOS, but only weak inhibition towards eNOS was observed and no significant inhibition against nNOS and iNOS. Genistein can inhibit LPS-induced NO production in macrophages. Other flavonoids including apigenin, quercetin and morin have shown activity against the production of NO from LPS/interferon-γ-activated C6 astrocytes (Sadowska-Krowicka et al., 1998; Soliman and Mazzio, 1998).

Flavonoids can also impact the expression of a number of cytokines. Compounds including genistein, amoradicin, silybin and baicalin, have been reported to suppress the expression of pro-inflammatory cytokines like IL-6 and TNF-α in LPS-treated cell lines (Cho et al., 2000; Winkel-Shirley, 2001). Considering the overall inhibition of a wide range of pro-inflammatory genes by flavonoids, the underlying therapeutic mechanism was investigated and it appears that flavonoids may inhibit various signal transduction protein kinases such protein kinase C, leading to inhibited phosphorylation of IκB kinase and suppressed IκB kinase activation (Benoit et al., 1996; Geng et al., 1993)

1.3 Flavonoid Alkaloids

1.3.1 Chemistry of Flavonoid Alkaloids

Flavonoid alkaloids (flavoalkaloids) are a group of flavonoid compounds with the attachment of one or more nitrogenous moieties, such as piperidine, and pyrrolidine. Flavonoids with phenol groups are generally acidic while alkaloids with amine groups are basic. Flavonoid alkaloids, as a combination of these two properties from flavonoids and alkaloids, are usually amphoteric. There are only a limited number of flavonoid alkaloids compounds from natural sources reported in the past decades, majority of which are summarized in Table 1. Their representative structures are shown in Figure 6. The flavonoid moieties are shown in Figure 7, including flavonols (quercetin), flavanone (naringenin), flavone and flavan and epicatechin. The hydroxyl groups at position 5, 3' or 4' of flavonoid group may be methylated and co-exist with un-methylated ones in the natural source. All flavonoid moieties have at least two phenol groups attached at *meta* positions. The phenol group may be methylated or cyclized into a ring structure. The nitrogenous moieties generally locate at ring A, either at position 6 or 8. The nitrogenous moieties will always be in a cyclized ring form ranging from 5-atom to 7-atom (Figure 8). Fused rings may also appear, such as 4,7-dimethyloctahydro-1H-cyclopenta[c]pyridine in kopsirachin (Katharina Homberger, 1984). In most cases, it is the alpha position carbon of the nitrogenous moiety that binds with the flavonoids. But for chromone alkaloids, this rule doesn't apply and the binding carbon would be several atoms away from the nitrogen. The nitrogen atom would also be part of an amide group, as in the case of pyrrolidinone and dracocephin (Ren et al., 2008). They could also be alkylated, such as compounds

phyllospadine, buchenavianine (Beutler et al., 1992). Considering the structural similarities, chromone alkaloids are generally treated as a special class or a very related class of flavonoid alkaloids. Distinct from the general flavonoid alkaloids, chromone alkaloids have a methyl group attached at position 2 instead of a phenyl group. Representative chromone alkaloid is compound rohitukine extracted from plant *Amoora rohituka*. Later on this compound and its regio-isomer dysoline were also isolated from the stem barks of another plant *Dysoxylum binectariferum*. Both of regio-isomers have shown promising cytotoxicity and anti-inflammatory activity (Jain et al., 2013).

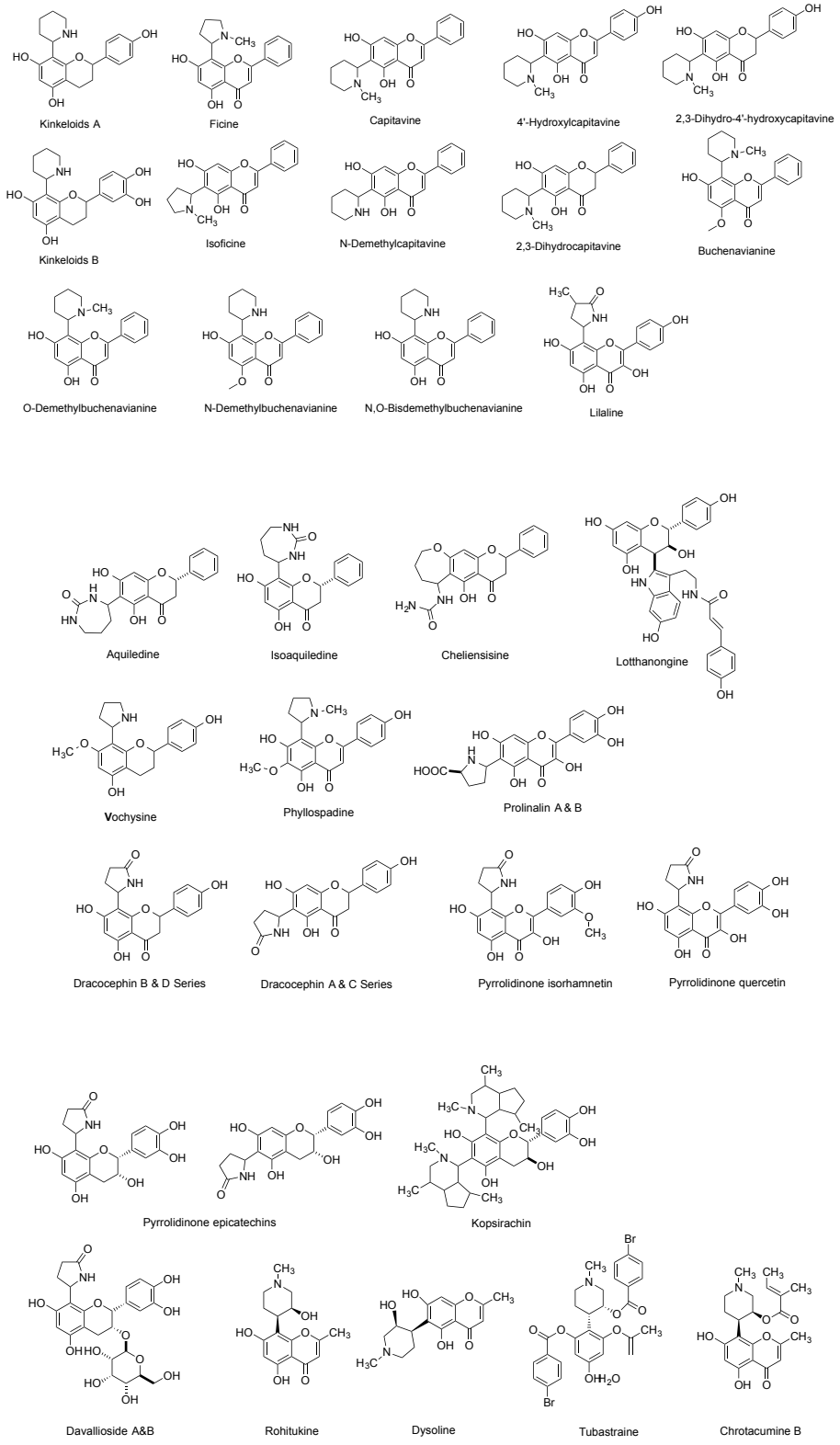

Figure 6. The structures of representative flavonoid alkaloids

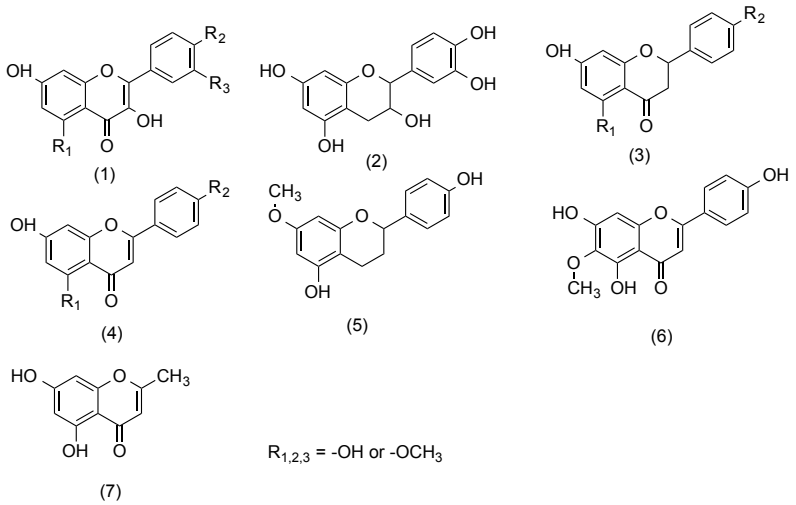

Figure 7. Representative flavonoid moieties of the flavonoid alkaloids

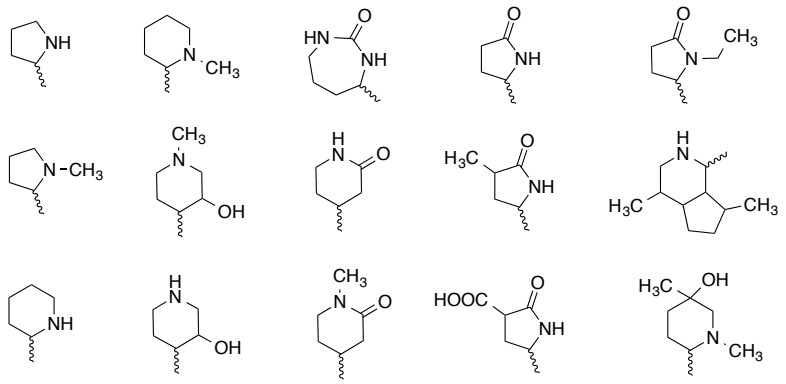

Figure 8. Representative nitrogenous moieties of the flavonoid alkaloids

Table 1. Representative flavonoid alkaloids and their natural sources.

Compound	Source	Reference
Kinkéloids	*Combretum micranthum*	Welch, 2008
Ficine	*Ficus pantoniana*	Leete, 1982
Isoficine	*Ficus pantoniana*	Leete, 1982
Capitavine	*Buchenavia macrophylla*	Ahond, 1984
N-Demethylcapitavine	*Buchenavia macrophylla*	Ahond, 1984
4'-Hydroxycapitavine	*Buchenavia macrophylla*	Ahond, 1984
2,3-Dihydrocapitavine	*Buchenavia macrophylla*	Ahond, 1984
2,3-Dihydro-4'-hydroxycapitavine	*Buchenavia macrophylla*	Ahond, 1984
Buchenavianine	*Buchenavia macrophylla*	Beutler et al., 1992
O-Demethylbuchenavianine	*Buchenavia macrophylla*	Beutler et al., 1992
N-Demethylbuchenavianine	*Buchenavia macrophylla*	Beutler et al., 1992
N,O-Bisdemethylbuchenavianine	*Buchenavia macrophylla*	Beutler et al., 1992
Aquiledine	*Aquilegia ecalcarata*	Chen et al., 2001
Isoaquiledine	*Aquilegia ecalcarata*	Chen et al., 2001
Lilaline	*Lilium candidum*	Masterova et al., 1987
Vochysine	*Vochysia guianensis*	Geneviève Baudouin, 1983
Phyllospadine	*Phyllospadix iwatensis*	Takagi et al., 1980
Lotthanongine	*Trigonostemon reidioides*	Kanchanapoom et al., 2002
Dracocephins (A-D)	*Dracocephalum rupestre*	Ren et al., 2008
Pyrrolidinone epicatechins	*Actinidia arguta*	Jang et al., 2009
Prolinalin A, B	*Bombyx mori*	Hirayama et al., 2006
Pyrrolidinone quercetin	*Senecio argunensis*	Li et al., 2008
Pyrrolidinone isorhamnetin	*Senecio argunensis*	Li et al., 2008
Kopsirachin	*Kopsia dasyrachis*	Katharina Homberger, 1984
Davallioside A B	*Davallia mariesii*	Cui et al., 1990
Ethylpyrrolidinonyl theasinensin A	*Camellia sinensis*	Tanaka et al., 2005
Rohitukine	*Amoora rohituka*	Kumara et al., 2014
Tubastraine	*Tubastrea micrantha*	Alam et al., 1988
Chrotacumine A-F	*Dysoxylum acutangulum*	Lazim et al., 2013
Cassiadinine	*Cassia siamea*	Biswas and Mallik, 1986

1.3.2 Flavonoid Alkaloids Biological Activities

Except their unique amphoteric physiochemical properties, flavonoid alkaloids either from nature or their synthetic analogues have shown a wide range of bioactivities, such as anti-inflammatory, anti-diabetes, anti-cancer and anti-HIV (Khadem and Marles, 2011). Some of these bioactive flavonoid alkaloids may serve as a lead molecule for new drug discoveries and pharmacological researches. For example, flavonoid alkaloids 6-(2-pyrrolidinone-5-yl)-(-)-epicatechin and its conformational isomer 8-(2-pyrrolidinone-5-yl)-(-)-epicatechin were isolated by Jang et al., in 2009. They have shown inhibitory activity on the formation of advanced glycation end products (AGEs) *in vitro* with IC_{50} of 36.0 μM and 47.8 μM, indicating potential use for diabetes treatment (Jang et al., 2009). In an AIDS-antiviral drug screening project conducted by National Cancer Institute, *O*-Demethylbuchenavianine isolated from *Buchenavia macrophylla* by Beutler et al, showed both potent anti-virus activity (ED_{50} = 0.26 μM) and anti-neoplastic activity (IC_{50} = 0.66 μM) on HIV infected CEM-SS host cells. Further cytotoxicity exploration showed that melanoma cancer cells are also very sensitive to this compound with IC_{50} in micromole range (Beutler et al., 1992). Structure activity relationship studies indicated that the removal of methyl group on the nitrogen atom resulted in a dramatic decrease of anti-HIV activity. In 2014 Zhang et al, discovered compound cheliensisine, which would induce p53-mediated apoptosis and inhibit the anchorage-independent growth of human colon cancer HCT116 cells. The mechanism has been unveiled, as cheliensisine can induce the phosphorylation of p53 protein at amino acid Ser20 and Ser15. The phosphorylated one is comparatively more stable. Except that their experiments demonstrated cheliensisine also induces hydrogen peroxide generation, which serves as a

precursor for the signaling events and downstream biological activities (Zhang et al., 2014). Another flavonoid alkaloids discovered for cancer treatment is flavopiridol. It is a synthetic analogue compound derived from chromone alkaloid rohitukine. Rohitukine was firstly discovered in *Amoora rohituka* and later isolated from plant *Dysoxylum binectariferum* and other species (Mohana Kumara et al., 2012). Rohitukine has been reported with various biological activities, such as anti-cancer, anti-inflammatory activities. The synthetic analogue flavopiridol was found with much improved anti-proliferation activities on a number of different cell lines, especially the breast carcinoma cell lines (IC_{50} ranges from 25 to 160 nM) (Tan and Swain, 2002). It can potently inhibit several cyclin dependent kinases (CDKs) including CDK1, CDK2, and CDK4 and cause cell cycle arrest at the G_1/S and G_2/M transitions (Kaur et al., 1992). The IC_{50} of flavopiridol towards CDKs ranges from 100 to 400 nM. In addition, flavopiridol is reported to have antiangiogenic effects as well. In preclinical studies, flavopiridol has shown potent efficacy on the treatment of a variety of tumors, and especially breast cancer. Yet, now the compound is going to be studied in phase III clinical trials to explore the combination of flavopiridol with other anti-cancer drugs as a combo for cancer treatment. (Blagosklonny, 2004; Tan and Swain, 2002)

1.3.3 Flavonoid Alkaloids Biosynthesis

The biosynthesis of flavonoid alkaloids is poorly understood. It was reported that amino acid constituent N^5-ethyl-L-glutamine in tea products would be transformed to an active metabolite N-ethyl-4-oxobutanamide through Strecker degradation. N-ethyl-4-

oxobutanamide then undergoes cyclization reaction and forms the ring compound 1-ethyl-5-hydroxypyrrolidin-2-one, which could react with theasinensin A and as shown in Figure 9 forms flavonoid alkaloid ethylpyrrolidinonyl theasinensin, (Tanaka et al., 2005). The biosynthesis of the nitrogenous moieties have been reported in other phytochemicals, especially in alkaloids. For example, the piperidine group attached at *N*-demethylcapitavine also exists in alkaloid anabasine from tree tabacco (*Nicotiana glauca*). As reported, its biosynthesis starts from amino acid L-lysine (Szőke et al., 2013), which could form an active aldehyde 5-aminopentanal through Strecker degradation. The aldehyde later cyclizes and forms intermediate compound Δ^1- piperideine. Based on these reviewed papers, the nitrogenous moieties on flavonoid alkaloids are more likely to be synthesized independently from the flavonoid moieties. After their individual syntheses, the active nitrogenous intermediate will bind with the flavonoids at 6 or 8 position through a chemical reaction, such as Mannich reaction.

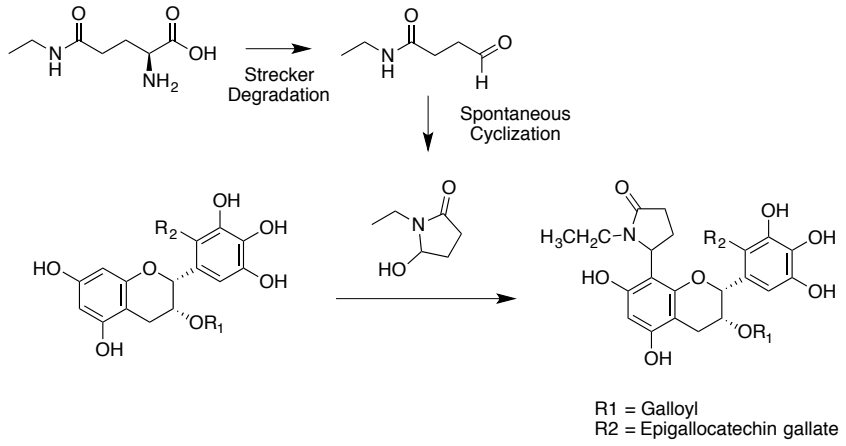

Figure 9. Bio-generation pathway of flavonoid alkaloid ethylpyrrolidinonyl theasinensin A

The biosynthesis of flavonoid moieties of flavonoid alkaloids has been very well established. The core structure of flavonoids is synthesized from three malonyl-CoAs and one 4-coumaroyl-CoA (Shirley, 1996; Winkel-Shirley, 2001, 2002). Ring A has been shown to be synthesized from the tree malonyl-CoAs and ring B comes from 4-coumaroyl-CoA. The flavan biosynthesis scheme is shown in Figure 10**.** Flavonoid synthesis starts from L-phenylalanine, and forms a key intermediate p-coumarate under the catalysis of PAL (phenylalanine ammonialyase), C4H (cinnamate 4-hydroxylase), and 4CL (p-coumaroyl-CoA ligase). *P*-coumarate then gets activated by coenzyme A, and was added three malonyl groups with the loss of three carbon dioxide molecules, yielding natural product chalcone. Chalcone is then cyclized to flavanone naringenin under the catalysis of enzyme chalcone isomerase (CHI). Extra hydroxyl group can be added to the B ring of naringenin under the catalysis of enzyme flavanone-3-hydroxylase (F3H) to form another flavanone compound eriodictyol. Both naringenin and eriodictyol could be reduced by flavanone reductase (FR) to achieve the flavanol compounds. Flavanols can be dehydrated under the help of anthocyanidin synthase (ANS) to achieve another special category of flavonoid, anthocyanidin. Flavans are usually achieved through the reduction of anthocyanidin compounds under the catalysis of anthocyanidin reductase (ANR).

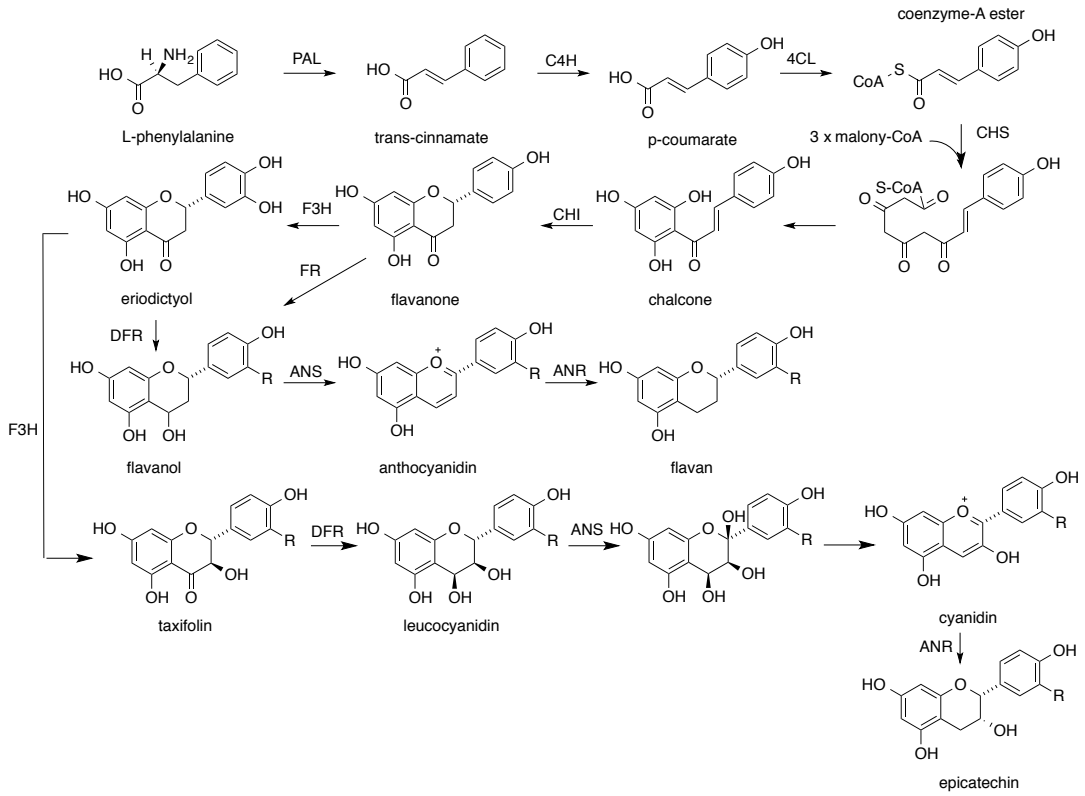

Figure 10. The biosynthesis of representative flavonoids. Abbreviations: PAL, phenylalanine ammonialyase; C4H, cinnamate 4-hydroxylase; 4CL, p-coumaroyl-CoA ligase; CHS, chalcone synthase; CHI, chalcone isomerase; F3H, flavanone 3-hydroxylase; DFR, dihydroflavonol reductase; FR, flavanone reductase; ANS, anthocyanidin synthase; ANR, anthocyanidin reductase;

1.4 References

Aaltonen, K.J., Virkki, L.M., Malmivaara, A., Konttinen, Y.T., Nordstrom, D.C., Blom, M., 2012. Systematic review and meta-analysis of the efficacy and safety of existing TNF blocking agents in treatment of rheumatoid arthritis. Plos One 7, e30275.

Ahond, A.F., A.; Moretti, C.; Philogene, E.; Poupat, C.; Thoison, O.; Potier, P, 1984. Premiers alcaloïdes vrais isolés de Combretacées: Buchenavia macrophylla Eichl. et *Buchenavia capitata* Eichl. Bulletin de la Société Chimique de France Partie I 41-45.

Ajay, M., Chai, H.J., Mustafa, A.M., Gilani, A.H., Mustafa, M.R., 2007. Mechanisms of the anti-hypertensive effect of *Hibiscus sabdariffa* L. calyces. *J* Ethnopharmacol 109, 388-393.

Alam, M., Sanduja, R., Wellington, G.M., 1988. Tubastraine - Isolation and Structure of a Novel Alkaloid from the Stony Coral Tubastraea-Micrantha. Heterocycles 27, 719-723.

Amic, D., Davidovic-Amic, D., Beslo, D., Rastija, V., Lucic, B., Trinajstic, N., 2007. SAR and QSAR of the antioxidant activity of flavonoids. Current medicinal chemistry 14, 827-845.

Andersen, O.M., Markham, K.R., 2005. Flavonoids: chemistry, biochemistry and applications. CRC Press.

Baeuerle, P.A., Baltimore, D., 1996. NF- κ B: Ten Years After. Cell 87, 13-20.

Bassène, E., Olschwang, D., Pousset, J., 1981. Plantes medicinales africaines I: Caracterisation de l'inositol et du sorbitol, principes actifs probables du Kinkéliba ("*Combretum micranthum*" G. Don.). Dakar medical 26, 219-225.

Bassene, E.O., D.; Pousset, J.-L., 1986. Plantes medicinales africaines. Les alcaloides du *Combretum micranthum* G. Don (Kinkéliba). Annales pharmaceutiques francaises 44, 191-196.

Ben-Erik Van Wyk, N.G., 2000. People's Plants. Briza Publications, 30.

Benoit, F., Valentin, A., Pelissier, Y., Diafouka, F., Marion, C., Kone-Bamba, D., Kone, M., Mallie, M., Yapo, A., Bastide, J., 1996. In vitro antimalarial activity of vegetal extracts used in West African traditional medicine. The American journal of tropical medicine and hygiene 54, 67-71.

Beutler, J.A., Cardellina, J.H., 2nd, McMahon, J.B., Boyd, M.R., Cragg, G.M., 1992. Anti-HIV and cytotoxic alkaloids from *Buchenavia capitata*. *J* Nat Prod 55, 207-213.

Biswas, K.M., Mallik, H., 1986. Cassiadinine, a Chromone Alkaloid and (+)-6-Hydroxymellein, a Dihydroisocoumarin from *Cassia-Siamea*. Phytochemistry 25, 1727-1730.

Blagosklonny, M.V., 2004. Flavopiridol, an inhibitor of transcription: implications, problems and solutions. Cell cycle 3, 1537-1542.

Bradley, J., 2008. TNF - mediated inflammatory disease. The Journal of pathology 214, 149-160.

Chang, H.C., Peng, C.H., Yeh, D.M., Kao, E.S., Wang, C.J., 2014. *Hibiscus sabdariffa* extract inhibits obesity and fat accumulation, and improves liver steatosis in humans. Food & function 5, 734-739.

Cheikhyoussef, A., Shapi, M., Matengu, K., Ashekele, H.M., 2011. Ethnobotanical study of indigenous knowledge on medicinal plant use by traditional healers in Oshikoto region, Namibia. J Ethnobiol Ethnomed 7.

Chen, J.H., Wang, C.J., Wang, C.P., Sheu, J.Y., Lin, C.L., Lin, H.H., 2013. *Hibiscus sabdariffa* leaf polyphenolic extract inhibits LDL oxidation and foam cell formation involving up-regulation of LXRalpha/ABCA1 pathway. Food Chem 141, 397-406.

Chen, S.B., Gao, G.Y., Leung, H.W., Yeung, H.W., Yang, J.S., Xiao, P.G., 2001. Aquiledine and isoaquiledine, novel flavonoid alkaloids from *Aquilegia ecalcarata*. J Nat Prod 64, 85-87.

Chivandi, E., Davidson, B.C., Erlwanger, K.H., 2008. A comparison of the lipid and fatty acid profiles from the kernels of the fruit (nuts) of *Ximenia caffra* and *Ricinodendron rautanenii* from Zimbabwe. Ind Crop Prod 27, 29-32.

Cho, J.Y., Kim, P.S., Park, J., Yoo, E.S., Baik, K.U., Kim, Y.-K., Park, M.H., 2000. Inhibitor of tumor necrosis factor- α production in lipopolysaccharide-stimulated RAW264. 7 cells from A*morpha fruticosa*. J Ethnopharmacol 70, 127-133.

Christian, K.R., Nair, M.G., Jackson, J.C., 2006. Antioxidant and cyclooxygenase inhibitory activity of sorrel (*Hibiscus sabdariffa*). J Food Compos Anal 19, 778-783.

Cui, C.B., Tezuka, Y., Kikuchi, T., Nakano, H., Park, J.H., 1990. Davallioside-a and Davallioside-B, Novel Flavan-3-Ol Derivatives with a Gamma-Lactam, from the Rhizomes of Davallia-Mariesii Moore. Chemical & pharmaceutical bulletin 38, 2620-2622.

Cushnie, T.T., Lamb, A.J., 2005. Antimicrobial activity of flavonoids. International journal of antimicrobial agents 26, 343-356.

Dinarello, C.A., 2000. Proinflammatory cytokines. Chest Journal 118, 503-508.

Engelhart, M.J., Geerlings, M.I., Ruitenberg, A., van Swieten, J.C., Hofman, A., Witteman, J.C., Breteler, M.M., 2002. Dietary intake of antioxidants and risk of Alzheimer disease. Jama 287, 3223-3229.

Erlund, I., 2004. Review of the flavonoids quercetin, hesperetin naringenin. Dietary sources, bioactivities, and epidemiology. Nutrition research 24, 851-874.

Fujisawa, S., Ishihara, M., Kadoma, Y., 2002. Kinetic evaluation of the reactivity of flavonoids as radical scavengers. SAR and QSAR in Environmental Research 13, 617-627.

Gabor, M., 1986. Anti-inflammatory and anti-allergic properties of flavonoids. Progress in clinical and biological research 213, 471-480.

Garcia-Mediavilla, V., Crespo, I., Collado, P.S., Esteller, A., Sanchez-Campos, S., Tunon, M.J., Gonzalez-Gallego, J., 2007. The anti-inflammatory flavones quercetin and kaempferol cause inhibition of inducible nitric oxide synthase, cyclooxygenase-2 and reactive C-protein, and down-regulation of the nuclear factor kappaB pathway in Chang Liver cells. European journal of pharmacology 557, 221-229.

Geleijnse, J.M., Launer, L.J., Hofman, A., Pols, H.A., Witteman, J.C., 1999. Tea flavonoids may protect against atherosclerosis: the Rotterdam Study. Archives of internal medicine 159, 2170-2174.

Geneviève Baudouin, F.T., Michel Koch, Marc Vuilhorgne, Jean-Yves Lallemand, Henri Jacquemin, 1983. Isolement, Structure et Synthèse de la Vochysine, Pyrrolidinoflavanne de *Vochysia guianensis*. J Nat Prod 46, 681–687.

Geng, Y., Zhang, B., Lotz, M., 1993. Protein tyrosine kinase activation is required for lipopolysaccharide induction of cytokines in human blood monocytes. The Journal of Immunology 151, 6692-6700.

Gosain, S., Ircchiaya, R., Sharma, P.C., Thareja, S., Kalra, A., Deep, A., Bhardwaj, T.R., 2010. Hypolipidemic effect of ethanolic extract from the leaves of *Hibiscus sabdariffa* L. in hyperlipidemic rats. Acta Pol Pharm 67, 179-184.

Grisham, M.B., Jourd'Heuil, D., Wink, D.A., 1999. I. Physiological chemistry of nitric oxide and its metabolites: implications in inflammation. American Journal of Physiology-Gastrointestinal and Liver Physiology 276, G315-G321.

Guardia, T., Rotelli, A.E., Juarez, A.O., Pelzer, L.E., 2001. Anti-inflammatory properties of plant flavonoids. Effects of rutin, quercetin and hesperidin on adjuvant arthritis in rat. Farmaco 56, 683-687.

Guzik, T., Korbut, R., Adamek-Guzik, T., 2003. Nitric oxide and superoxide in inflammation. Journal of physiology and pharmacology 54, 469-487.

Hamalainen, M., Nieminen, R., Vuorela, P., Heinonen, M., Moilanen, E., 2007. Anti-inflammatory effects of flavonoids: genistein, kaempferol, quercetin, and daidzein inhibit STAT-1 and NF-kappaB activations, whereas flavone, isorhamnetin, naringenin, and pelargonidin inhibit only NF-kappaB activation along with their inhibitory effect on iNOS expression and NO production in activated macrophages. Mediators of inflammation 2007, 45673.

Harleen Kaur Sandhar, B.K., Sunil Prasher, Prashant Tiwari, Manoj Salhan, Pardeep Sharma, 2011. A Review of Phytochemistry and Pharmacology of Flavonoids. Internationale Pharmaceutica Sciencia 1, 25-41.

Heim, K.E., Tagliaferro, A.R., Bobilya, D.J., 2002. Flavonoid antioxidants: chemistry, metabolism and structure-activity relationships. The Journal of nutritional biochemistry 13, 572-584.

Herrera-Arellano, A., Flores-Romero, S., Chavez-Soto, M.A., Tortoriello, J., 2004. Effectiveness and tolerability of a standardized extract from *Hibiscus sabdariffa* in patients with mild to moderate hypertension: a controlled and randomized clinical trial. Phytomedicine 11, 375-382.

Hirayama, C., Ono, H., Tamura, Y., Nakamura, M., 2006. C-prolinylquercetins from the yellow cocoon shell of the silkworm, Bombyx mori. Phytochemistry 67, 579-583.

Hollman, P.C., Katan, M.B., 1999. Dietary flavonoids: intake, health effects and bioavailability. Food and chemical toxicology : an international journal published for the British Industrial Biological Research Association 37, 937-942.

Iwu, M.M., 2014. Handbook of African medicinal plants. CRC press.

Jain, S.K., Meena, S., Qazi, A.K., Hussain, A., Bhola, S.K., Kshirsagar, R., Pari, K., Khajuria, A., Hamid, A., Shaanker, R.U. and Bharate, S.B., 2013. Isolation and biological evaluation of chromone alkaloid dysoline, a new regioisomer of rohitukine from *Dysoxylum binectariferum*. Tetrahedron Letters, 54(52), pp.7140-7143.

Jang, D.S., Lee, G.Y., Lee, Y.M., Kim, Y.S., Sun, H., Kim, D.H., Kim, J.S., 2009. Flavan-3-ols Having a gamma-Lactam from the Roots of *Actinidia arguta* Inhibit the Formation of Advanced Glycation End Products in Vitro. Chemical & pharmaceutical bulletin 57, 397-400.

Juliani, H.R., Koelliker, Y., Bucuk, M., Welch, C., Tepper, B.J., Jefthas, E., Simon, J.E., 2009a. Quality and consumer studies in the USA of African herbal teas for the natural product industry development in Sub-Sahara Africa, ACS symposium series. Oxford University Press, pp. 403-420.

Juliani, H.R., Welch, C.R., Wu, Q., Diouf, B., Malainy, D., Simon, J.E., 2009b. Chemistry and Quality of Hibiscus (*Hibiscus sabdariffa*) for Developing the Natural-Product Industry in Senegal. J Food Sci 74, S113-S121.

Kanchanapoom, T., Kasai, R., Chumsri, P., Kraisintu, K., Yamasaki, K., 2002. Lotthanongine, an unprecedented flavonoidal indole alkaloid from the roots of Thai medicinal plant, *Trigonostemon reidioides*. Tetrahedron Lett 43, 2941-2943.

Kao, E.S., Hsu, J.D., Wang, C.J., Yang, S.H., Cheng, S.Y., Lee, H.J., 2009. Polyphenols Extracted from Hibiscus sabdariffa L. Inhibited Lipopolysaccharide-Induced Inflammation by Improving Antioxidative Conditions and Regulating Cyclooxygenase-2 Expression. Biosci Biotech Bioch 73, 385-390.

Katharina Homberger, M.H., 1984. Kopsirachin, ein ungewöhnliches Alkaloid aus der Apocynaceae Kopsia dasyrachis Ridl. 189. Mitteilung über organische Naturstoffe. Helv Chim Acta 67, 237-248.

Kaur, G., Stetler-Stevenson, M., Sebers, S., Worland, P., Sedlacek, H., Myers, C., Czech, J., Naik, R., Sausville, E., 1992. Growth inhibition with reversible cell cycle arrest of

carcinoma cells by flavone L86-8275. Journal of the National Cancer Institute 84, 1736-1740.

Kawai, M., Hirano, T., Higa, S., Arimitsu, J., Maruta, M., Kuwahara, Y., Ohkawara, T., Hagihara, K., Yamadori, T., Shima, Y., 2007. Flavonoids and related compounds as anti-allergic substances. Allergology International 56, 113-123.

Khadem, S., Marles, R.J., 2011. Chromone and flavonoid alkaloids: occurrence and bioactivity. Molecules 17, 191-206.

Kim, H.P., Son, K.H., Chang, H.W., Kang, S.S., 2004. Anti-inflammatory plant flavonoids and cellular action mechanisms. J Pharmacol Sci 96, 229-245.

Kim, J.-B., Han, A.-R., Park, E.-Y., Kim, J.-Y., Cho, W., Lee, J., Seo, E.-K., Lee, K.-T., 2007. Inhibition of LPS-Induced iNOS, COX-2 and Cytokines Expression by Poncirin through the NF-κB Inactivation in RAW 264.7 Macrophage Cells. Biological and Pharmaceutical Bulletin 30, 2345-2351.

Kumara, P.M., Soujanya, K.N., Ravikanth, G., Vasudeva, R., Ganeshaiah, K.N., Shaanker, R.U., 2014. Rohitukine, a chromone alkaloid and a precursor of flavopiridol, is produced by endophytic fungi isolated from *Dysoxylum binectariferum* Hook.f and Amoora rohituka (Roxb).Wight & Arn. Phytomedicine 21, 541-546.

Lanni, C., Becker, E., 1985. Inhibition of neutrophil phospholipase A2 by p-bromophenylacyl bromide, nordihydroguaiaretic acid, 5, 8, 11, 14-eicosatetrayenoic acid and quercetin. International Archives of Allergy and Immunology 76, 214-217.

Lans, C.A., 2006. Ethnomedicines used in Trinidad and Tobago for urinary problems and diabetes mellitus. J Ethnobiol Ethnomed 2, 45.

Lawrence, T., 2009. The nuclear factor NF- κ B pathway in inflammation. Cold Spring Harbor perspectives in biology 1, a001651.

Lazim, M.I.M., Ismail, I.S., Shaari, K., Abd Latip, J., Al-Mekhlafi, N.A., Morita, H., 2013. Chrotacumines E and F, Two New Chromone-Alkaloid Analogs from *Dysoxylum acutangulum* (Meliaceae) Leaves. Chem Biodivers 10, 1589-1596.

Lee, T.-P., Matteliano, M.L., Middleton, E., 1982. Effect of quercetin on human polymorphonuclear leukocyte lysosomal enzyme release and phospholipid metabolism. Life Sci 31, 2765-2774.

Leete, E., 1982. A One-Step Synthesis of Ficine and Isoficine. J Nat Prod 45, 605-607.

Li, N., Shao, L., Zhang, C.F., Zhang, M., 2008. Two new flavonoid alkaloids from Senecio argunensis. Journal of Asian natural products research 10, 1143-1146.

Liang, Y.-C., Huang, Y.-T., Tsai, S.-H., Lin-Shiau, S.-Y., Chen, C.-F., Lin, J.-K., 1999. Suppression of inducible cyclooxygenase and inducible nitric oxide synthase by apigenin and related flavonoids in mouse macrophages. Carcinogenesis 20, 1945-1952.

Lin, H.H., Chan, K.C., Sheu, J.Y., Hsuan, S.W., Wang, C.J., Chen, J.H., 2012. *Hibiscus sabdariffa* leaf induces apoptosis of human prostate cancer cells in vitro and in vivo. Food Chem 132, 880-891.

Lin, H.H., Chen, J.H., Kuo, W.H., Wang, C.J., 2007. Chemopreventive properties of *Hibiscus sabdariffa* L. on human gastric carcinoma cells through apoptosis induction and JNK/p38 MAPK signaling activation. Chem-Biol Interact 165, 59-75.

Luque, I., Gélinas, C., 1997. Rel/NF-κB and IκB factors in oncogenesis, Seminars in cancer biology. Elsevier, pp. 103-111.

MacMicking, J., Xie, Q.-w., Nathan, C., 1997. Nitric oxide and macrophage function. Annual review of immunology 15, 323-350.

Mahadevan, N., Shivali, K.P., Kamboj, P., 2009. Hibiscus sabdariffa Linn.-an overview. Natural product radiance 8, 77-83.

Masterova, I., Uhrin, D., Tomko, J., 1987. Lilaline - a Flavonoid Alkaloid from Lilium-Candidum. Phytochemistry 26, 1844-1845.

Mohana Kumara, P., Zuehlke, S., Priti, V., Ramesha, B.T., Shweta, S., Ravikanth, G., Vasudeva, R., Santhoshkumar, T.R., Spiteller, M., Uma Shaanker, R., 2012. Fusarium proliferatum, an endophytic fungus from *Dysoxylum binectariferum* Hook.f, produces rohitukine, a chromane alkaloid possessing anti-cancer activity. Antonie van Leeuwenhoek 101, 323-329.

Muhammad, S.A., A N, 2005. The Important Food Crops and Medicinal Plants of North-western Nigeria. Research Journal of Agriculture and Biological Sciences 1, 254-260.

Mulaudzi, R.B., Ndhlala, A.R., Kulkarni, M.G., Finnie, J.F., Van Staden, J., 2011. Antimicrobial properties and phenolic contents of medicinal plants used by the Venda people for conditions related to venereal diseases. J Ethnopharmacol 135, 330-337.

Müller, C.W., Harrison, S.C., 1995. The structure of the NF-κB p50:DNA-complex a starting point for analyzing the Rel family. FEBS letters 369, 113-117.

Nagai, T., Moriguchi, R., Suzuki, Y., Tomimori, T., Yamada, H., 1995. Mode of action of the anti-influenza virus activity of plant flavonoid, 5, 7, 4′-trihydroxy-8-methoxyflavone, from the roots of *Scutellaria baicalensis*. Antiviral research 26, 11-25.

Nair, J.J., Mulaudzi, R.B., Chukwujekwu, J.C., Van Heerden, F.R., Van Staden, J., 2013. Antigonococcal activity of *Ximenia caffra* Sond. (Olacaceae) and identification of the active principle. S Afr J Bot 86, 111-115.

Nijveldt, R.J., van Nood, E., van Hoorn, D.E., Boelens, P.G., van Norren, K., van Leeuwen, P.A., 2001. Flavonoids: a review of probable mechanisms of action and potential applications. The American journal of clinical nutrition 74, 418-425.

Ochani, P.C., D'Mello, P., 2009. Antioxidant and antihyperlipidemic activity of *Hibiscus sabdariffa* Linn. leaves and calyces extracts in rats. Indian journal of experimental biology 47, 276.

Olajide, O.A., Makinde, J.M., Okpako, D.T., 2003. Evaluation of the anti-inflammatory property of the extract of *Combretum micranthum* G. Don (Combretaceae). Inflammopharmacology 11, 293-298.

Onyenekwe, P.C., Ajani, E.O., Ameh, D.A., Gamaniel, K.S., 1999. Antihypertensive effect of roselle (*Hibiscus sabdariffa*) calyx infusion in spontaneously hypertensive rats and a comparison of its toxicity with that in Wistar rats. Cell Biochemistry and Function 17, 199-206.

Orwa, C., Mutua, A., Kindt, R., Jamnadass, R., Simons, A., 2012. Agroforestree database: a tree reference and selection guide version 4.0. 2009.

Pan, M.H., Lai, C.S., Ho, C.T., 2010. Anti-inflammatory activity of natural dietary flavonoids. Food & function 1, 15-31.

Raso, G.M., Meli, R., Di Carlo, G., Pacilio, M., Di Carlo, R., 2001. Inhibition of inducible nitric oxide synthase and cyclooxygenase-2 expression by flavonoids in macrophage J774A. 1. Life Sci 68, 921-931.

Read, M.A., 1995. Flavonoids: naturally occurring anti-inflammatory agents. The American journal of pathology 147, 235-237.

Ren, D.M., Guo, H.F., Yu, W.T., Wang, S.Q., Ji, M., Lou, H.X., 2008. Stereochemistry of flavonoidal alkaloids from Dracocephalum rupestre. Phytochemistry 69, 1425-1433.

Robak, J., Gryglewski, R., 1995. Bioactivity of flavonoids. Polish journal of pharmacology 48, 555-564.

Ross, I., 2003. Hibiscus sabdariffa, Medicinal Plants of the World. Humana Press, pp. 267-275.

Sacandé, M., Sanon, M., Schmidt, L., 2007. *Combretum micranthum* G. Don. Seed Leaflet.

Sadowska-Krowicka, H., Mannick, E.E., Oliver, P.D., Sandoval, M., Zhang, X.J., Eloby-Childess, S., Clark, D.A., Miller, M.J., 1998. Genistein and gut inflammation: role of nitric oxide. Proceedings of the Society for Experimental Biology and Medicine. Society for Experimental Biology and Medicine 217, 351-357.

Saw, C.L.L., Guo, Y., Yang, A.Y., Paredes-Gonzalez, X., Ramirez, C., Pung, D., Kong, A.-N.T., 2014. The berry constituents quercetin, kaempferol, and pterostilbene synergistically attenuate reactive oxygen species: Involvement of the Nrf2-ARE signaling pathway. Food and Chemical Toxicology 72, 303-311.

Scalbert, A., Johnson, I.T., Saltmarsh, M., 2005. Polyphenols: antioxidants and beyond. The American journal of clinical nutrition 81, 215S-217S.

Serhan, C.N., Ward, P.A., Gilroy, D.W., 2010. Fundamentals of inflammation. Cambridge University Press.

Shirley, B.W., 1996. Flavonoid biosynthesis: 'New' functions for an 'old' pathway. Trends Plant Sci 1, 377-382.

Simon, J.E., Wu, Q. and Welch, C., 2014. Peperidine-flavan alkaloid compounds derived from African herb tea kinkeliba as anti-diabetic agents. U.S. Patent 8,642,769.

So, A., De Smedt, T., Revaz, S., Tschopp, J., 2007. A pilot study of IL-1 inhibition by anakinra in acute gout. Arthritis Research and Therapy 9, R28.

Soliman, K.F., Mazzio, E.A., 1998. In vitro attenuation of nitric oxide production in C6 astrocyte cell culture by various dietary compounds. Proceedings of the Society for Experimental Biology and Medicine. Society for Experimental Biology and Medicine 218, 390-397.

Surh, Y.-J., Chun, K.-S., Cha, H.-H., Han, S.S., Keum, Y.-S., Park, K.-K., Lee, S.S., 2001. Molecular mechanisms underlying chemopreventive activities of anti-inflammatory phytochemicals: down-regulation of COX-2 and iNOS through suppression of NF-κB activation. Mutation Research/Fundamental and Molecular Mechanisms of Mutagenesis 480, 243-268.

Szoke, É., Lemberkovics, É., Kursinszki, L., 2013. Alkaloids derived from lysine: piperidine alkaloids, Natural Products. Springer, pp. 303-341.

Takagi, M., Funahashi, S., Ohta, K., Nakabayashi, T., 1980. Phyllospadine, a New Flavonoidal Alkaloid from the Sea-Grass *Phyllosphadix-Iwatensis*. Agr Biol Chem Tokyo 44, 3019-3020.

Tan, A.R., Swain, S.M., 2002. Review of flavopiridol, a cyclin-dependent kinase inhibitor, as breast cancer therapy. Semin Oncol 29, 77-85.

Tanaka, T., Watarumi, S., Fujieda, M., Kouno, I., 2005. New black tea polyphenol having N-ethyl-2-pyrrolidinone moiety derived from tea amino acid theanine: isolation, characterization and partial synthesis. Food Chem 93, 81-87.

Tilley, S.L., Coffman, T.M., Koller, B.H., 2001. Mixed messages: modulation of inflammation and immune responses by prostaglandins and thromboxanes. Journal of Clinical Investigation 108, 15.

Udoh, I., Nworu, C., Eleazar, C., Onyemelukwe, F., Esimone, C., 2012. Antibacterial profile of extracts of *Combretum micranthum* G. Don against resistant and sensitive nosocomial isolates.

Van Wyk, B.E., 2011. The potential of South African plants in the development of new food and beverage products. S Afr J Bot 77, 857-868.

Vauzour, D., Rodriguez-Mateos, A., Corona, G., Oruna-Concha, M.J., Spencer, J.P.E., 2010. Polyphenols and Human Health: Prevention of Disease and Mechanisms of Action. Nutrients 2, 1106-1131.

Villani, T., Juliani, R., Simon, E.J., Wu, Q.L., 2013. *Hibiscus sabdariffa*: Phytochemistry, Quality Control, and Health Properties. ACS Symposium Series 1127, 209–230.

Welch, C.R., 2010. Chemistry and pharmacology of Kinkéliba (*Combretum micranthum*), a west African medicinal plant. Rutgers, The State University of New Jersey.

Winkel-Shirley, B., 2001. Flavonoid biosynthesis. A colorful model for genetics, biochemistry, cell biology, and biotechnology. Plant Physiol 126, 485-493.

Winkel-Shirley, B., 2002. Biosynthesis of flavonoids and effects of stress. Curr Opin Plant Biol 5, 218-223.

Xia, E.Q., Deng, G.F., Guo, Y.J., Li, H.B., 2010. Biological Activities of Polyphenols from Grapes. Int J Mol Sci 11, 622-646.

Yao, H., Xu, W.Z., Shi, X.L., Zhang, Z., 2011. Dietary Flavonoids as Cancer Prevention Agents. J Environ Sci Heal C 29, 1-31.

Zhang, J., Gao, G., Chen, L., Li, J., Deng, X., Zhao, Q.S., Huang, C., 2014. Hydrogen peroxide/ATR-Chk2 activation mediates p53 protein stabilization and anti-cancer activity of cheliensisin A in human cancer cells. Oncotarget 5, 841-852.

CHAPTER TWO

Phytochemical Analysis and Anti-Inflammatory Activity of the Extracts of the African Medicinal Plant *Ximenia caffra*

2.1 Introduction

Ximenia caffra, also known as "large sourplum" or just ximenia, is a member of a genus of flowering plants in the Olacaceae family, which is indigenous to the southern African region (Ben-Erik Van Wyk, 2000; Cheikhyoussef et al., 2011). Ximenia has been used in foods and traditional medicine. Its fruit, considered to be rich in vitamin C, potassium, and protein, has been commonly added into porridges and made into jam (Ndhlala et al., 2008; Van Wyk, 2011). The dried seed of *X. caffra* contains a substantial quantity of unsaturated fatty acids; the most abundant is oleic acid (Khumalo et al., 2002). As such, the extracted seed oil would be used as a feed ingredient and domestic biofuel (Chivandi et al., 2012). As a traditional medicine, local herbalists have been using the leaves and root of *X. caffra* for treatment of wounds, infections, fever, infertility and diarrhea (De Wet et al., 2012; Mulaudzi et al., 2011; Nair et al., 2013). Recent modern research confirmed that the leaf and root extracts of *X. caffra* have antigonococcal, antibacterial and antifungal activities, which corroborate very well with its traditional use (Fabry et al., 1998; Mulaudzi et al., 2011; Nair et al., 2013; Tafadzwa Munodawafaa, 2013). Compared with the research that has been undertaken on the fruits for its nutritional and/or

pharmacological activities, only one paper has been published on the phytochemical composition analysis of *X. caffra* leaf, in which the total flavonoid content was only roughly estimated using a vanillin assay (Mulaudzi et al., 2011). Bioactive phytochemicals contained in the leaf of related species *X. americana*, from western and eastern sub-Sahara Africa were investigated and led to the identification of sambunigrin, gallic acid, and quercetin and the glycosides by spectrometric methods (Le et al., 2012).

Most of the studies with Ximenia focus on the fruit and seed, as these represent the products of current commerce and traditional use, rather than the leaf. In this study, we purposefully investigated the phytochemical profile of the leaf, which had not been previously examined using LC/UV/MS. Interestingly, though not unexpectedly, a number of polyphenol compounds were discovered in the leaf. Polyphenols are a class of compounds characterized by the presence of large multiples of phenol structural units, and abundantly exist in food products, including crops, fruit, vegetables, tea, and wine (Erlund, 2004; Vauzour et al., 2010; Xia et al., 2010). These compounds have shown a wide range of biological activities including anti-inflammation, the prevention of cancer and cardiovascular diseases (Hamalainen et al., 2007; Scalbert et al., 2005).

Based upon the chemical profile determined and to further explore new applications for the leaves while extending the traditional uses, we investigated the leaves for their antioxidant activity, total phenolic content, and anti-proliferation activity using the Folin Ciocalteu assay, ABTS radical scavenging assay, and the MTS cell proliferation assay,

respectively. Additionally, the effects of extracts on the mRNA expression of pro-inflammatory genes were assessed by RT-qPCR through the quantification of inducible nitric oxide synthetase (iNOS), interleukin-6 (iL-6), and tumor necrosis factor α (TNF-α) induced by lipopolysaccharide (LPS) in murine RAW 264.7 macrophage cells. Interleukin 6 (iL-6), a cytokine secreted by T cells and macrophages, is produced at the inflammation sites during infection and tissue damage. iL-6 has stimulatory effects on immune cells and can induce chronic inflammatory responses. Thus, targeting iL-6 would help prevent or treat rheumatoid arthritis and other chronic inflammatory diseases (Gabay, 2006). iNOS is one of the key enzymes generating nitric oxide (NO), which regulates a number of pathophysiological conditions including infection, inflammation, and neoplastic diseases. Reagents that can inhibit iNOS would reduce the generation of NO and have potential anti-inflammatory effects (Hamalainen et al., 2007). Anther biomarker TNF-α, an adipokine, is involved in series of inflammation reactions during immune response. Its antagonists have also shown effects in the treatment of a range of inflammatory diseases, including rheumatoid arthritis, psoriasis, and ankylosing spondylitis (Bradley, 2008).

To further explore the mechanism of anti-proliferation and anti-inflammatory activities, extracts of *X. caffra* were evaluated in cells for suppression of NF-κB (nuclear factor kappa-light-chain-enhancer of activated B cells), a protein complex that regulates the transcription of DNA and is involved in cellular responses to stress. The activation of NF-κB is generally considered to up-regulate a range of genes encoding growth factors, cytokines, apoptosis, and immunomodulatory molecules. As a shared key signal pathway

of proliferation and inflammation in cells, the pro-longed activation of NF-κB has been reported to be involved in inflammatory conditions, autoimmune disease, and cancer (Dabek et al., 2010; Dutta et al., 2006; Gilmore, 2006; Tak and Firestein, 2001; Wang et al., 2014). The results demonstrate that the underlying therapeutic mechanism involves the suppression of NF-κB, a shared pathway between cell death and inflammation.

2.2 Materials and Methods

2.2.1 Plant Materials

Standard compounds, gallic acid, rutin, catechin, quercetin, kaempferol and ABTS (2,2'-azino-bis (3-ethylbenzthiazoline-6-sulfonic acid)) reagent were purchased from Sigma Aldrich (St.Louis, MO). HPLC-grade methanol (MeOH), acetonitrile (ACN) and formic acid were purchased from Fisher Scientific Co (Fair Lawn, NJ). Folin Ciocalteu's Phenol Reagent was purchased from MP Biomedicals (Solon, OH). The plant samples of *X. caffra* leaves were field collected from Northeastern Namibia using a research permit from the Ministry of Environment and Tourism, Namibia and in concert with the University of Namibia and the National Botanical Research Institute (NBRI). Voucher specimens were prepared during field collection and sent to the NBRI where the collected plants were taxonomically authenticated. The voucher specimens were also deposited in both the National Botanical Research Institute, Windhoek, Namibia and the Chrysler Herbarium & Mycological Collection, Biological Sciences Building, Rutgers University, New Brunswick, NJ. For chemical screening, the leaves were manually harvested using NBRI guidelines and were air dried under ambient temperature for two weeks, then

packaged for later experimental analysis. The dried leaf materials were air shipped to Rutgers University where each was ground into a fine powder with a laboratory mill (Perten 3100) and stored at room temperature in the dark.

2.2.2 Analytical Equipment and Methods

Separation on HPLC was performed using column Prodigy ODS3 5μm, 150 × 3.2 mm, 5 micro (Phenomenex Inc. Torrace, CA). The separation, identification and quantification were performed on Hewlett-Packard Agilent 1100 series HPLC-MS (Agilent Technologies, Waldbronn, Germany) equipped with a quaternary pump system, a degasser, an autosampler, a DAD detector, an MSD trap with an electrospray ion source (ESI), and software HP ChemStation, Data Analysis 4.2.

HPLC separation was performed with mobile phase of solvent A and B in gradient, where A was 0.1% formic acid (v/v) in water and B was 0.1% formic acid (v/v) in acetonitrile. The gradient starts from 5% B to 30% B in 50 min. The detection wavelength was set at 280 nm for gallic acid and catechin, 370 nm for quercetin, and kaempferol derivatives. The flow rate is 1.0 ml/min. The electrospray was conducted in negative and positive modes in two separated runs. The optimized collision energy is of 80 %, scanning from *m/z* 100 to 700. ESI was conducted at voltage of 3.5 kV for positive model and -3.5 kV for negative model. High-purity liquid nitrogen 99.999% was used as dry gas and nebulizer at a flow rate of 12 L/min, and the capillary temperature was 350℃. Nitrogen was used as nebulizer at 60 psi and helium as collision gas. The ESI interface and mass spectrometer

parameters were optimized to obtain maximum sensitivity.

2.2.3 Sample Preparation

For quantitative and qualitative studies, ~ 500 mg of the finely ground plant leaves were extracted using 10 ml 70% methanol in water with 0.1% acetic acid and sonicated for 10 min. Then, the extract was conditioned at room temperature overnight and later filtered through a 0.45 μm filter. 10 μl of the extract was injected for both qualitative and quantitative analysis. The extraction procedure was adopted from our prior studies (Wu et al., 2003). For total phenolic assay, *in vitro* antioxidant assay: around 20 mg of each plant sample was extracted using 10 ml 70% Methanol/Water (0.1% acetic acid) followed by sonication for 10 min, and then conditioned at room temperature for overnight. The extract was filtered through a 0.45μm nylon filter. For cell-based bioactivity assays, the leaf extract above was dried on rotavapor and lyophilizer to powder and subsequently dissolved in DMSO to different concentrations.

Individual stock solution (~1.0 mg/ml) of the standard compound was prepared by dissolving ~10.0 mg of each compound in 10 ml methanol. The stock solution was diluted with methanol to obtain working solutions ranging from 3.91 to 500 μg /ml. Calibration curve was built upon each group of the working solutions. In each standard curve, six or more concentration levels were used for calibration on HPLC. The concentration of quercetin ($y = 0.052x - 0.8257$, $R^2 = 0.9999$) and kaempferol ($y = 0.0383x - 1.7818$, $R^2 = 0.9999$) ranges from 3.91 to 500 μg /ml. For gallic acid ($y = 0.0373x - 12.437$, $R^2 = 0.9999$)

and catechin ($y = 0.1516x - 3.5055$, $R^2 = 0.9999$), the concentration ranges from 31.25 to 500 µg /ml. All calibrations curves had good linearity.

2.2.4 Cell Culture and Treatment

The murine RAW 264.7 macrophage cell, a widely used model for inflammatory studies were obtained from the American Type Culture Collection (ATCC). PC-3/N cell, a stable clone transfected with an NF-κB luciferase construct were established and obtained from Dr. Xi Zheng's laboratory as previously described (Zhou et al., 2014). The RAW cell and PC-3/N cell were routinely cultured in Dulbecco's Modified Eagle's Medium (DMEM, Invitrogen, Carlsbad, CA, USA) supplemented with 10% fetal bovine serum (FBS, Invitrogen, Carlsbad, CA, USA), 100U/ml penicillin and streptomycin in a humidified incubator with 5% CO_2 at 37°C.

2.2.5 Folin-Ciocalteu Assay

Total phenolic content was measured on UV-Vis spectrophotometer according to the Folin-Ciocalteu's method (Singleton, 1985). 40 µl of the extract was mixed with 900 µl Folin Ciocalteu's reagent followed by incubation at room temperature for 5 min. After that 400 µl of 15% sodium carbonate was added and the mixture stayed at r.t for 45 min. Then the UV absorption at wavelength of 752 nm was measured against a blank solution. The standard curve was measured based on the prepared gallic acid standard solution (1.0, 0.5, 0.25, 0.125, 0.0625 mg/ml) and the result was transformed as milligrams of gallic acid per

gram of sample ± SD (GAE ± SD).

2.2.6 ABTS Scavenging Assay

The total antioxidant capacity of leaf extract was measured according to the decolorization of the ABTS radical cation as percentage of inhibition. ~38.4 mg of ABTS and 6.6 mg potassium persulfate ($K_2S_2O_8$) were co-dissolved in 10 ml of water and reacted for 16 hours in dark environment to form stable radicals. The ABTS working solution was prepared by dissolving ABTS radicalized solution in ethanol to an absorbance of 0.700 ± 0.20 at λ = 734 nm. The wavelength selected is corresponding to the highest extinction coefficient ($\varepsilon = 1.7 \times 10^4$ $mol^{-1}L$ cm^{-1} in ethanol). 990 µl of the diluted ABTS radical solution was mixed with 10 µl of the sample extract followed by reaction for 20 minutes at room temperature. The decoloration of the solution indicates that ABTS radical cations were reduced by the antioxidants in the sample and was determined by the measurement of the decrease of absorbance at 734 nm against a blank solution of ethanol at 25°C. The percentage decrease of absorbance at 734 nm has a linear relationship with the amount of antioxidant compounds in the extract and can be calculated using the following equation:

$$\text{Percentage inhibition (\%)} = [1- (\text{Absorbance}_{\text{sample}})/(\text{Absorbance}_{\text{control}})] \times 100.$$

Standard solution of Trolox was prepared in ethanol. The linear relationship was buildup between decreased absorbance percentage and Trolox concentration (r^2 = 0.99). All samples are prepared in triplicate and the result was expressed as mmol of Trolox Equivalent per gram of sample ± SD (TE ± SD).

2.2.7 Anti-proliferation Assay

The anti-proliferative effect of *X. caffra* leaves extract was tested in RAW cells using the MTS assay. MTS assay, usually called "one step" MTT assay, is used for assessing cell viability. NAD(P)H-dependent cellular oxidoreductase enzymes from live cells can reduce MTS reagent and form a formazan product with maximum absorption at 490-500 nm. The RAW cells were seeded in a 96-well tissue culture plate at an initial density of 10,000 cells/ml. After 24 hr, the cells were treated with various concentration of *X. caffra* leaf extract in DMSO for another 24 hr. The MTS assay was then performed using the CellTiter 96 aqueous nonradioactive cell proliferation assay kit [MTS: 3-(4,5-dimethylthiazol-2-yl)-5-(3-carboxymethoxyphenyl)-2-(4-sulfophenyl)-2H-tetrazolium, inner salt] (Promega, Madison, WI, USA) as previously described (Saw et al., 2014; Wang et al., 2014). The absorbance of the formazan product was measured at 490 nm using a μQuant Biomolecular Spectrophotometer (Bio-Tek Instruments, Inc., Winooski, VT, USA). The cell viability (%) was expressed as follows: (optical density of sample) / (optical density of DMSO) x 100%.

2.2.8 Quantitative Real-Time Polymerase Chain Reaction (qPCR)

The RAW cells were seeded in 6-well tissue culture plates at the density of 10,000 cells/ml. After 24 hours, the cells were treated with LPS (1 μg/ml, Sigma, St. Louis, MO, USA) alone or co-treated with the leaf extract (78.13-312.5 μg/ml) dissolved in DMSO. Then RAW cells were harvested 24 hours after each treatment. Briefly, the cell culture medium was removed and the cells were washed twice with ice-cold phosphate-buffered

saline (1X PBS, pH = 7.4) to remove the dead cells. Then RNA lysis buffer was added to each well and the total RNA of the rest live cells was isolated and purified using a RNeasy Mini Kit (Qiagen, Valencia, CA, USA) according to the manufacturer's manual. RNA concentration was quantified using Nanodrop (Thermo Scientific, Wilmington, DE, USA). Volume of 1 μg RNA was calculated for each sample and added to PCR tubes to synthesize cDNA using the TaqMan Reverse Transcription Reagents (Applied Biosystems, Foster City, CA, USA). The gene expression of iL-6, iNOS, and TNF-α was quantitated by qPCR performed on an Applied Biosystems 7900HT Fast Real-Time PCR System (Applied Biosystems, Foster City, CA, USA) with SYBR Green PCR Master Mix using synthesized cDNA as template. Glyceraldehyde 3-phosphate dehydrogenase (Gapdh) was used as endogenous reference gene. The primer sequences were described previously (Lee et al., 2014). The relative fold change of gene expression of iL-6, iNOS, and TNF-α was calculated by comparative CT method ($2^{-\Delta\Delta CT}$) with the following equation:

$$\Delta\Delta Ct = \Delta Ct\ (sample) - \Delta Ct\ (reference)$$

ΔΔCt value describes the differences between the average ΔCt value of the sample of interest (e.g., extract treated cells) and the average ΔCt value of a reference sample (e.g., extract untreated cells). In this equation, ΔCt (sample) is the CT value for any treatment normalized to the CT value of endogenous reference gene Gapdh. ΔCt (reference) is the CT value for blank DMSO treatment normalized to the CT value of endogenous reference gene Gapdh. The use of an endogenous reference gene corrects the variation in RNA content, variation in reverse transcription efficiency, possible RNA degradation, variation in nucleic acid recovery and differences in sample handling.

2.2.9 Luciferase Assay of NF-κB-dependent Reporter Gene Activity

The PC-3/N cells were seeded in 12-well tissue culture plates at an initial density of 10,000 cells/ml. After 24 hours, the cells were treated with the leaf extract (78.13-312.5 μg/ml) dissolved in DMSO. Then cells were harvested 24 hours after each treatment. The luciferase activity was measured using a luciferase reporter assay system (Promega, Madison, WI, USA) according to the manufacturer's manual. Briefly, the treated PC-3/N cells were washed twice with ice-cold 1X PBS (pH 7.4) and harvested in 1X reporter lysis buffer. After centrifugation at 12,000 rpm for 5 min at 4 °C, a 10 μl aliquot of the supernatants were mixed with 50 μl of luciferase assay substrate and the mixture was assayed for luciferase activity using a SIRIUS luminometer (Berthold Detection System GmbH, Pforzheim, Germany). Considering different amount of cells in each well, the measured luciferase activity was normalized to total protein concentration of each sample, which is measured by BCA protein assay (Pierce, Rockford, IL, USA). The NF-κB luciferase activity was finally expressed as percent of the control. This PC-3/N cells were stable transfected with NF-κB luciferase reporter gene, once NF-κB is activated, it will initiate the expression of reporter gene and start the synthesis of the protein luciferase, which could be measured by luminometer. The luciferase activity was further normalized by the total protein amount in the live cells from each treatment, so the toxicity won't affect the relative quantitation.

2.3 Results and Discussion

2.3.1 Identification of Phytochemical Constituents

Identification of each compound was mainly based on the mass spectrometric data, UV-Vis spectrum, and comparison with authentic standards. Each compound was analyzed on mass spectrometry under both negative and positive modes. The UV and MS chromatograms are illustrated in Figure 11. The identity, retention time, molecular ions, fragment ions and maximum UV absorption wavelength for each identity are summarized in Table 2.

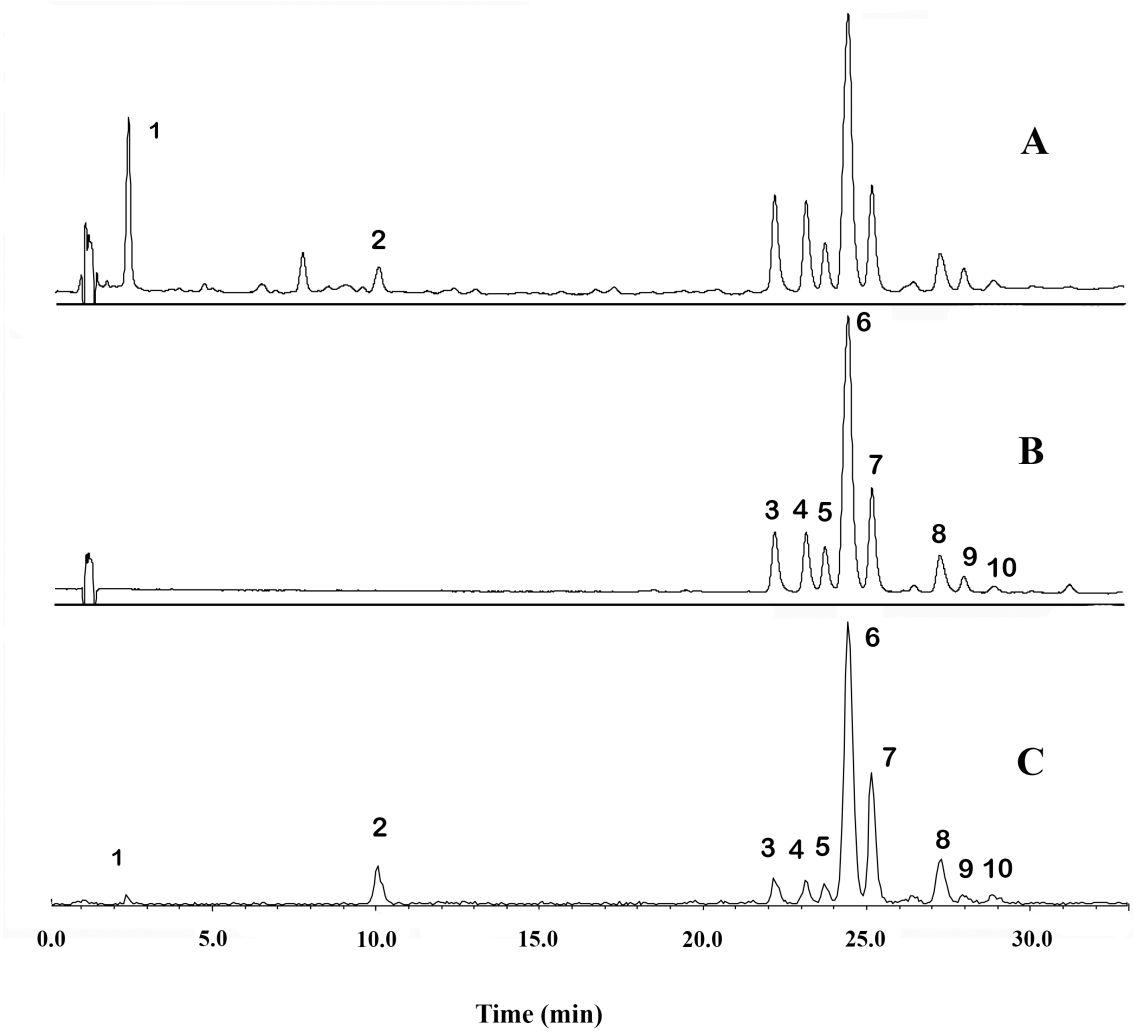

Figure 11. Chromatograms of *Ximenia caffra* leaf extract. (A) UV Chromatogram at 280 nm; (B) UV chromatogram at 370 nm; (C) Processed MS chromatogram

The major compounds (3-10) detected in *X. caffra* leaf are flavonol glycosides. Compounds 3-10 were identified as glycosylated derivatives of quercetin and kaempferol based on their characteristic aglycone fragment ions (*m/z*= 303, *m/z*=287 under positive ionization). The main glycosides attached are galactoside/glucoside, xyloside and rutinoside. The UV-Vis absorption of these identified compounds have a

maximum absorption at ~ 356 nm, which is consistent with previous reports (B. Ducrey, 1995). The structure of each derivative was identified based on the molecular and fragment ions. For example, MS spectrum of compound **6** (t_R 24.3 min) indicates that it has molecular ions at *m/z* 611 ($[M+H]^+$), *m/z* 609 ($[M-H]^-$) and is fragmented to *m/z* 465 $[M–rhamnosyl+H]^+$ and *m/z* 303 ($[M–rhamnosyl–glucosyl+H]^+$), which corresponds to quercertin-rutinoside, and the identity was further confirmed with commercially available authentic standard. The same identification was applied to the derivatives of galloylglucoside/galloylgalactoside. For example compound **3/4** (t_R 22.1 min or t_R 23.1 min), has a molecular ion at *m/z* 617 ($[M+H]^+$), and is further fragmented to *m/z* 465 ($[M-galloyl+H]^+$), and *m/z* 303 ($[M-galloylglucoside+H]^+$ or $[M-galloylgalactoside+H]^+$). The MS spectra of the flavonol glycosides under positive ion mode are illustrated in Figure 12 and the structures of representative compounds are shown in Figure 13.

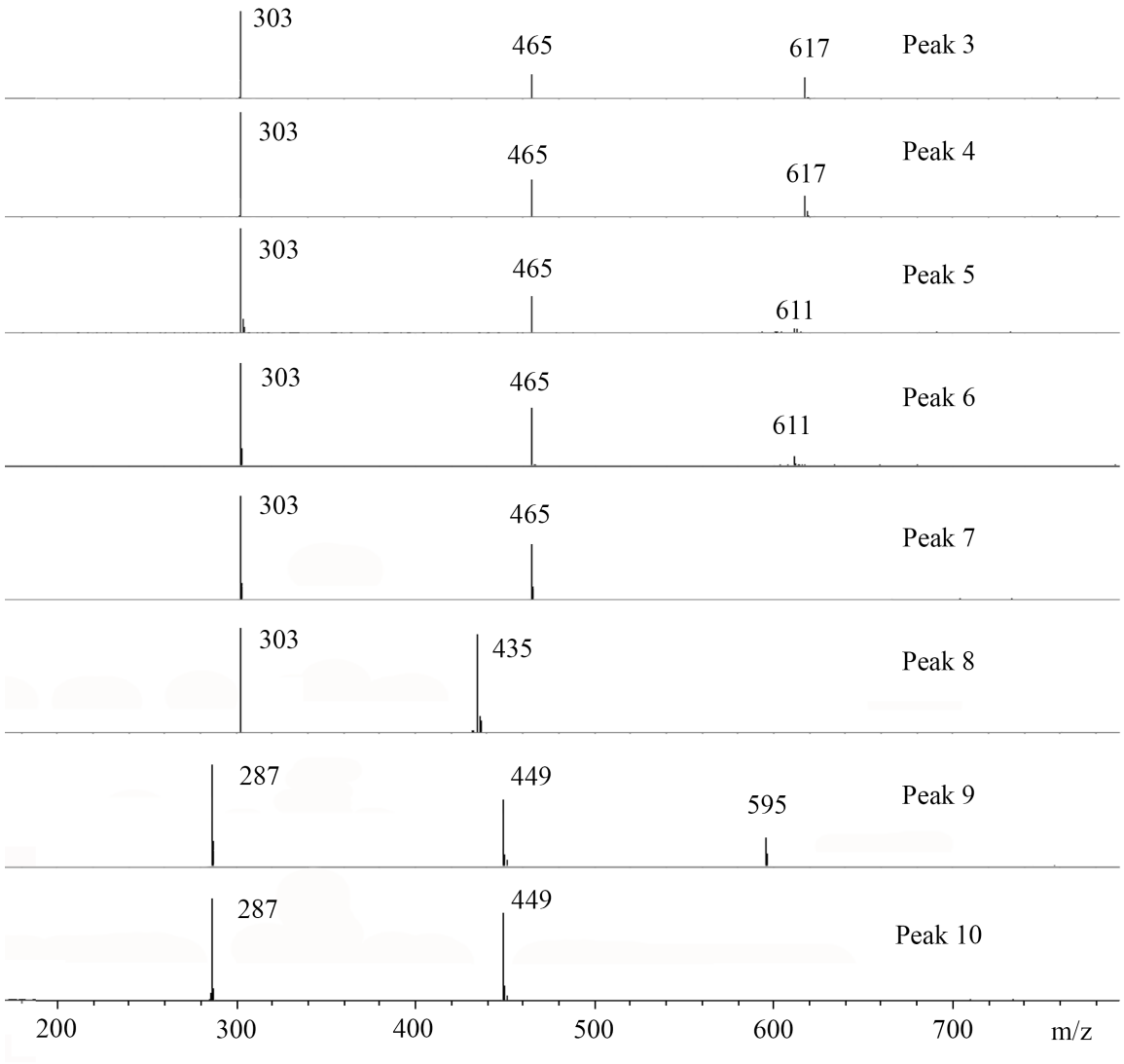

Figure 12. The mass spectra of flavonol glycosides (peak 3 to peak 10) under positive ion mode

Some components give the same MS, UV-Vis spectrum, such as compound 3/4 and 5/6. Compound 3 and 4 may have different glycosides (galactoside or glucoside) attached, or same glycosides but at different positions. Compound 6 can be

differentiated from 5 based on comparison with commercial available standard and determined as quercetin-3-O-rutinoside.

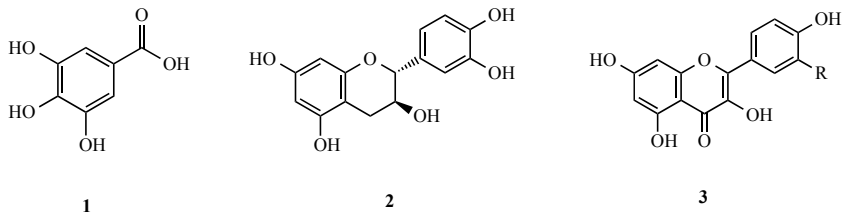

Figure 13. Representative structures of identified polyphenols. (1) Gallic acid; (2) Catechin; (3) The aglycone of compound 3-10: quercertin (R=OH) and kaempferol (R=H). Sugar moieties are usually attached at position 3

Other polyphenol compounds including gallic acid and catechin were also determined. Their detection under negative mode yields better sensitivity. Gallic acid has a molecular ion at *m/z* 169 ($[M-H]^-$), and a fragment ion at *m/z* 125 ($[M-CO_2-H]^-$). Catechin has a molecular ion at *m/z* 289 ($[M-H]^-$). Both have characteristic maximum absorption at ~ 280 nm. To further confirm the identities of gallic acid and catechin, each sample was co-injected with respective authentic standard.

2.3.2 Quantification of each Phytochemical

The leaves of *X. caffra* were found to contain copious amounts of different flavonol glycosides and other polyphenol compounds. The content of flavonol glycoside products

were quantified at UV wavelength of 370 nm. To approximate the content of compounds without commercially available standards, the response factor was used and adjusted by the ratio of the molecular weight to that of the aglycone (Dubber and Kanfer, 2004). Gallic acid and catechin were quantified at 280 nm. The content of each individual polyphenol is included in Table 2. The total amount of polyphenols measured by HPLC is 19.46 mg/g, 81% of which is contributed by quercetin and its derivatives (15.64 mg/g), while kaempferol derivatives represent only 5% of the total amount. The most abundant single compound was rutin (9.08 mg/g), accounting for 47% of the total polyphenol composition. Phenolic acid, gallic acid, is 0.95 mg/g, representing 5% of the total polyphenol amount. The flavanol catechin (1.77 mg/g) contributed to the last 9% of the total composition.

Table 2. Phytochemicals identified from leaf extracts of *Ximenia caffra.*

Peak	Retention time (min)	UV-Vis λ_{max}(nm)	Molecular and fragment ions		Compound Name	Content (mg/g)
			Negative Ions	Positive Ions		
1	2.4	278	125,169	-	Gallic acid*	0.96
2	10.0	280	289	291	Catechin*	1.77
3	22.1	356	615	303,465,617	Quercetin-G-Gall	1.70
4	23.1	358	615	303,465,617	Quercetin-G-Gall	1.59
5	23.6	357	609	303, 465, 611	Quercetin-G-Rha	1.12
6	24.3	357	463, 609	303, 465,611	Quercetin-Glc-Rha (Rutin)*	9.08
7	25.1	356	463	303, 465	Quercetin-G	2.03
8	27.2	356	433	303, 435	Quercetin-Xyl	0.11
9	27.9	356	593	287, 449, 595	Kaempferol-G-Rha	0.82
10	28.9	356	447	287, 449	Kaempferol-G	0.26

Abbreviations: G: glucosyl/galactosyl; Glc: glucosyl; Gla: galactosyl; Rha: rhamnosyl; Gall: galloyl; Xyl: xylosyl; “ * ” indicates that compounds were confirmed through the comparison with authentic standards.

2.3.3 Total Phenolics and *In Vitro* Antioxidant Capacities

The content of phenolics in the sample is expressed as mg of gallic acid equivalents (GAE) per gram of ground powder. The total content of phenolics determined by Folin-Ciocalteu assay in the leaf is 261.87 ± 7.11 mg GAE /g, suggesting its potent antioxidant activity. While not directly compared at the same time, in a comparative manner, the total phenolics observed is higher than functional tea green tea (165 mg GAE/g) and black tea (124 mg GAE/g), even if it is not used as tea product (Lee, K. W, et al, 2003). While recognizing that there would be an expected wide range across all green and black teas, this data indicates that comparatively *X. caffra* can be considered a rich source of total phenols. The antioxidant capacity of the samples is indicated using mmol of Trolox equivalents per gram of ground plant material. The total antioxidant capacity of the leaf extract determined by ABTS radical cation was 1.46 ± 0.01 mmol TEAC/g. The measured values are slightly below green tea (1.77 ± 0.32 mmol TEAC/g) and black tea (1.33 ± 0.21 mmol TEAC/g), yet show potent anti-oxidant activity (Rusaczonek, A, et al, 2010). As polyphenol compounds are known to reduce radicals *in vitro* and *in vivo*, it is highly possible this activity is due to its content of flavonoids described above.

2.3.4 Anti-proliferation Activity

The MTS assay was applied to investigate the effect of *X. caffra* leaf extract on the growth of cultured RAW 264.7 cells. As illustrated in Figure 14, after 24 hours treatment with leaf extract, the cell viability of RAW cells decreased dose-dependently. When the concentration of raw leaf extract is 312.5 μg/ml, the viability of the RAW cell is 46.83 ±

3.46%. The IC_{50} value of the raw leaf extract was determined to be 239.0 ± 44.5 μg/ml. This data implies that the leaf extract inhibits the growth of RAW cell, potential possessing a cytotoxic effect.

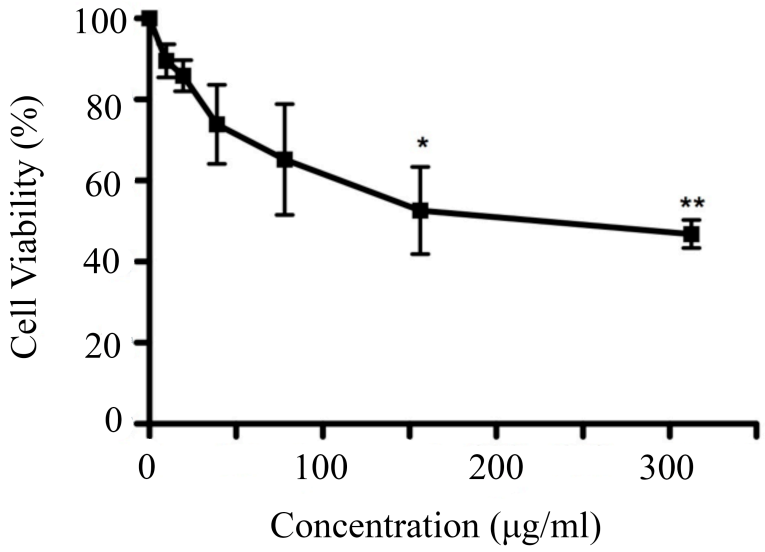

Figure 14. Cell viability vs the concentrations of leaf extract measured by MTS assay

2.3.5 Anti-inflammatory Activity

To evaluate the effect of *X. caffra* leaf extract on the LPS-stimulated expression of inflammatory enzymes and pro-inflammatory cytokines, the mRNA expression of inflammatory markers iL-6, iNOS, and TNF-α were measured by qPCR. Treatment of cells with leaf extract at a variety of concentrations demonstrated a dose-dependent response on the expression of iL-6, iNOS, and TNF-α, as shown in Figure 15. The strongest response was seen for iL-6, (Figure 15A) wherein treatment at 312.5 μg/mL induced a nearly 10-fold decrease in expression vs. background expression, and nearly

100-fold decrease in expression vs. LPS induced cells which were not treated by *X. caffra* leaf extract. This demonstrates clearly the impact of *X. caffra* leaf extract on the expression of iL-6, an indication of potentially significant anti-inflammatory activity. The effect of *X. caffra* extract on TNF-α and iNOS was measurable, but less significant than the results for iL-6. The expression of iNOS in cells treated with 312.5 µg/mL leaf extract was comparable to background expression, a two-fold decrease in expression compared to LPS induced cells (Figure 15B). A two-fold decrease in the expression of TNF-α was measured in cells treated with 312.5 µg/ml when compared to background expression, which is a three-fold decrease in the expression compared to LPS induced cells that were not treated with *X. caffra* extract (Figure 15C). These results corroborate well with the iL-6 results, further supporting the anti-inflammatory activity of *X. caffra* leaf extracts in a cell system.

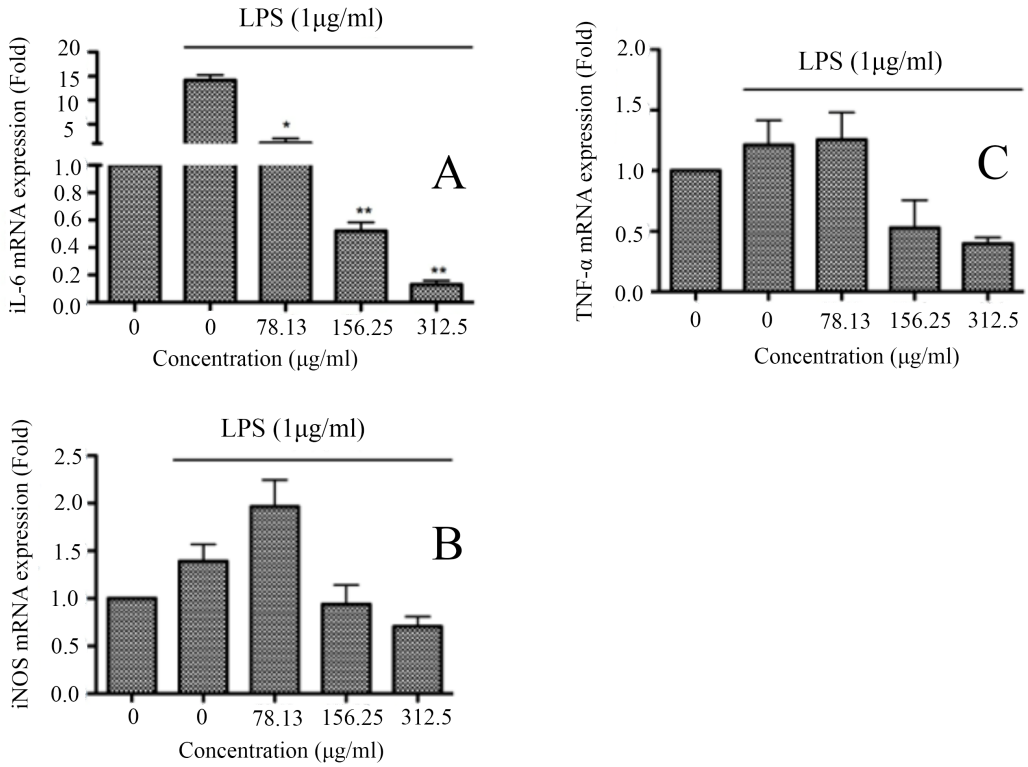

Figure 15. Anti-inflammatory activity of *Ximenia caffra* leaf extract measured by RT-qPCR in RAW 264.7 macrophage cells (A) iL-6 mRNA expressions after treatment; (B) iNOS mRNA expression after treatment; (C) TNF-α mRNA expression after treatment

2.3.6 NF-ϰB Transcription Activity

As described above, the leaf extract of *X. caffra* exhibited both anti-proliferation and anti-inflammatory activities in RAW cells. NF-κB protein complex is involved in a number of cellular responses to stimuli such as free radical, stress, and cytokine (Saw et al., 2011; Saw et al., 2013). To investigate the effects of *X. caffra* leaf extract on the NF-κB transcription activity, the luciferase activity of PC-3/N cells, with a stably transfected NF-

κB luciferase constructs, was measured. In this assay, protein NF-κB was co-expressed with protein luciferase and directly quantified by luminometer. The data demonstrated that *X. caffra* leaf extract significantly attenuated the NF-κB transcription activity in a dose-dependent manner after 24 h treatment (Figure 16). At the concentration of 312.5 μg/ml, the expression of NF-κB was decreased to approximately 60% of the vehicle control. The data obtained is consistent with the results from MTS and qPCR assays, indicating that the inhibition of NF-κB activation might be one of the mechanisms underlying the anti-proliferation and anti-inflammatory effects of the leaf extract of *X. caffra*.

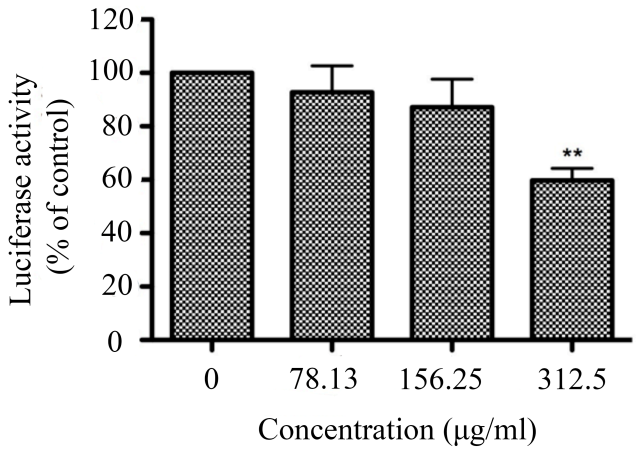

Figure 16. NF-κB transcription activity vs the concentrations of *Ximenia caffra* leaf extract after treatment

2.4 Conclusion

This is the first study examining the leaves, rather than the fruit or seeds of *X. caffra*, which can be sustainably harvested yet is underutilized by local indigenous peoples. The chemical profile of *X. caffra* leaf was comprehensively analyzed and led to the identification of 10 polyphenol compounds, including phenolic acid and flavonoids. The individual polyphenols were successfully quantitated using UV detection. Further bioactivity investigations showed that the extracts of *X. caffra* leaf exhibit anti-oxidant, anti-proliferation, and anti-inflammatory activities. The underlying molecular mechanism may partially be contributed by the inhibition of NF-κB activation, a shared signal pathway between proliferation and inflammation. In the future, it would be of high interest to use flow cytometry to test the extract's cytotoxicity on PC-3 cells and other cells. Same techniques would also be used to quantity the amount of activated cells with fluoresces. These experiments would provide more detailed information about the affects on cell status. Further investigations are needed to explore whether these polyphenol compounds could work synergistically to achieve much improved activities than each single component. The chemical profile and bioactivities determined support its traditional use and may help for its further pharmacological studies and nutraceutical applications. Considering that some botanical supplements on market have similar polyphenol profile, the compounds found in *X. caffra* leaf would also be of interest as a new source of these natural products. The development of a sustainable production and collection system for *X. caffra* leaves could compliment interest in this plant's fruit and seeds.

2.5 Acknowledgement

This work was commissioned by the Millennium Challenge Account Namibia with funding from the Millennium Challenge Corporation in support of the Commissioned project, *Inventory and rapid throughput screening of indigenous utilized plant species for development of new natural products* (MCAN/LMEF/2010/01), to Rutgers, The State University of New Jersey with Prof. Simon as PI. We thank Dave Cole and Loide Uahengo of MCA-Namibia for their support and guidance, the National Botanical Research Institute for providing the botanical authentication services and their collaborative partnership, to Danielle Mortensen for her assistance in field collection, to the Namibian Indigenous Plant Task Team for providing oversight to our work, to the Namibian Ministry of Environment and Tourism for their assistance with permits and other compliance requirements, and to both the University of Namibia and to the Rutgers New Jersey Agricultural Station who also provided financial and logistical support.

2.6 References

B. Ducrey, J.L.W., A. Marston, K. Hostettmann, 1995. Analysis of flavonol glycosides of thirteen Epilobium species (Onagraceae) by LC-UV and thermospray LC-MS. Phytochemistry 38, 129–137.

Ben-Erik Van Wyk, N.G., 2000. People's Plants. Briza Publications, 30.

Bradley, J.R., 2008. TNF-mediated inflammatory disease. The Journal of pathology 214, 149-160.

Cheikhyoussef, A., Shapi, M., Matengu, K., Ashekele, H.M., 2011. Ethnobotanical study of indigenous knowledge on medicinal plant use by traditional healers in Oshikoto region, Namibia. J Ethnobiol Ethnomed 7.

Chivandi, E., Davidson, B.C., Erlwanger, K.H., 2012. Red Sour Plum (*Ximenia caffra*) Seed: A Potential Non-conventional Energy and Protein Source for Livestock Feeds. Int J Agric Biol 14, 540-544.

Dabek, J., Kulach, A., Gasior, Z., 2010. Nuclear factor kappa-light-chain-enhancer of activated B cells (NF-kappaB): a new potential therapeutic target in atherosclerosis? Pharmacological reports : PR 62, 778-783.

De Wet, H., Nzama, V.N., Van Vuuren, S.F., 2012. Medicinal plants used for the treatment of sexually transmitted infections by lay people in northern Maputaland, KwaZulu-Natal Province, South Africa. S Afr J Bot 78, 12-20.

Dubber, M.J., Kanfer, I., 2004. High-performance liquid chromatographic determination of selected flavonols in Ginkgo biloba solid oral dosage forms. Journal of pharmacy & pharmaceutical sciences : a publication of the Canadian Society for Pharmaceutical Sciences, Societe canadienne des sciences pharmaceutiques 7, 303-309.

Dutta, J., Fan, Y., Gupta, N., Fan, G., Gelinas, C., 2006. Current insights into the regulation of programmed cell death by NF-kappa B. Oncogene 25, 6800-6816.

Erlund, I., 2004. Review of the flavonoids quercetin, hesperetin naringenin. Dietary sources, bioactivities, and epidemiology. Nutrition research 24, 851-874.

Fabry, W., Okemo, P.O., Ansorg, R., 1998. Antibacterial activity of East African medicinal plants. J Ethnopharmacol 60, 79-84.

Gabay, C., 2006. Interleukin-6 and chronic inflammation. Arthritis research & therapy 8 Suppl 2, S3.

Gilmore, T.D., 2006. Introduction to NF-kappaB: players, pathways, perspectives. Oncogene 25, 6680-6684.

Hamalainen, M., Nieminen, R., Vuorela, P., Heinonen, M., Moilanen, E., 2007. Anti-inflammatory effects of flavonoids: genistein, kaempferol, quercetin, and daidzein inhibit STAT-1 and NF-kappaB activations, whereas flavone, isorhamnetin, naringenin, and pelargonidin inhibit only NF-kappaB activation along with their inhibitory effect on iNOS expression and NO production in activated macrophages. Mediators of inflammation 2007, 45673.

Khumalo, L.W., Majoko, L., Read, J.S., Ncube, I., 2002. Characterisation of some underutilised vegetable oils and their evaluation as starting materials for lipase-catalysed production of cocoa butter equivalents. Ind Crop Prod 16, 237-244.

Le, N.H.T., Malterud, K.E., Diallo, D., Paulsen, B.S., Nergard, C.S., Wangensteen, H., 2012. Bioactive polyphenols in *Ximenia americana* and the traditional use among Malian healers. J Ethnopharmacol 139, 858-862.

Lee, J.H., Lee, K.R., Su, Z.Y., Boyanapalli, S.S., Barman, D.N., Huang, M.T., Chen, L., Magesh, S., Hu, L., Kong, A.N., 2014. In vitro and in vivo anti-inflammatory effects of a novel 4,6-bis ((E)-4-hydroxy-3-methoxystyryl)-1-phenethylpyrimidine-2(1H)-thione. Chemical research in toxicology 27, 34-41.

Lee, K.W., Kim, Y.J., Lee, H.J. and Lee, C.Y., 2003. Cocoa has more phenolic phytochemicals and a higher antioxidant capacity than teas and red wine. Journal of agricultural and food chemistry, 51(25), pp.7292-7295.

Mulaudzi, R.B., Ndhlala, A.R., Kulkarni, M.G., Finnie, J.F., Van Staden, J., 2011. Antimicrobial properties and phenolic contents of medicinal plants used by the Venda people for conditions related to venereal diseases. J Ethnopharmacol 135, 330-337.

Nair, J.J., Mulaudzi, R.B., Chukwujekwu, J.C., Van Heerden, F.R., Van Staden, J., 2013. Antigonococcal activity of Ximenia caffra Sond. (Olacaceae) and identification of the active principle. S Afr J Bot 86, 111-115.

Ndhlala, A.R., Muchuweti, M., Mupure, C., Chitindingu, K., Murenje, T., Kasiyamhuru, A., Benhura, M.A., 2008. Phenolic content and profiles of selected wild fruits of Zimbabwe: *Ximenia caffra,* Artobotrys brachypetalus and Syzygium cordatum. Int J Food Sci Tech 43, 1333-1337.

Rusaczonek, A., Swiderski, F. and Waszkiewicz-Robak, B., 2010. Antioxidant properties of tea and herbal infusions-a short report. Polish Journal of Food and Nutrition Sciences, 60(1).

Saw, C.L., Cintron, M., Wu, T.Y., Guo, Y., Huang, Y., Jeong, W.S., Kong, A.N., 2011. Pharmacodynamics of dietary phytochemical indoles I3C and DIM: Induction of Nrf2-mediated phase II drug metabolizing and antioxidant genes and synergism with isothiocyanates. Biopharmaceutics & drug disposition 32, 289-300.

Saw, C.L., Guo, Y., Yang, A.Y., Paredes-Gonzalez, X., Ramirez, C., Pung, D., Kong, A.N., 2014. The berry constituents quercetin, kaempferol, and pterostilbene synergistically attenuate reactive oxygen species: Involvement of the Nrf2-ARE signaling pathway. Food and chemical toxicology : an international journal published for the British Industrial Biological Research Association 72, 303-311.

Saw, C.L., Yang, A.Y., Guo, Y., Kong, A.N., 2013. Astaxanthin and omega-3 fatty acids individually and in combination protect against oxidative stress via the Nrf2-ARE pathway. Food and chemical toxicology : an international journal published for the British Industrial Biological Research Association 62, 869-875.

Scalbert, A., Johnson, I.T., Saltmarsh, M., 2005. Polyphenols: antioxidants and beyond. The American journal of clinical nutrition 81, 215S-217S.

Singleton, V.L., 1985. Citation Classic - Colorimetry of Total Phenolics with Phosphomolybdic-Phosphotungstic Acid Reagents. Cc/Agr Biol Environ, 18-18.

Tafadzwa Munodawafaa, L.S.C., Sylvester Rodgers Moyob, 2013. Antimicrobial and Phytochemical Screening of some Zimbabwean Medicinal Plants. Journal of Biologically Active Products from Nature 3, 323-330.

Tak, P.P., Firestein, G.S., 2001. NF-kappaB: a key role in inflammatory diseases. The Journal of clinical investigation 107, 7-11.

Van Wyk, B.E., 2011. The potential of South African plants in the development of new food and beverage products. S Afr J Bot 77, 857-868.

Vauzour, D., Rodriguez-Mateos, A., Corona, G., Oruna-Concha, M.J., Spencer, J.P.E., 2010. Polyphenols and Human Health: Prevention of Disease and Mechanisms of Action. Nutrients 2, 1106-1131.

Wang, L., Zhang, C., Guo, Y., Su, Z.Y., Yang, Y., Shu, L., Kong, A.N., 2014. Blocking of JB6 Cell Transformation by Tanshinone IIA: Epigenetic Reactivation of Nrf2 Antioxidative Stress Pathway. The AAPS journal.

Wu, Q., Wang, M., Simon, J.E., 2003. Determination of isoflavones in red clover and related species by high-performance liquid chromatography combined with ultraviolet and mass spectrometric detection. Journal of chromatography. A 1016, 195-209.

Xia, E.Q., Deng, G.F., Guo, Y.J., Li, H.B., 2010. Biological Activities of Polyphenols from Grapes. Int J Mol Sci 11, 622-646.

Zhou, D.Y., Ding, N., Van Doren, J., Wei, X.C., Du, Z.Y., Conney, A.H., Zhang, K., Zheng, X., 2014. Effects of curcumin analogues for inhibiting human prostate cancer cells and the growth of human PC-3 prostate xenografts in immunodeficient mice. Biological & pharmaceutical bulletin 37, 1029-1034.

CHAPTER THREE

Phytochemistry, Antioxidant Capacity, Total Phenolic Content And Anti-Inflammatory Activity of *Hibiscus sabdariffa* Leaves

3.1 Introduction

Hibiscus sabdariffa, commonly known as Roselle, Bissap or Hibiscus, is member of a genus of flowering plants in the Malvaceae family. Native to tropical Africa, this species is now naturalized and grown worldwide in sub-tropic and tropic areas (Ross, 2003). Hibiscus plays an important role in local foods and nutraceuticals. Its bright red calyx is popular ingredient in beverages and foods such as teas, jams, and jellies providing both color and with its own unique flavor (Mahadevan et al., 2009). Hibiscus tea, a popular herbal tea around the world, is found in international commerce as a sole ingredient in herbal infusions or blend imparting a characteristic red color and unique flavor to such beverages (Villani et al., 2013). Research has shown hibiscus to exhibit nutraceutical properties, and this plant has been recognized in traditional medicines where it has been used as medicine for the treatment of hypertension, inflammation, and liver disorders (Lans, 2006; Lin et al., 2007). Compared with the calyx, the leaf of *H. sabdariffa*, the most abundant portion of roselle foliage, is underutilized. The leaf is usually discarded, except in sub-Sahara Africa where some consume it as vegetable in soups and sauces. The hibiscus leaf also has been reported to exhibit various bioactivities both *in vitro* and

in vivo including anti-oxidant, anti-hyperlipidemic, anti-atherosclerotic, and anti-proliferation (Chen et al., 2013; Gosain et al., 2010; Lin et al., 2012; Ochani and D'Mello, 2009).

In spite of increasing volume of pharmacological research that has focused upon the calyx and leaf of *H. sabdariffa*, only a few studies have sought to identify the phytochemicals in the leaf. Major components identified in *H. sabdariffa* leaf include different phenolic acids and flavonoids (Chen et al., 2013; Rodriguez-Medina et al., 2009). However, these analyses lack satisfactory separation, quantification, and comparison between different accessions. Due to the potential beneficial roles of hibiscus leaf, as well as its increasing popularity in use for foods, drinks and nutritional supplements, we sought to systematically quantify the major chemical constituents, explore additional bioactivities and ensure all studies are conducted with authenticated varieties and genetic materials using well-established quality control method. As such, this research investigated bioactive polyphenol chemical profile qualitatively and quantitatively using LC/UV/MS, and conducted bioactivities research using Folin-Ciocalteu assay, Trolox equivalent antioxidant capacity (TEAC) radical scavenging assay and nitric oxide synthetase inhibition assay on LPS (lipopolysaccharide) induced macrophage RAW 264.7 cells cell lines. Leaf samples of 25 populations of *H. sabdariffa* collected from around the world, then cultivated at the same time and place under identical environmental conditions in Baton Rouge, LA, USA, were phytochemically compared.

The content of flavonol aglycones, quercetin and kaempferol, were prepared for quantification using acid induced hydrolysis. Interestingly, compound 5-HMF (5-(hydroxymethyl)furfural) was identified as one major component in the dried leaf sample. Bioactivity studies indicate that *H. sabdariffa* leaf has moderate antioxidant activities and anti-inflammatory activities, suggesting potential new applications in the future. The relationship between the 5-HMF content and measured bioactivities was investigated in our study, and the potential of using 5-HMF as a marker for quality control in *H. sabdariffa* leaves was also explored. This comprehensive investigation of the phytochemistry of *Hibiscus sabdariffa* leaf conducted in this study enabled the development of quality control methodology for its production.

3.2 Materials And Methods

3.2.1 Chemicals and Reagents

Standard compounds including rutin hydrate, chlorogenic acid, neochlorogenic acid, cryptochlorogenic acid, kampferol, and formic acid, ABTS (2,2'-azino-bis(3-ethylbenzothiazoline-6-sulphonic acid), potassium persulfate were purchased from Sigma Aldrich (St. Louis, MO). Quercetin and 5-HMF were purchased from Acros Organics (Geel, Belgium) and Folin Ciocalteu's Phenol Reagent was purchased from MP Biomedicals (Solon, OH). HPLC grade solvents including water, methanol, acetonitrile

and hydrochloric acid (HCl) were purchased from Fisher Scientific (Fair Lawn, NJ). Ethyl alcohol was purchased from Pharmco-AAPER (Brookfield, CT).

3.2.2 Plant Samples

A field trial was conducted during the 2009 growing season from April to November in Baton Rouge, LA, USA for the 25 *Hibiscus sabdariffa* populations from 22 roselle accessions (Appendix I). The seeds of the accessions with plant identification numbers were obtained from the USDA Agricultural Research Service (ARS) Plant Genetic Resources Conservation Unit in Griffin, Georgia. The seeds without plant identification numbers were collected by the Southern University Agricultural Research and Extension Center *Hibiscus* Research Group. The seeds of all the accessions were planted in seed trays in a greenhouse in mid-March and germinated within a two-week period. The seedlings were kept in the greenhouse for four weeks and then transplanted to a field plot at the Horticulture Farm (30.524 ºN, 91.190 ºW, and elevation 22 m) located on the campus of Southern University and A&M College in Baton Rouge, Louisiana, USA at the end of April. The university is located on Scott's Bluff overlooking the Mississippi River. Baton Rouge has a subtropical humid climate with mild winters, hot and humid summers. This area has an average annual precipitation of 1,700 mm. The average annual temperature for Baton Rouge is 19.7°C while the average temperature for January is 10.67°C and August is 26.97°C. The field plot had 22 rows. Each row was randomly assigned to one accession, with 20-25 plants planted per accession. The planting space was 142 cm between two adjacent rows and 122 cm between two adjacent plants within a

row. The soil type in the area is classified as prairies series with poorly drained soils formed from loess deposits. The soil type is a silt clay loam with soil pH of 6.9. Observations were made for each accession including botanical, growth and developmental characteristics. Young and mature leaves along with branches were collected for herbarium uses and deposited at the Southern University Agricultural Research and Extension Center. For chemical analysis, 25 mature sun-exposed leaves were collected from the top to mid sections of the plants for each accession at the end of September. The leaves were placed in a sterilized plastic bag in a cooler for transportation to the laboratory. Leaf samples after removal of their petioles were oven-dried at 60 °C for 48 hour, then grounded into powder and stored in Ziploc bags for chemical analyses.

3.2.3 Sample Preparation

The dried hibiscus leaves were ground into powder. Around 100 mg of each sample was then accurately measured and placed in a volumetric flask and added 25 ml of 70% (v/v) methanol/water with 0.1% acetic acid solution. The sample extraction was then put in ultrasonic water bath for 10 min followed by shaking at room temperature for overnight (Xu et al., 2011). The extract of each sample was then filtered through 0.45 µm filter and used for qualification, quantification, Folin-Ciocalteu assay, ABTS radical scavenging assay. Samples were injected to HPLC immediately or stored in freezer of – 20 °C for further test. For cell-based nitrite assay, the leaf extract above was dried on rotavapor and

lyophilized to powder and subsequently dissolved in solvent DMSO with final concentrations of DMSO in the culture medium less than 0.05%.

For the hydrolysis of quercetin and kaempferol glycosides, the method used was based upon that first published by Xu et al (2012). An accurately weighed ~60 mg of dried ground hibiscus powder was placed in a volumetric flask with 2 ml of 2.7 M HCl solution and hydrolyzed in water bath at temperature of 90 °C for 60 min. The volume was filled up to 5 ml after hydrolysis and then each extract was filtered through 0.45 µm filter before injection into HPLC. The recovery test was performed with quercetin rutinoside (rutin) at three different concentrations corresponding approximately 100%, 150%, 200% of the expected value in a representative sample. The recoveries of the different concentrations are 95%, 98%, and 100% indicating that the hydrolysis method and extraction method we used to quantify the flavonol aglycones is precise and accurate.

Each standard compound was measured accurately and dissolved in 70% (v/v) methanol/water with 0.1% acetic acid as stock solution. The stock solution was then diluted using methanol into a series of concentrations as working solutions. The concentration range and calibration curve of each compound are as follows: 5-(hydroxymethyl)furfural (0.31-20.00 µg/ml, $y = 0.0149x - 199.49$, $R^2 = 0.999$), chlorogenic acid (1.60-1000.00 µg/ml, $y = 0.0366x + 1199.6$, $R^2 = 0.999$), quercetin (2.37-379.80 µg/ml, $y = 0.0288x - 1413.4$, $R^2 = 0.999$), kaempferol (2.19-351.00 µg/ml, y

= 0.0275x - 1028, R^2 = 0.999). All standards' calibration curves have good linearity. Every sample was filtered through 0.45 μm nylon filter before injection.

3.2.4 HPLC-MS Conditions

The separation and identification were performed on Hewlett-Packard Agilent 1100 series HPLC-MS (Agilent Technologies, Waldbronn, Germany) equipped with a quaternary pump system, a degasser, an autosampler, a DAD detector, an MSD trap with electrospray ion source (ESI). The electrospray ion mass spectrometer was under positive model and negative mode in separated runs with scan range from *m/z* 100 to 800. The needle voltage was 3.5 kV for positive mode and -3.5 kV for negative mode, nitrogen (99.999%) flow rate was 12 L/min and the capillary temperature was 350˚C. Nitrogen was set as nebulizer at 60 psi and helium as a collision gas. HP ChemStation software, and Data Analysis 4.2 were used in qualitative experiments. For identification, the column used was Polaris TM Amide C18 column, 5 μm, 250 × 4.6 mm (Varian) at temperature of 25°C. The flow rate was 1.0 ml/min. The mobile phases consist of solvent A (0.1% formic acid in water (v/v)) and solvent B (0.1% formic acid in acetonitrile (v/v)). The gradient starts from 5% to 10% B in 0 to 10 min, 10% to 34% B in 10 to 34 min, 34% to 60% B in 34 to 35 min, and continues at 60 % B to 50 min.

For quantitative analysis, the experiment was performed on Waters 2695 separation module equipped with a photodiode array detector (PDA). Solvents were degassed in a separate bath sonicator. The spectral scan range of UV-DAD detector was 200-520 nm.

The column used was Prodigy ODS3 5µm, 150 × 3.2 mm 5 micro (Phenomenex Inc. Torrace CA) and flow rate was 1 ml/min. Solvent A is 0.1% formic acid in water (v/v), solvent B is 0.1% formic acid in acetonitrile (v/v). 5-HMF and chlorogenic acids were quantified at 280 and 330 nm respectively, and the gradient was 5 to 10% B in 0 to 10 min, 10 to 20% B in 10 to 20 min. Flavonol aglycones from acid induced hydrolysis were quantified at 370 nm, and the gradient was isocratic 30% solvent B for 10 min.

3.2.5 Folin-Ciocalteu Assay

The total phenolic content was determined based on Folin Ciocalteu assay with a few modifications (Singleton, 1985). 40 µl of the leaf extract prepared as described above was mixed with 900 µl diluted Folin Ciocalteu's reagent followed by incubation at room temperature for 5 min. Then, 400 µl of 15% sodium carbonate was added and the mixture reacted at r.t for 45 min. The UV absorption at wavelength of 752 nm was measured against a blank solution. The standard curve was measured based on the prepared gallic acid standard solution (0.38, 0.19, 0.095, 0.475 mg/ml) and the result was transformed as milligrams of gallic acid per g ± SD. Results were calculated from the mean of three replicates.

3.2.6 ABTS Radical Scavenging Assay

The *in vitro* antioxidant activity was measured based the decolorization of the ABTS radical cation (Re et al., 1999). The procedure was as follows: 38.4 mg of ABTS and 6.6

mg potassium persulfate ($K_2S_2O_8$) were co-dissolved in 10 ml of water and stored for 16 hours in dark environment to form stable radical cation (ABTS·+). The stored radical solution was then diluted using ethanol to a concentration with UV absorption of 0.70 ± 0.20 at 734 nm. 990 µl of the diluted ABTS radical working solution was mixed with 10 µl of the leaf extract prepared as described above followed by reaction for 20 minutes at room temperature. The decolorization of mixed solution indicates that antioxidant compounds in the extract quenched ABTS radical cations. There is a quantitative relationship between the reduction of absorbance at 734 nm and the concentration of antioxidants present in the sample. The standard curve was generated by plotting the concentrations of Trolox against the percentage of inhibition. The value of antioxidant capacity of each sample can be calculated out as TEAC (Trolox equivalent antioxidant capacity). The final results were expressed as µmol TE /g ± SD. Results were calculated from the mean of three replicates.

3.2.7 Cell Culture

RAW 264.7 cells were derived from murine macrophages and achieved from American Type Culture Collection (Rockville, MD, USA). Cells were cultured in DMEM (Dulbecco's modified Eagle's medium) supplemented with 10% endotoxin-free, heat-inactivated fetal calf serum (GIBCO, Grand Island, NY, USA), 100-unites/ml penicillin, and 100 µg/ml streptomycin. The culture media was changed to serum-free DMEM when the density reached 2-3 × 10^6 cells/ml. Then the cells were activated by incubation in the media with *Escherichia coli* lipopolysaccharide (LPS, 100 ng.ml). Different

concentrations of the leaf extract dissolved in dimethyl sulfoxide (DMSO) were added into the cell lines subsequently with final concentration of 20, 40, 80 μg/ml, while control group was treated with only 0.05% DMSO solution.

3.2.8 Nitrite Assay

Murine macrophage RAW 264.7 cells were treated with lipopolysaccharide (LPS) to induce an inflammatory response, measured by the concentration of nitric oxide (NO) generated by the cells. The nitrite concentration in the culture medium was measured as an indicator of NO production, according to the Griess reaction. Extracts exhibiting anti-inflammatory activity show a decreased content of nitrite in the culture medium, evidence of the inhibition of the enzyme nitric oxide synthetase, well known for its role in inflammation. Cells were treated solely with LPS (negative control), or with extracts at concentrations of 20 μg/ml, 40 μg/ml and 80 μg/ml and incubated for 24 hours at 37 °C. After centrifugation at 1000 *g* for 20 min, 100 μL of each supernatant medium was mixed with the same volume of Griess reagent (1% sulfanilamide in 5% phosphoric acid and 0.1% naphthylethylenediamine dihydrochloride in water). Absorbance of the mixture at 550 nm was then measured and values were expressed as mean ± standard error of triplicate tests.

3.2.9 Statistical Analysis

Experimental data was subjected to one-way analysis of variance (ANOVA) and Tukey's multiple-comparison tests using Statistical Analysis System (SAS, version 9.4). Differences were considered statistically significant at $P < 0.05$ level.

3.3 Results And Discussions

3.3.1 Phytochemical Identifications

Identification of each single compound was mainly based on its retention time, UV absorption spectrum, mass spectrum and the comparison or co-injection with standard compounds. Most compounds were identified under both negative and positive modes. The retention time, wavelength of maximum UV absorption and detected mass ions for each compound are summarized in Table 3. Ten major polyphenol compounds were identified in this investigation using LC/UV/MS, which correlate very well with previous reports (Rodriguez-Medina et al., 2009). Three different chlorogenic acid isomers, which were not fully determined in previous study, were successfully differentiated and quantified in these experiments based on comparison with authentic standards.

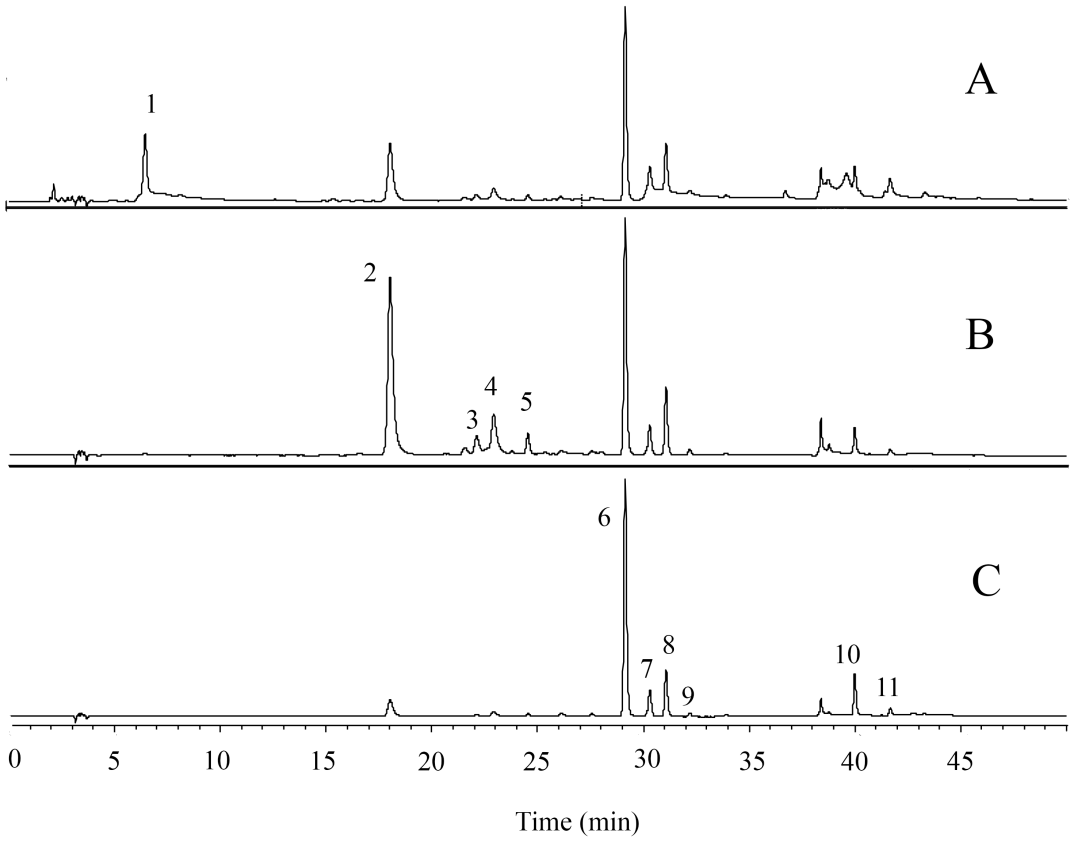

Figure 17. Representative chromatograms of *Hibiscus sabdariffa* leaf extract. (A) UV chromatogram at 280 nm; (B) UV chromatogram at 330 nm; (C) UV chromatogram at 370 nm. The identities of the labeled peaks are listed in Table 3.

Table 3. The phytochemicals identified in *Hibiscus sabdariffa* leaf.

Peak Number	t_R (min)	UV λ_{max} (nm)	Molecular and Fragment Ions		Compound Identified
			Positive Mode	Negative Mode	
1	6.5	285, 230	109, 127	-	5-(hydroxymethyl)furfural
2	18.1	328	355	191, 353	Neochlorogenic acid
3	22.5	328	355	191, 353	Chlorogenic acid
4	23.6	328	355	173, 353	Cryptochlorogenic acid
5	25.7	328	337	335	Caffeoylshikimic acid
6	29.1	356	611, 465, 303	609	Quercetin-rutinoside (Rutin)
7	30.2	356	465, 303	463	Quercetin-G
8	31	356	595, 449, 287	593	Kaempferol-G-Rha
9	32.2	356	287,449	447	Kaempferol-G
10	39.9	369	303	301	Quercetin
11	41.5	369	287	286	Kaempferol

Abbreviations: g:glucosyl/galactosyl; rha: rhamnosyl

The major compounds in the hibiscus leaf extracts are flavonol glycosides (peak 6-11) as shown in Figure 17C. Compounds 6-9 were identified as glycosylated derivatives of the

flavonols, quercetin and kaempferol, based on their characteristic aglycone fragment ions (*m/z* = 303, *m/z* = 287 under positive mode), as well as the free aglycones quercetin and kaempferol (peak 10, 11). Maximal UV-Vis absorptions of these compounds were consistent with reported values of around 365 nm from the literature for quercetin, and kaempferol (Ducrey, Wolfender, Marston, & Hostettmann, 1995). The general structure of each derivative is determined based on the molecular and fragment ions. For example, the MS spectrum of compound 6 (t_R 29.1 min) indicates that it has a molecular ion at *m/z* of 611 ($[M+H]^+$), which was fragmented to *m/z* 465 ($[M\text{-rhamnosyl}+H]^+$) and *m/z* 303 ($[M\text{-rhamnosyl-glucosyl}+H]^+$. The identity was tentatively determined as quercetin-rutinoside and then further confirmed through the co-injection with authentic standard. The same identification principle was applied to the kaempferol glycosides. For example, compound 9 (t_R 32.2 min) has a molecular ion at *m/z* of 449 ($[M+H]^+$), and is fragmented to *m/z* 287 ($[M\text{-glucosyl}+H]^+$ or ($[M\text{-galactosyl}+H]^+$) which corresponds to kaempferol-glucoside or kaempferol-galactoside. Representative mass spectra for each analyte under positive ionization are shown in Figure 18. To positively confirm the identity of the aglycones, hydrolyzed leaf samples were compared with authentic standards by HPLC, as shown in Figure 19.

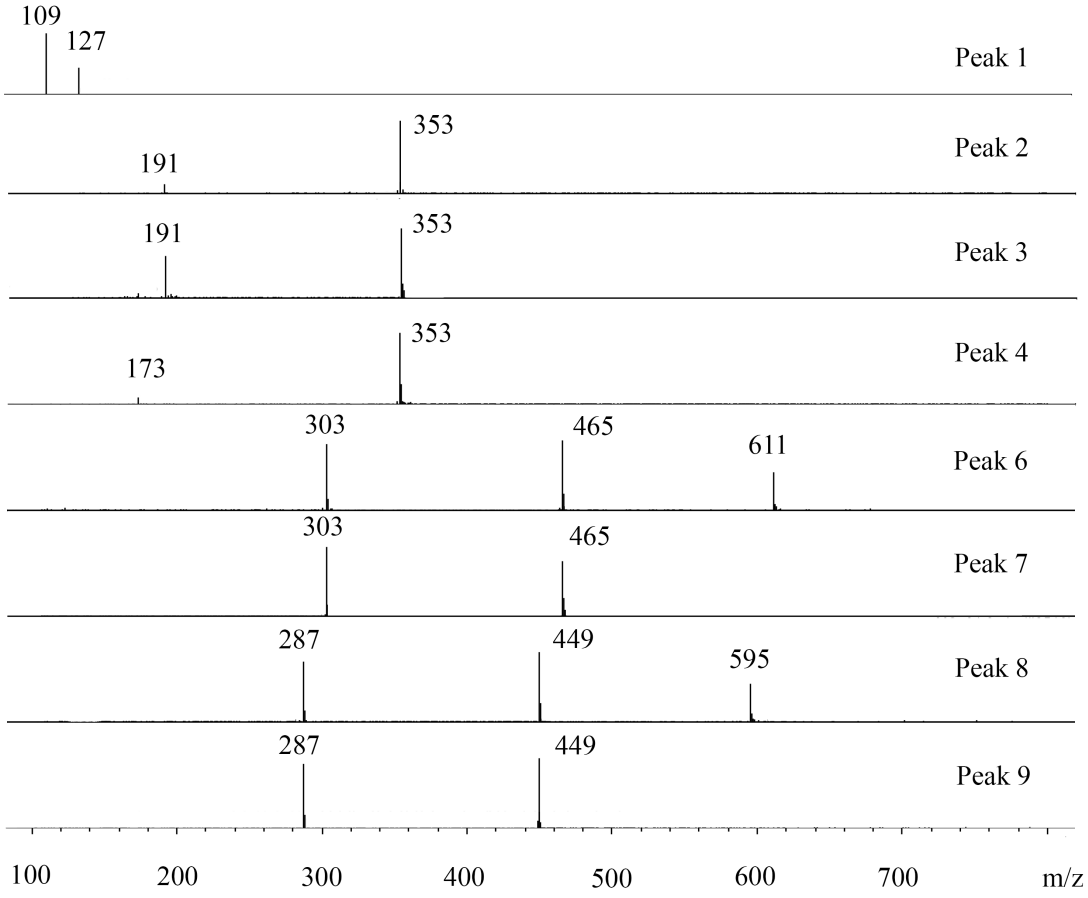

Figure 18. The mass spectrum of representative compounds. Peaks 1-4 are under negative mode; Peaks 6-9 are under positive mode

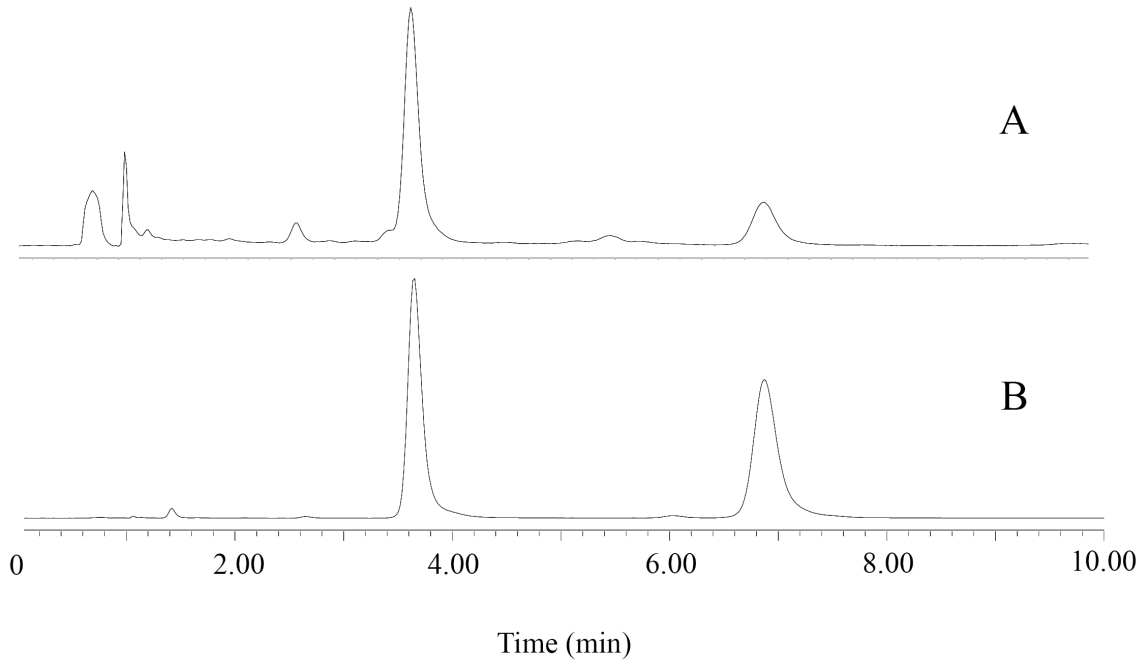

Figure 19. The chromatograms of flavonol aglycones. (A) Representative chromatogram of hydrolyzed extract of *Hibiscus sabdariffa* leaf at 370 nm; (B) The mixture of standard compounds of quercetin and kaempferol

Three different chlorogenic acids isomers (peaks 2-4, Figure 17B) were identified in the leaf sample. They share similar UV absorption spectrum with maximum wavelength at ~ 328 nm and same molecular ions in mass spectrometry. Peak 4 had a distinct mass fragment ion at *m/z* 173 and a loss of fragment ion at *m/z* 191 under negative mode, which led to its identification as cryptochlorogenic acid (4-*O*-caffeoylquinic acid) based upon the report by Clifford et al (2003). To further confirm the assumption and distinguish the other two isomers, authentic standards were purchased and injected on HPLC separately for comparison. Then three different isomers of chlorogenic acids were positively determined as follows: peak 2 is neochlorogenic acid (5-*O*-caffeoylquinic acid), peak 3 is chlorogenic acid (3-*O*-caffeoylquinic acid) and peak 4 is cryptochlorogenic acid (4-*O*-caffeoylquinic acid).

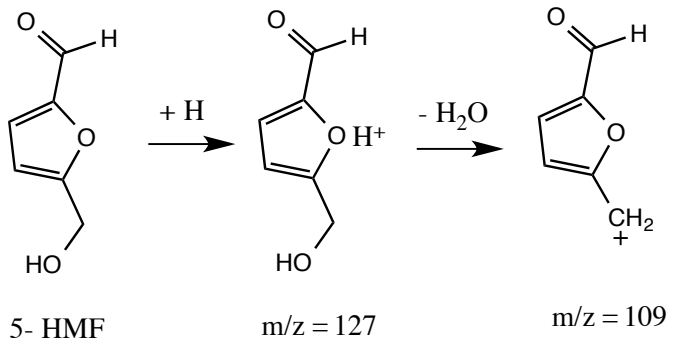

Figure 20. The formation of detected fragment ions of 5-HMF in mass spectrometer

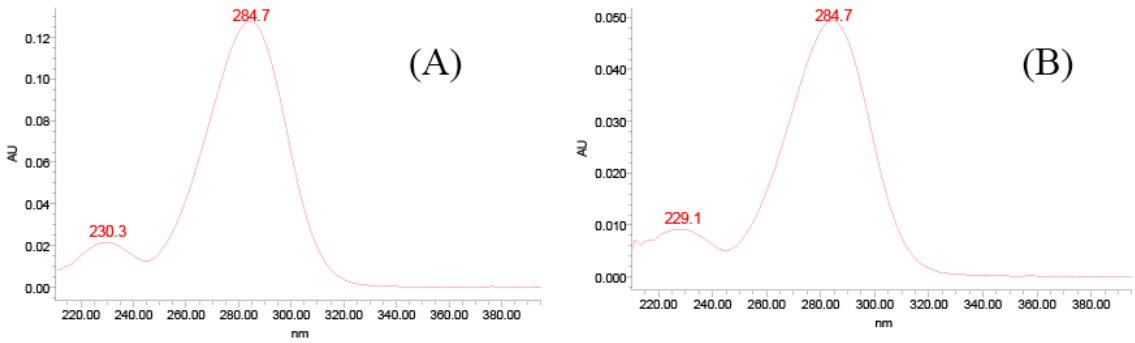

Figure 21. The UV absorption spectrum of 5-HMF; (A): The 5-HMF commercial standard; (B): The 5-HMF from *Hibiscus sabdariffa*

The compound 5-(hydroxymethyl)furfural (5-HMF, peak 1, Figure 17A) was identified as a significant component in the dried *Hibiscus sabdariffa* leaf for the first time. Molecular ion at *m/z* 127 ($[M+H]^+$) was observed along with its most abundant fragment ion at *m/z* 109 ($[M-H_2O]^+$), which correlates very well with previous report (Herrero et al., 2012; Zhao et al., 2014). To positively confirm its identity, the UV-Vis spectrum of peak 1 was compared with commercial available standard and identical absorptions were observed at ~ 280 nm and ~230 nm. The identity of this compound was further confirmed by retention time comparison on HPLC.

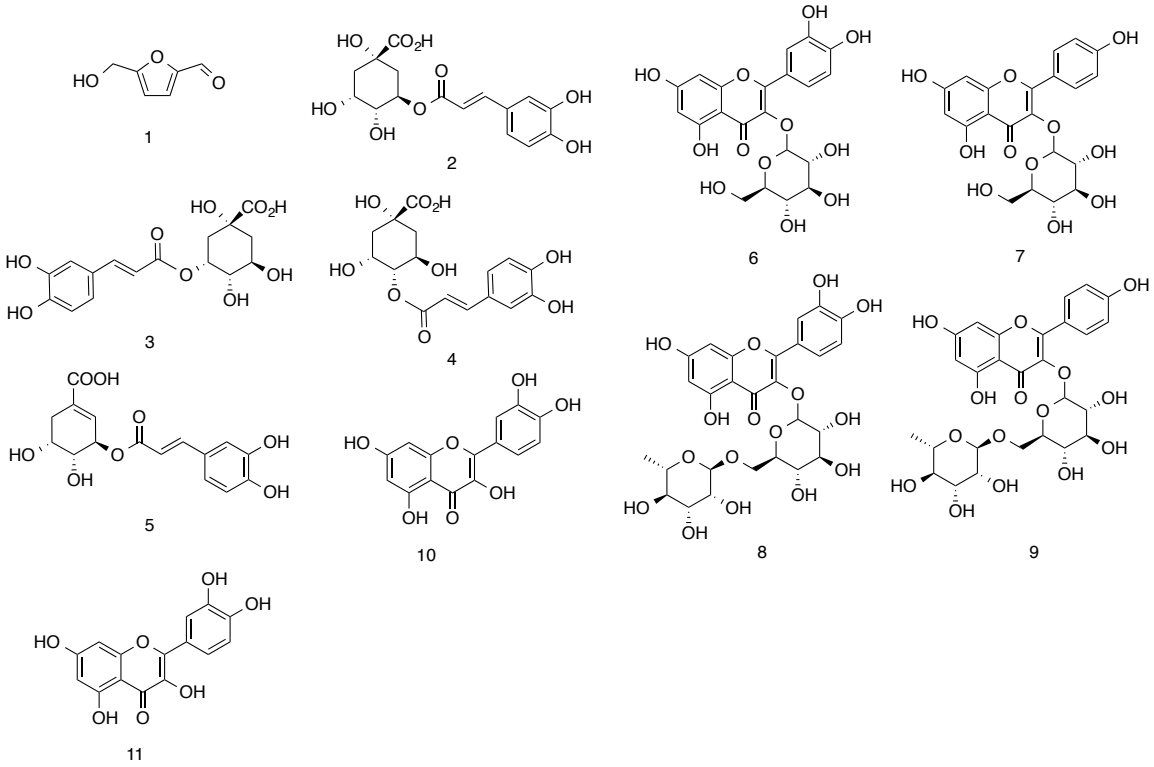

Figure 22. Chemical structures of compounds identified from the leaf of *Hibiscus sabdariffa*

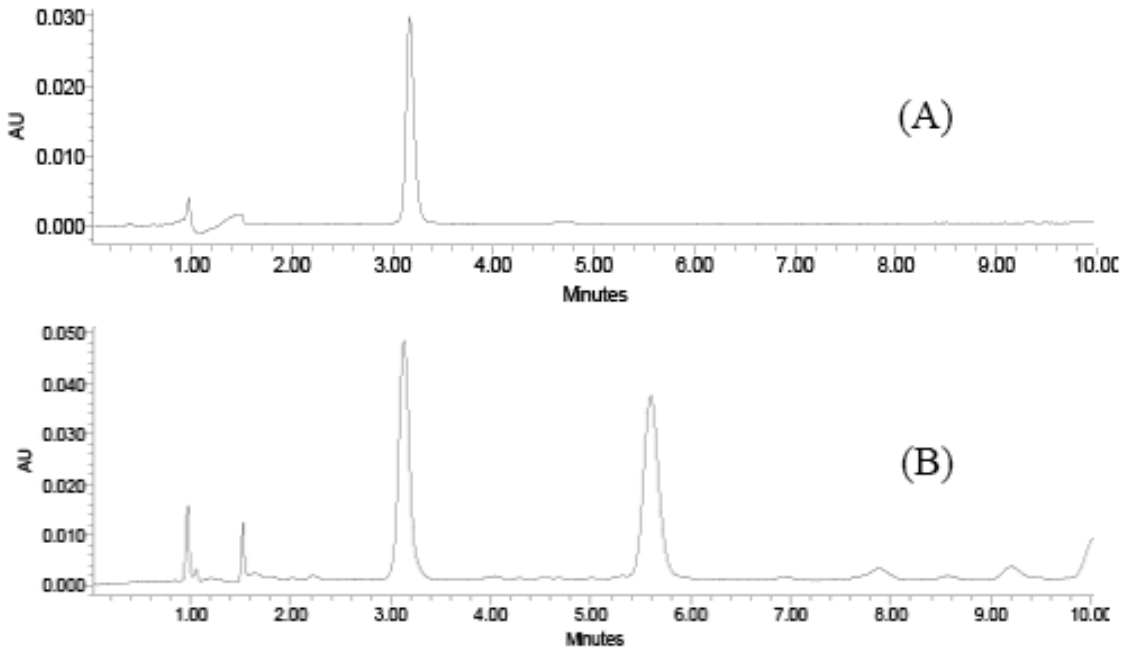

Figure 23. The HPLC chromatograms of 5-HMF at 280 nm. (A) Commercial standard 5-HMF; (B) The 70% methanol extract of *Hibiscus sabdariffa*

3.3.2 Quantitative Analysis of 25 *Hibiscus sabdariffa* Populations

Quantification of flavonol aglycones, chlorogenic acids and 5-HMF was performed on HPLC with UV detection. The summarized results of quantitative analysis of 25 *Hibiscus sabdariffa* samples are shown in Table 4. As calculated, the flavonol aglycones content varies from 2.76 mg/g to 7.31 mg/g in dried hibiscus leaf. The average chemical composition of the 25 samples is shown in Figure 24A. The quercetin glycosides are the major flavonol, representing on average 26% of the total composition measured by HPLC, while kaempferol contributes only 6%. The total amount of chlorogenic acids and its isomers varied from 4.80 to 10.30 mg/g in the dried leaf, representing the majority of the

average composition. Neochlorogenic acid was present in content with a range from 2.87 to 7.16 mg/g, representing an average of 40% of the total content measured; the second most abundant phenolic acid is cryptochlorogenic acid, ranging from 1.14 to 2.72 mg/g, representing an average of 14% of the total. The following 6% is chlorogenic acid, ranging from 0.42 to 1.49 mg/g.

Table 4. Content of each component, total phenolics and total antioxidant capacity in 25 *Hibiscus sabdariffa* leaf samples.

Code	Amount of chemical constituent (mg/g)[(a)]								Content of total phenolics	Total antioxidant capacity [(c)]
	5-HMF	Neo	Chl	Cry	TC	Q	K	TF		
Cuba-1	1.30	6.84	0.85	2.13	9.82	5.18	1.55	6.73	29.9 ± 0.5 [a]	135.3 ± 11.9 [abcd]
Cuba-2	0.65	5.06	0.89	1.96	7.91	4.21	1.19	5.40	22.2 ± 2.4 [f]	111.5 ± 7.9 [abcd]
Georgia, USA	0.45	4.05	0.42	1.57	6.04	3.29	0.92	4.21	20.5 ± 1.2 [m]	134.2 ± 18.9 [abcd]
Ghana-1	0.43	7.16	0.46	2.50	10.12	2.64	0.68	3.32	23.2 ± 4.0 [cd]	128.0 ± 14.0 [abcd]
Ghana-2	1.22	7.02	0.95	2.33	10.30	3.01	0.85	3.86	22.3 ± 3.0 [gh]	108.2 ± 11.6 [cd]
India	1.13	6.35	0.90	2.26	9.51	5.86	1.31	7.17	25.7 ± 2.1 [de]	128.5 ± 11.5 [abcd]
Jamaica	1.35	5.34	0.78	1.87	7.99	3.04	0.68	3.72	23.8 ± 3.8 [fg]	111.4 ± 7.2 [abcd]
Malaysia	1.65	6.50	0.42	2.16	9.08	2.54	0.59	3.12	20.6 ± 3.5 [gh]	110.7 ± 10.3 [bcd]
Nigeria-1	1.33	5.84	0.89	1.88	8.61	4.59	0.55	5.14	23.7 ± 0.8 [f]	137.6 ± 14.5 [abc]
Nigeria-2	1.06	6.28	0.87	2.72	9.87	3.19	0.74	3.93	21.1 ± 2.3 [ijk]	114.9 ± 10.9 [abcd]
Nigeria-3	1.46	5.44	0.85	1.82	8.11	3.52	0.63	4.15	23.1 ± 2.3 [hij]	112.5 ± 6.7 [abcd]
Poland	0.82	5.39	0.74	2.15	8.28	5.73	1.58	7.31	27.2 ± 1.2 [b]	142.6 ± 14.2 [abcd]
Senegal-1	1.24	5.05	1.49	1.88	8.42	3.49	0.75	4.23	24.1 ± 2.8 [hi]	132.7 ± 16.8 [abcd]
Senegal-2	1.22	5.35	0.78	2.00	8.13	5.44	0.79	6.24	20.4 ± 3.2 [m]	111.0 ± 8.3 [abcd]
South Africa-1	1.45	5.19	0.99	1.72	7.90	3.43	0.85	4.28	25.5 ± 3.9 [e]	130.9 ± 11.8 [abcd]
South Africa-2	1.30	5.52	0.83	2.12	8.47	5.68	0.81	6.50	23.6 ± 2.8 [fg]	133.0 ± 13.8 [a]
South Africa-3	1.75	6.38	0.49	2.01	8.88	2.79	0.71	3.49	21.5 ± 2.8 [jk]	101.5 ± 17.5 [d]
South Africa-4	1.82	6.03	0.80	1.81	8.64	3.18	0.83	4.01	21.6 ± 2.6 [fgh]	115.6 ± 16.1 [abcd]
Sudan-1	0.75	5.96	1.36	1.94	9.26	2.82	0.70	3.52	20.4 ± 2.5 [kl]	136.8 ± 17.8 [abcd]
Sudan-2	0.35	2.87	0.79	1.14	4.80	3.86	0.87	4.73	24.9 ± 3.3 [c]	152.5 ± 18.8 [ab]
Sudan-3	0.81	5.46	1.00	1.72	8.18	2.16	0.60	2.76	19.0 ± 2.7 [lm]	120.5 ± 11.8 [abcd]
Taiwan	1.08	5.23	0.97	2.01	8.21	3.21	0.64	3.86	22.2 ± 0.9 [ijk]	128.7 ± 8.5 [abcd]
Thailand	0.37	3.15	0.64	1.23	5.02	2.44	0.79	3.23	22.4 ± 3.1 [fg]	126.7 ± 5.9 [abcd]
Zambia-1	0.77	5.82	0.93	2.21	8.96	3.17	1.02	4.19	22.2 ± 2.0 [fgh]	141.4 ± 21.3 [abcd]
Zambia-2	0.71	6.49	0.88	1.94	9.31	2.91	0.98	3.89	21.9 ± 2.0 [kl]	126.3 ± 18.2 [abcd]

(a) Abbreviations. 5-HMF: 5-(Hydroxymethyl)furfural; Neo: neochlorogenic acid; Chl: chlorogenic acid; Cry: cryptochlorogenic acid; TC: Total chlorogenic acids; Q: Quercetin; K: kaempferol; TF: Total flavonol aglycones; (b) Expressed as mg gallic acid per gram. The data are shown as means ± SD of three independent experiments. Means in the same column followed by the same letter are not significantly different at $p < 0.05$; (c) Expressed as μmol Trolox equivalent per gram. The data are shown as means ± SD of three independent experiments. Means in the same column followed by the same letter are not significantly different at $p < 0.05$; All measurements are based on leaves' dry weight

The amount of 5-HMF in *H. sabdariffa* leaf varied in different samples from 0.35 to 1.82 mg/g. The amount of 5-HMF has been used as an indicator for the freshness of some fruits or juices. This compound usually is formed from ketopentoses when dehydration occours in acid environments or high temperature, and commonly found in food with sugar under drying or baking (Roman-Leshkov et al., 2006). The maximum amount of 5-HMF recommended in fruit concentrate by The International Federation of Fruit Juice Processors (IFFJP) is 25 mg/kg in concentrate (Güray et al., 2013). Monakhova and Lachenmeier (2012) estimated that the consumption and daily intake of the 5-HMF up to levels of more than 150 mg/day, and average daily consumption varies in different countries (Monakhova and Lachenmeier, 2012). The average content of 5-HMF detected in the leaf samples in this investigation is 1.06 mg/g, which may be an indicator of improper drying or storage. The 5-HMF found in processed *H. sabdariffa* leaf would be a concern if consumed in beverage or food, and further investigation into its formation is warranted.

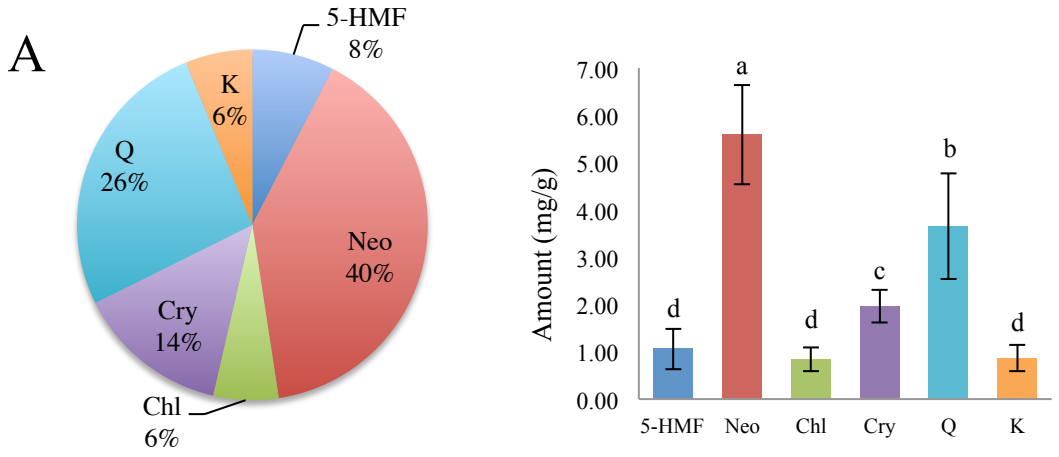

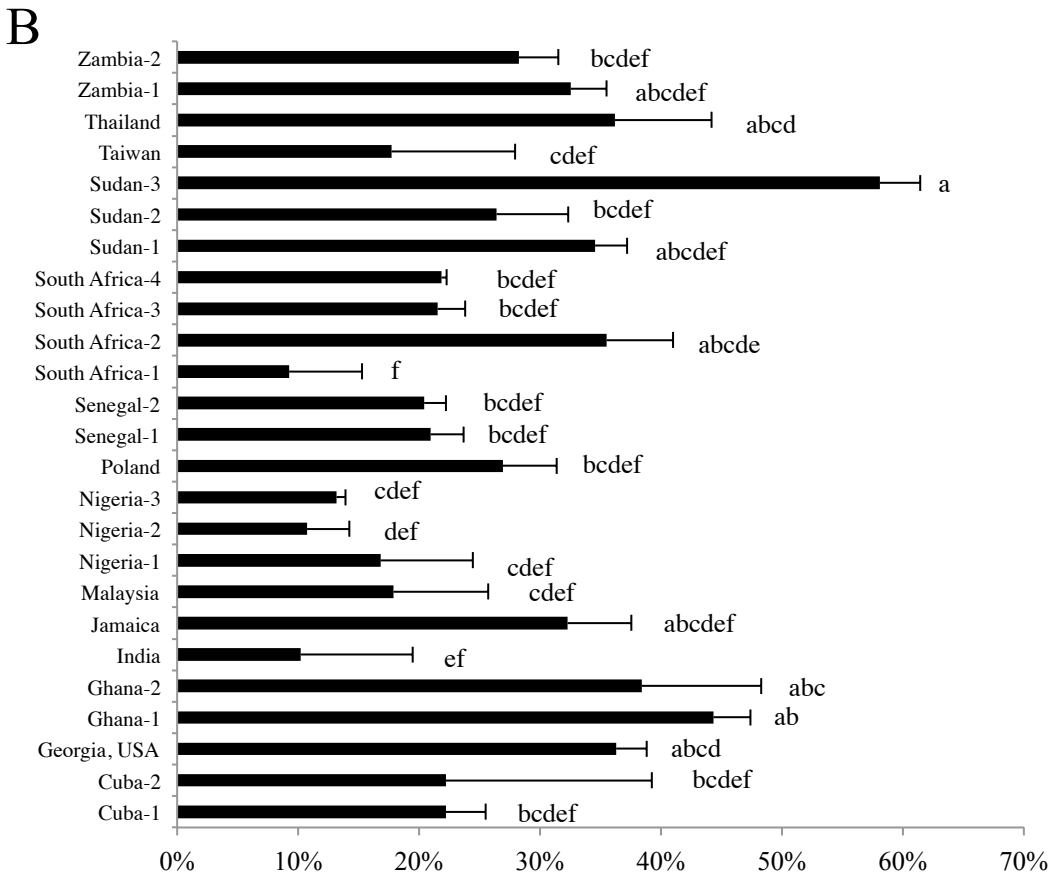

Figure 24. (A) Relative and absolute mean chemical compositions of the population of *H. sabdariffa* leaf. Abbreviations: "5-HMF" 5-(hydroxymethyl)furfural; "Neo" means neochlorogenic acid; "Chl" means chlorogenic acid; "Cry" means cryptochlorogenic acid; "Q" means quercetin; "K" means kaempferol; Values with the same letter are not significantly different ($P < 0.05$) between chemical compositions. (B) Inhibition of nitric oxides production by extracts of *H. sabdariffa* leaf (80 µg/mL) on LPS induced RAW 264.7 cells; Values with the same letter are not significantly different ($P<0.05$) between samples.

3.3.3 Total Phenolic Content and *In Vitro* Antioxidant Capacities

The total polyphenol content measured by the Folin-Ciocalteu assay was expressed as mg gallic acid equivalents (GAE) per gram of plant material. The total phenolic content determined using Folin-Ciocalteu assay, ranged from 18.98 ± 2.7 to 29.9 ± 0.5 mg GAE /g with an average value of 22.92 mg GAE /g. The antioxidant activity measured by ABTS radical scavenge assay is indicated using mmol or µmol of Trolox equivalent per gram of ground leaf powder. The *in vitro* antioxidant capacity measured in the 25 samples ranged from 101.5 ± 17.5 to 152.5 ± 18.8 µmol TE /g. As polyphenols can reduce radicals *in vitro* and *in vivo*, these observed antioxidant activities are at least partially due to its polyphenol components as described above.

3.3.4 Anti-inflammatory Activity

To evaluate the potential anti-inflammatory activities of the *H. sabdariffa* leaf extracts, the extracts were screened against RAW 264.7 murine macrophage cells *in vitro*. Inhibition of nitric oxide synthetase (NOS) was determined by treating the cells with lipopolysaccharide induced inflammatory response. Cells treated with *H. sabdariffa* extracts exhibited a dose-dependent inhibition of NOS. There was wide variation between *H. sabdariffa* accessions, with a range from a minimum inhibition of 9.1% inhibition to 57.9% inhibition at 80 µg/ml. The average response was 26.4 ± 11.4% inhibition at a

concentration of 80 μg/ml. Results are summarized in Figure 24B. It was reported that each single component of flavonol quercetin, kaempferol and chlorogenic acid, has shown anti-inflammatory activities *in vitro*, so it is possible that these components discovered in *H. sabdariffa* may work as a combination in this assay (Hämäläinen, Nieminen, Vuorela, Heinonen, & Moilanen, 2007; Shan, Fu, Zhao, Kong, Huang, Luo, et al., 2009).

3.3.5 Correlation between 5-HMF and Quality

The presence of 5-HMF, reported here for the first time in this plant species may be related to quantifiable aspects of quality control. To examine potential relationships among the data, a correlation matrix was computed. An inverse correlation was determined between the content of 5-HMF and corresponding antioxidant and anti-inflammatory activities. There is a moderate negative correlation (R = - 0.5305) between the content of 5-HMF and the measured Trolox equivalent antioxidant capacity in the leaf extracts. This relationship is reasonable, since the formation of 5-HMF is related to over-drying, exposure to elevated temperatures, pH value, and other storage conditions (Craig Jr et al., 1961; Janzowski et al., 2000). Such exposure would be expected to decrease the total antioxidant capacity, as exposure to oxygen over time consumes the anti-oxidants. A negative correlation was also detected between the content of 5-HMF and the measured inhibition of nitric oxide synthetase. Although the specific compounds in *H. sabdariffa* leaf extract responsible for the nitric oxide synthetase inhibition are not yet known, there is a relationship between 5-HMF, and a decrease in this activity. It is

possible that during processing, the compounds that imbue the leaf extracts with anti-inflammatory activity decomposed. These results indicate a relationship between the quantity of 5-HMF and a decrease in the measurable bioactivity for *H. sabdariffa* leaf extracts.

To further confirm that the formation of 5-HMF was due to the over-drying or other improper process steps, fresh leaf samples of *H. sabdariffa* were collected from field and immediately stored in -20 °C for further analysis without drying. The sample preparation procedure is the same as described above, but sample was extracted and analyzed immediately on the HPLC. The chemical profile of fresh leaves and dried leaves were compared with each other. As clearly shown in Figure 27, 5-HMF doesn't exist in freshly grown and immediately analyzed samples, but yet is observed in the dried one. These results suggest that to avoid potential health related problems and to prevent decreased anti-inflammatory activity, proper processing procedures must be implemented to avoid the formation of 5-HMF in the leaf samples.

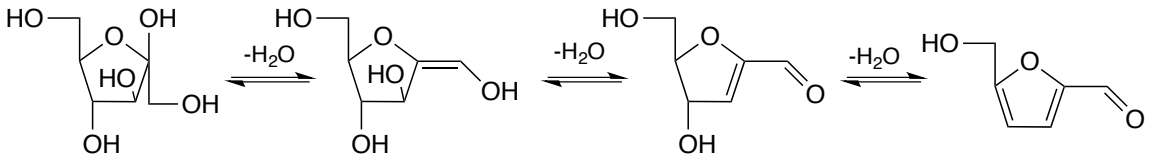

Figure 25. Hypothesized mechanism for the generation of 5-HMF from fructose

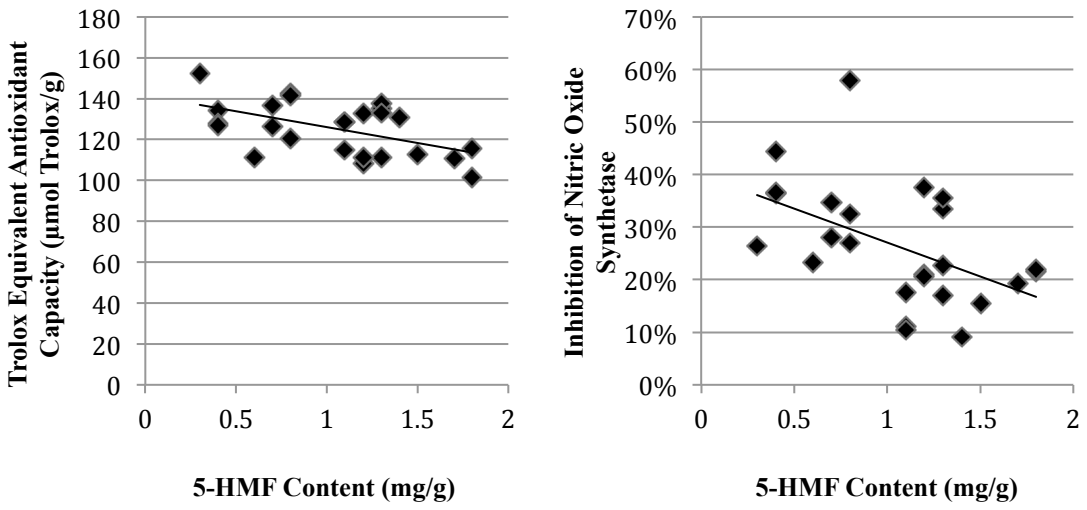

Figure 26. The relationship between 5-HMF from *Hibiscus sabdariffa* leaves content and *in vitro* bioactivities. (A) Negative correlation between 5-HMF and the measured Trolox Equivalent Antioxidant Capacity (R = -0.5305); (B) Negative correlation between 5-HMF content and inhibition of nitric oxide synthetase (NOS) activity (R = -0.4927).

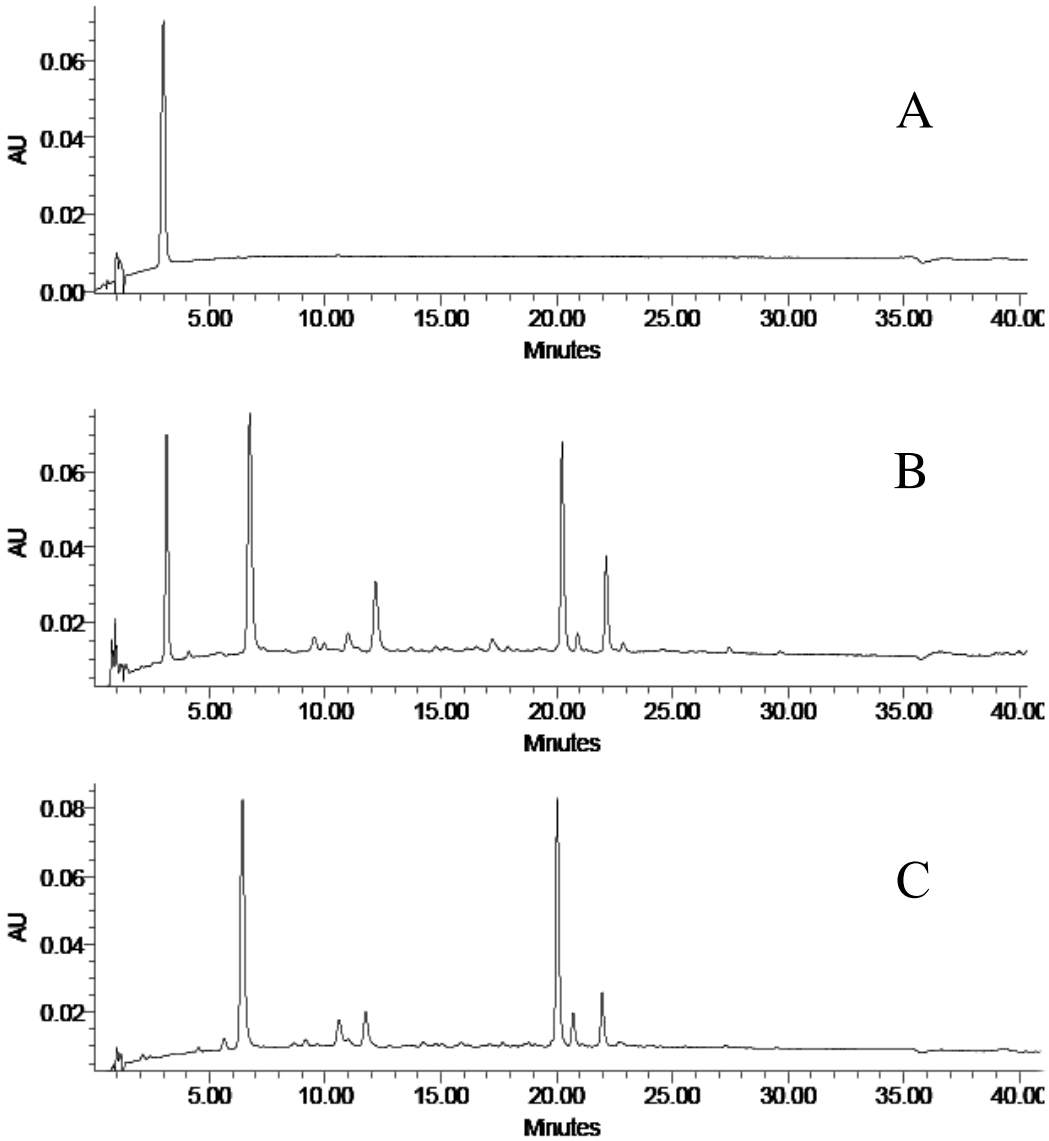

Figure 27. The chemical profile comparisons between fresh and dried *Hibiscus sabdariffa* leaves. (A): Standard compound 5-HMF; (B): Dried leaf sample; (C): Fresh leaf sample

3.4 Conclusion

Hibiscus sabdariffa leaves consumed in many countries were found to contain high levels of polyphenol compounds, mainly chlorogenic acid and its isomers, quercetin and kaempferol glycosides, which may contribute to its anti-oxidant capacity and anti-inflammatory activity. Leaf extracts can reduce the amount of free radicals in ABTS assay and the amount of nitric oxide produced in LPS induced cell lines, proving its traditional use as functional beverage. In addition, the compound 5-HMF was found in the dry hibiscus leaf samples for the first time, and that compound may have been formed due to improper processing or storage. The amount of 5-HMF in leaves has a moderate negative correlation with the antioxidant and anti-inflammatory activities, indicating its potential use as a marker for the quality control during the harvest process and manufacturing. As there is an increasing consumption of *H. sabdariffa* globally, this study would significantly help further biological research and its industrial applications in the future. Considering that some botanical supplements on market have similar phytochemical profiles to the polyphenols found in hibiscus, compounds contained in *H. sabdariffa* should also be of interest as a new source of these natural products.

3.5 Acknowledgement

This work was supported by the USDA-NIFA grants #2008-38814-04772 (to KLC) and #2012-38821-20092 (to KLC) and Southern University Agricultural Research and Extension Center. We also thank the Rutgers New Use Agriculture and Natural

Plant Products Program and the New Jersey Agricultural Experiment Station, Rutgers, The State University of New Jersey for their partial funding and support.

3.6 References

Chen, J.H., Wang, C.J., Wang, C.P., Sheu, J.Y., Lin, C.L., Lin, H.H., 2013. *Hibiscus sabdariffa* leaf polyphenolic extract inhibits LDL oxidation and foam cell formation involving up-regulation of LXRalpha/ABCA1 pathway. Food Chem 141, 397-406.

Clifford, M.N., Johnston, K.L., Knight, S., Kuhnert, N., 2003. Hierarchical scheme for LC-MSn identification of chlorogenic acids. J Agr Food Chem 51, 2900-2911.

Craig Jr, J., Aceto, N., Della Monica, E., 1961. Occurrence of 5-hydroxymethylfurfural in vacuum foam-dried whole milk and its relation to processing and storage. Journal of dairy science 44, 1827-1835.

Gosain, S., Ircchiaya, R., Sharma, P.C., Thareja, S., Kalra, A., Deep, A., Bhardwaj, T.R., 2010. Hypolipidemic effect of ethanolic extract from the leaves of *Hibiscus sabdariffa* L. in hyperlipidemic rats. Acta Pol Pharm 67, 179-184.

Güray, T., Tuncel, M., Uysal, U.D., 2013. A rapid determination of patulin using capillary zone electrophoresis and its application to analysis of apple juices. Journal of chromatographic science 51, 310-317.

Herrero, M., Castro-Puyana, M., Rocamora-Reverte, L., Ferragut, J.A., Cifuentes, A., Ibanez, E., 2012. Formation and relevance of 5-hydroxymethylfurfural in bioactive subcritical water extracts from olive leaves. Food Res Int 47, 31-37.

Janzowski, C., Glaab, V., Samimi, E., Schlatter, J., Eisenbrand, G., 2000. 5-Hydroxymethylfurfural: assessment of mutagenicity, DNA-damaging potential and reactivity towards cellular glutathione. Food and chemical toxicology : an international journal published for the British Industrial Biological Research Association 38, 801-809.

Lans, C.A., 2006. Ethnomedicines used in Trinidad and Tobago for urinary problems and diabetes mellitus. J Ethnobiol Ethnomed 2, 45.

Lin, H.H., Chan, K.C., Sheu, J.Y., Hsuan, S.W., Wang, C.J., Chen, J.H., 2012. *Hibiscus sabdariffa* leaf induces apoptosis of human prostate cancer cells in vitro and in vivo. Food Chem 132, 880-891.

Lin, H.H., Chen, J.H., Kuo, W.H., Wang, C.J., 2007. Chemopreventive properties of *Hibiscus sabdariffa* L. on human gastric carcinoma cells through apoptosis induction and JNK/p38 MAPK signaling activation. Chem-Biol Interact 165, 59-75.

Mahadevan, N., Shivali, K.P., Kamboj, P., 2009. *Hibiscus sabdariffa* Linn.-an overview. Natural product radiance 8, 77-83.

Monakhova, Y.B., Lachenmeier, D.W., 2012. The Margin of Exposure of 5-Hydroxymethylfurfural (HMF) in Alcoholic Beverages. Environmental health and toxicology 27, e2012016.

Ochani, P.C., D'Mello, P., 2009. Antioxidant and antihyperlipidemic activity of *Hibiscus sabdariffa* Linn. leaves and calyces extracts in rats. Indian journal of experimental biology 47, 276.

Re, R., Pellegrini, N., Proteggente, A., Pannala, A., Yang, M., Rice-Evans, C., 1999. Antioxidant activity applying an improved ABTS radical cation decolorization assay. Free radical biology & medicine 26, 1231-1237.

Rodriguez-Medina, I.C., Beltran-Debon, R., Molina, V.M., Alonso-Villaverde, C., Joven, J., Menendez, J.A., Segura-Carretero, A., Fernandez-Gutierrez, A., 2009. Direct characterization of aqueous extract of *Hibiscus sabdariffa* using HPLC with diode array detection coupled to ESI and ion trap MS. Journal of separation science 32, 3441-3448.

Roman-Leshkov, Y., Chheda, J.N., Dumesic, J.A., 2006. Phase modifiers promote efficient production of hydroxymethylfurfural from fructose. Science 312, 1933-1937.

Ross, I., 2003. *Hibiscus sabdariffa*, Medicinal Plants of the World. Humana Press, pp. 267-275.

Singleton, V.L., 1985. Citation Classic - Colorimetry of Total Phenolics with Phosphomolybdic-Phosphotungstic Acid Reagents. Cc/Agr Biol Environ, 18-18.

Villani, T., Juliani, R., Simon, E.J., Wu, Q.L., 2013. *Hibiscus sabdariffa*: Phytochemistry, Quality Control, and Health Properties. ACS Symposium Series 1127, 209–230.

Xu, Y.P., Simon, J.E., Ferruzzi, M.G., Ho, L., Pasinetti, G.M., Wu, Q.L., 2012. Quantification of anthocyanidins in the grapes and grape juice products with acid assisted hydrolysis using LC/MS. J Funct Foods 4, 710-717.

Xu, Y.P., Simon, J.E., Welch, C., Wightman, J.D., Ferruzzi, M.G., Ho, L., Passinetti, G.M., Wu, Q.L., 2011. Survey of Polyphenol Constituents in Grapes and Grape-Derived Products. Journal of agricultural and food chemistry 59, 10586-10593.

Zhao, M., Xu, J., Qian, D.W., Guo, J.M., Jiang, S., Shang, E.X., Duan, J.A., Du, L.Y., 2014. Characterization of the metabolism of 5-hydroxymethylfurfural by human intestinal microflora using ultra-high performance liquid chromatography-quadrupole time-of-flight mass spectrometry. Anal Methods-Uk 6, 3826-3833.

CHAPTER FOUR

Identification of Kinkéloids in *Combretum micranthum*

4.1 Introduction

Kinkéliba (*Combretum micranthum*), a popular African herbal tea of Senegal and neighboring countries has been playing an important role as a hot beverage and in traditional medicine in West Africa. Our previous research, showed that different leaf extracts of kinkéliba can induce glucose-lowering activity, which would be potentially applied for the treatment of diabetes (Welch, 2010; Simon et al. 2014). Previous phytochemical profile investigation of *C. micranthum* from Senegal in our lab has led to the isolation and identification of four groups of novel skeleton nitrogen-containing compounds. The structures of these compounds were preliminarily identified using LC-MS at the beginning of the study, which indicated the existence of a nitrogen moiety. Through further chromatographic separation and the elucidation using NMR, the basic structure frame was identified as a series of piperidine-flavan alkaloids with increasing number of hydroxyl groups attached (Figure 28). These compounds were named as kinkéloids in honor of this plant. Simultaneously, we observed that that each group of the kinkéloids has two or more chiral centers and two regioisomers with piperidine ring attached at either 6 or 8 position. Because of the limited amount of compounds purified, even if the existence of different regioisomers, as shown on LC/MS were understood, we could not further distinguish them from the plant material. Thus, in this study and in

order to elucidate their identities, the kinkéloids A were synthesized through three-step semi-synthetic reactions. The regioisomers of kinkéloids in the plant extract, which had not been resolved in previous study, were differentiated through comparison with synthetic standards. The chirality analysis of the kinkéloids is still undergoing in our lab.

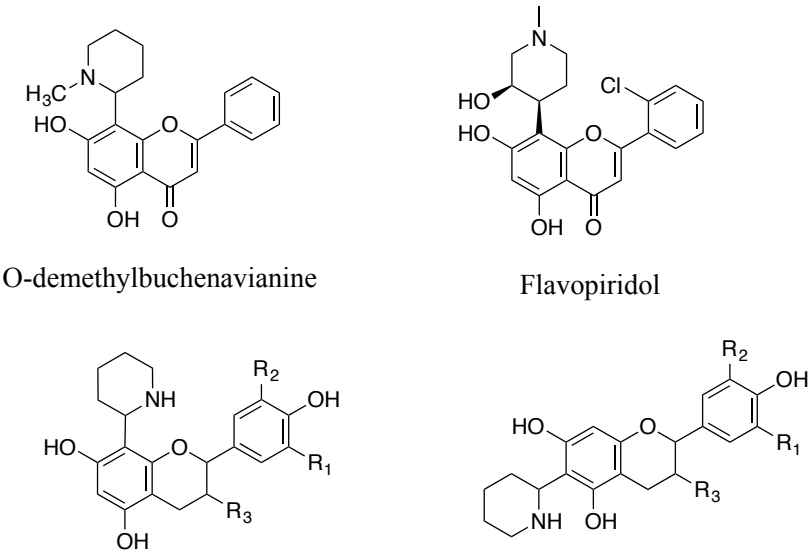

1 Kinkeloids A: R_1 = H, R_2 = H, R_3 = H; **3** Kinkeloids C: R_1 = OH, R_2 = OH, R_3 = H
2 Kinkeloids B: R_1 = OH, R_2 = H, R_3 = H; **4** Kinkeloids D: R_1 = OH, R_2 = OH, R_3 = OH

Figure 28. The structure of *O*-demethylbuchenavianine, flavopiridol and kinkéloids

Kinkéloids, as a group of novel skeleton flavan alkaloids, belong to a small family of natural products, the flavonoid alkaloids, which is characterized by two components in the structure: a flavonoid moiety and a nitrogenous moiety. Compounds of flavonoid alkaloid family have shown a wide range of biological activities including anti-HIV, anti-

cancer and anti-diabetic activities (Beutler et al., 1992; Mohana Kumara et al., 2012; Jang et al., 2009). For example, flavopiridol (Figure 28) derived from natural product chrome alkaloid rohitukine, which was originally extracted from *Dysoxylum binectariferum*, can inhibit the activity of cyclin-dependent kinases (CDKs) and is being developed in clinical trial for cancer treatment (Tan and Swain, 2002). Compound *O*-demethylbuchenavianine from *Buchenavia capitata* has shown HIV-inhibitory activity with EC_{50} of 0.26 uM (Beutler et al., 1992).

A biosynthetic pathway of these novel kinkéloids in the plant was proposed based upon the published literature and using *Camellia sinensis* (the evergreen shrub used as the source of Chinese tea) as a model given that many of the same amino acids and condensed tannins are found also in kinkéliba. It was suggested that some amino acid(s), constituents found in Chinese tea products would be transformed to a number of metabolites, which could react with polyphenols through cross-condensation reactions to form novel nitrogen-containing flavonoids (Diana and Cirrincione, 2015; Tanaka et al., 2005). For example, compound ethylpyrrolidinonyl theasinensin, which was first discovered in black tea extract, is formed through a reaction between polyphenol theasinensin A with N^5-ethyl-L-glutamine (Tanaka et al., 2005). Considering the similarities between compound kinkéloids and ethylpyrrolidinonyl theasinensin, we propose in our study that the piperidine may originally come from amino acid L-lysine through two-step metabolism reactions. Then an intermediate compound Δ^1-piperideine may react with the flavan molecule through series of Mannich reactions. We tested this using this same reaction to generate artificially the synthesis of kinkéloids.

4.2 Materials and Methods

4.2.1 Plant Materials

Kinkéliba samples utilized for this study was collected from shrubs within a localized population in Leen, Pout, in central Senegal. Plant materials were gathered by ASNAPP (Agribusiness In Sustainable Natural African Plant Products)-Senegal, a local registered Senegalese NGO, accompanied by members of the community and with prior written consent from the community and community leaders for collection and scientific analysis. Locally communities often dry the leaves and branch together forming a long bundle and then sold locally as an herbal tea. The leaves and branches were manually harvested, air-dried under shade in ambient conditions and off the ground on white tarp. Once dried, the leaves were manually separated from the branches, and cleaned. The trees from which the leaves were harvested were taxonomically identified as *Combretum micranthum* by the people who have been working with this same plant population and species in Senegal with the community as an indigenous herbal tea to provide additional local income opportunities; and was later confirmed by the staff of ASNAPP-Senegal trained in the identification of Senegalese botanicals. The dried leaf material were originally air-shipped to South Africa where the leaves were processed by Cape Natural Teas, Cape Town, South Africa and packaged into a Mpuntu line of African herbal teas and then air-shipped to Rutgers University for chemical analysis. Additional dried leaves from same plant populations were air-shipped with the proper forms directly from ASNAPP-Senegal, Dakar, Senegal to Rutgers University for chemical profiling and other studies.

4.2.2 Equipment and Methods

1D and 2D NMR spectroscopy were performed on a Bruker Avance 400 MHz spectrometer (Billerica, MA). HPLC grade solvents including water, methanol, ethanol, acetonitrile and hydrochloric acid were purchased from Fisher Scientific (Fair Lawn, NJ). Column chromatography was performed using silica gel (230 - 400 mesh; Selecto Scientific, Suwanee, GA), Sephadex LH-20 (25-100 μ, Sigma-Aldrich, St. Louis, MO). Preparative HPLC was performed on a Waters 600/2487 system with a UV detector. Analytical LC-MS was performed on Hewlett-Packard Agilent 1100 series HPLC-MSD (Agilent Technologies, Waldbronn, Germany) equipped with a quaternary pump system, a degasser, an auto-sampler, a DAD detector, a MSD trap with electrospray ion source (ESI). The electrospray ion mass spectrometer was performed under positive model with scan range from *m/z* 100 to 800. The needle voltage was 3.5 kV for positive mode, nitrogen (99.999%) flow rate was 12 L/min and the capillary temperature was 350˚C. Nitrogen was set as nebulizer at 60 psi and helium as a collision gas. Software HP ChemStation and Data Analysis 4.2 were used.

4.2.3 Extraction and Sample Preparation

The sample preparation of kinkéloid was based on previous published reports from our laboratory (Welch, 2010). Basically, the dried leaves were ground to a fine powder followed by extraction with ethanol two times, and twenty-four hour maceration using 80%

ethanol/water (v/v). The combined extract was concentrated using a rotary evaporator and re-dissolved in water/ethanol (95:5, v/v), which was then partitioned between hexane (labeled LH), chloroform (LC), ethyl acetate (LE), and *n*-butanol (LB), with the remaining water fraction as LW. The *n*-butanol fraction, LB, was further separated by silica gel column chromatography using methanol in chloroform in gradient from 0 to 100%. The eluted fractions were combined into 20 final fractions, LB-1 to LB-20. The thirteen fraction LB-1 was purified by preparative HPLC (10% to 40% acetonitrile/water with 0.1% formic acid) with column Luna Phenyl Hexyl (3 μm, 3.9 x 150 mm) to yield kinkéloids A. Fractions LB-16, 17, 19 were purified by preparative HPLC (15% to 40% acetonitrile/water with 0.1% formic acid)) with column Microsorb C_{18} (10 μm, 41.4 x 300 mm) and yielded kinkéloids B, C, D, respectively (Welch, 2010). The NMR data of each purified compounds and more detailed experimental procedures have been described by Cara Welch in her dissertation while working in this laboratory (Welch, 2010).

4.2.4 Semi-synthesis of Kinkéloids A

Step 1. Synthesis of tri-TMS protected naringenin

To a solution of naringenin (272 mg, 1.00 mmol) in dry pyridine (1 mL), hexamethyldisilazane (HMDS, 1 ml) and trimethylchlorosilane (TMSCl, 0.6 ml) were added. The mixture was stirred with a stirring bar at room temperature for 1 hour. Then the volatile constituents were distilled off under reduced pressure. The residue was suspended in solvent toluene and the precipitate was filtered off.

Step 2. Synthesis o f 2-(4-hydroxyphenyl)chromane-5,7-diol

The toluene solution was concentrated under reduced pressure and the residue was re-dissolved in tetrahydrofuran (THF, 2.5 ml) followed by addition of $LiBH_4$ (11 mg, 0.5 mmol). The mixture was further stirred at room temperature for half an hour. Then 0.5 mg of methyl orange and sodium cyanoborohydride (63 mg, 1.0 mmol) were added into the solution. Then the mixture was slowly titrated using hydrochloric acid solution (1 N) with the release of hydrogen to the point when the color of the solution turns into red. The color of the solution was kept in red by further slow addition of HCl solution. After approximate 2 hours, extra amount of hydrochloric acid (1 to 1.5 ml) was added to keep the color permanent and the reaction was stirred for overnight at room temperature. Then solvent THF was distilled off under reduced pressure and the residue was extracted with ethyl acetate and washed with 1 N hydrochloric acid solution, distilled water, and brine. The organic phase was dried using anhydrous sodium sulfate, concentrated under vacuum and purified on silica gel column using 10 to 30 % ethyl acetate in hexane. The final yield is 65%. ^{1}H-NMR (400 MHz, MeOD-d_4): δ 7.22 (d, 2H, J = 8.6 Hz, H-3', 5'), 6.77 (d, 2H, *J* = 8.6 Hz, H-2' 6'), 5.90 (d, 1H, *J* =2.3, H-6), 5.83 (d, 1H, *J* =2.3, H-8), 4.82 (br, d, 1H, H-2), 2.54-2.71 (m, 2H, H-4), 1.87-2.13 (m, 2H, H-3). ^{13}C NMR (100 MHz, MeOD-d4) δ 158.09, 157.99, 157.49, 157.33 (C-5, 7, 9, 4'), 134.34 (C-1'), 128.47 (C-3', 5'), 116.05 (C-2', 6'), 96.02 (C-6), 95.94 (C-8), 78.84 (C-2), 30.88 (C-3), 20.43 (C-4)

Step 3. Synthesis of kinkéloids A

The synthesized flavan intermediate (258 mg, 1.0 mmol) from step 2 was dissolved in 2 ml of THF solution followed by addition of 4 ml of water. Then the solution was added Δ^1- piperideine (1.0 eq) dropwise. After being stirred at 80 °C for 4 hours with the protection of nitrogen gas, the solution was concentrated under reduced pressure and loaded directly on silica gel column for purification with 15 % methanol in dichloromethane as elution solvent. White solid with pale yellow was achieved as kinkéloids A. Further separation of 6-, 8-, regioisomers of kinkéloids A, was performed on Sephadex LH-20 using 100% methanol as elution solvent. ^{1}H NMR (400 MHz, DMSO-d_6, 6-piperidyl kinkéloids A) δ 1.41-1.76 (6H, m, H-4'', 5'', 6''), 1.83 (1H, m, H-3), 2.01 (1H m, H-3), 2.53 (2H, m, H-4), 2.67 (1H, m, H-3''), 3.12 (1H, m, H-3''), 4.15 (1H, m, H-1''), 4.80 (1H, H-2), 5.82 (1H, H-8), 6.75 (2H, H-2', 6'), 7.17 (2H, H-3', 5'); ^{13}C NMR (100 MHz, DMSO-d6) δ 19.29 (C-4), 23.79, 24.06 (C-4'', 5'') 28.89 (C-3), 29.83 (C-6''), 45.60 (C-3'') 52.74 (C-1''), 76.41 (C-2), 94.17 (C-8), 101.18 (C-10), 106.71 (C-6), 114.98 (C-2', 6'), 127.37 (C-3', 5'), 131.97 (C-1'), 156.93, 155.53, 154.87, 153.38 (C-5, 7, 9, 4'). ^{1}H NMR (400 MHz, DMSO-d_6, 8-piperidyl kinkéloids A) δ 1.51-1.80 (6H, m, H-4'', 5'', 6''), 1.81 (1H, m, H-3), 2.06 (1H m, H-3), 2.51 (2H, m, H-4), 2.87 (1H, m, H-3''), 3.24 (1H, m, H-3''), 4.30 (1H, m, H-1''), 5.02 (1H, m, H-2), 6.14 (1H, H-6), 6.77 (2H, d, H-2', 6'), 7.20 (2H, d, H-3', 5'), ^{13}C NMR (100 MHz, DMSO-d6) δ 19.64 (C-4), 21.67, 22.93 (C-4'', 5'') 28.60 (C-6''), 28.67 (C-3), 45.45 (C-3'') 52.70 (C-1''), 76.31 (C-2), 95.35 (C-6), 101.78 (C-10), 104.80 (C-8), 114.98 (C-2', 6'), 127.29 (C-3', 5'), 157.00, 155.51, 154.06, 153.90 (C-5, 7, 9, 4').

4.3 Results and Discussion

4.3.1 Identification of Kinkéloids

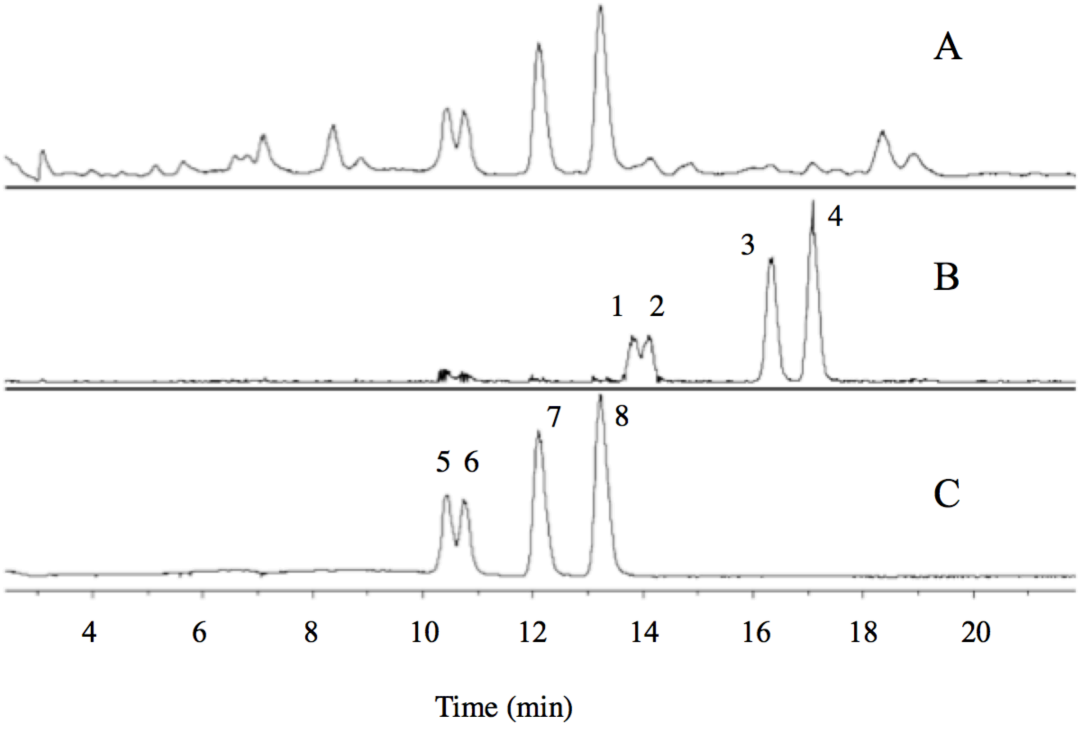

Figure 29. Representative chromatograms of methanol extract of kinkéliba. A: The total ion chromatogram; B: The extracted ion chromatogram at *m/z* 342 of kinkéloids A; C: The extracted ion chromatogram at *m/z* 358 of kinkéloids B

From the methanol extract of kinkéliba, a total of four series of kinkéloids were separated and identified using LC/MS (Figure 29) and NMR. The extraction and identification was previously investigated by Welch (2010) and Simon et al (2014) and the original NMR

data of purified kinkéloids was previously described (Welch, 2010; Simon et al. 2014). As determined by mass spectrometry, their molecular weights are 341 Da (kinkéloids A), 357 Da (kinkéloids B), 373 Da (kinkéloids C), 389 Da (kinkéloids D), indicating that these compounds differ only by one hydroxyl group and the oxygen atom accounts for the 16 units difference. Kinkéloids B, the most abundant component among these series, was obtained as white solid. Its molecular formula was established as $C_{20}H_{23}NO_5$ from the analysis of HRESIMS at *m/z* 358.1638 ($[M+H]^+$). The odd number of molecular weight (357 Da) deduced from molecular ion suggests the presence of a nitrogen atom in the molecule. It shares similar UV absorption spectrum with flavan molecules with maximum absorption at ~ 280 nm (Zhang et al., 2006). The purified compounds were analyzed on NMR with methanol-d_4 and the data has been fully described (Welch, 2010). In 1H-1H COSY NMR, the correlation between one methine (δ 5.0 ppm, H-2) and two methylene groups (δ 2.13 & 1.87 ppm, H-3; δ 2.62 ppm, H-4) suggests the presence of partial structure $–CH_2-CH_2-CH-$. The methine (-CH-) group was attached to an oxygen atom based on its shift to down field in ^1H and ^{13}C NMR spectra. Its long range coupling with aromatic carbon (δ 134.02 ppm, C-1') in ring C was also observed in HMBC spectrum. One methylene group ($-CH_2-$, δ 2.62 ppm, H-4) has a long-range correlation with another aromatic carbon (δ 103.1 ppm, C-10) in ring B, and this carbon has no hydrogen attached as shown in HMQC. The 3', 4'-dihydroxy group in ring C was deduced from a typical ABX aromatic resonances system between δ 6.86 ppm (H-2'), δ 6.78 ppm (H-5') and δ 6.72 ppm (H-6') (Liu et al., 2006). The appearance of only one proton signal around δ 6.07 indicates that one of the 6 or 8 position of ring B is substituted. Totally, there are fifteen signals displaced in the ^{13}C NMR spectrum, parts of

which match the structure of flavan very well. These include five oxygenated aromatic carbons (δ 146.2, 146.5, 155.0, 155.6, 157.9 ppm); seven non-oxygenated aromatic carbons (δ 96.0, 103.0, 103.1, 114.4, 116.2, 118.7, 134.6 ppm); two methylene carbons (δ 20.1 ppm, C-4; δ 30.3 ppm, C-3) and one methine carbon (δ 79.5 ppm). The flavan skeleton was further confirmed through the comparison with synthesized analytical standard 3', 4', 5, 7-tetrahydroxyflavan (see Chapter 5).

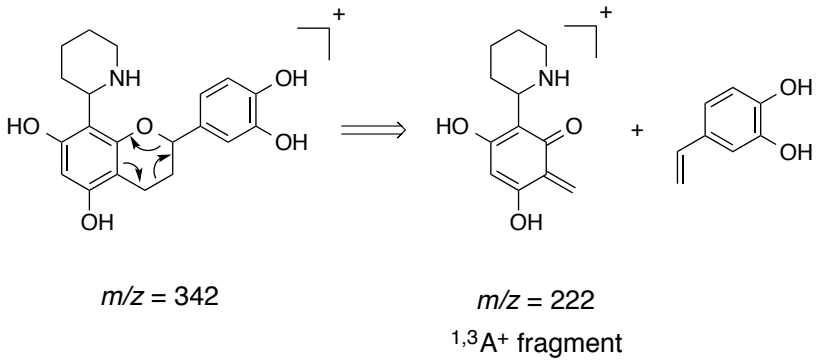

Figure 30. The retro Diels-Alder (RDA) mass spectrometric fragmentation of kinkéloids B (8-substituted isomer)

The weight difference between the kinkéloid and their corresponding flavan is 84 Da with a formula of $C_5H_{10}N$, indicating a ring structure may exist in the substituted group. Considering the lack of methyl group and double bonds in the substitute, we hypothesized that a six-member ring structure, piperidyl group, exists in the substitute. The identity of the piperidyl group was initially determined through the main mass fragment ion ($^{1,3}A^+$, *m/z* = 222) formed in LC/MS analysis (Figure 30). The $^{1,3}A^+$

fragment ion formed through retro Diels-Alder (RDA) cleavage in kinkéloid is 83 Da heavier than the one from flavan molecule ($^{1,3}A^{+}$, *m/z* = 139) (Tsimogiannis et al., 2007). Based on the observed disappearance of 6- or 8-H in the ^{1}H-NMR spectrum, the piperidine ring was determined to be located at either one of these two positions. Further analysis of 1H-1H COSY, HMQC, and HMBC spectra confirmed that the piperidine ring is attached at 6 / 8 position of ring B with nitrogen locates at 2'' position. Hydrogen (δ 4.54 ppm, H-1'') attached carbon 1'' was much shifted to the down field by nitrogen atom and aromatic ring B in ^{1}H and ^{13}C NMR spectra. It also has a J^{3} coupling with two oxygenated aromatic carbons C5, C7 (δ155.7 ppm, δ 155.0 ppm) or C7, C9 (δ 155.0, 158.0 ppm) in HMBC analysis. In ^{1}H NMR, signals at δ 2.97 - 3.40 ppm (1H) were assigned to H-3''; δ 1.62 - 2.31 ppm (6H) were assigned to H-4'', H-5'', H-6''. Their ^{13}C signals mainly locating at the up-field are assigned by HSQC to be δ 46.82 ppm (C-3''), δ 24.23 ppm (C-4''), δ 23.53 ppm (C-5''), δ 29.54 ppm (C-6''). The signals of H-3'', C-3'' were shifted to down-field by nitrogen molecule at position 2''. The identity of the piperidine ring was further confirmed through the NMR spectra comparison with previous reports (Ahond et al., 1984). The major 1H-1H COSY and HMBC of kinkéloids B are illustrated in Figure 31. Through similar ways, the overall structures of kinkéloids C and D were also deduced from the analysis of LC/MS and NMR data (Welch, 2010). The extracted ion chromatograms of kinkéloids C and D indicated that they may have much more structural isomers and be more complex than kinkéloids A and B (Figure 32). These must be caused by extra hydroxyl groups, which could be attached at either 3 position with one more chiral bond, or on the B ring, or may be both, making the identification of each isomer even more challenging. Previous phytochemical

investigation in our lab has successfully purified and confirmed the existence of some structures of C and D using NMR, without designation of chiral bonds (Welch, 2010) (Figure 32).

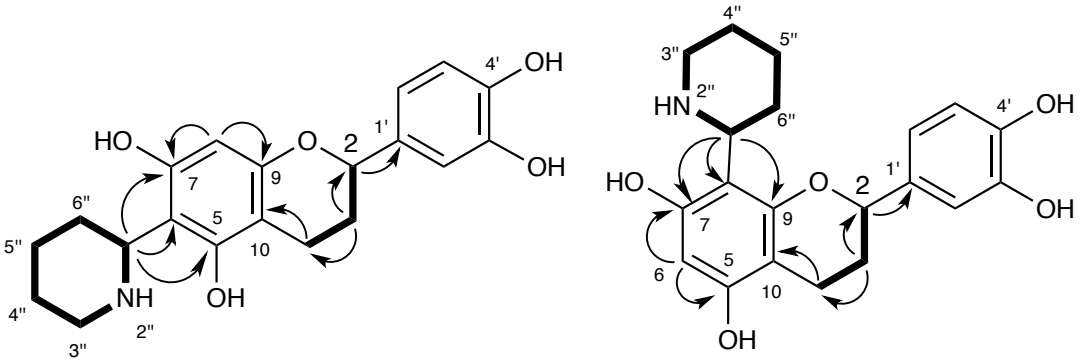

Figure 31. The structure of kinkéloids B and key ^{1}H-^{1}H COSY (▬) and HMBC (H→C) correlations

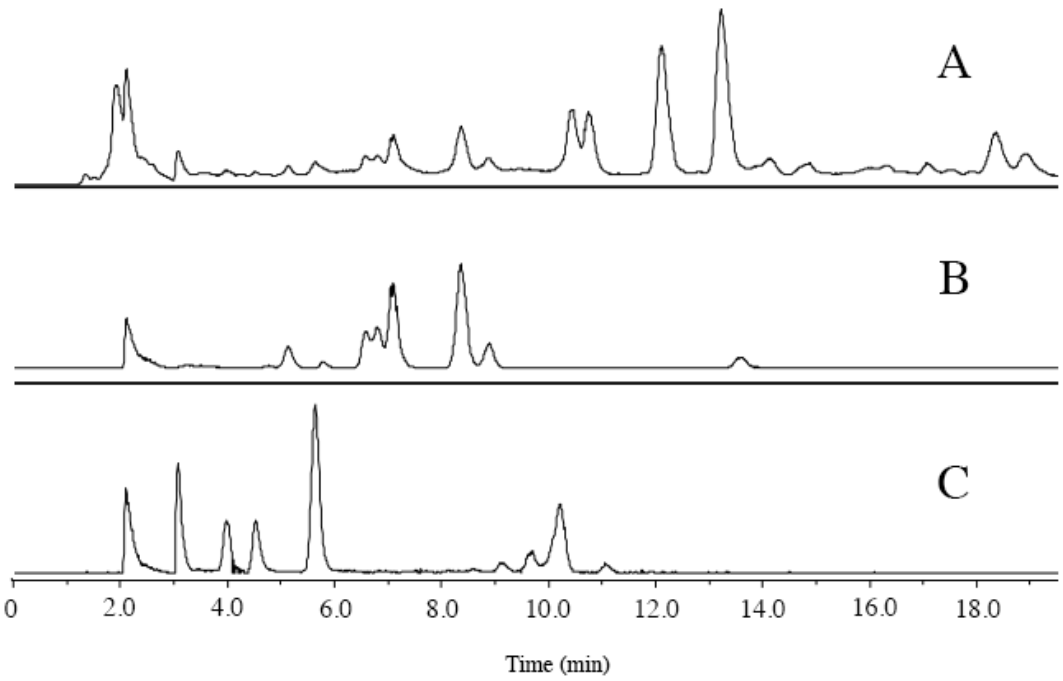

Figure 32. The chromatograms of methanol extract of kinkéliba. A: The total ion chromatogram; B: The extracted ion chromatogram at kinkéloids C *m/z* 374; C: The extracted ion chromatogram at kinkéloids D *m/z* 390

4.3.2 Semi-synthesis of Kinkéloids A

Due to the close physiochemical properties, kinkéloids in one series were isolated as a mixture of two sets of regioisomers with the piperidine ring attached at the 6 and 8 positions, respectively. The 6-H or 8-H has low pKa value and could exchange between free deuterium proton, resulting in "decreased" signals on the ^{1}H-NMR. This phenomenon was observed in our previous experiments when MeOD-d_4 was used as NMR solvent (Welch, 2010). For group A and B, there are two chiral centers present at position 2 and 1'', each set would be further divided into 4 individual compounds. So A

and B group of kinkéloids may have 8 different isomers. It is quite challenging to separate and differentiate each isomer considering their close physicochemical properties and subtle differences on NMR spectra. In order to further confirm the deduced kinkéloids structures and distinguish 6, 8 regioisomers, kinkéloids A were scaled up through artificially synthesis and its 6, 8 regioisomers were separated using Sephadex column LH-20. After comparison with the extract of kinkéliba on HPLC, the identity of kinkéloids A was further confirmed and elucidated (Figure 34). As shown in Figure 34, peak 1 and 2 belong to one regioisomer group, while peak 3 and 4 belong to anther group. Literature data supports that H-6/C-6 and H-8/C-8 have very close chemical shift with H-8/C-6 at a slightly higher field than H-6/C-8 in ^{1}H-NMR (Shen et al., 1993). The analysis method was adopted by a published paper (Cheng et al., 2008). Therefore, peaks 1, 2 in Figure 29 were assigned as 6-substituted isomer, and peak 3, 4 were assigned as 8-substituted isomer. The assignments of H-6/C-6 and H-8/C-6 were also supported by HMBC analysis (Figure 31). Conclusive confirmation of each isomer using X-ray crystallography may be necessary and could be done in the future. The chirality determination of carbons 2 and 1” of kinkéloids is discussed in Chapter 7.

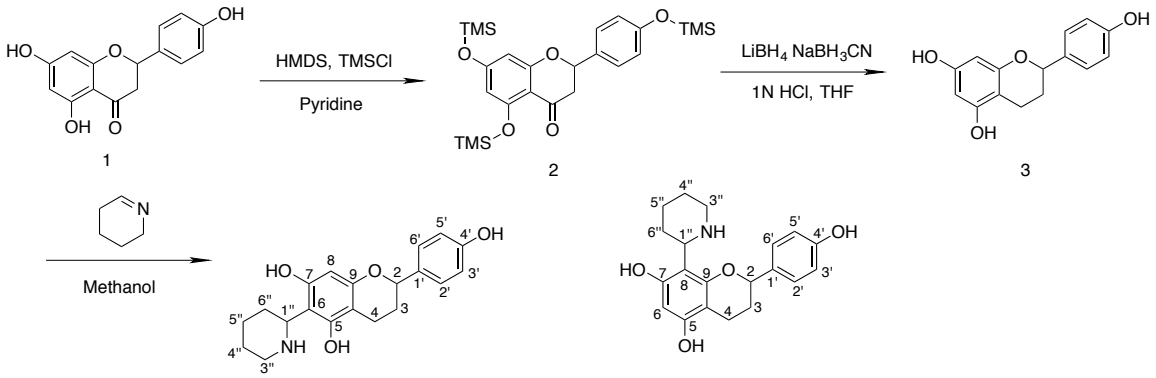

Figure 33. The semi-synthesis route of kinkéloids A

The synthesis route starts from material naringenin (**1**), which was protected with trimethylsilyl (TMS) groups under basic condition through a reaction with HMDS and TMSCl to yield intermediate compound (**2**) (Figure 33). Then the carbonyl group of compound (**2**) was deoxygenated using $NaBH_3CN$ and the TMS groups were subsequently removed in acidic condition to give the flavan intermediate (**3**). Through the well-known Mannich reaction, freshly prepared Δ^1- piperideine was attached to the 6 / 8 position of flavan intermediate (**3**) to yield the desired kinkéloids A (Claxton et al., 1988). This synthesis method described could be used to scale-up the production of kinkéloids for further bioactivity studies. We observed that the kinkéloids A would turn purple for a few hours if preserved in the air, indicating its instability. This may be caused by the oxidation at nitrogen atom and the formation of amine oxide or some other oxidized products. As observed on the chromatogram by us, it is a mixture of several oxidized products. We also noticed that the kinkéloids in the plant would be stable up to several years without being oxidized. Why there appears so much stability in the

kinkéloids when in the dried leaf in comparison to the pure artificially synthesized ones remains unclear.

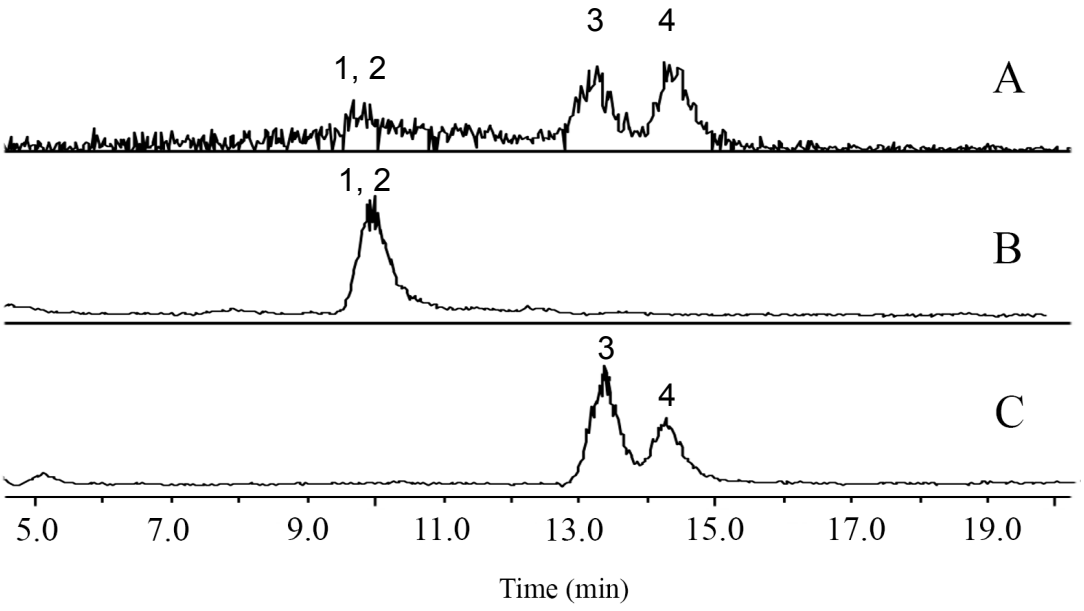

Figure 34. Comparison of kinkéloids A from plant extract to the synthesized ones. A: Extracted total ion chromatogram of kinkéliba methanol extract at *m/z* 342; B: The synthesized compound 6-piperidyl kinkéloids A; C: The synthesized compound 8-piperidyl kinkéloids

4.3.3 Tentative Biosynthetic Pathway Analysis

The biosynthetic pathway of the discovered kinkéloids was proposed based on literature review and using the proposed biochemistry reported from the secondary plant products from black tea as a model. The biosynthesis of kinkéloids initially proceeds from the flavonoid pathway, starting from amino acid phenylalanine, to *trans*-cinnamate, chalcone,

flavanone, flavanol, anthocyanidin, and to intermediate compound flavan (Figure 35) (Winkel-Shirley, 2002; Winkel-Shirley, 2001; Shirley, 1996). Like most piperidine alkaloids, the piperidyl group of kinkéloids may also come from Δ^1- piperideine-derived lysine (Szőke et al., 2013; Diana and Cirrincione, 2015). L-lysine can undergo decarboxylation under the catalysis of pyridoxal-5'-phosphate dependent enzymes and produce diamine compound cadaverine. The cadaverine can undergo oxidative deamidation and leads to compound 5-aminopentanal, which could cyclize intro compound Δ^1- piperideine. Then, the formed imine Δ^1- piperideine may couple to flavan molecule at position 6 or 8 through Mannich reaction to yield the discovered kinkéloids in *C. micranthum* Overall, the novel discovered molecules kinkéloids might originally come from two amino acids, L-phenylalanine and L-lysine. The detailed proposed biosynthetic mechanism is presented in Figure 35. The function of kinkéloids in the plant materials is still unknown. There are also very limited researches reported in other flavonoid alkaloids functions studies. Due to the unique structure, as a combination of a flavonoid moiety and a nitrogen moiety, flavonoid alkaloids may involve in the cell signaling pathways or serve as protective substances against animal or insect attacks. It would also be possible that they may be formed as byproducts of plant metabolism.

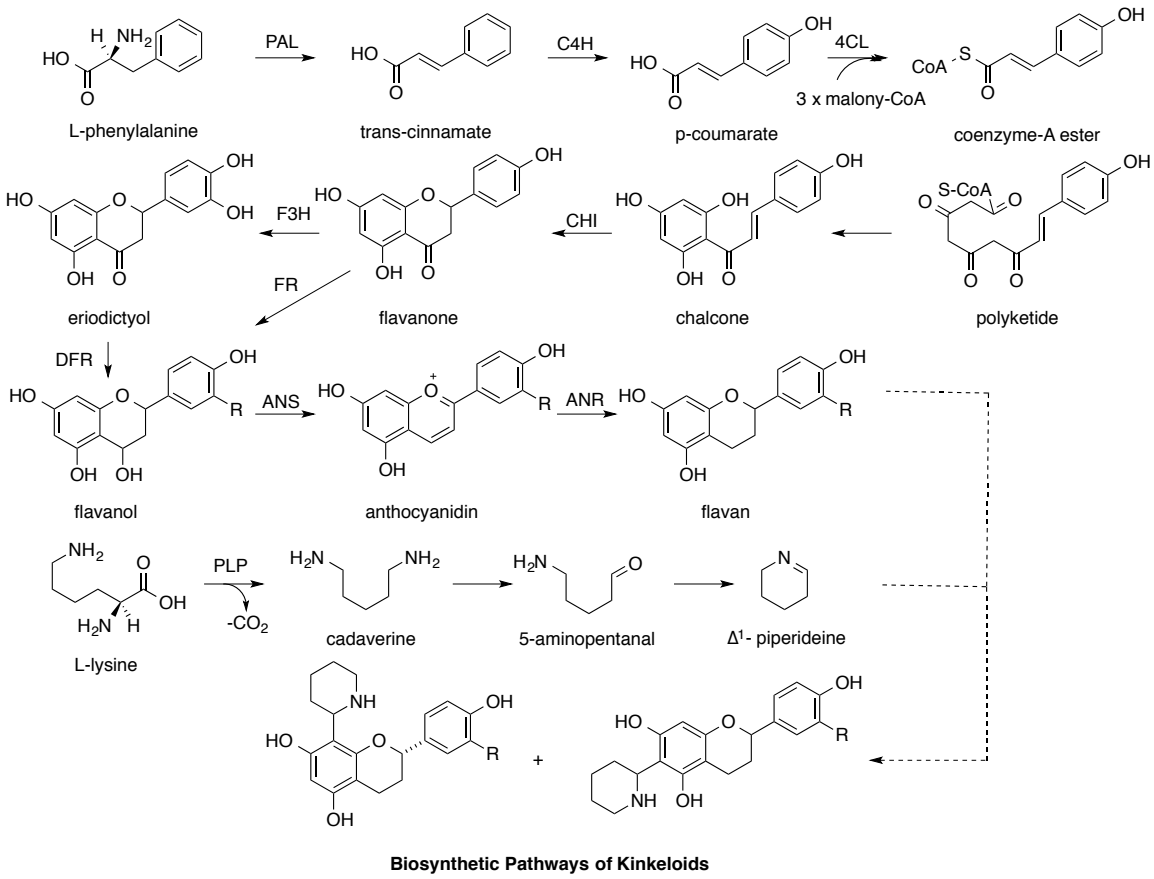

Figure 35. Known (solid arrows) and proposed (dashed arrows) biosynthetic pathways of kinkéloids. Abbreviations: R: H or OH; PAL: Phenylalanine ammonia lyase; C4H: Cinnamate 4-hydroxylase; 4CL: 4-coumarate: CoA ligase; CHS: Chalcone synthase; CHI: Chalcone flavanone isomerase; F3H: Flavanone 3-hydroxylase; FR: Flavanone reductase; DFR: Dihydroxyflavanone reductase; ANS: Anthocyanidin synthase; ANR: Anthocyanidin reductase; PLP: Pyridoxal-5'-phosphate

4.4 Conclusion

A series of novel skeleton flavan alkaloids compounds from kinkéliba were further examined in this study. The chemical profile of each group of kinkéloids were investigated using LC-MS, and which indicated that C and D groups are more complex than groups A and B. Kinkéloids A were artificially semi-synthesized from naturally abundant flavanone naringenin. The synthesized compounds serve as standard and confirmed the structure of kinkéloids identified from plant kinkéliba, even if chiral centers still remain unsolved. Semi-synthetic methods would be used for the convenient and efficient scale-up of kinkéloids preparation and for pharmacological activity studies. The two groups of regioisomers of kinkéloids A generated from synthesis were successfully separated on reverse phase HPLC and compared with the ones from plant extract. We observed that kinkéloids A were not stable and could be oxidized and turn to purple color when exposed to the air. This may be caused the oxidation of amine group in the air. Purification each regioisomer group was achieved on column of Sephadex LH20. One of the possible biosynthetic pathways of kinkéloids was proposed based on literature review, which indicates that kinkéloids may originally come from two amino acids L-lysine and L-phenylalanine.

4.6 Acknowledgements

We thank Babou Diouf and Diatta Malainy, Agri-Business in Sustainable Natural African Plant Product, ASNAPP-Senegal (www.asnapp.org) with whom we worked to commercialize this indigenous Senegalese plant as an herbal tea as an income generating

activity with the Senegalese communities. We thank the Senegalese communities who both worked so closely with us and also encouraged us to pursue new scientific-driven food and medicinal applications on this species to generate greater market interest in the use of this indigenous Senegalese plant. We thank the communities, which allowed us to carry out studies with the kinkéliba that was wild harvested manually by the authors, ANSAPP-Senegal and community members together on their lands. We recognize and thank the USAID for their support of our projects in sub-Saharan Africa to strengthen in-country African natural products industry through their support of the Partnership for Food and Industry in Natural Products (PFID/NP), a university led program supported by the Office of Economic Growth, Agriculture and Trade (EGAT/AG) of the USAID (Contract Award No. AEG-A-00-04-00012-00). The USAID project provided funding that was focused at the development of kinkéliba tea as a community income generating activity. We thank the New Jersey Agricultural Experiment Station and the School of Environmental and Biological Sciences at Rutgers and the New Use Agriculture and National Plant Products Program. This work was conducted as part of the dissertation research of Jing Zhen and also of Cara Welch.

4.7 References

Ahond, A., Fournet, A., Moretti, C., Philogene, E., Poupat, C., Thoison, O., Potier, P., 1984. Premiers alcaloides vrais isoles de Combretacees, Buchenavia macrophylla Eichl. et *Buchenavia capitata* Eichl. Bulletin de la Société chimique de France.

Beutler, J.A., Cardellina, J.H., Mcmahon, J.B., Boyd, M.R., 1992. Anti-Hiv and Cytotoxic Alkaloids from *Buchenavia-capitata*. J Nat Prod 55, 207-213.

Cheng, K.W., Wong, C.C., Cho, C.K., Chu, I.K., Sze, K.H., Lo, C., Chen, F., Wang, M.F., 2008. Trapping of Phenylacetaldehyde as a Key Mechanism Responsible for Naringenin's Inhibitory Activity in Mutagenic 2-Amino-1-methyl-6-phenylimidazo [4,5-b]Pyridine Formation. Chemical research in toxicology 21, 2026-2034.

Claxton, G.P., Allen, L., Grisar, J.M., 1988. 2,3,4,5-Tetrahydropyridine Trimer. Org Synth 50-9, 968-971.

Diana, P., Cirrincione, G., 2015. Biosynthesis of Heterocycles: From Isolation to Gene Cluster. John Wiley & Sons.

Jang, D.S., Lee, G.Y., Lee, Y.M., Kim, Y.S., Sun, H., Kim, D.H., Kim, J.S., 2009. Flavan-3-ols Having a gamma-Lactam from the Roots of Actinidia arguta Inhibit the Formation of Advanced Glycation End Products in Vitro. Chemical & pharmaceutical bulletin 57, 397-400.

Liu, X., Li, W., Hua, H., Li, W., Chen, F., Wu, L., 2006. An NMR Study of a Phenyl Propanoid-substituted Catechin from Polygonum bistorta. AJTM.

Mohana Kumara, P., Zuehlke, S., Priti, V., Ramesha, B.T., Shweta, S., Ravikanth, G., Vasudeva, R., Santhoshkumar, T.R., Spiteller, M., Uma Shaanker, R., 2012. Fusarium proliferatum, an endophytic fungus from *Dysoxylum binectariferum* Hook.f, produces rohitukine, a chromane alkaloid possessing anti-cancer activity. Antonie van Leeuwenhoek 101, 323-329.

Shen, C.C., Chang, Y.S., Ho, L.K., 1993. Nuclear-Magnetic-Resonance Studies of 5,7-Dihydroxyflavonoids. Phytochemistry 34, 843-845.

Shirley, B.W., 1996. Flavonoid biosynthesis: 'New' functions for an 'old' pathway. Trends Plant Sci 1, 377-382.

Simon, J.E., Wu, Q. and Welch, C., 2014. Peperidine-flavan alkaloid compounds derived from African herb tea kinkeliba as anti-diabetic agents. U.S. Patent 8,642,769.

Szőke, É., Lemberkovics, É., Kursinszki, L., 2013. Alkaloids derived from lysine: piperidine alkaloids, Natural Products. Springer, pp. 303-341.

Tan, A.R., Swain, S.M., 2002. Review of flavopiridol, a cyclin-dependent kinase inhibitor, as breast cancer therapy. Semin Oncol 29, 77-85.

Tanaka, T., Watarumi, S., Fujieda, M., Kouno, I., 2005. New black tea polyphenol having N-ethyl-2-pyrrolidinone moiety derived from tea amino acid theanine: isolation, characterization and partial synthesis. Food Chem 93, 81-87.

Tsimogiannis, D., Samiotaki, M., Panayotou, G., Oreopoulou, V., 2007. Characterization of flavonoid subgroups and hydroxy substitution by HPLC-MS/MS. Molecules 12, 593-606.

Welch, C.R., 2010. Chemistry and pharmacology of Kinkéliba (*Combretum micranthum*), a west African medicinal plant. Rutgers, The State University of New Jersey.

Winkel-Shirley, B., 2001. Flavonoid biosynthesis. A colorful model for genetics, biochemistry, cell biology, and biotechnology. Plant Physiol 126, 485-493.

Winkel-Shirley, B., 2002. Biosynthesis of flavonoids and effects of stress. Curr Opin Plant Biol 5, 218-223.

Zhang, X.Y., Li, B.G., Zhou, M., Yuan, X.H., Zhang, G.L., 2006. Chemical constituents of *Phacellaria compressa* Benth. Journal of Integrative Plant Biology 48, 236-240.

CHAPTER FIVE

The Total Synthesis Of Natural Products Kinkéloids

5.1 Introduction

Kinkéloids are groups of novel skeleton compounds, which were firstly discovered in our lab from the African plants *Combretum micranthum* (Welch, 2010; Simon et al 2014). Its structure consists of a flavan moiety and a piperidine ring attached at either 6 or 8 position. Kinkéloids A, B, C, D differ from each other only by the number of hydroxyl groups attached, resulting in 16 mass unit difference consecutively on mass spectrometry (Figure 36). Since kinkéloids were identified as major components contained in *C. micranthum*, which have been traditionally used as hot tea, it is of great interest for the further exploration of their biological activates. Due to the close physiochemical properties between these kinkéloids in the plant extract, direct separation and accumulation using chromatography is very challenging and time-consuming, especially for large-scale production for pharmacology research. Therefore, in this study, we aimed to design synthetic methods that could help totally synthesize kinkéloids A and B groups. The methods may also be applied for the synthesis of their analogues with modified structures for medicinal and pharmacological research in the future.

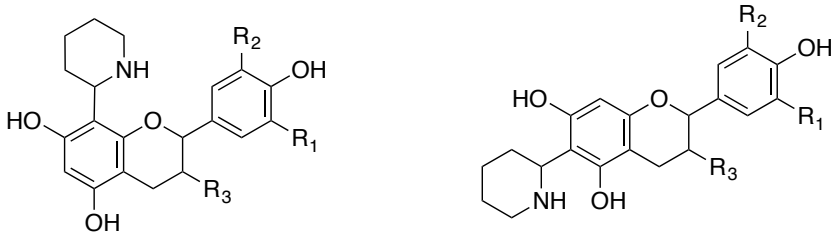

1 Kinkeloids A: R_1 = H, R_2 = H, R_3 = H; **3** Kinkeloids C: R_1 = OH, R_2 = OH, R_3 = H
2 Kinkeloids B: R_1 = OH, R_2 = H, R_3 = H; **4** Kinkeloids D: R_1 = OH, R_2 = OH, R_3 = OH

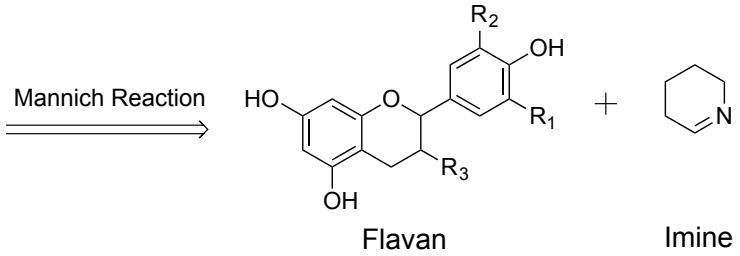

Figure 36. Kinkéloids and retrosynthetic analysis

Here, we report on two synthetic methods, which could be used for the preparation of kinkéloids. Both synthetic routes rely on the Mannich reaction in the connection between the flavan moiety and the piperidine moiety in the last step (Figure 36). In the family of flavonoids, only flavone and flavanone classes were reported in the synthesis of their corresponding flavonoid alkaloids through the reaction with cyclic imine (Leete, 1982; Nguyen et al., 2012; Chen et al., 2006). The chemical properties between different classes of flavonoids vary greatly and affect their reaction results. In our study, the Mannich reaction between a flavan molecule and cyclic imine was explored for the first time. As reported, the other flavonoid alkaloids usually have low solubility in alcohol and even in DMSO, and the 8-substitued groups generally are less soluble than the 6-substitued ones (Nguyen et al., 2011). In contrast to other flavonoid alkaloids, the synthesized flavan

alkaloids are very soluble in alcohol solvent, such as methanol and ethanol. As such, the solvent selected to perform the flavan Mannich reaction was 100% methanol. Due to the comparatively higher flexibility of flavan molecules, the substitution on 6-, 8- positions is lack of selectivity, even if different solvent systems were tried including MeOH, EtOH, H_2O/MeOH, H_2O/THF. However, this substitution selectivity was observed and reported in flavanone and flavone groups, indicating the carbonyl groups at position 4 can impact the nucleophilic activities of position 6 and 8 (Chen et al., 2006; Nguyen et al., 2011).

The synthesis of cyclic imine started from commercially available compound piperidine, which was converted to N-chloropiperidine **7** through the addition of N-chlorosuccinimide (NCS). Then, the treatment of formed N-chloropiperidine with potassium hydroxide in ethanol gave the corresponding synthetic intermediate Δ^1-piperidein **8**. In this step, low yield may be observed if excessive heating is used for solvent removal because of the low boiling point of compound **8**. Δ^1-piperidein was then crystalized out in its trimeric form as tripiperidein **9** in cold acetone (Claxton et al., 1988). The two synthetic methods presented here differ from each other on the synthesis of flavan moiety (Rouchaud and Braekman, 2009; Grundon and Reynolds, 1964). Synthetic method one was applied for the synthesis of kinkéloid B series, while method two was used for the kinkéloid A series.

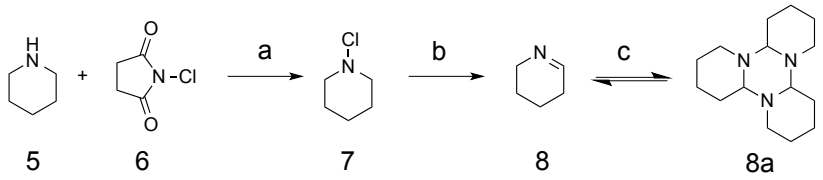

Figure 37. The synthesis of Δ^1-piperidein intermediate

Reaction conditions and reagents: (a) Ether, RT; (b) 20% KOH, ethanol, 0°C to RT, 62 %, (c) acetone, -20°C

Synthesis of Kinkéloids B

The synthetic route one starts from commercially available compounds 3,4-dihydroxybenzaldehyde (**9**) and 2,4,6-trihydroxyacetophone (**10**), which were protected with MOM groups to give compounds **11** and **12**. MOM group is an ideal compromise of stability in basic condition and facile cleavage in acidic condition. The ethanol mixture of **11** and **12** was basified with 40% KOH solution in ice bath and gradually warmed up to room temperature to give the fully protected chalcone **13** in 62% yield (Urgaonkar et al., 2005). De-protection of MOM groups using 10 % HCl in methanol under elevated temperature of 50 °C gave exclusively compound eriodictyol **14**, which was cyclized from de-protected chalcone intermediate. Then phenolic acid groups were fully protected with TMS (trimethylsilyl) groups before the step of reductive de-oxygenation using mild reducing reagent $NaBH_3CN$. $NaBH_3CN$, as a reducing agent, has remarkable stability in acidic environment, whose hydrolysis rate is 10^{-8} that of sodium borohydride (Clinton, 1975). A wide range of acids including BF_3•OEt_2, $ZnCl_2$, concentrated HCl, were compared in the reaction and it was found 10% HCl delivers the best conversion (60%

yield) without opening the A ring at 2 position (Srikrishna et al., 1995; Kulangiappar et al., 2014). The TMS protecting groups were also removed in the reaction by hydrolysis. Flavan **16** reacted with Δ^1-piperidein and yielded the kinkéloids B series with 20 % yield. Low yield may be due to the formation of side product, 6,8- di-piperidine substituted flavan and the low conversion percentage.

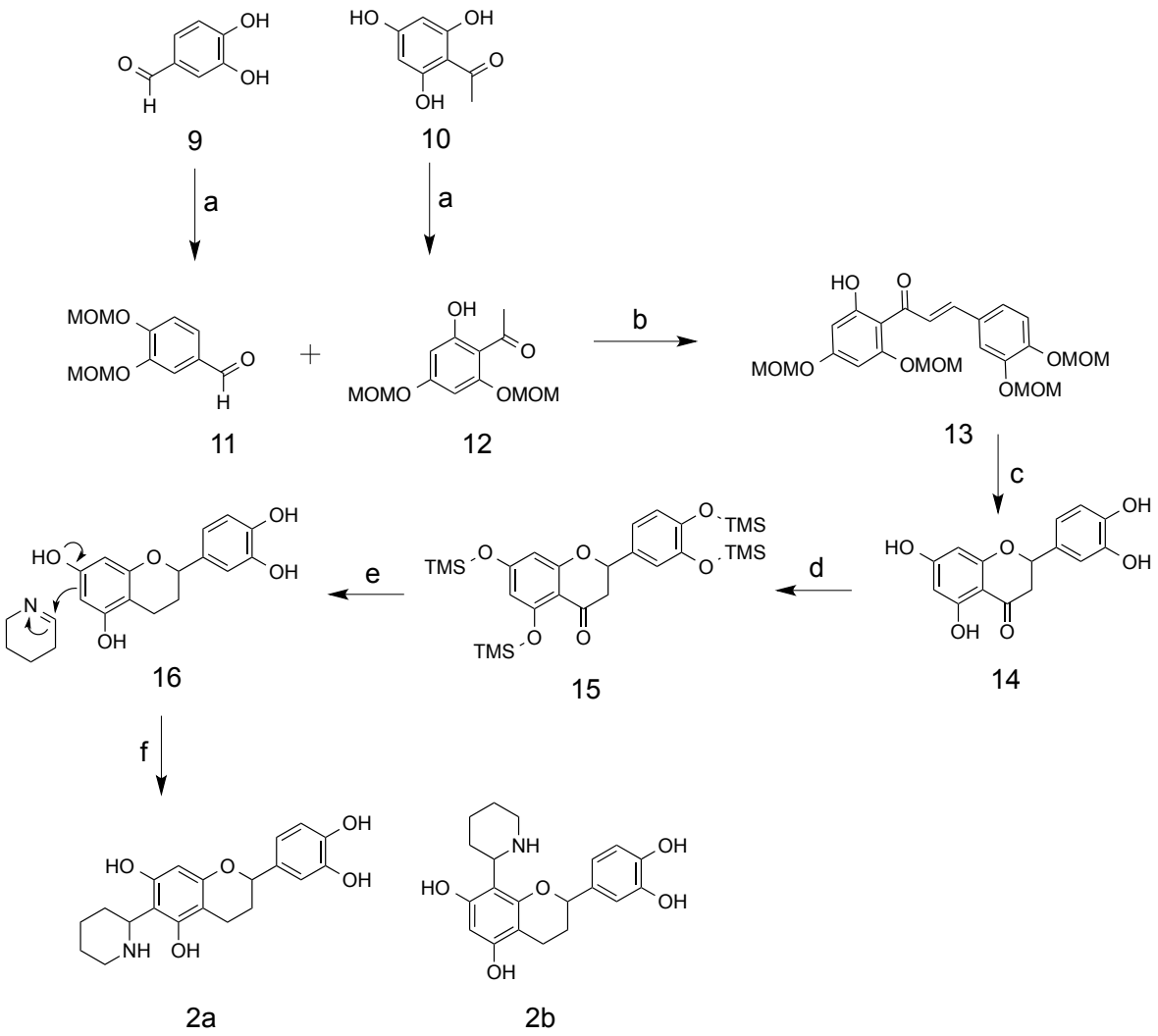

Figure 38. Route one for the synthesis of kinkéloids B[a]

[a] Reaction conditions and reagents: (a) DIPEA, MOMCl, DMAP, CH_2Cl_2, 0°C to RT (88% for **11**, 74% for **12**); (b) 40% KOH, ethanol, 0°C to RT (62 %); (c) 10% HCl, methanol, reflux (71 %); (d) TMSCl, HMDS, Pyridine (e) $LiAlH_4$, $NaBH_3CN$, THF, 10% HCl, RT (65 %); (f) Δ^1-piperideine, methanol, 70°C (20 %).

Synthesis of Kinkéloids A

The second method involves the application of *o*-quinone methide and the inverse electron-demand Diels-Alder reaction. Starting material 2,4,6-trihydroxybenzaldehyde (**17**) reacted with di-tert-butyl dicarbonate to form compound **18**, which is thermally unstable on silica column and can decompose to the di-boc substituted compound **18a** at room temperature in the purification process. The use of a cold solvent system (ethyl acetate/hexane) from -20 °C freezer for chromatographic separation prevented its decomposition and kept its tri-substituted status. Compound **18** was then used to generate *o*-quinone methides in combination with magnesium bromide and lithium aluminum hydride based on literature reports (Van De Water et al., 2000). The generation of *o*-quinone methides through Grignard regents requires extreme dryness. Subsequent 1,4-conjugate addition between *o*-quinone methide with electron-rich olefins through inverse Diels-Alder reaction yields protected flavan products. Selenski (2006) reported that the aldehydes, alkenes and other materials have to be extremely dried using sodium through Kugelrohr distillation. Low yield was observed in our experiment and we suggest that it was due to the lack of dryness in this process. This inverse Diels-Alder reaction has been

applied to the synthesis of modified flavonoid molecules in prior study (Selenski, 2006). The t-butyl and boc groups were subsequently removed using $ZnBr_2$ at room temperature and 4', 5, 7-trihydroxyl flavan was achieved (Selenski and Pettus, 2004). Kinkéloids A were synthesized through the reaction between flavan **21** and Δ^1-piperidein with yield 25 %. Compared with kinkéloids B series, the A series compounds are comparatively less stable and could be easily oxidized to purple compound in the air within a few hours. This phenomenon correlated very well with their relative amount that was originally accumulated and found in the extracted leaves, in which B series is very abundant while A series is relatively scarce, as shown in Figure 29. Both synthesized kinkéloids A and B have been further positively confirmed through the comparison with compounds contained in kinkéliba's leaves extract on LC/UV/MS. The synthesized compounds share identical UV profile, mass spectrum and retention time with the ones extracted from kinkéliba leaves.

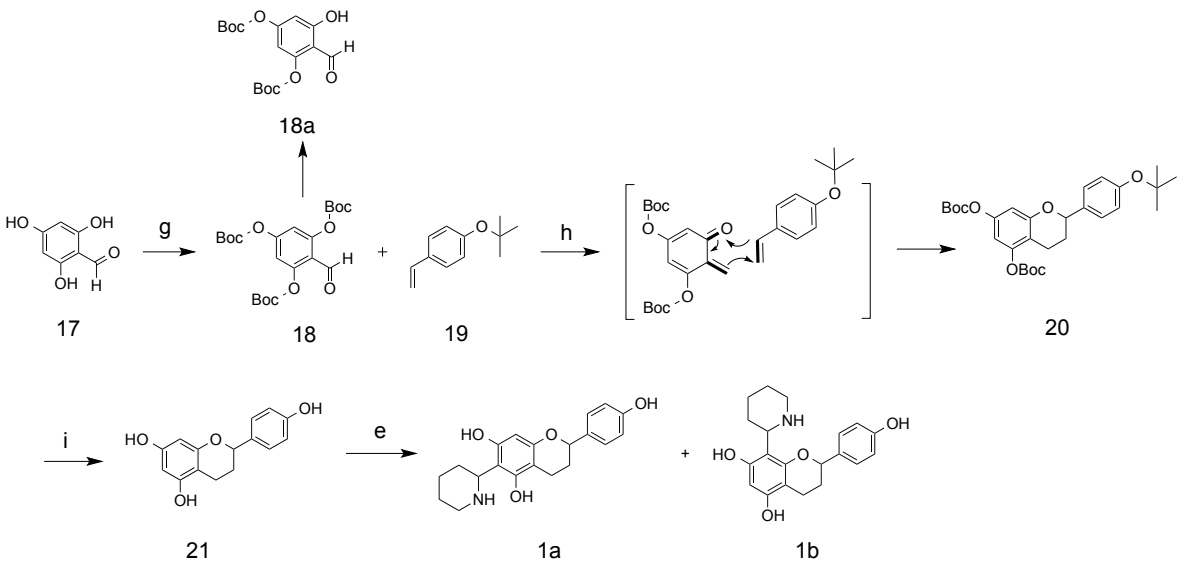

Figure 39. Route two for the synthesis of kinkéloids A[a]

[a] Reaction conditions and reagents: (g) Boc_2O, DIPEA, DMAP, CH_2Cl_2, RT, overnight (46.5%); (h) $MgBr_2{\cdot}OEt_2$, $LiAlH_4$, Ether, -78°C to RT; (i) $ZnBr_2$, CH_2Cl_2 (9.7%); (e) Δ^1-piperideines, methanol, 70°C (25 %).

This study presents the first synthesis of kinkéloids, a group of newly discovered flavan alkaloids with novel skeleton. Efficient synthesis would help prepare flavan alkaloids in larger quantities for future biological activity studies. The synthetic methods could also contribute to the *in vivo* disposition, metabolism and pharmacokinetic studies through the incorporation of stable radioisotopes.

5.2 Experimental Procedures:

5.2.1 General Experimental Procedures

^{1}H and ^{13}C NMR spectra were performed on Bruker Avance 400 MHz spectrometer (Billerica, MA). Analytical LC-MS was performed on Hewlett-Packard Agilent 1100 series HPLC-MSD (Agilent Technologies, Waldbronn, Germany) equipped with a quaternary pump system, a degasser, an auto-sampler, a DAD detector, a MSD trap with electrospray ion source (ESI). Column chromatography was performed using silica gel (230 - 400 mesh; Selecto Scientific, Suwanee, GA), Sephadex LH-20 (25-100 μ, Sigma-Aldrich, St. Louis, MO). All synthetic materials are purchased from Sigma Aldrich, St. Louis, MO. All solvents were purchased from Fisher Scientific, Hampton, NH.

5.2.2 Synthesis Δ^1-Piperidein

Into a suspension solution of N-chlorosuccinimide **6** (5.9 g, 45.0 mmol) in ether (50 ml), piperidine **5** (2.5 ml, 25.25 mmol) was added drop wise over a 30 min time period. After being stirred for 3 hours at room temperature, the suspension was filtered and washed with ether (20 ml). The combined organic solvent was washed with water (20 ml), brine (20 ml), and then dried using anhydrous sodium sulfate. The solvent was removed under reduced pressure and yields intermediate N-chloropiperidine **7**, which was added dropwise into a solution of potassium hydroxide (3 g) in ethanol (15 ml) followed by being stirred for another 5 hours at room temperature. After the reaction, ether (25 ml) was added into the solution, and washed with water, brine and dried using anhydrous

sodium sulfate. Solvent ether was then removed under reduced pressure without heating and yielded product Δ^1-piperidein (1.30 g, 62 %). Low yield was observed if solvent was removal under heating on the rotavapor. Δ^1-piperidein was crystalized as tripiperidein in cold acetone at -20°C. ^{1}H NMR (400 MHz $CDCl_3$), a mixture of monomeric and trimeric forms; monomeric form (some peaks overlapped with the trimeric form): δ 7.77-7.86 (m, 1H, N=C-H), 3.52-3.60 (m, 2H, -CH_2-), 2.33 (m, 2H, -CH_2-), 2.13 (m, 2H, -CH_2-); trimeric form: 3.07-3.11 (m, 1H, -CH-), 2.76-2.78 (m, 1H, -CH_2-), 1.95-1.99 (m, 1H, -CH_2-), 1.65-1.69 (m, 3H, 2 × -CH_2-), 1.52-1.54 (m, 2H, -CH_2-), 1.12-1.29 (m, 2H, -CH_2-). ^{13}C NMR (100 MHz $CDCl_3$) monomeric form (some peaks overlapped with the trimeric form): δ 163.2 (CH, -N=CH-), 49.35 (CH_2, -CH_2-N=), 28.85 (CH_2, -CH_2-CH=), 18.80 (CH_2, -CH_2-); trimeric forms: 82.05 (CH, -N-CH (CH_2)-N-); 46.48 (CH2, -CH_2-N-), 29.27 (CH_2, -CH_2-), 25.87 (CH_2, -CH_2-), 22.41 (CH_2, -CH_2-).

5.2.3 Total Synthesis of Kinkéloids B

*3,4-Bis(methoxymethoxy)benzaldehyde (**11**)*

Into an ice-cooled suspension of 3,4- dihydroxybenzaldehyde (500 mg, 3.62 mmol) in 10 mL of dichloromethane, *N,N*-diisopropylethylamine (6.0 mL) and DMAP (5 crystals) were added. Then MOMCl (chloromethyl methyl ether, 642 mg, 7.96 mmol) was added dropwise at 0 °C, and then reaction was gradually warmed up to room temperature with stirring for overnight. After the disappearance of starting material on TLC, the reaction was poured into water (10 mL) and extracted with organic solvent DCM (2 × 20 mL). The combined organic phase was washed with water, brine and dried over anhydrous

sodium sulfate. The solvent was then removed under reduced pressure and the residue was further purified on silica gel column using hexane/ethyl acetate (9:1) to yield compound **11** as white solid (720 mg, 88 %). ^{1}H NMR (400 MHz $CDCl_3$) δ 3.51 (3H, s, -OCH_3), 3.52 (3H, s, -OCH_3), 5.28 (2H, s, -OCH_2O-), 5.32 (2H, s, -OCH_2O-), 7.27 (1H, d, *J* = 8.4 Hz, H-5'), 7.50 (1H, dd, *J* = 8.4 and 1.9 Hz, H-6'), 7.67 (1H, d, *J* = 1.9 Hz, H-2'), 9.86 (1H, s, -CHO); ^{13}C NMR (100 MHz $CDCl_3$) 56.5 (CH_3, -OCH_3), 56.6 (CH_3, -OCH_3), 95.1 (CH_2, -OCH_2O-), 95.5 (CH_2, -OCH_2O-), 115.6 (CH, C-5'), 116.1 (CH, C-2'), 126.4 (CH, C-6'), 131.3 (C, C1'), 147.6 (C, C-3'), 152.8 (C, C-4'), 190.9 (C, CHO).

*1-(2-Hydroxy-4,6-bis(methoxymethoxy)phenyl)ethan-1-one (**12**)*

2,4,6-trihydroxyacetophone (500 mg, 2.97 mmol) was suspended in ice-old dichloromethane (10 ml) followed by addition of *N,N*-diisopropylethylamine (6.0 mL), and DMAP (5 crystals). After about 10 mins, MOMCl (515 mg, 6.40 mmol) was added dropwise at 0 °C and the mixture was kept stirring for overnight at room temperature. After the disappearance of starting material shown on TLC, the mixture was poured into water (10 mL), extracted with dichloromethane (2 × 20 mL) two times. The organic phase was washed with water (10 mL) and brine (10 mL), and dried using anhydrous sodium sulfate. The solvent was then removed under reduced pressure and the residue was purified on silica gel column using hexane/ethyl acetate (9:1) to yield compound **12** (560 mg, 73.4 %) as colorless oil and crystalized as white solid. ^{1}H NMR (400 MHz $CDCl_3$) δ 2.66 (s, 3H, -$COCH_3$), 3.47 (s, 3H, -OCH_3), 3.51 (3H, s, -OCH_3), 5.17 (2H, s, -OCH_2O-), 5.25 (2H, s, -OCH_2O-), 6.24 (1H, d, *J* = 2.3 Hz, Ar-H), 6.27 (1H, d, *J* = 2.3 Hz,

Ar-H); ^{13}C NMR (100 MHz $CDCl_3$) δ 33.1 (CH_3, -$COCH_3$), 56.6 (CH_3, -OCH_3), 56.9 (CH_3, -OCH_3), 94.2 (CH_2, 2 × -OCH_2O-), 94.7 (CH, C-5'), 97.4 (CH, C-3'), 107.1 (C, C-1'), 160.5 (C, C-6'), 163.6 (C, C-4'), 167.0 (C, C-2'), 203.4 (C=O, C-1).

*3-(3,4-Bis(methoxymethoxy)phenyl)-1-(2-hydroxy-4,6-bis(methoxymethoxy)phenyl)prop-2-en-1-one (**13**)*

Compound **11** (160 mg, 0.71 mmol) and **12** (150 mg, 0.59 mmol) were co-suspended in ice-cold solution of ethanol (5 mL) followed by the addition of 40% KOH solution (1 mL). The mixture was gradually warmed to room temperature and stirred for overnight. After that, the reaction was poured into water (10 mL) and extracted with dichloromethane (3 × 20 mL). The combined organic phase was washed with water (10 mL), brine (10 mL) and dried using anhydrous Na_2SO_4. The solvent was then purified on silica gel column using hexane/ethyl acetate (5:1) to yield compound **13** (170 mg, 62.0 %) as yellow solid. ^{1}H NMR (400 MHz $CDCl_3$) δ 3.48 (3H, s, -OCH_3), 3.52 (3H, s, -OCH_3), 3.53 (3H, s, -OCH_3), 3.54 (3H, s, -OCH_3), 5.18 (2H, s, -OCH_2O-), 5.27 (2H, s, -OCH_2O-), 5.28 (2H, s, -OCH_2O-), 5.30 (2H, s, -OCH_2O-), 6.27 (1H, d, J = 2.3 Hz, H-3'), 6.31 (1H, d, J = 2.3 Hz, H-5'), 7.17-7.22 (2H, m, H-5, 6), 7.51 (1H, d, J = 1.7 Hz, H-2). 7.74 (1H, d, J = 15.5 Hz, H-α), 7.86 (1H, d, J = 15.5 Hz, H-β), 13.92 (1H, s, -OH); ^{13}C NMR (100 MHz $CDCl_3$) δ 56.4 (CH_3, -OCH_3), 56.5 (CH_3, -OCH_3), 56.6 (CH_3, -OCH_3), 57.0 (CH_3, -OCH_3), 94.2 (CH_2, -OCH_2O-), 94.9 (CH_2, -OCH_2O-), 95.2 (CH_2, -OCH_2O-), 95.3 (CH_2, -OCH_2O-), 95.7 (CH, C-5'), 97.7 (CH, C-3'), 107.7 (C, C-1'), 115.5 (CH, C-2), 116.4 (CH, C-5), 124.3 (CH, C-6), 126.1 (CH, C- α), 130.1 (C, C-1), 142.5 (CH, C- β), 147.7

(C, C-4), 149.3 (C, C-3), 160.1 (C, C-2'), 163.5 (C, C-6'), 167.5 (C, C-4'), 192.9 (C, C=O).

*2-(3,4-Dihydroxyphenyl)-5,7-dihydroxychroman-4-one (**14**)*

Compound **13** (70 mg, 0.15 mmol) was suspended in methanol (5 mL) followed by the addition of 37% HCl solution (1 mL). The mixture was heated up and refluxed for 5 hours. After the reaction, the solution was cooled down and poured into water, extracted with EtOAc (3 × 10 mL). The combined organic phases was washed with water, brine, and dried using anhydrous Na_2SO_4. Then solvent was then removed under reduced pressure. The residue was dissolved in methanol (0.5 mL) and purified over Sephadex LH-20 column using 100% methanol to yield compound **10** (30.5 mg, 71%) as white solid. It would also be purified on silica gel column using solvent hexane/ethyl acetate (4:1). ^{1}H NMR (400 MHz $CDCl_3$) δ 2.67 (1H, dd, *J* = 3.0 Hz and 17.1 Hz, H-3), 3.19 (1H, dd, *J* = 17.1 and 12.5 Hz, H-3), 5.37 (1H, dd, *J* = 12.5 and 3.0 Hz, H-2), 5.87 and 5.88 (2H, d, H-6 and 8), 6.74 (2H, s, H-5' and 6'), 6.87 (1H, s, H-2); ^{13}C NMR (100 MHz $CDCl_3$) δ 42.1 (CH, C-3), 78.4 (CH, C-2), 94.9 (CH, C-6), 95.7 (CH, C-8), 101.8 (C, C-10), 114.3 (CH, C-2'), 115.3 (CH, C-5'), 117.9 (CH, C-6'), 129.4 (C, C-1'), 145.2 (C, C-4'), 145.7 (C, C-3'),162.9 (C, C-5), 163.4 (C, C-9), 166.6 (C, C-7), 196.3 (C, C-4)

*2-(3,4-Dihydroxyphenyl)chromane-5,7-diol (**16**)*

Into a solution of compound **14** (288 mg, 1.0 mmol) in dry pyridine (1 mL) was added hexamethyldisilazane (1 ml), and trimethylchlorosilane (0.6 ml). The mixture was then further stirred at room temperature for an hour. The volatile constituents were then distilled off under reduced pressure on rotavapor. The residue was then suspended in toluene and the precipitate was then filtered off. Solvent toluene solution was then distilled off under reduced pressure and the residue was dissolved in THF (2.5 ml) followed by the addition of $LiBH_4$ (11 mg, 0.5 mmol). The mixture was further stirred at room temperature for half an hour. Then 0.5 mg of methyl orange and sodium cyanoborohydride (63 mg, 1.0 mmol) were added into the solution. The mixture then was slowly titrated using hydrochloric acid solution (1 N) with the release of hydrogen until the color of the solution turns into red. The color of the solution was controlled in red by continuous slow addition of hydrochloric acid. After approximate 2 hours, extra amount of hydrochloric acid (1 to 1.5 ml) was added slowly and gently to keep the color permanent and the reaction was stirred for overnight at room temperature. After that, solvent THF was distilled off under reduced pressure and the residue was extracted with ethyl acetate and washed with 1 N hydrochloric acid solution, distilled water, and brine. The organic solution was then dried using anhydrous sodium sulfate and purified on silica column using 10 to 20 % ethyl acetate in hexane as eluent with 65 % yield. ^{1}H NMR (400 MHz, MeOD-d4) δ 1.88 (1H, m, H-3), 2.08 (1H, m, H-3), 2.61 (2H, m, H-4), 4.77 (1H, dd, H-2), 5.84 (1H, d, J = 2.3 Hz, H-8), 5.90 (1H, d, J = 2.3 Hz, H-6), 6.67 (2H, m, H-5', 6'), 6.85 (1H, d, J = 1.84 Hz, H-2'); ^{13}C NMR (100 MHz, MeOD-d4) δ 20.35 (C-4), 30.89 (C-3), 78.848 (C-2), 96.00 (C-8), 96.08 (C-6) 102.6 (C-10), 114.47 (C-5'),

116.17 (C-2'), 118.83 (C-6'), 135.14 (C-1'), 145.93 (C-3'), 146.24 (C-4'), 157.31, 157.49, 157.97 (C-5, 7, 9)

Kinkéloids B

The synthesized flavan compound **16** (40 mg, 0.15 mmol) was dissolved in methanol (4 ml) followed by the addition of Δ^1-piperideines **8** (12.1 mg, 0.15 mmol). The mixture was stirred at 70°C under nitrogen atmosphere for 4 hours. After the reaction, the solvent was removed under reduced pressure and the residue was firstly purified on a short Sephadex column LH-20 using solvent methanol to give mixture of compound 3 and 4 (10.5 mg, 20 %, low yield may be due to the formation of di-piperidine substituted products and some dead absorption to the column). Then the mixture was reloaded to a ~1.5 m long Sephadex LH-20 column for the separation of two groups of regioisomers. The elution solvent is methanol. As each group of regioisomers is a mixture of diastereoisomers, the coupling constants were not calculated. ^{1}H NMR (400 MHz DMSO-d_6, 6-piperidyl kinkéloids B): δ 1.37-1.80 (6H, m, H-4'', 5'', 6''), 1.80-1.83 (1H, m, H-3), 2.00 (1H, m, H-3), 2.50 (2H, m, H-4), 2.60 (1H, m, H-3''), 3.08 (1H, m, H-3''), 4.10 (1H, m, H-1''), 4.73 (1H, m, H-2), 5.78 (1H, H-8), 6.61-6.72 (2H, m, H-5', 6'), 6.76 (1H, d, *J* = 1.92 Hz, H-2'); ^{13}C NMR (100 MHz, DMSO-d_6) δ 19.0 (C-4), 24.0, 24.5 (C-4'', 5''), 29.0 (C-3), 30.3 (C-6''), 45.7 (C-3'') 52.8 (C-1''), 76.4 (C-2), 93.9 (C-8), 101.4 (C-10), 107.1 (C-6), 113.7 (C-2'), 115.3 (C-5'), 117.1 (C-6'), 132.7 (C-1'), 144.8, 145.1 (C-3', 4') 153.2, 154.6, 155.9 (C- 5, 7, 9). ^{1}H NMR (400 MHz DMSO-

d_6, 8-piperidyl kinkéloids B): δ 1.37-1.80 (6H, m, H-4'', 5'', 6''), 1.80 (1H, m, H-3), 2.00 (1H, m, H-3), 2.49 (2H, m, H-4), 2.70 (1H, m, H-3''), 3.16 (1H, m, H-3''), 4.20 (1H, m, N-H), 4.86 (1H, m, H-2), 5.97 (1H, H-6), 6.61-6.8 (3H, m, H-5', 6', 2'); ^{13}C NMR (100 MHz, DMSO-d_6) δ 18.7 (C-4), 23.3 23.5 (C-4'', 5''), 28.6 (C-3), 29.6 (C-6''), 45.5 (C-3'') 52.5 (C-1''), 76.4 (C-2), 95.3 (C-6), 100.2 (C-10), 104.0 (C-8), 113.4 (C-2'), 115.4 (C-5'), 116.5 (C-6'), 132.7 (C-1'), 144.8, 145.2 (C-3', 4') 152.7, 155.3, 155.5 (C- 5, 7, 9).

5.2.4 Total Synthesis of Kinkéloid A

*Tri-tert-butyl (2-formylbenzene-1,3,5-triyl) tricarbonate (**18**)*

2,4,6-trihydroxybenzaldehyde (1.0 g, 6.50 mmol) was placed in an oven-dried flask filled with nitrogen followed by dissolution using solvent CH_2Cl_2. Then *N,N*-diisopropylethylamine (DIPEA) (0.7 mL), catalyst DMAP (four crystals) and Boc_2O (5 ml, 21.8 mmol) were added and the mixture was stirred at room temperature for overnight. The reaction was stopped using excessive 1 M NH_4Cl and extracted using organic solvents dichloromethane (2 × 20 mL). The combined organic solvent is washed with water (10 mL), brine (10 mL) and then dried using anhydrous $MgSO_4$. The solution was filtered and dried under reduced pressure. The residue was purified on silica gel column using refrigerated/cold hexane/ethyl acetate (95:5) and yielded compound **12** (1.37 g, 46.5%) as colorless glue. Cold solvents for purification were necessary due to the instability of tri-Boc protected material, which could decompose to di-Boc protected side

product at elevated temperature. ^{1}H NMR (400 MHz $CDCl_3$) δ 1.55 (9H, s, 3 × -CH_3), 1.56 (18H, s, 6 × -CH_3), 7.10 (2H, s, 2 × Ar-H), 10.20 (1H, s, -CHO)

*2-(4-Hydroxyphenyl)chromane-5,7-diol (**21**)*

The synthesized intermediate compound **18** (100 mg, 0.22 mmol) was dissolved in anhydrous ether and added to a flask containing 1-tert-butoxy-4-vinylbenzene (4 ml, 21 mmol) and magnesium bromide ethyl etherate $MgBr_2{\cdot}OEt_2$ (58 mg, 0.22 mmol) at -78°C with the protection of argon. Then into the mixture was added $LiAlH_4$ (9.0 mg, 0.24 mmol) solution in anhydrous ether through a cannula. The reaction was gradually warmed to room temperature and stirred for another 3 hours at room temperature. The reaction was quenched using 1M $NaHCO_3$ and extracted using ether (3 × 10 mL). The combined organic phase was then washed with water (5 mL), brine (5 mL) and dried using anhydrous Na_2SO_4. The solvent was removed and the residue was re-dissolved in the DCM (5 mL) followed by the addition of $ZnBr_2$ (250 mg, 2.2 mmol). The mixture was then stirred at room temperature for overnight. The reaction was quenched with 1 M HCl solution followed by extraction with EtOAc (3 × 10 mL). The combined organic phase was dried under reduced pressure and purified on silica column with hexane/ethyl acetate (3:1) to yield compound 16 (5.5 mg, 9.7 %) as white solid. The part is based on published method (Selenski and Pettus, 2004). Due to the reaction's extreme water sensitivity, low yield was observed when compared with reported result (Selenski and Pettus, 2004). ^{1}H-NMR (400 MHz, MeOD-d4): δ 7.22 (2H, d, *J* = 8.6 Hz, H-3', 5'), 6.77 (2H, d, *J* = 8.6 Hz, H-2' 6'), 5.90 (1H, d, *J* =2.3 Hz, H-6), 5.83 (1H, d, *J* =2.3 Hz, H-8), 4.82 (1H, br, d, H-2), 2.54-2.71 (2H, m, H-4), 1.87-2.13 (2H, m, H-3). ^{13}C NMR (100

MHz, MeOD-d4) δ 158.09, 157.99, 157.49, 157.33 (C-5, 7, 9, 4'), 134.34 (C-1'), 128.47 (C-3', 5'), 116.05 (C-2', 6'), 96.02 (C-6), 95.94 (C-8), 78.84 (C-2), 30.88 (C-3), 20.43 (C-4)

Kinkéloids A

The synthesized flavan compound **21** (200 mg, 0.78 mmol) was dissolved in methanol followed by the addition of Δ^1-piperideines (77 mg, 0.93 mmol). The mixture was stirred at 70°C under nitrogen atmosphere for 5 hours. After the reaction, the solvent was removed under reduced pressure and the residue was purified on silica column using methanol/dichloromethane (15:85) to yield a mixture of kinkéloids A. Further purification on a short Sephadex column LH-20 with methanol yields compound kinkéloids A as white solid (25 %). Here too, we observed that synthesized kinkéloids A would be oxidized to purple compounds after exposure to the air for a while. The purified mixture was reloaded to a ~1.5 m long Sephadex LH-20 column for the separation of two groups of regioisomers. As each group of regioisomers is a mixture of diastereoisomers, the coupling constants were not calculated. ^{1}H NMR (400 MHz, DMSO-d_6, 6-piperidyl kinkéloids A): δ 1.41-1.76 (6H, m, H-4'', 5'', 6''), 1.83 (1H, m, H-3), 2.01 (1H m, H-3), 2.53 (2H, m, H-4), 2.67 (1H, m, H-3''), 3.12 (1H, m, H-3''), 4.15 (1H, m, H-1''), 4.80 (1H, H-2), 5.82 (1H, H-8), 6.75 (2H, H-2', 6'), 7.17 (2H, H-3', 5'); ^{13}C NMR (100 MHz, DMSO-d6) δ 19.29 (C-4), 23.79, 24.06 (C-4'', 5'') 28.89 (C-3), 29.83 (C-6''), 45.60 (C-3'') 52.74 (C-1''), 76.41 (C-2), 94.17 (C-8), 101.18 (C-10), 106.71 (C-6), 114.98 (C-2', 6'), 127.37 (C-3', 5'), 131.97 (C-1'), 156.93, 155.53, 154.87, 153.38 (C-5, 7, 9, 4'). ^{1}H NMR (400 MHz, DMSO-d_6, 8-piperidyl kinkéloids A): δ 1.51-1.80 (6H, m, H-4'', 5'',

6''), 1.81 (1H, m, H-3), 2.06 (1H m, H-3), 2.51 (2H, m, H-4), 2.87 (1H, m, H-3''), 3.24 (1H, m, H-3''), 4.30 (1H, m, H-1''), 5.02 (1H, m, H-2), 6.14 (1H, H-6), 6.77 (2H, d, H-2', 6'), 7.20 (2H, d, H-3', 5'), ^{13}C NMR (100 MHz, DMSO-d_6) δ 19.64 (C-4), 21.67, 22.93 (C-4'', 5'') 28.60 (C-6''), 28.67 (C-3), 45.45 (C-3'') 52.70 (C-1''), 76.31 (C-2), 95.35 (C-6), 101.78 (C-10), 104.80 (C-8), 114.98 (C-2', 6'), 127.29 (C-3', 5'), 157.00, 155.51, 154.06, 153.90 (C-5, 7, 9, 4').

5.3 References

Akeem, A.A., Ejikeme, U.C., Okarafor, E.U., 2012. Antibacterial Potentials of the Ethanolic Extract of the Stem Bark of *Combretum micranthum* G. Don and Its Fractions. Journal of Plant Studies 1, p75.

Ancolio, C., Azas, N., Mahiou, V., Ollivier, E., Di Giorgio, C., Keita, A., Timon-David, P., Balansard, G., 2002. Antimalarial activity of extracts and alkaloids isolated from six plants used in traditional medicine in Mali and Sao Tome. Phytother Res 16, 646-649.

Beutler, J.A., Cardellina, J.H., Mcmahon, J.B., Boyd, M.R., 1992. Anti-Hiv and Cytotoxic Alkaloids from *Buchenavia-capitata*. J Nat Prod 55, 207-213.

Chen, L., Hu, T.S., Zhu, J., Wu, H.M., Yao, Z.J., 2006. Application of a regioselective Mannich reaction on naringenin and its use in fluorescent labeling. Synlett, 1225-1229.

Claxton, G.P., Allen, L., Grisar, J.M., 1988. 2,3,4,5-Tetrahydropyridine Trimer. Org Synth 50-9, 968-971.

Clinton, F., 1975. Sodium cyanoborohydride—a highly selective reducing agent for organic functional groups. Synthesis 3, 135-146.

Grundon, M., Reynolds, B., 1964. 459. Δ1-piperideines. J. Chem. Soc., 2445-2450.

Houghton, P.J., 2000. Chemistry and biological activity of natural and semi-synthetic chromone alkaloids. Studies in Natural Products Chemistry 21, 123–155.

Kulangiappar, K., Anbukulandainathan, M., Raju, T., 2014. Synthetic Communications: An International Journal for Rapid Communication of Synthetic Organic Chemistry. Synthetic Commun 1, 2494-2502.

Leete, E., 1982. A One-Step Synthesis of Ficine and Isoficine. J Nat Prod 45, 605-607.

Nguyen, T.B., Lozach, O., Surpateanu, G., Wang, Q., Retailleau, P., Iorga, B.I., Meijer, L., Gueritte, F., 2012. Synthesis, Biological Evaluation, and Molecular Modeling of Natural and Unnatural Flavonoidal Alkaloids, Inhibitors of Kinases. Journal of medicinal chemistry 55, 2811-2819.

Nguyen, T.B., Wang, Q., Gueritte, F., 2011. An Efficient One-Step Synthesis of Piperidin-2-yl and Pyrrolidin-2-yl Flavonoid Alkaloids through Phenolic Mannich Reactions. Eur J Org Chem, 7076-7079.

Rouchaud, A., Braekman, J.C., 2009. Synthesis of New Analogues of the Tetraponerines. Eur J Org Chem, 2666-2674.

Selenski, C., 2006. General method for the construction of type-A proanthocyanidins: Synthesis of racemic-diinsininone. University of California, Santa Barbara.

Selenski, C., Pettus, T.R., 2004. Enantioselective [4+ 2] Cycloadditions of o-Quinone Methides: Total Synthesis of (+)-Mimosifoliol and Formal Synthesis of (+)-Tolterodine. The Journal of organic chemistry 69, 9196-9203.

Simon, J.E., Wu, Q. and Welch, C., 2014. Peperidine-flavan alkaloid compounds derived from African herb tea kinkeliba as anti-diabetic agents. U.S. Patent 8,642,769.

Srikrishna, A., Sattigeri, J., Viswajanani, R., Yelamaggad, C., 1995. A simple and convenient one step method for the reductive deoxygenation of aryl ketones to hydrocarbons. Synlett 1995, 93-94.

Tan, A.R., Swain, S.M., 2002. Review of flavopiridol, a cyclin-dependent kinase inhibitor, as breast cancer therapy. Semin Oncol 29, 77-85.

Urgaonkar, S., La Pierre, H.S., Meir, I., Lund, H., RayChaudhuri, D., Shaw, J.T., 2005. Synthesis of antimicrobial natural products targeting FtsZ:(±)-dichamanetin and (±)-2'''-hydroxy-5''-benzylisouvarinol-B. Organic letters 7, 5609-5612.

Van De Water, R.W., Magdziak, D.J., Chau, J.N., Pettus, T.R., 2000. New construction of ortho ring-alkylated phenols via generation and reaction of assorted o-quinone methides. Journal of the American Chemical Society 122, 6502-6503.

Welch, C.R., 2010. Chemistry and pharmacology of Kinkéliba (*Combretum micranthum*), a west African medicinal plant. Rutgers, The State University of New Jersey.

CHAPTER SIX

Synthesis of Kinkéloids Analogues and α-Glucosidase Inhibition

6.1 Introduction

Diabetes is one of the most common chronic diseases with an estimated 387 million patients worldwide and 4.9 million associated deaths in 2014 (International Diabetes Federation, 2014). The number of diabetes patients is projected to rise to 592 million in 2035 (Guariguata et al., 2014). Diabetes is a group of metabolic diseases characterized by high blood glucose level. One of the important therapeutic approaches is to inhibit digesting enzymes such as α-amylase, α-glucosidase, to slow down the digestion and absorption of polysaccharides to suppress postprandial hyperglycemia (Tundis et al., 2010). α-Amylase hydrolyzes large α-linked polysaccharides, such as starch and glycogen, to low-molecular-weight carbohydrates, such as maltose and dextrin (Brayer et al., 2000). α-Glucosidase is an enzyme that is present in the intestine, can hydrolyze α glucose residue from the non-reducing side of oligosaccharides to release a single α-glucose, acting as the final step in the digestion of dietary carbohydrates (He, 1998). Inhibitors of α-glucosidase, such as acarbose, miglitol and voglibose, which are carbohydrate mimetics or derivatives, have been marketed for the treatment of Type II diabetes mellitus (Scheen, 2003). These drug molecules are competitive inhibitors of α-glucosidase and can decrease postprandial hyperglycaemia. However, they do have

gastrointestinal adverse effects including diarrhea, flatulence and abdominal discomfort, which limit a long-term compliance to therapy (Hollander, 1992). There is a need to develop more selective and safer inhibitors of α-glucosidase for control of hyperglycemia in diabetes.

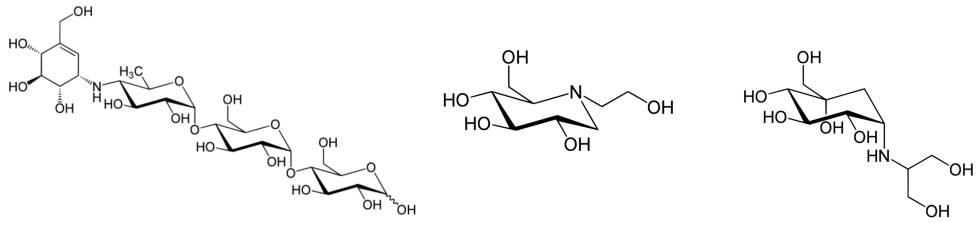

Acarbose Miglitol Voglibose

Figure 40. Anti-diabetic drugs targeting α-glucosidase

Flavonoid compounds, such as luteolin, naringenin, also exhibit potent α-glucosidase inhibitory activities both *in vitro* and *in vivo* and have shown protective effects in the development of diabetes (Iio et al., 1984; Priscilla et al., 2014; Yan et al., 2014; Wang et al., 2011). However their clinical uses for the treatment of diabetes are limited by the low

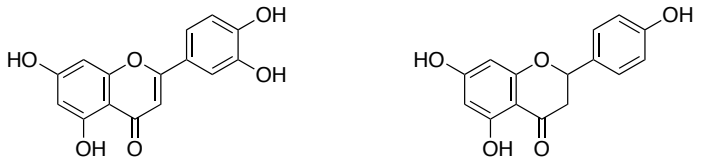

Luteolin Naringenin

Figure 41. Chemical structure of flavonoids luteolin and naringenin

bioavailability and the lack of selectivity. Helgren et al reported that the attachment of nitrogen moieties can increase the solubility of parent flavonoid compounds, because the

product can form a salt with acids, such as hydrochloric or trifluoroacetic acid (Helgren et al., 2015).

Structure modifications on flavonoids could also further increase their selectivity and inhibitory potency toward a specific target. Using compound 6-C-(E-phenylethenyl)-naringenin as an example, the introduction of phenylethenyl group at the 6 position of naringenin dramatically increases the inhibitory activity toward cyclooxygenase-1 (COX-1) and has much improved anticancer activity *in vitro* and *in vivo* (Li et al., 2014). Another example is compound flavopiridol, derived from flavone. It would selectively

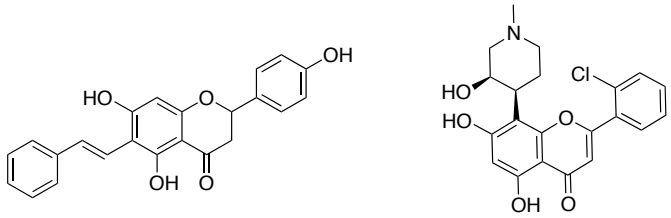

6-C-(E-Phenylethenyl)-naringenin Flavopiridol

Figure 42. Chemical structures of 6-C-(E-phenylethenyl)-naringenin and flavopiridol

inhibit cyclin-dependent kinases CDK1 and CDK2 and serves as an anticancer drug candidate in clinical trials for the treatment of breast cancer (Sedlacek, 2001). This kind of flavonoid derivative with a nitrogen moiety is conventionally categorized into a small class of natural products, named flavonoid alkaloids (Khadem and Marles, 2011). The introduction of various nitrogen moieties may increase the binding affinity toward specific enzymes with potential therapeutic applications.

In this study we set out to synthesize novel flavonoid alkaloids with potentially improved α-glucosidase inhibitory activities to address current concerns about diabetes. We are also trying to learn the structure activity relationships and inhibitory mechanisms between our synthesized flavonoid derivatives and α-glucosidase, which could help drug molecule design targeting α-glucosidase in the future. In this study, different nitrogen containing moieties were attached to four different flavonoid subclasses, including flavanone (I), flavone (II), isoflavone (III) and flavan (IV) (Figure 43). Based on the traditional uses of kinkéliba and the previous discovered *in vivo* glucose tolerance activity in our lab (Welch, 2010; Simon et al. 2014), kinkéloids were screened in this experiment for anti-α-glucosidase activity. The inhibitory activities of the synthesized derivatives were tested on α-glucosidase produced from yeast *Saccharomyces cerevisiae*, among

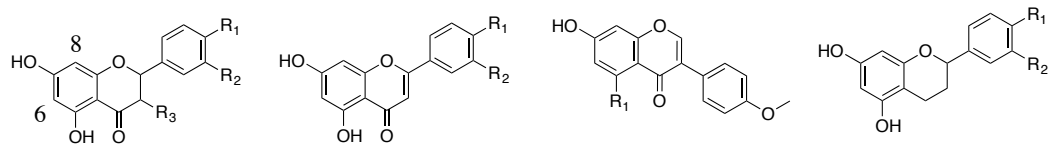

Naringenin
R_1= OH, R_2 = H, R_3 = H

Hesperetin
R1= OCH_3, R_2 = OH, R_3 = H

Chrysin
R_1= H, R_2 = H

Apigenin
R_1= OH, R_2 = H

Formononetin
R_1= H

4', 5, 7- trihydroxyflavan
R_1= OH, R_2 = H

3', 4', 5, 7- tetrahydroxyflavan
R_1= OH, R_2 = OH

Figure 43. The flavonoid subclasses used for derivatives synthesis

which compounds **15** and **23** (Figure 44) proved to have the best inhibitory activity with IC_{50} value of 23 and 4.1 μM, respectively. The inhibitory kinetics and mechanism of two

potent compounds **15** and **23** were further explored using Lineweaver–Burk plot and Dixon plot.

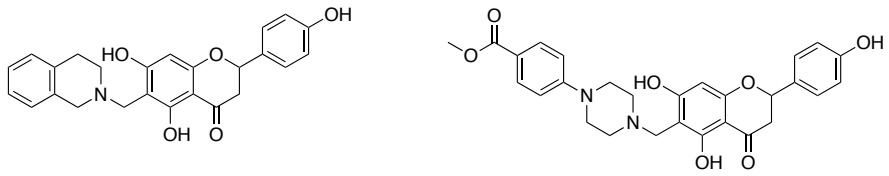

15 **23**

Figure 44. The structure of representative flavonoid alkaloids

Molecular docking studies of compounds **15** and **23** were performed on Autodock vina. Three locations were identified as the potential binding sites on the surface of α-glucosidase (Appendix III), in which location A with the highest binding affinity correlates very well with literatures reports and our experimental data (Brindis et al., 2010). Based on the binding analysis and the comparisons of different compounds and their inhibitory activities, structure activity relationships were further generalized in this study.

6.2 Results and Discussion

6.2.1 Synthesis

In the synthesis of flavonoid alkaloids **1-10** (Figure 45), the flavonoid was dissolved in methanol or THF followed by the addition of cyclic imine Δ^1-piperideine (1.25 eq).

These two compounds reacted with each other through Mannich reaction at elevated temperature. TLC was used to monitor the completion of reactions. Afterward, the solvent of each reaction was removed and the residue was applied on silica gel chromatography for purification using various solvent systems. The synthesis of Δ^1-piperideine from piperidine has been fully described in Chapter Five. Representative reaction mechanism of compounds **1-10** is illustrated in Figure 46.

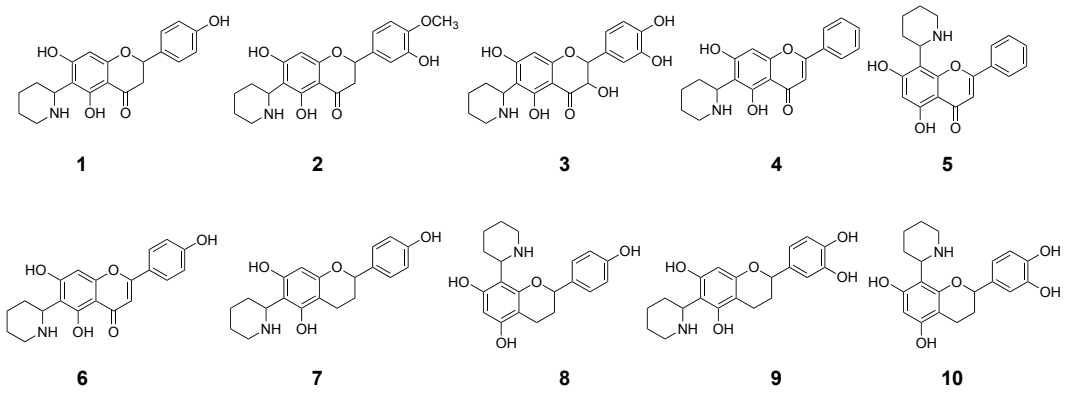

Figure 45. Chemical structures of compounds **1-10**

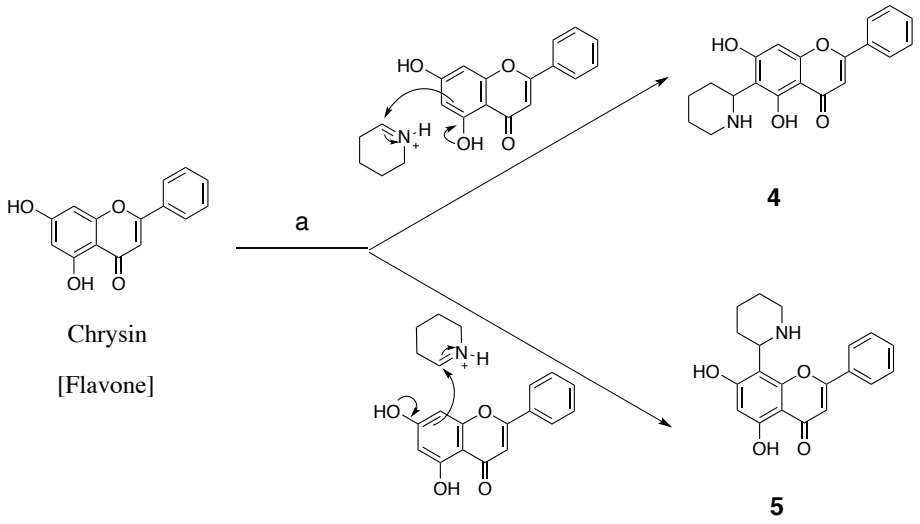

Figure 46. Synthesis of flavonoid alkaloids **4** and **5**; (a) Δ^1-piperideine, methanol/THF, 80 °C

In the synthesis of flavonoid alkaloids **11-25** (Figure 47), a 37% aqueous solution of formaldehyde (1.25 eq) was added to the appropriate flavonoid and secondary amine (1.25 eq), which were dissolved in methanol or THF. The mixture was then stirred and heated for several hours depending upon the amine and flavonoid. The reaction was also performed through Mannich reaction. The imine intermediate was formed through the reaction between formaldehyde and a secondary amine, and then reacted with flavonoid. A representative reaction mechanism is illustrated in Figure 48.

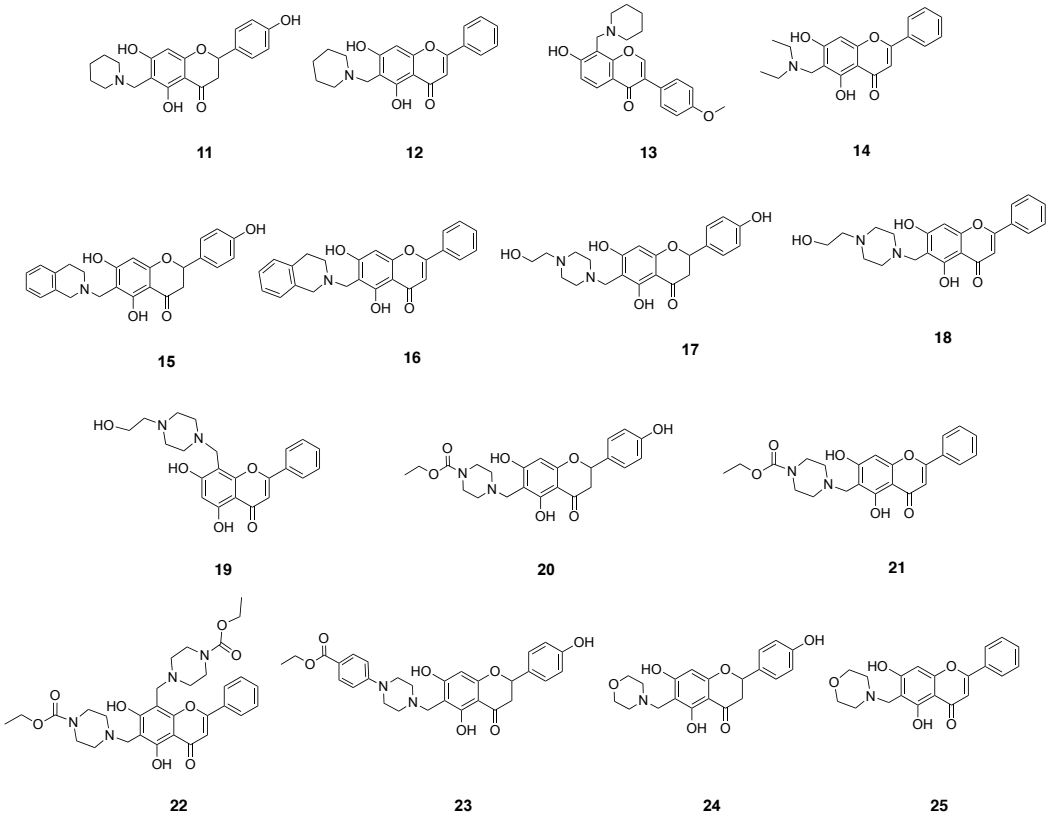

Figure 47. Chemical structures of compounds **11-25**

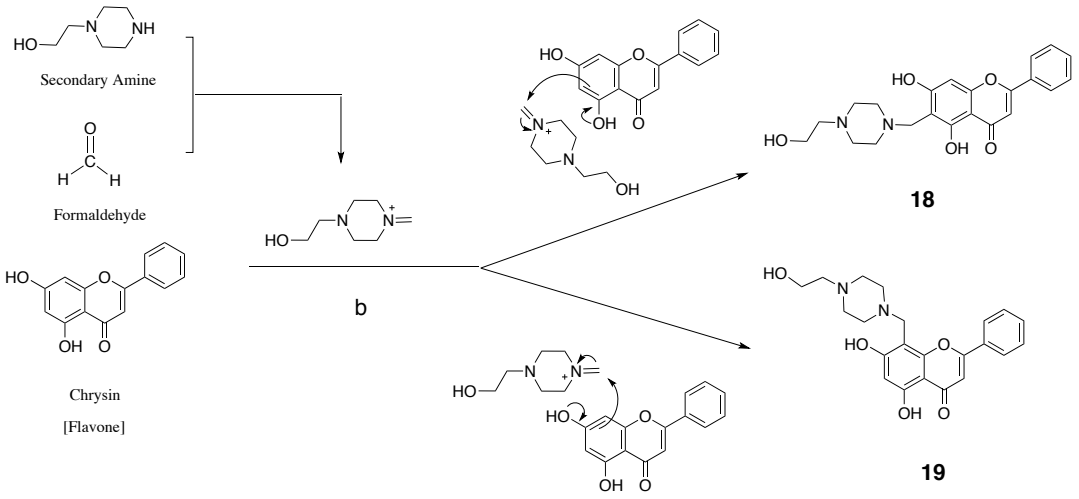

Figure 48. Synthesis of flavonoid alkaloids **18** and **19**; (b) secondary amine, 37% HCHO, methanol or THF, 65 °C

In both reactions, we observed that some of the synthesized flavonoids alkaloids were likely absorbed on silica column during purification reducing the relative yields. This observation correlates very well to previous report by Chen et al (2006). Due to the very close chemical properties between the 6 and 8 positions of flavonoid compounds, the site of alkylation under Mannich reaction varies depending on the solvent, temperature and reaction time. Different flavonoids with different chemical properties have different regioselectivities in electrophilic substitution. Chen et al (2006) reported imine has high regioselectivity toward the 6 position of flavanone compound naringenin if the reaction is performed well under mild conditions within limited hours (Chen et al, 2006). Nguyen et al (2011) reported that the use of solvent system H_2O /THF (2:1) at 40 °C would yield 99:1 selectivity between 6 and 8 positions for flavones. The addition of base may render the reaction reversible and would change the ratio of formed products.

For synthesized compounds present in this study, each compound was fully elucidated based on ^{1}H and ^{13}C NMR. Some of them were further characterized using 2D NMR. Substitution at 6 or 8 positions was determined either based on previous literature reports, or by the proton NMR peaks. For example, flavonoid chrysin has proton NMR chemical shift at 6.17 ppm for H-6 and 6.40 ppm for H-8, in which H-6 is around 0.2 ppm higher field than H-8. In the H-NMR spectra of synthesized derivatives, the H-6 peak (5.78 ppm) of compound **5** is still around ~ 0.2 ppm higher field than the H-8 peak (5.98 ppm) of compound **4**. This observation was also confirmed by HMBC, such as the correlation between H-8 and C-7, C-9 of compound **4,** H-6 and C-5, C-7 of compound **5** (Figure 49). High regioselectivity for C-6 position of naringenin was achieved under the optimized conditions, as reported by Chen et al (Chen et al., 2006).

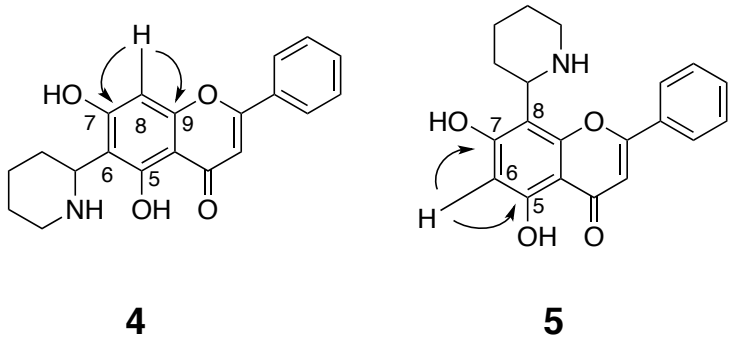

Figure 49. Structures of synthesized regioisomers of the chrysin derivatives, **4** and **5**, their HMBC correlations

6.2.2 Biological Activity

All synthesized compounds were screened against α-glucosidase enzyme from yeast along with the flavonoid compound naringenin, which is a known α-glucosidase inhibitor

and used as a positive control in our study. The concentration of compounds measured against α-glucosidase ranges from 3.15 to 806 μM. Some compounds were evaluated at only relatively lower concentrations due to the lower solubility in the experimental buffer employed. The inhibitory potency of each compound was evaluated by its IC_{50} value, which was determined by fitting to a sigmoidal dose-response curve with variable slope. At least three independent experiments were performed to determine the IC_{50} values for each compound. Among these screened compounds, **11**, **15**, **20** and **23** exhibited strong inhibition against α-glucosidase with IC_{50} values of 83, 23, 65 and 4.1 μM, respectively. Their dose-response curves are shown in Figure 50.

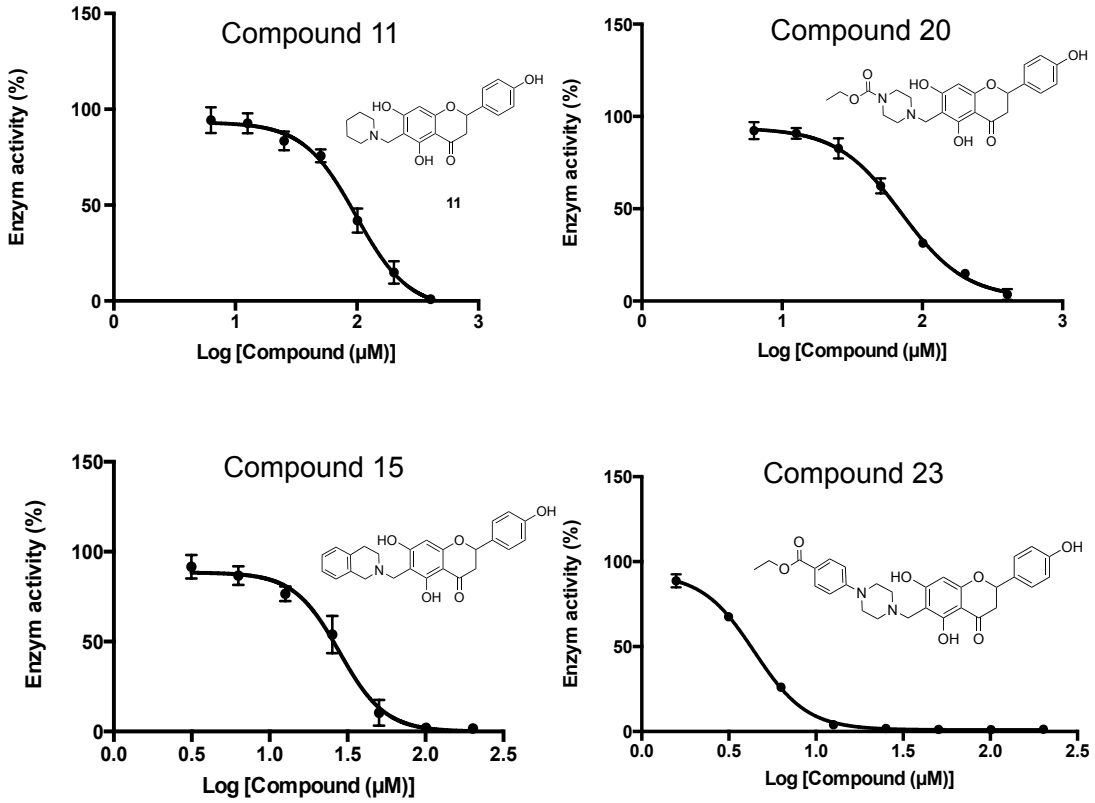

Figure 50. α-Glucosidase inhibitory activity of compounds **11**, **15**, **20** and **23**

Table 5. Summary of synthesized compounds and their inhibitory activities (**1-10**)

No.	Flavonoid Moiety*	Alkaloid Moiety	Position	Substituted Groups			Inhibitory Activity (IC_{50} in μM)
				R_1	R_2	R_3	
1	I		6	OH	H	H	249
2			6	OCH_3	OH	H	> 500
3			6	OH	OH	OH	> 500
4	II		6	H	H	-	> 500
5			8				> 500
6			6	OH	H	H	293
7	IV		6	OH	-	-	> 500
8			8	OH	-	-	> 500
9			6	OH	OH	-	> 500
10			8	OH	OH	-	> 500

* Classes of flavonoids: I: Flavanone; II: Flavone; IV: Flavan

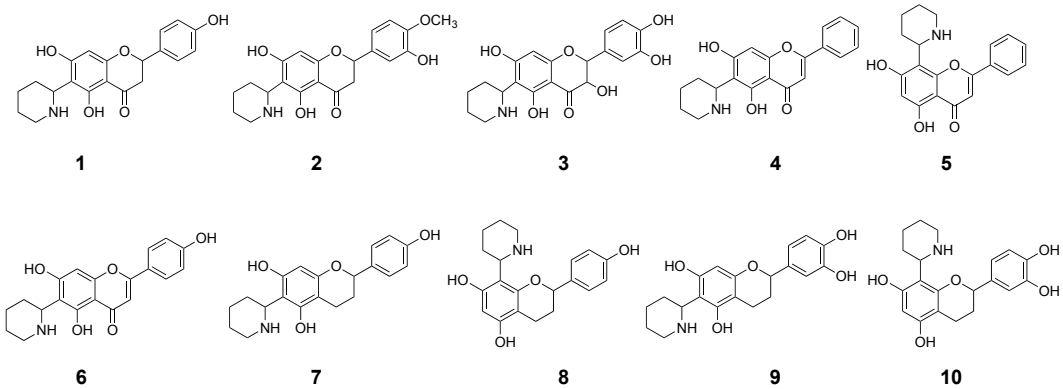

Figure 51. The chemical structures of synthesized flavonoid alkaloids (**1-10**)

Compounds **1-10** were synthesized through the reaction with Δ^1-piperideine. The piperidine ring is connected to the 6 or 8 position of the flavonoid through the 2'' position (carbon next to the nitrogen atom) giving a secondary amine group in the product. Compounds **1** and **6** have inhibitory activities toward α-glucosidase with IC_{50}

values of 249.4 μM and 293.3 μM, respectively. The kinkéloids (**7-10**) tested did not have potent inhibitory activities with IC_{50} less than 500 μM.

Table 6. Summary of synthesized compounds and their inhibitory activities (**11-14**)

No.	Flavonoid Moiety*	Alkaloid Moiety	Position	Substituted Groups			Inhibitory Activity (IC_{50} in μM)
				R_1	R_2	R_3	
11	I		6	OH	H	H	83
12	II		6	H	H	-	> 500
13	III		8	H	-	-	> 500
14	II		6	H	H	-	217

* Classes of flavonoids: I: Flavanone; II: Flavone; III: Isoflavone;

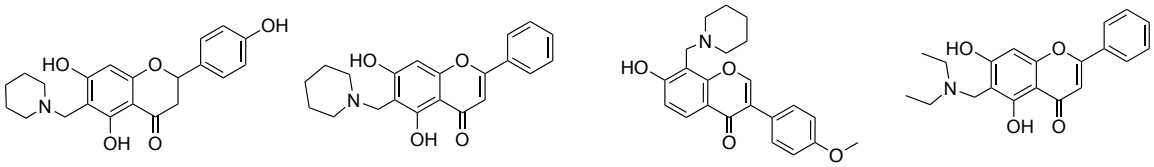

Figure 52. The chemical structures of synthesized flavonoid alkaloids (**11-14**)

Compounds **11-14** were synthesized through the reaction between flavonoids and piperidine or diethylamine. The nitrogen moiety is connected to the flavonoid through a methylene group resulting a tertiary amine group in the product. Compound **11** and **14** have inhibitory activity with IC_{50} value of 83 μM and 217 μM, respectively.

Table 7. Summary of synthesized compounds and their inhibitory activities (**15** & **16**)

No.	Flavonoid Moiety*	Alkaloid Moiety	Position	Substituted Groups			Inhibitory Activity (IC_{50} in μM)
				R_1	R_2	R_3	
15	I	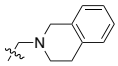	6	OH	H	H	23
16	II		6	H	H	-	> 500

* Classes of flavonoids: I: Flavanone; II: Flavone;

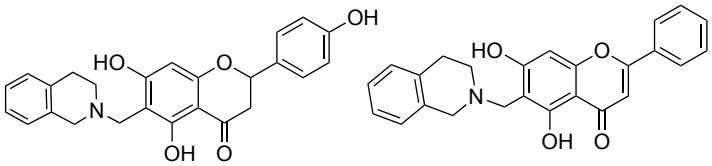

15 **16**

Figure 53. The chemical structures of synthesized flavonoid alkaloids (**15-16**)

Compound **15** and **16** were synthesized with starting material secondary amine 1,2,3,4- tetrahydroisoquinoline. Compound **15** has much improved inhibitory activity with IC_{50} of 23 μM, which could be contributed by enhanced hydrophobic interactions between the tetrahydroisoquinolinen and the protein molecule. However, compound **16** did not show potent inhibitory activity, suggesting the importance of 4'-hydroxyl group and the double bond at 2-3 positions.

Table 8. Summary of synthesized compounds and their inhibitory activities (**17-23**)

No.	Flavonoid Moiety*	Alkaloid Moiety	Position	Substituted Groups			Inhibitory Activity (IC_{50} in μM)
				R_1	R_2	R_3	
17	I	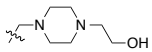	6	OH	H	H	521
18	II		6	H	H	-	> 500
19			8				> 500
20	I	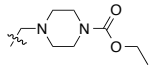	6	OH	H	H	65
21	II		6	H	H	-	> 500
22			Di	H	H	-	> 500
23	I	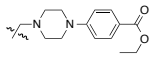	6	OH	H	H	4.1

* Classes of flavonoids: I: Flavanone; II: Flavone;

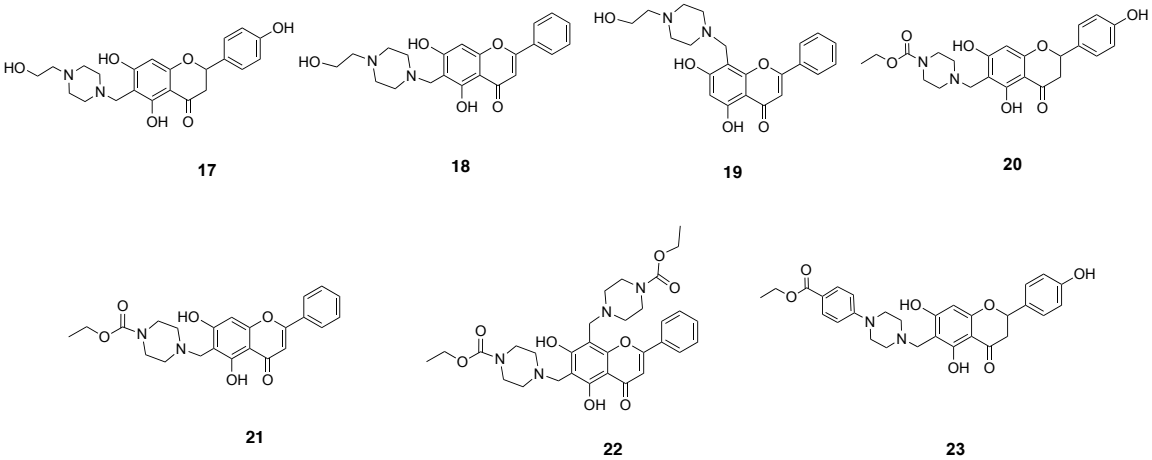

Figure 54. The chemical structures of synthesized flavonoid alkaloids (**17-23**)

Compounds **17-23** were synthesized with the attachment of a piperazine group, which has two nitrogen atoms. Other chemical groups, such as ester, ethyl alcohol, were also added to diverse their structures. In these compounds, compound **23** has the most potent inhibitory activity with IC_{50} value of 4.1 μM. Compound **20** also has good inhibitory activity with IC_{50} value of 65 μM.

Table 9. Summary of synthesized compounds and their inhibitory activities (**24-25**)

No.	Flavonoid Moiety*	Alkaloid Moiety	Position	Substituted Groups			Inhibitory Activity (IC_{50} in μM)
				R_1	R_2	R_3	
24	I		6	OH	H	H	203
25	II		6	H	H	-	> 500

* Classes of flavonoids: I: Flavanone; II: Flavone;

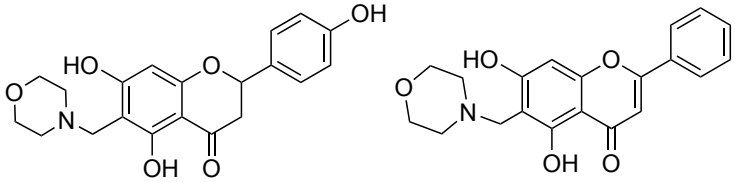

24 **25**

Figure 55. The chemical structures of synthesized flavonoid alkaloids (**24-25**)

Compounds **24-25** were synthesized flavanone and flavone derivatives and with the attachment of a morpholine group. Among them, **24** showed inhibitory activity with IC_{50} of 203 μM.

The enzyme kinetic assays were performed on the most potent two compounds **15** and **23** to investigate their mode of inhibition toward α-glucosidase. In the kinetic studies, a range of concentrations of test compounds and substrate pNPG (*p*-nitrophenyl- α-D-glucoside) were used. The data was analyzed using Lineweaver-Burk and Dixon plots (Figure 56) (Cornish-Bowden, 1974). The Lineweaver-Burk plot was drawn by plotting inverse velocity (*1/V*) as a function of the inverse substrate concentration (*1/[S]*), while the Dixon plot was created by plotting inverse velocity (*1/V*) as a function of the

compound concentration (*[I]*). The result showed that both compounds **15** and **23** are very close to the non-competitive model inhibitor of α-glucosidase. Their *Ki* value achieved from Dixon plot, are 37.8 ± 0.8 and 13.2 ± 0.6 μM, respectively.

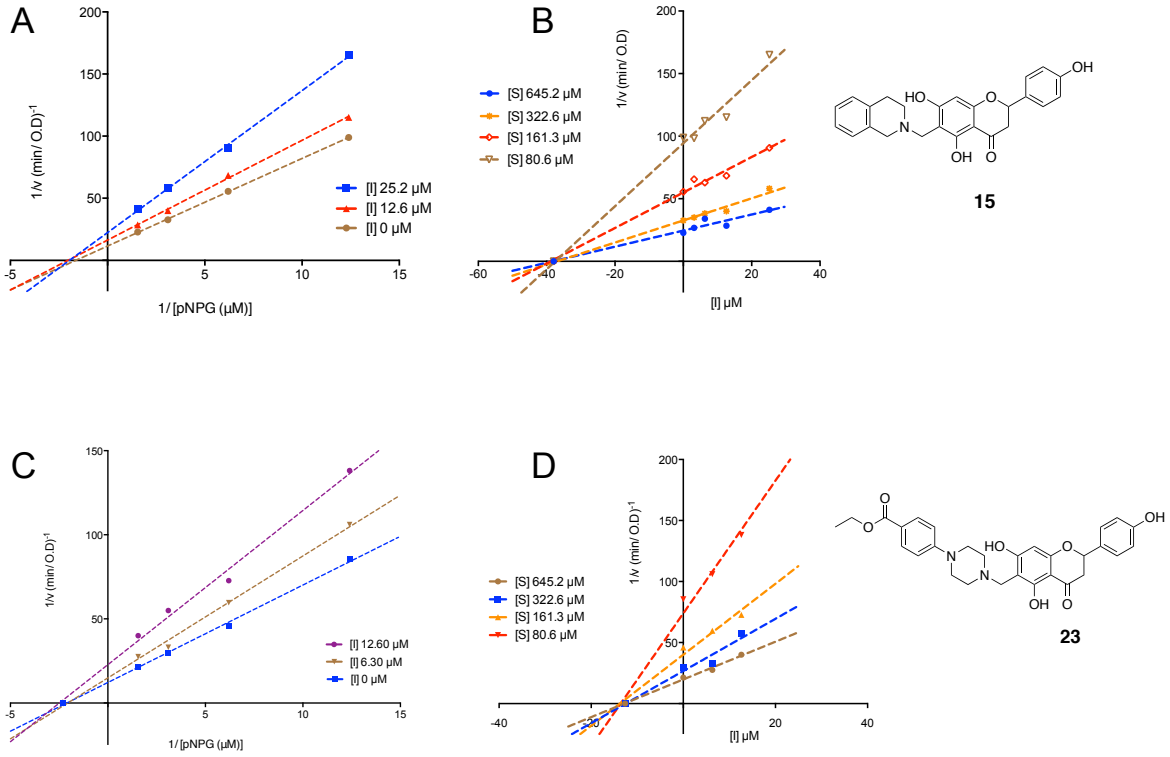

Figure 56. Lineweaver-Burk and Dixon plots of compound **15** and **23** toward the inhibition of α-glucosidase. (A) Lineweaver-Burk plot of compound **15**; (B) Dixon plot of compound **15**; (C) Lineweaver-Burk plot of compound **23**; (D) Dixon plot of compound **23**

6.2.3 Molecular Modeling

In order to develop a binding model between the synthesized inhibitor and α-glucosidase, a molecular docking study was performed. After geometric optimization, both enantiomers of compounds **15** and **23** were docked into the entire protein molecule. There are mainly three different docking sites (Appendix III), in which site A (Figure 57A) has the best correlation with non-competitive features and highest binding affinity (Brindis et al., 2010). From the preliminary docking results of compounds **15**, **23**, we

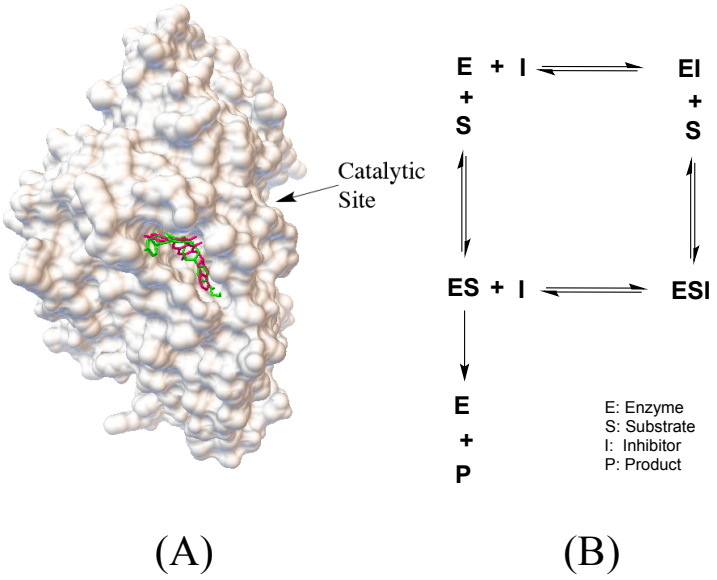

Figure 57. (A). The discovered binding site A between synthesized compounds **15**, **23** and α-glucosidase; (B) The scheme of non-competitive inhibition

found that the R or S isomers share almost the same binding sites on the protein through random screening. Their positions and configurations are very close at binding site A, indicating the chirality at position 2 may has limited effect on docking results, but this

observation will require further confirmation in the future. Even if site A is not directly responsible for the hydrolysis of carbohydrates, but after binding with a small molecule, it may alter protein conformation and interfere the catalytic function indirectly (Figure 57). A secondary docking was then performed on site A within a smaller area and yields refined results for binding analysis. The binding site A is close to the catalytic center and formed by amino acid residues ARG 263, ARG 270, HIS 295, GLY 269, ASN 259, TRP 15, LYS 16, LEU 297, SER 298, TRP 343 (Figure 58). There are two arginine amino acids, ARG 263, ARG 270 at the entrance of the pocket, which are positively charged at experimental pH 6.8 and may interact with the 4'-hydroxyl group on flavonoid ring C. At the end, a hydrophobic pocket formed by two tryptophan amino acids TRP 15 and TRP 343 is likely to interact with the hydrophobic groups, like the tetrahydroisoquinoline group of compound **15** and the ethyl benzoate group of compound **23**. Three hydrogen bonds were observed for compound **15**: the carbonyl group of position 4 and HIS 295, phenol groups of position 5, 7 and amino acids ASN 259 and SER 298. For compound **23**, there are two hydrogen bonds: phenol of position 7 and HIS 295, the carbonyl group of ester group and LYS 16.

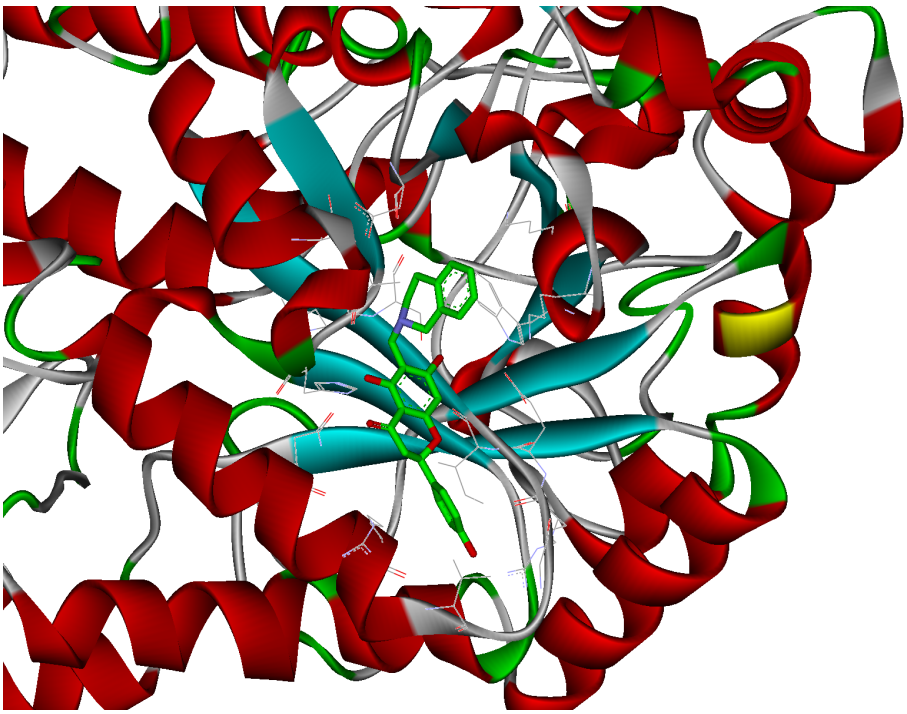

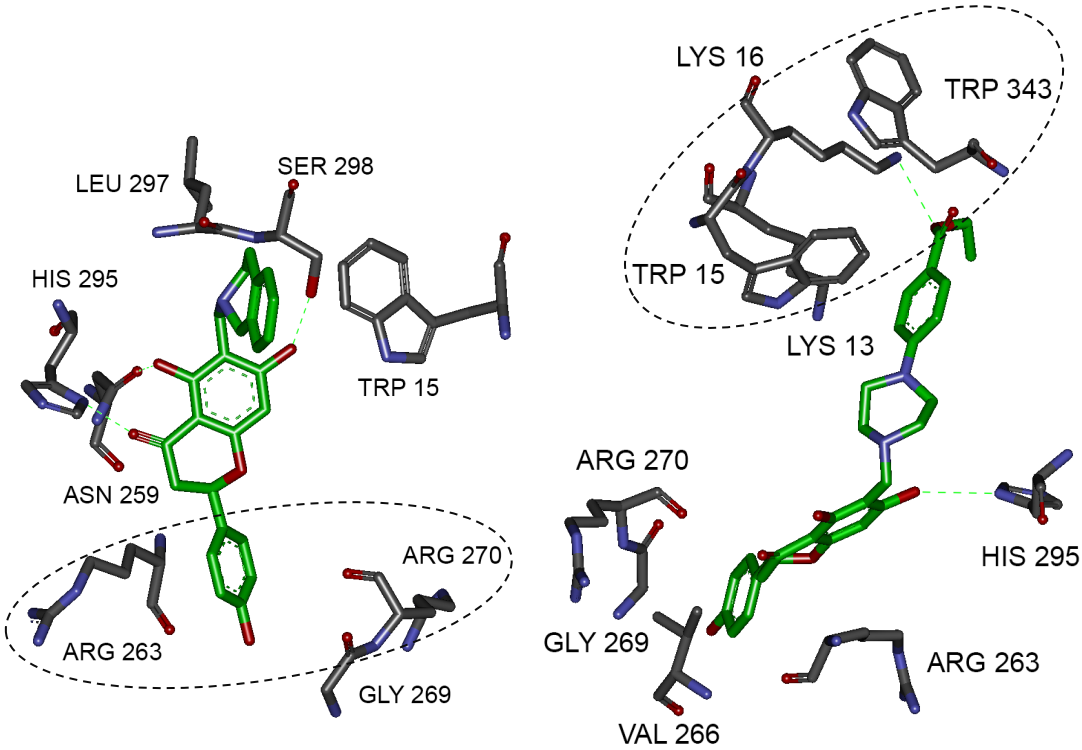

Figure 58. The binding model between compounds **15** and **23** and α-glucosidase at binding site A

6.2.4 Summary of Structure Activity Relationships

In this study, most of the analogues were synthesized from the flavanone naringenin and flavone chrysin. Several structure activity relationships were found through the comparisons of different compound's inhibitory activities and the analysis of docking results. From the comparison between compounds **4** (IC_{50} = 500 μM) and **6** (IC_{50} = 293 μM) in Figure 59, our data suggests that the hydroxyl group attached at ring position 4'

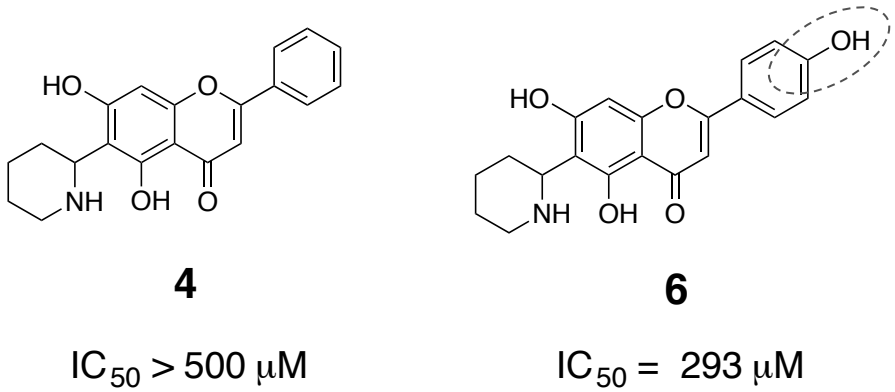

Figure 59. Chemical structures of compound **4** and **6**

on ring B is important for maintaining inhibitory activity. The importance of 4'-hydroxyl group would also be anticipated from the docking results. As seen in Figure 58, there is an interaction between ring B of flavonoid moiety and the positively charged arginine groups (ARG 263, ARG 270) at the entrance of the binding pocket. The positively charged arginine groups prefer the more hydrophilic phenol group than the hydrophobic phenyl group. This may also explain that why most of the chrysin derivatives synthesized in this study without 4'-hydroxyl group have comparatively lower inhibitory activities.

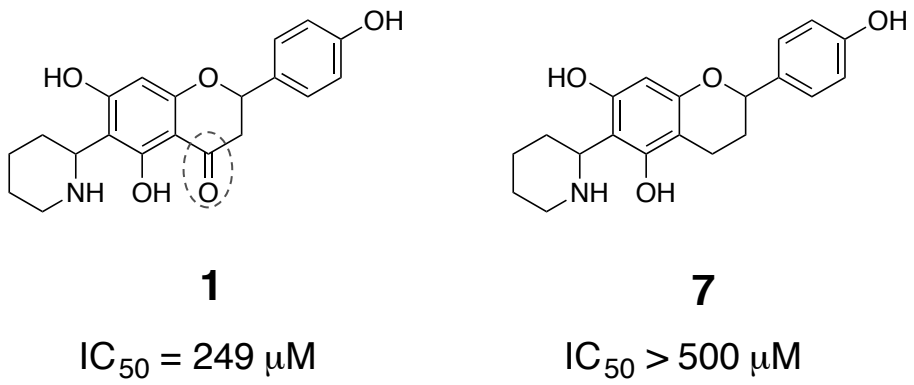

Figure 60. Chemical structures of compound **1** and **7**

In comparing the bioactivity of compound **1** (IC_{50} = 249 μM) and **7** (IC_{50} > 500 μM), the importance of carbonyl group at position 4 in the maintaining of inhibitory activity is clearly evident. The carbonyl group at 4-position may contribute to hydrogen bonding between the protein and the compound as shown in Figure 58, or it may increase the molecular rigidity presenting a more suitable conformation toward the binding pocket.

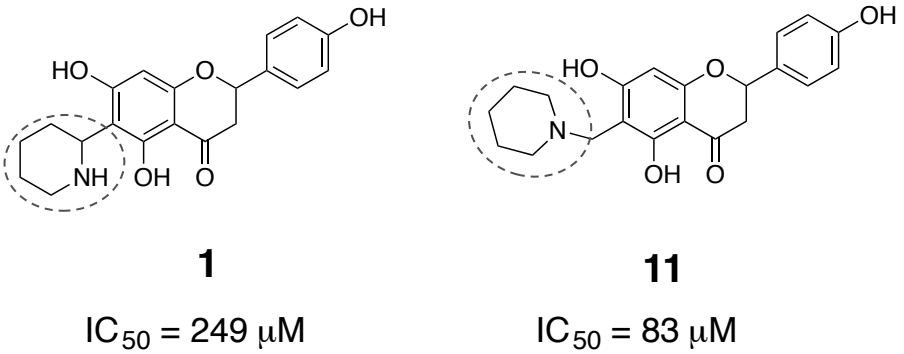

Figure 61. Chemical structures of compound **1** and **11**

We also observed that a tertiary amine is likely to yield better inhibitory activity than a secondary amine group, as suggested from the comparison between compound **1** (IC_{50} = 249 μM) and compound **11** (IC_{50} = 83 μM). Attachment of hydrophobic groups at ring A of the flavonoid moiety is generally associated with improved inhibitory activity as

compound **15** (IC_{50} = 23 μM) is significantly more potent than **17** (IC_{50} = 521 μM); Similarly it can be seen that compound **23** (IC_{50} = 4.1 μM) is much more potent than **20** (IC_{50} = 65 μM). This observation correlates very well with the binding analysis from the docking result. As shown in Figure 58, there is a hydrophobic pocket formed by two tryptophan amino acids, which prefers to have interaction with hydrophobic groups rather than hydrophilic ones.

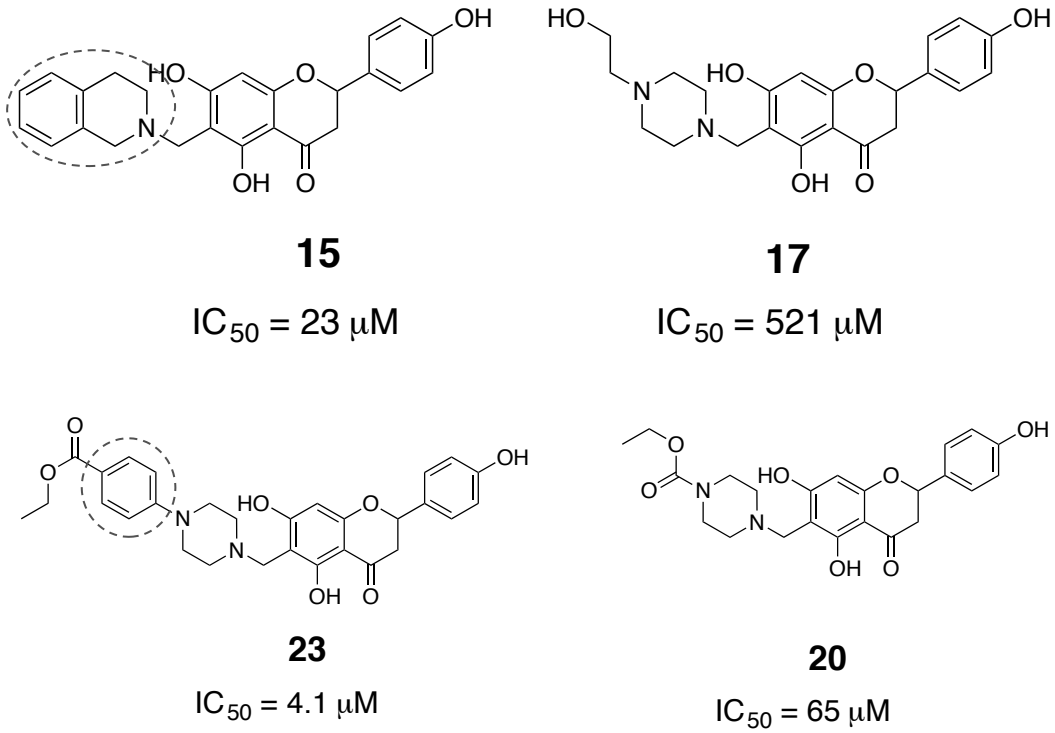

Figure 62. Chemical structures of compound **15**, **17**, **23** and **20**

We also noticed that the addition of extra hydrogen bond acceptor at the end of attached nitrogen moiety may increase the binding between α-glucosidase through the addition of hydrogen bonding. For example compound **23** (IC_{50} = 4.1 μM) have a hydrogen bond with LYS 16 through the carbonyl group of ester moiety, which may

explain the higher inhibitory activity than compound **15** (IC_{50} = 23 μM). Based on these observations, the overall structure activity relationships are generalized in Figure 64.

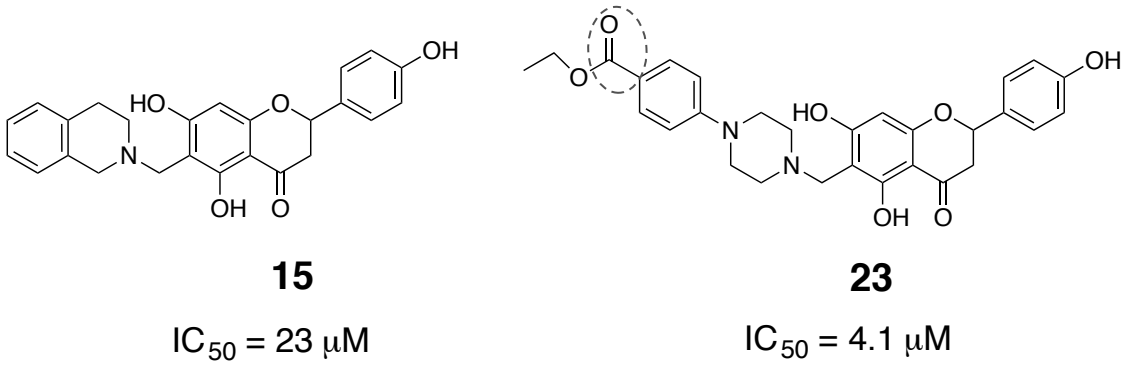

Figure 63. Chemical structures of compound **15** and **23**

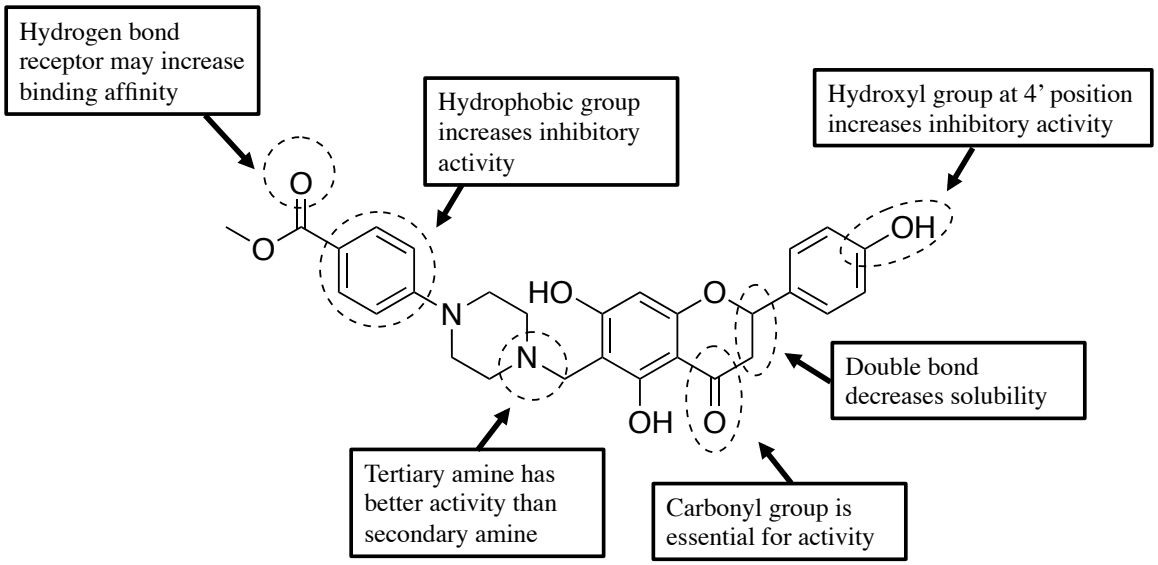

Figure 64. The generalized structure activity relationships

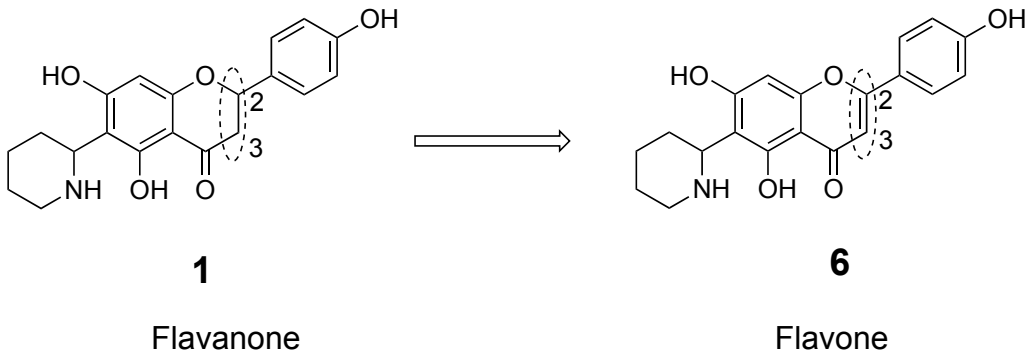

Figure 65. Chemical structures of compound **1** and **6**

Through the comparison between **1** and **6**, we found that the double bond at 2-3 positions will decrease the solubility, meaning in general the flavanone derivatives have better solubility than flavone derivatives, which have a double bond at 2-3 positions. We also tried to link flavone chrysin with ethyl 4-(1-piperazinyl)benzoate group to synthesize an analogue of the most potent compound **23**, but the synthesized compound has much decreased solubility in the assay buffer and could not be assayed for inhibitory activity.

It would be of considerable interest to modify the ethyl 4-(1-piperazinyl)benzoate moiety of compound **23** to increase its overall solubility making it more compatible to other flavonoid moieties, while maintaining the inhibitory activity. Considering the high pK_b value of the phenylamine group ($pK_b \sim 11$), one possible strategy is to insert one or two methylene group between the benzene moiety and the attached piperazine moiety. With this insertion, the original phenylamine is converted to an alkyl tertiary amine with much decreased pK_b value ($pK_b \sim 9$ or 5) making the whole molecule much easier to be ionized in experimental pH of 6.8 and potentially more soluble under our experimental assay conditions (Figure 66).

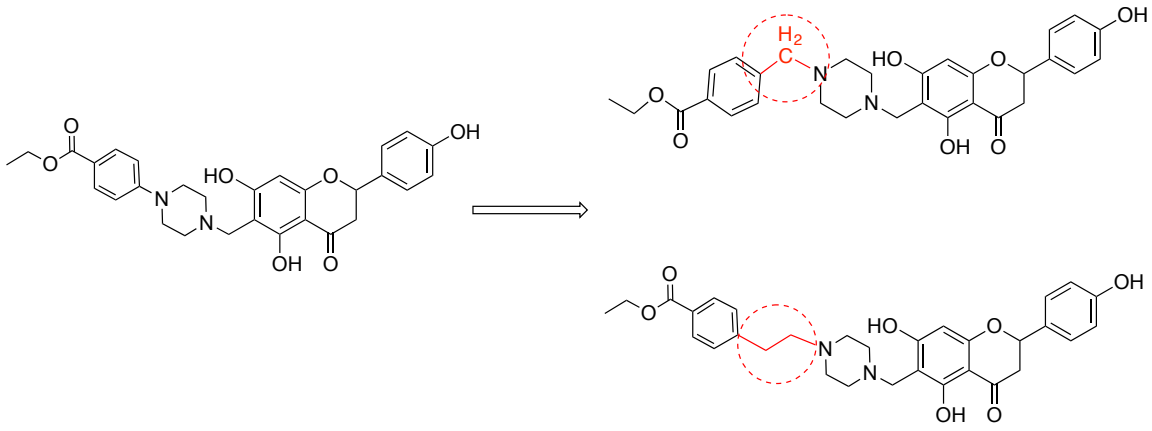

Figure 66. The modified structure of compound **23** with insertion of one or two methylene group between benzene and the piperazine moieties

The structure of **23** could also be modified with the introduction of more hydrophilic groups on the flavonoid moieties. Based on the generalized structure activity relationships above, other synthesized analogues could also be rationally designed through the modifications of compound **15** and **23** to provide better inhibitory activity and for diabetes drug development. These further structure modifications will require more complicated synthetic routes designs, especially the modifications of the functional groups attached at ring A of flavonoids. Studies described in this paper only serve as an initial investigation of structure activity relationships between α-glucosidase and flavonoid alkaloids. The biological activities of synthesized compounds in this study are far below the activities of drugs on the market targeting α-glucosidase, such as acarbose (IC_{50} of 430 nM) and voglibose (IC_{50} of 5.5 nM) (Matsui et al., 2002). So in order to potentially achieve lead compounds in the future, additional work is necessary to design synthetic methods to modify the structures of interest in this study.

6.3 Conclusion

In summary, a collection of flavonoid alkaloids were synthesized through Mannich reaction targeting α-glucosidase. Most of the compounds synthesized from flavanone naringenin exhibit potent bioactivities with IC_{50} values below 500 μM, in which the most potent compound **23** has an IC_{50} value of 4.1 μM. The enzyme kinetic investigations suggested that the synthesized compounds **15** and **23** inhibit enzyme in the non-competitive manner with *Ki* value of 37.8 ± 0.8 and 13.2 ± 0.6 μM, respectively. Results from the molecular docking study suggested that the synthesized derivatives might bind to a pocket close the catalytic center and interfere the catalysis process indirectly. The binding model between α-glucosidase and compounds **15**, **23** at location A were carefully analyzed, in which several hydrogen bonds and hydrophobic interactions were revealed. Based on tested inhibitory activities of synthesized compounds and the binding analysis from the docking study, several structure activity relationships were further generalized. We found that the 4'-position hydroxyl group and 4-position carbonyl group are essential to maintain the inhibitory activity. The introduction of hydrophobic groups and hydrogen bond acceptors at flavonoid ring A would potentially increase the binding affinity. Several recommendations were also given in our study as potential future work to further increase the inhibitory activities of compounds **15**, **23**. Overall, this study is serving as structure activity relationships exploratory studies between flavonoid alkaloids and enzyme α-glucosidase, potentially contributing anti-diabetic drug development in the future.

6.4 Materials and Methods

6.4.1 Instrument and Reagents

^{1}H and ^{13}C NMR spectra were performed on Bruker Avance 400 MHz spectrometer (Billerica, MA). Analytical LC-MS was performed on Hewlett-Packard Agilent 1100 series HPLC-MSD (Agilent Technologies, Waldbronn, Germany) equipped with a quaternary pump system, a degasser, an auto-sampler, a DAD detector, a MSD trap with electrospray ion source (ESI). Column chromatography was performed using silica gel (230 - 400 mesh; Selecto Scientific, Suwanee, GA). All synthetic materials are all purchased from Sigma Aldrich, St. Louis, MO. All solvents were purchased from Fisher Scientific, Hampton, NH.

6.4.2 *In vitro* α-glucosidase Assay

The assay was performed with slight modifications based on a chromogenic method reported by Wang et al (2015). First, 10 µl of enzyme solution (1 U/ml) was diluted with 120 µl of 0.1 M phosphate buffer (pH 6.8). Then, 5 µl of the compounds dissolved in DMSO of various concentrations were added into the enzyme solution. The final concentration of DMSO was around 2%. The mixture was then incubated at 37 °C for 15 min. Afterward 20 µl of 5 mM substrate p-nitrophenyl- α-D-glucopyranoside in phosphate buffer (pH 6.8) was added and incubated for additional 30 min at 37 °C. The reaction was quenched using 80 µl of 0.2 M Na_2CO_3. Absorption was subsequently

measured using UV spectrometer at wavelength of 405 nm. The reaction without enzyme was treated as blank and each experiment was triplicated. Reaction with the treatment of compound naringenin was used as a positive control in the experiment. The inhibitory activity was calculated using the following equation:

Inhibition % = [(control absorption – sample absorption) / control absorption] × 100

The IC_{50} value of each sample was calculated from the fitting of sigmoidal dose-response curve with variable slope.

6.4.3 Enzymatic Kinetics of α-glucosidase Inhibition

Mode of the inhibition of synthesized flavonoid alkaloids against yeast α-glucosidase activity was measured with different concentrations of pNPG (0.625, 1.25, 2.5, 5.0 mM). The control group had no compound added. Mode of inhibition of each tested compound was determined by Lineweaver-Burk plot analysis. The Dixon plots were applied to determined the inhibitory constants with the following equation:

V is the reaction velocity, S is substrate concentration, V_{max} is the maximum enzyme velocity, K_m is Michaelis-Menten constant, I is inhibitor concentration, K_i is inhibition constant, α is the constant that determines mechanism. In this study, for non-competitive inhibitor, $\alpha = 1$.

$$V = \frac{Vm\,S}{Km\left(1 + \frac{I}{Ki}\right) + S\,(1 + \frac{I}{\alpha Ki})}$$

If α is very large, then the mode approaches a competitive model. If α is very small but greater than zero, the mode is more close to uncompetitive model (Brindis et al., 2010).

6.4.4 Molecular Docking

The crystallographic structure of α-glucosidase (PDB: 3A4A) was downloaded from the Protein Data Bank (http://www.rcsb.org/pdb/). Enzyme docking experiment is based on previous published report (Rivera-Chávez et al., 2015). All polar hydrogen atoms and charges were assigned to the receptor using AutoDockTools 1.5.4. Compounds used for docking study were built using the molecular builder function in MOE 2010.11 (http://www.chemcomp.com/), the energy of each compound was minimized to its local minima using MMF94X force field to a constant value of 0.05 kcal/mol. Docking simulation and binding pocket prediction was performed using AutoDock Vina (http://vina.scripps.edu/) (Trott and Olson, 2010). The protein was held rigid in the docking process. The inhibitors were allowed to be flexible. The initial grid box size was 62 Å× 78 Å×1 72Å in the *x, y, z* dimensions and the grid box center was put on x = 23.8, y = -3.834 and z = 19.691. The protein was positioned at the center of the box. The docking method was validated using its competitive inhibitor acarbose. The resulting docked poses were analyzed with AutoDockTools using cluster analysis, PyMOL (https://www.pymol.org) (DeLano, 2002). Using this established method, the control compound acarbose was docked into the catalytic binding pocket, which correlates very well with literature report and its competitive inhibition mechanism on α-glucosidase.

6.4.5 Chemical Synthesis

*General procedure for the synthesis of Compounds **1-10***

The flavonoid compound was dissolved in methanol, ethanol or methanol/ tetrahydrofuran followed by the addition of Δ^1-piperideine. The mixture was then stirred at 80 °C under nitrogen atmosphere for 5 hours. After the reaction, the solvent was removed under reduced pressure and the residue was purified on silica column using methanol/dichloromethane to yield desired compound.

*5,7-Dihydroxy-2-(4-hydroxyphenyl)-6-(piperidin-2-yl)chroman-4-one (**1**)*

Naringenin (136 mg, 0.5 mmol) was dissolved in ethanol (8 ml) followed by addition of Δ^1-piperideine (64 mg, 0.75 mmol). The mixture was stirred at 70 °C for overnight. Then product was precipitated out as white solid. The precipitate was filter out for purity analysis on LC/MS and NMR. Yield: 78%; white powder; mp > 232 °C (dec.); ESI-MS: *m/z* 356 $[M+H]^+$, ^{1}H NMR (400 MHz, DMSO-d_6): δ 1.50-1.90 (6H, m, H- 4'', 5'', 6''), 2.47 (1H, m, H-3), 2.75 (1H, m, H-3''), 2.98 (1H, m, H-3), 3.29 (1H, m, H-3''), 4.16 (1H, m, H-1''), 5.20 (1H, m, H-2), 5.33 (1H, s, H-8), 6.78 (2H, m, H-3', 5'), 7.28 (2H,m, H-2', 6'); ^{13}C NMR (100 MHz, DMSO-d_6): δ 22.44, 22.54 (C-4'', 5''), 28.15 (C-6''), 41.86 (C-3), 43.52 (C-3''), 52.05 (C-1''), 77.48 (C-2), 96.91 (C-10), 98.01 (C-8), 104.58 (C-6), 115.05 (C-2', 6'), 128.01 (C-3', 5'), 129.75 (C-1'), 157.40, 160.01, 161.56, 177.67 (C-4', 5, 7, 9), 191.51 (C-4, C=O).

*5,7-Dihydroxy-2-(3-hydroxy-4-methoxyphenyl)-6-(piperidin-2-yl)chroman-4-one (**2**)*

Hesperetin (250 mg, 0.83 mmol) was dissolved in methanol (5 ml) followed by addition of Δ^1-piperideine (82.7 mg, 1.0 mmol). The mixture was stirred at 65 °C for overnight. Then the solvent of the reaction was removed on rotavapor. The dried sample was mixed with small amount of silica gel and then loaded on silica gel column for purification using solvent system (5% methanol in dichloromethane). Yield: 60%; white solid; mp 172-174 °C. ESI-MS: m/z 386 $[M+H]^+$; ^{1}H NMR (400 MHz, DMSO-d_6): δ 1.50-1.90 (6H, m, H- 4'', 5'', 6''), 2.54 (1H, m, H-3), 3.27 (1H, m, H-3''), 2.92 (1H, m, H-3), 3.27 (1H, m, H-3''), 3.76 (1H, s, -OCH_3), 4.16 (1H, m, H-1''), 5.18 (1H, m, H-2), 5.35 (1H, s, H-8), 6.84-6.91 (3H, m, H-2', 5', 6'); ^{13}C NMR (100 MHz, DMSO-d_6): δ 22.45, 22.54 (C-4'', 5''), 28.2 (C-6''), 41.9 (C-3), 43.5 (C-3''), 52.0 (C-1''), 55.7 (-OCH_3), 77.3 (C-2), 96.9 (C-8), 98.5 (C-10), 104.6 (C-6), 112.0 (C-5'), 113.9 (C-2'), 117.3 (C-6'), 132.1 (C-1'), 146.5, 147.6 (C-3', 4'), 161.5, 160.0, 177.7 (C-5, 7, 9), 191.4 (C-4, C=O).

*2-(3,4-Dihydroxyphenyl)-3,5,7-trihydroxy-6-(piperidin-2-yl)chroman-4-one (**3**)*

(±) Taxifolin (24.4 mg, 0.08 mmol) was dissolved in methanol (1 ml) followed by addition of Δ^1-piperideine (7.3 mg, 0.08 mmol). The mixture was stirred at 40 °C. After the reaction, the solvent of the reaction was removed on rotavapor and the sample was purified on silica gel column using solvent system (20% methanol in dichloromethane). Yield: 25%; yellow solid; mp > 200 °C (dec.); ESI-MS: *m/z* 388 $[M+H]^+$; ^{1}H NMR (400 MHz, DMSO-d_6) (mixture of isomers): δ 1.53-1.70 (6H, m, H-4'', 5'', 6''), 2.79 (1H, m, H-3''), 3.30 (1H, m, H-3''), 4.21 (1H, m, H-1''), 4.27 (1H, d, J = 10 Hz, H-3), 4.75 (1H,

d, J = 10 Hz, H-2), 5.40 (1H, s, H-8), 6.84 (1H, m, H-5'), 6.70 (2H, m, H-2', 6'); ^{13}C NMR (100 MHz, DMSO-d_6): δ 22.41, 27.80, 29.48 (C-4'', 5'', 6''), 43.78 (C-3''), 51.90 (C-1''), 82.42 (C-2), 104.59 (C-6), 97.80 (C-10), 95.95 (C-8), 119.10 (C-2', 6'), 115.10 (C-5'), 145.51, 160.78 (C-3', C-4'), 159.98, 161.43 (C-5, 9), 161.32 (C-7), 192.6 (C-4).

*5,7-Dihydroxy-2-phenyl-6-(piperidin-2-yl)-4H-chromen-4-one (**4**)*

Chrysin (200 mg, 0.79 mmol) was dissolved in MeOH/THF (4 ml / 8 ml). Then, the mixture was added Δ^1-piperideine (80 mg, 0.96 mmol). The mixture was stirred at 40 °C. TLC was used to monitor the completion of the reaction. Afterward, the solvent was removed under vacuum and the residue was purified on silica gel column using 5% methanol in dichloromethane. Pale yellow solid (yield: 26%); mp 202-204 °C ESI-MS: *m/z* 338 $[M+H]^+$; ^{1}H NMR (400 MHz, DMSO-d_6): δ 1.55-1.85 (6H, m, H-4'', 5'', 6''), 2.75 (1H, m, H-3''), 3.31 (1H, m, H-3''), 4.26 (1H, J = 11.4, 3.8 Hz, H-1''), 5.98 (1H, s, H-8), 6.71 (1H, s, H-3), 7.55 (3H, m, H-3', 4', 5'), 7.99 (2H, m, H-2', 6'); ^{13}C NMR (100 MHz, DMSO-d_6): δ 22.52, 22.80, 28.12 (C-4'', 5'', 6''), 43.49 (C-3''), 52.01 (C-1''), 95.90 (C-8), 99.34 (C-10), 108.67 (C-8), 125.00 (C-2', 6'), 130.00 (C-3', 5'), 131.37 (C-4'), 157.46, 157.28, 161.26 (C-5, 9, 2), 173.88 (C-7), 180.14 (C-4).

*5,7-Dihydroxy-2-phenyl-8-(piperidin-2-yl)-4H-chromen-4-one (**5**)*

Chrysin (200 mg, 0.79 mmol) was dissolved in MeOH/THF (4 ml / 8 ml). Then, the mixture was added Δ^1-piperideine (80 mg, 0.96 mmol). The mixture was stirred at 40 °C.

TLC was used to monitor the completion of the reaction. Afterward, the solvent was removed under vacuum and the residue was purified on silica gel column using 5% methanol in dichloromethane. Yellow solid (yield: 14%); mp 212-214 °C; ESI-MS: *m/z* 338 $[M+H]^+$; ^{1}H NMR (400 MHz, DMSO-d_6): δ 1.55-1.83 (6H, m, H-4'', 5'', 6''), 2.89 (1H, m, H-3''), 3.31 (1H, m, H-3''), 4.48 (1H, *J* = 11.8, 3.5 Hz, H-1''), 5.78 (1H, s, H-6), 6.78 (1H, s, H-3), 7.59 (3H, m, H-3', 4', 5'), 8.00 (2H, m, H-2', 6'); ^{13}C NMR (100 MHz, DMSO-d_6): δ 22.77, 22.98, 28.93 (C-4'', 5'', 6''), 43.58 (C-3''), 52.69 (C-1''), 101.57 (C-6), 103.77 (C-10), 104.70 (C-8), 125.95 (C-2', 6'), 129.20 (C-3', 5'), 131.48 (C-4'), 153.63, 160.67, 161.05 (C-5, 9, 2), 173.14 (C-7), 180.27 (C-4).

*5,7-Dihydroxy-2-(4-hydroxyphenyl)-6-(piperidin-2-yl)-4H-chromen-4-one (**6**)*

Apigenin (20 mg, 0.07 mmol) was dissolved in 3 ml H_2O/THF (2:1). Then the mixture was added Δ^1-piperideine (8.3 mg, 0.1 mmol). The mixture was then stirred at 40 °C. TLC was used to monitor the completion of the reaction. Afterward, the solvent was removed under vacuum and the residue was purified on silica gel column using 10% methanol in dichloromethane. Yellow solid (yield: 38%); mp > 230 °C (dec.); ESI-MS: *m/z* 354 $[M+H]^+$; ^{1}H NMR (400 MHz, DMSO-d_6): δ 1.53-1.78 (6H, m, H-4'', 5'', 6''), 2.80 (1H, m, H-3''), 3.30 (1H, m, H-3''), 4.25 (1H, *J* = 11.6 3.4 Hz, H-1''), 6.07 (1H, s, H-8), 6.58 (1H, s, H-3), 6.89 (2H, m, H-3', 5'), 7.83 (2H, m, H-2', 6'); ^{13}C NMR (100 MHz, DMSO-d_6): δ 22.61, 22.86, 28.21 (C-4'', 5'', 6''), 43.80 (C-3''), 51.95 (C-1''), 102.11 (C-6), 99.74 (C-10), 95.45 (C-8), 127.98 (C-2', 6'), 115.86 (C-3', 5'), 160.78 (C-4'), 157.43, 157.16, 162.28 (C-5, 9, 2), 171.87 (C-7), 180.56 (C-4).

*2-(4-Hydroxyphenyl)-6-(piperidin-2-yl)chromane-5,7-diol (**7**)*

The synthesized 4', 5, 7-trihydroxyflavan (200 mg, 0.78 mmol) was dissolved in methanol followed by the addition of Δ^1-piperideine (77 mg, 0.93 mmol). The mixture was stirred at 70 °C under nitrogen atmosphere for 5 hours. After the reaction, the solvent was removed under reduced pressure and the residue was purified on silica column using methanol/dichloromethane (15:85) to yield a mixture of kinkéloids A. Further purification on a short Sephadex column LH-20 with methanol yields compound kinkéloids A as white solid (25%). We observed that synthesized kinkéloids A were oxidized to purple compounds after exposure to the air for a while at room temperature. The purified mixture was reloaded to a ~1.5 m long Sephadex LH-20 column for the separation of two groups of regioisomers. As each group of regioisomers is a mixture of chiral isomers, the coupling constants were not calculated. Melting point was not measured due to its instability at room temperature; ^{1}H NMR (400 MHz, DMSO-d_6, 6-piperidyl kinkéloids A): δ 1.41-1.76 (6H, m, H-4'', 5'', 6''), 1.83 (1H, m, H-3), 2.01 (1H m, H-3), 2.53 (2H, m, H-4), 2.67 (1H, m, H-3''), 3.12 (1H, m, H-3''), 4.15 (1H, m, H-1''), 4.80 (1H, H-2), 5.82 (1H, H-8), 6.75 (2H, H-2', 6'), 7.17 (2H, H-3', 5'); ^{13}C NMR (100 MHz, DMSO-d6) δ 19.29 (C-4), 23.79, 24.06 (C-4'', 5'') 28.89 (C-3), 29.83 (C-6''), 45.60 (C- 3'') 52.74 (C-1''), 76.41 (C-2), 94.17 (C-8), 101.18 (C-10), 106.71 (C-6), 114.98 (C-2', 6'), 127.37 (C-3', 5'), 131.97 (C-1'), 156.93, 155.53, 154.87, 153.38 (C-5, 7, 9, 4').

*2-(4-Hydroxyphenyl)-8-(piperidin-2-yl)chromane-5,7-diol (**8**)*

The synthesized 4', 5, 7-trihydroxyflavan (200 mg, 0.78 mmol) was dissolved in methanol followed by the addition of Δ^1-piperideine (77 mg, 0.93 mmol). The mixture was stirred at 70 °C under nitrogen atmosphere for 5 hours. After the reaction, the solvent was removed under reduced pressure and the residue was purified on silica column using methanol/dichloromethane (15:85) to yield a mixture of kinkéloids A. Further purification on a short Sephadex column LH-20 with methanol yields compound kinkéloids A as white solid (25%). We observed that synthesized kinkéloids A were gradually oxidized to purple compounds after exposure to the air for a while at room temperature. The purified mixture was reloaded to a ~1.5 m long Sephadex LH-20 column for the separation of two groups of regioisomers. As each group of regioisomers is a mixture of chiral isomers, the coupling constants were not calculated. Melting point was not measured due to its instability at room temperature; ^{1}H NMR (400 MHz, DMSO-d_6, 8-piperidyl kinkéloids A): δ 1.51-1.80 (6H, m, H-4'', 5'', 6''), 1.81 (1H, m, H-3), 2.06 (1H m, H-3), 2.51 (2H, m, H-4), 2.87 (1H, m, H-3''), 3.24 (1H, m, H-3''), 4.30 (1H, m, H-1''), 5.02 (1H, m, H-2), 6.14 (1H, H-6), 6.77 (2H, d, H-2', 6'), 7.20 (2H, d, H-3', 5'), ^{13}C NMR (100 MHz, DMSO-d_6) δ 19.64 (C-4), 21.67, 22.93 (C-4'', 5'') 28.60 (C-6''), 28.67 (C-3), 45.45 (C-3'') 52.70 (C-1''), 76.31 (C-2), 95.35 (C-6), 101.78 (C-10), 104.80 (C-8), 114.98 (C-2', 6'), 127.29 (C-3', 5'), 157.00, 155.51, 154.06, 153.90 (C-5, 7, 9, 4').

*2-(3,4-Dihydroxyphenyl)-6-(piperidin-2-yl)chromane-5,7-diol (**9**)*

The synthesized flavan compound 3', 4', 5, 7-tetrahydroxyflavan (40 mg, 0.15 mmol) was dissolved in methanol (4 ml) followed by the addition of Δ^1-piperideines (12.1 mg, 0.15 mmol). The mixture was stirred at 70°C under nitrogen atmosphere for 4 hours. After the reaction, the solvent was removed under reduced pressure and the residue was firstly purified on a short Sephadex column LH-20 using solvent methanol to give mixture of compound 6-piperidyl kinkéloids B (**9**) and 8-piperidyl kinkéloids B (**10**) (10 mg, 20%, low yield may be due to the formation of di-piperidine substituted products and some dead absorption to the column). Then the mixture was reloaded to a ~1.5 m long Sephadex LH-20 column for the separation of two groups of regioisomers. The elution solvent is methanol. As each group of regioisomers is a mixture of chiral isomers, the coupling constants were not calculated. ^{1}H NMR (400 MHz DMSO-d_6, 6-piperidyl kinkéloids B): δ 1.37-1.80 (6H, m, H-4'', 5'', 6''), 1.80-1.83 (1H, m, H-3), 2.00 (1H, m, H-3), 2.50 (2H, m, H-4), 2.60 (1H, m, H-3''), 3.08 (1H, m, H-3''), 4.10 (1H, m, H-1''), 4.73 (1H, m, H-2), 5.78 (1H, s, H-8), 6.61-6.72 (2H, m, H-5', 6'), 6.76 (1H, d, J = 1.92, H-2'); ^{13}C NMR (100 MHz, DMSO-d_6) δ 19.0 (C-4), 24.0, 24.5 (C-4'', 5''), 29.0 (C-3), 30.3 (C-6''), 45.7 (C-3'') 52.8 (C-1''), 76.4 (C-2), 93.9 (C-8), 101.4 (C-10), 107.1 (C-6), 113.7 (C-2'), 115.3 (C-5'), 117.1 (C-6'), 132.7 (C-1'), 144.8, 145.1 (C-3', 4') 153.2, 154.6, 155.9 (C- 5, 7, 9).

*2-(3,4-Dihydroxyphenyl)-8-(piperidin-2-yl)chromane-5,7-diol (**10**)*

The synthesized flavan compound 3', 4', 5, 7-tetrahydroxyflavan (40 mg, 0.15 mmol) was dissolved in methanol (4 ml) followed by the addition of Δ^1-piperideines (12.1 mg, 0.15 mmol). The mixture was stirred at 70 °C under nitrogen atmosphere for 4 hours. After the reaction, the solvent was removed under reduced pressure and the residue was firstly purified on a short Sephadex column LH-20 using solvent methanol to give mixture of compound 6-piperidyl kinkéloids B (**9**) and 8-piperidyl kinkéloids B (**10**) (10 mg, 20%, low yield may be due to the formation of di-piperidine substituted products and some dead absorption to the column). Then the mixture was reloaded to a ~1.5 m long Sephadex LH-20 column for the separation of two groups of regioisomers. The elution solvent is methanol. As each group of regioisomers is a mixture of chiral isomers, the coupling constants were not calculated. ^{1}H NMR (400 MHz DMSO-d_6, 8-piperidyl kinkéloids B): δ 1.37-1.80 (6H, m, H-4'', 5'', 6''), 1.80 (1H, m, H-3), 2.00 (1H, m, H-3), 2.49 (2H, m, H-4), 2.70 (1H, m, H-3''), 3.16 (1H, m, H-3''), 4.20 (1H, m, N-H), 4.86 (1H, m, H-2), 5.97 (1H, s, H-6), 6.61-6.8 (3H, m, H-5', 6', 2'); ^{13}C NMR (100 MHz, DMSO-d_6) δ 18.7 (C-4), 23.3 23.5 (C-4'', 5''), 28.6 (C-3), 29.6 (C-6''), 45.5 (C-3'') 52.5 (C-1''), 76.4 (C-2), 95.3 (C-6), 100.2 (C-10), 104.0 (C-8), 113.4 (C-2'), 115.4 (C-5'), 116.5 (C-6'), 132.7 (C-1'), 144.8, 145.2 (C-3', 4') 152.7, 155.3, 155.5 (C- 5, 7, 9).

*General synthetic procedure of Compounds (**11-25**)*

The flavonoid compound was dissolved in methanol followed by the addition of 37% formaldehyde solution and the corresponding amine. The mixture was then stirred at 65 °C for various hours. After the reaction, the solvent was removed under reduced

pressure and the residue was purified on silica column using methanol/dichloromethane to yield each desired compound.

*5,7-Dihydroxy-2-(4-hydroxyphenyl)-6-(piperidin-1-ylmethyl)chroman-4-one (**11**)*

Naringenin (150 mg, 0.55 mmol) was dissolved in methanol followed by the addition of 37% formaldehyde solution (52 µl, 0.64 mmol) and the corresponding amine piperidine (82 µl, 0.83 mmol). The mixture was then stirred at 65 °C for 1 hour. After the reaction, the solvent was removed under reduced pressure and the residue was purified on silica column using 5-7.5% methanol/dichloromethane to yield each desired compound. Yield: 65%); yellow solid; mp 132-134 °C. ^{1}H NMR (400 MHz, DMSO-d_6): δ 1.29 (2H, H-5''), 1.40 (4H, H-4'', 6''), 2.44 (1H, H-3, dd, *J* = 2.8, 17 Hz), 2.49 (4H, H-3'', 7''), 3.01 (1H, H-3, dd, *J* = 12.6, 17 Hz), 5.17 (1H, H-2, dd, *J* = 2.8, 12.6 Hz), 5.50 (1H, s, H-8), 6.62 (2H, d, *J* = 8 Hz, H-3', 5'), 7.13 (2H, d, *J* = 8 Hz, H-2', 6'); ^{13}C NMR (100 MHz, DMSO-d_6): δ 22.77 (C-5''), 24.50 (C-4'', 6''), 41.83 (C-3), 52.27 (C-1''), 52.32 (C-3'', 7''), 78.07 (C-2), 95.86 (C-8), 99.34 (C-10), 99.80 (C-6), 115.09 (C-3'), 128.20 (C-2'), 129.14 (C-1'), 157.60 (C-4'), 160.99, 161.89, 171.60 (C-9, 5, 7), 194.79 (C-4).

*5,7-Dihydroxy-2-phenyl-6-(piperidin-1-ylmethyl)-4H-chromen-4-one (**12**)*

Chrysin (100 mg, 0.39 mmol) was dissolved in methanol followed by the addition of 37% formaldehyde solution (36 µl, 0.45 mmol) and the corresponding amine piperidine (49.6 µl, 0.50 mmol). The mixture was then stirred at 65 °C for 1 hour. After the reaction, the

solvent was removed under reduced pressure and the residue was purified on silica column using 5% methanol/dichloromethane to yield each desired compound. Yield: 21%; yellow solid; mp 196-198 °C; ^{1}H NMR (400 MHz, DMSO-d_6): δ 1.47 (2H, m, H-5''), 1.60 (4H, m, H-4'', 6''), 2.70 (4H, m, H-3'', 7''), 3.86 (2H, m, H-1''), 6.41 (1H, s, H-8), 6.92 (1H, s, H-3), 7.57-7.59 (3H, m, H-3', 4', 5'), 8.05 (2H, d, *J* = 6.72 Hz, H-2', 6'); ^{13}C NMR (100 MHz, DMSO-d_6): δ 22.82 (C-5''), 24.55 (C-4'', 6''), 48.54 (C-3'', 7''), 52.51 (C-1''), 94.46 (C-10), 94.85 (C-8), 105.01 (C-6), 105.22 (C-3) 126.26 (C-2', 6'), 129.11 (C-3', 5'), 131.28 (C-4'), 162.04 (C-2), 181.67 (C-4).

*7-Hydroxy-3-(4-methoxyphenyl)-8-(piperidin-1-ylmethyl)-4H-chromen-4-one (**13**)*

Formononetin (10 mg, 0.04 mmol) was dissolved in methanol followed by the addition of 37% formaldehyde solution (4.5 µl, 0.06 mmol) and the corresponding amine piperidine (5.9 µl, 0.06 mmol). The mixture was then stirred at 90 °C over the weekend. After the reaction, the solvent was removed under reduced pressure and the residue was purified on Sphedex- LH20 column using elution solvent of methanol. Yield: 51%; pale yellow solid; ^{1}H NMR (400 MHz, DMSO-d_6): δ 1.46 (2H, m, H-5''), 1.57 (4H, m, H-4'', 6''), 2.58 (4H, m, H3'', 7''), 3.78 (3H, s, -OCH_3), 3.90 (2H, s, H-1'') 6.83 (1H, d, *J* = 8.8 Hz, H-6), 7.0 (2H, d, *J* = 8.6 Hz, H-3', 5'), 7.5 (2H, d, *J* = 8.6 Hz, H-2', 6'), 7.88 (1H, d, *J* = 8.8 Hz, H-5), 8.35 (1H, s, H-2); ^{13}C NMR (100 MHz, DMSO-d_6): δ 23.24 (C-5''), 25.26 (C-4'', 6''), 52.97 (C-1''), 53.15 (C-3'', 7''), 55.11 (-OCH_3), 107.86 (C-8), 113.67 (C-3', 5'), 115.31 (C-6), 115.92 (C-10), 122.93 (C-1'), 124.22 (C-3), 125.56 (C-5), 130.05 (C-2', 6'), 152.68 (C-2), 155.01 (C-9), 158.92 (C-4'), 163.99 (C-7), 174.64 (C-4).

*6-((Diethylamino)methyl)-5,7-dihydroxy-2-phenyl-4H-chromen-4-one (**14**)*

Chrysin (150 mg, 0.59 mmol) was dissolved in methanol followed by the addition of 37% formaldehyde solution (62 µl, 0.77 mmol) and the corresponding amine diethyl amine (91 µl, 0.89 mmol). The mixture was then stirred at 65 °C overnight. After the reaction, the solvent was removed under reduced pressure and the residue was purified on silica column with 3% methanol in dichloromethane. Yield: 45% (together with 6,8 di-substituted side product); yellow solid; mp 184-186 °C ^{1}H NMR (400 MHz, DMSO-d_6): δ 1.27 (3H, t, J = 7.2 H, 2 × -CH_3), 2.61 (4H, q, J = 7.2 Hz, 2 × -$\underline{CH_2}$-CH_3), 4.01 (2H, s, H-1''), 6.30 (1H, s, H-8), 6.64 (1H, s, H-3), 7.53 (3H, m, H-3', 4', 5'), 7.80 (2H, dd, J = 1.68, 7.28 Hz, H-2', 6'); ^{13}C NMR (100 MHz, DMSO-d_6): δ 14.77 (-CH_3), 43.52 (C-4'', 6''), 52.55 (C-1''), 53.97 (C-3'', 7''), 61.82 (-OCH_2-), 98.23 (C-8), 100.45 (C-10), 105.03 (C-3), 106.09 (C-6), 126.21, 129.35, 131.66, 131.96 (C-2', 3', 4', 1'), 154.94 (C-9), 155.36 (-OC=O), 161.94, 163.29, 165.38 (C-2, 5, 7), 182.51 (-C=O).

*6-((3,4-Dihydroisoquinolin-2(1H)-yl)methyl)-5,7-dihydroxy-2-(4-hydroxyphenyl) chroman-4-one (**15**)*

Naringenin (300 mg, 1.1 mmol) was dissolved in methanol followed by the addition of 37% formaldehyde solution (107 µl, 1.32 mmol) and the corresponding amine 1,2,3,4-tetrahydroisoquinoline (185 µl, 1.32 mmol). The mixture was then stirred at 65 °C 2 hours. After the reaction, the solvent was removed under reduced pressure and the residue was purified on silica column with 2.5% methanol in dichloromethane. White

solid (yield 52%); mp > 162 °C (dec.). ^{1}H NMR (400 MHz, MeOD-d_4): δ 2.76 (1H, H-3, dd, *J* = 2.8, 17.2 Hz), 2.97 (4H, -NCH_2CH_2Ar-, br), 3.08 (1H, H-3, dd, *J* = 12.8, 17.2 Hz), 3.84 (2H, -NCH_2Ar, br), 3.97 (2H, H-1'', s), 5.32 (1H, H-2, dd, *J* = 2.8, 12.8 Hz), 5.97 (1H, s, H-8), 6.85 (2H, H-2', 6', d, *J* = 8.8 Hz) 7.00- 7.20 (4H, m, Ar-H), 7.30 (2H, H-3', 5', d, *J* = 8.8 Hz); ^{13}C NMR (100 MHz, MeOD-d_4): 28.41 (-CH_2-Ar), 43.22 (C-3), 49.96, 52.95, 55.18 (3 × -N-CH_2-), 78.78 (C-1), 96.29 (C-8), 100.22 (C-10), 101.89 (C-6), 115.67 (C-3', 5'), 127.89 (C-2', 6'), 126.19, 126.62, 126.87, 128.74 (4 × Ar-H), 130.43, 132.62, 133.15 (C-2 and 2 × Ar-C), 156.47, 161.30, 162.46 (C-5, 9, 4'), 169.27 (C-7), 195.79 (C-4).

6-((3,4-Dihydroisoquinolin-2(1H)-yl)methyl)-5,7-dihydroxy-2-phenyl-4H-chromen-4-one ***(16)***

Chrysin (150 mg, 0.59 mmol) was dissolved in 10 ml of methanol/tetrahydrofuran (1:1) followed by the addition of 37% formaldehyde solution (62 µl, 0.77 mmol) and the corresponding amine 1,2,3,4-tetrahydroisoquinoline (124 µl, 0.89 mmol). The mixture was then stirred at 65 °C 2 hours. After the reaction, the solvent was removed under reduced pressure and the residue was purified as yellow solid from silica column with elution solvent of 4% ethyl acetate in hexane. Yield: 12% (low yield due to 6,8 di-substituted side-product formation). Yellow solid; mp 210-212 °C (dec.); ^{1}H NMR (400 MHz, $CDCl_3$): δ 3.01 (4H, -Ar-CH_2-CH_2-), 3.89, 4.18 (4H, 2 × -N-CH_2-Ar), 6.32 (1H, s, H-8), 6.65 (1H, s, H-2), 7.04-7.19 (4H, m, -Ar-H), 7.50 (3H, m, -Ar-H), 7.85 (2H, m, -Ar-H); ^{13}C NMR (100 MHz, $CDCl_3$): 28.62 (Ar-CH_2-), 50.38, 53.56, 55.90 (3 × -N-CH_2-

), 94.95 (C-8), 100.65 (C-10), 105.00, 106.15 (C-3, 6), 126.32, 126/44, 126.48, 126.86, 127.03, 127.13, 128.97, 129.28, 129.42 (-ArH), 131.98, 132.88, 133.41 (C-1'' and –Ar-C), 155.04, 161.95, 163.32, 166.16 (C-2, 5, 7, 9), 182.64 (-C=O).

5,7-Dihydroxy-6-((4-(2-hydroxyethyl)piperazin-1-yl)methyl)-2-(4-hydroxyphenyl) chroman-4-one ***(17)***

Naringenin (300 mg, 1.1 mmol) was dissolved in methanol followed by the addition of 37% formaldehyde solution (107 µl, 1.32 mmol) and the corresponding amine 1-(2-hydroxyethyl)piperazine (162 µl, 1.32 mmol). The mixture was then stirred at 65 °C 2 hours. After the reaction, the solvent was removed under reduced pressure and the residue was purified on silica column with 5-15% methanol in dichloromethane. Yield: 64%; white solid; mp 118-120 °C; ^{1}H NMR (400 MHz, MeOD-d_4): δ 2.56- 2.59 (2H, -NCH_2-, t, *J* = 5.8 Hz), 2.66-2.71 (5H, -N-CH_2-CH_2-N- and H-3, br), 2.90 (4H, -N-CH_2-CH_2-N-, br), 3.03 -3.10 (1H, H-3, dd, *J* = 12.6, 17.1 Hz), 3.67-3.70 (2H, -CH_2-OH, t, *J* = 5.8 Hz), 3.92 (2H, H-1'', s), 5.29 (1H, H-2, dd, *J* = 3.1, 12.6 Hz), 5.82 (1H, H-8, s), 6.82-6.84 (2H, H -3', 5', d, *J* = 8.56 Hz), 7.30-7.32 (2H, H-2', 6', d, *J* = 8.56 Hz); ^{13}C NMR (100 MHz, MeOD-d_4): 43.84 (C-3), 52.65 (C-1''), 52.84 and 53.22 (-N-CH_2-CH_2-N-), 59.89 (-N-CH_2-), 60.79 (-CH_2-OH), 80.19 (C-2), 97.73 (C-8), 100.94 (C-10), 101.63 (C-6), 116.35 (C-3', 5'), 128.98 (C-2', 6'), 131.31 (C-1'), 158.97, 163.50, 164.43 (C-5, 9, 4'), 173.55 (C-7), 196.70 (C-4).

5,7-Dihydroxy-6-((4-(2-hydroxyethyl)piperazin-1-yl)methyl)-2-phenyl-4H-chromen-4-one ***(18)***

Chrysin (150 mg, 0.59 mmol) was dissolved in methanol/tetrahydrofuran (1:1) followed by the addition of 37% formaldehyde solution (62 µl, 0.77 mmol) and the corresponding amine 1-(2-hydroxyethyl)piperazine (115 µl, 0.89 mmol). The mixture was then stirred at 65 °C 2 hours. After the reaction, the solvent was removed under reduced pressure and the residue was purified on silica column with 3% methanol in dichloromethane. Yield: 45%; yellow solid; mp 180-182 °C; ^{1}H NMR (400 MHz, $CDCl_3$): δ 2.57-2.61 (10H, br, 5 × -CH_2-N-), 3.64 (2H, t, *J* = 5.2 Hz, -OCH_2-), 3.88 (2H, s, Ar-CH_2-N-), 6.41 (1H, s, H-8), 6.63 (1H, s, H-3), 7.52 (3H, m, H-3', 4', 5'), 7.87 (2H, dd, *J* = 1.5, 7.4 Hz, H-2', 6'); ^{13}C NMR (100 MHz, DMSO-d_6): δ 52.58, 53.27 (-NCH_2CH_2N-), 53.88 (C-1''), 57.98 (-OCH_2-), 59.26 (-CH_2-N-), 94.69 (C-8), 103.58 (C-10), 104.42 (C-6), 105.69 (C-3), 126.38 (C-2', 6'), 129.17 (C-3', 5'), 131.57 (C-4'), 131.82 (C-1'), 157.36 (C-9), 159.35 (C-5), 163.82 (C-2), 165.97 (C-7), 182.53 (C=O).

5,7-Dihydroxy-8-((4-(2-hydroxyethyl)piperazin-1-yl)methyl)-2-phenyl-4H-chromen-4-one ***(19)***

Chrysin (150 mg, 0.59 mmol) was dissolved in methanol/tetrahydrofuran (1:1) followed by the addition of 37% formaldehyde solution (62 µl, 0.77 mmol) and the corresponding amine 1-(2-hydroxyethyl)piperazine (115 µl, 0.89 mmol). The mixture was then stirred at 65 °C 2 hours. After the reaction, the solvent was removed under reduced pressure and the residue was purified on silica column with 3% methanol in dichloromethane. Yield:

55%; yellow solid; mp 171-173 °C; ^{1}H NMR (400 MHz, $CDCl_3$): δ 2.589-2.62 (10H, br, 5 × -CH_2-N-), 3.64 (2H, t, *J* = 5.3 Hz, -OCH_2-), 4.02 (2H, s, Ar-CH_2-N-), 6.30 (1H, s, H-6), 6.64 (1H, s, H-3), 7.56 (3H, m, H-3', 4', 5'), 7.82 (2H, dd, *J* = 1.6, 7.4 Hz, H-2', 6'); ^{13}C NMR (100 MHz, $CDCl_3$): δ 52.87, 52.68 (-NCH_2CH_2N-), 53.88 (C-1''), 57.97 (-OCH_2-), 59.17 (-CH_2-N-), 98.46, 100.43, 104.94, 106.05 (C-6, 10, 8, 3), 126.23 (C-2', 6'), 129.35 (C-3', 5'), 131.73 (C-4'), 131.95 (C-1'), 154.91 (C-9), 161.83 (C-5), 163.27 (C-2), 165.74 (C-7), 182.54 (C=O).

*Ethyl-4-((5,7-dihydroxy-23-(4-hydroxyphenyl)-4-oxochroman-6-yl)methyl) piperazine-1-carboxylate (**20**)*

Naringenin (300 mg, 1.1 mmol) was dissolved in methanol followed by the addition of 37% formaldehyde solution (107 µl, 1.32 mmol) and the corresponding amine ethyl-1-piperazinecarboxylate (162 µl, 1.32 mmol). The mixture was then stirred at 65 °C 2 hours. After the reaction, the solvent was removed under reduced pressure and the residue was purified on silica column with 5% methanol in dichloromethane. Yield: 64%; white solid; mp 112-114 °C; ^{1}H NMR (400 MHz, MeOD-d_4): δ 1.13-1.18 (3H, m, -CH_3), 2.52 (4H, br, -N-CH_2-CH_2-N-), 2.58-2.63 (1H, H-3, dd, *J* = 3.0, 17.1 Hz), 2.96- 3.04 (1H, H-3, dd, *J* = 12.7, 17.1 Hz), 3.44 (4H, br, -N-CH_2-CH_2-N-), 3.67 (2H, s, H-1''), 4.02 (2H, m, -OCH_2-) 5.21-5.28 (1H, dd, *J* = 3.0, 12.7 Hz, H-2,), 5.80 (1H, H-8, s), 6.70-6.72 (2H, d, *J* = 8.6 Hz, H-3', 5',), 7.19-7.21 (2H, d, *J* = 8.6 Hz, H-2', 6',); ^{13}C NMR (100 MHz, MeOD-d_4): 14.89 (-CH_3), 43.95 (C-3), 44.34 (-N-CH_2-CH_2-N-), 52.51 (C-1''), 53.12 (-N-CH_2-CH_2-N-), 62.89 (-OCH_2-), 80.44 (C-2), 96.61 (C-8), 101.96 (C-6), 116.36 (C-3', 5'), 129.02

(C-2’, 6’), 131.19 (C-1’’), 157.5, 159.05, 163.15, 164.20 (C-5, 7, 9, 4’), 169.65 (-N-C=O), 197.74 (-C=O).

*Ethyl-4-((5,7-dihydroxy-4-oxo-2-phenyl-4H-chromen-6-yl)methyl)piperazine-1-carboxylate (**21**)*

Chrysin (150 mg, 0.59 mmol) was dissolved in methanol/tetrahydrofuran (1:1) followed by the addition of 37% formaldehyde solution (62 µl, 0.77 mmol) and the corresponding amine ethyl-1-piperazinecarboxylate (140 µl, 0.89 mmol). The mixture was then stirred at 65 °C 2 hours. After the reaction, the solvent was removed under reduced pressure and the residue was purified on silica column with 2% methanol in dichloromethane. Yield: 50%; yellow solid; mp 170-172 °C; ^{1}H NMR (400 MHz, DMSO-d_6): δ 1.27 (3H, t, *J* = 7.0 Hz, -CH_3), 2.61 (4H, br, H-3’’, 7’’), 3.5 (4H, br, H-4’’, 6’’), 4.01 (2H, s, H-1’’), 4.14 (2H, m, -OCH_2-), 6.30 (1H, s, H-8), 6.64 (1H, H-3), 7.53 (3H, m, H-3’, 4’, 5’), 7.80 (2H, dd, *J* = 1.4, 7.5 Hz, H-2’, 6’); ^{13}C NMR (100 MHz, DMSO-d_6): δ 14.77 (-CH_3), 43.52 (C-4’’, 6’’), 52.55 (C-1’’), 53.97 (C-3’’, 7’’), 61.82 (-OCH_2-), 98.23 (C-8), 100.45 (C-10), 105.03 (C-3), 106.09 (C-6), 126.21, 129.35, 131.66, 131.96 (C-2’, 3’, 4’, 1’), 154.94 (C-9), 155.36 (-OC=O), 161.94, 163.29, 165.38 (C-2, 5, 7), 182.51 (-C=O).

*Diethyl-4,4'-((5,7-dihydroxy-4-oxo-2-phenyl-4H-chromene-6,8-diyl)bis(methylene))bis(piperazine-1-carboxylate) (**22**)*

Chrysin (150 mg, 0.59 mmol) was dissolved in methanol/tetrahydrofuran (1:1) followed

by the addition of 37% formaldehyde solution (62 µl, 0.77 mmol) and the corresponding amine ethyl-1-piperazinecarboxylate (140 µl, 0.89 mmol). The mixture was then stirred at 65 °C 2 hours. After the reaction, the solvent was removed under reduced pressure and the residue was purified on silica column with 2% methanol in dichloromethane. Yield: 37%; yellow solid; mp 130-132 °C; ^{1}H NMR (400 MHz, $CDCl_3$): δ 1.28 (6H, m, 2 × -CH_3), 2.62 (4H, br, H-3'', 7''), 3.56 (4H, br, H-4'', 6''), 3.87 (4H, 2 × s, H-1''), 4.14 (4H, m, 2 × -OCH_2-), 6.67 (1H, s, H-3), 7.55 (3H, m, H-3', 4', 5'), 7.87 (2H, dd, *J* = 1.4, 7.5 Hz, H-2', 6'); ^{13}C NMR (100 MHz, $CDCl_3$): representative peaks: δ 14.52 (-CH_3), 43.09, 43.31 (C-4'', 6''), 51.63, 52.04 (C-1''), 54.87 (C-3'', 7''), 60.65, 60.74 (-OCH_2-), 101.35, 102.53, 104.54, 104.8 (C-6, 8, 10, 3), 126.27, 129.19, 131.04, 131.87 (C-2', 3', 4', 1'), 154.50 (C-9), 154.69 (-OC=O), 181.68 (-C=O).

*Ethyl 4-(4-((5,7-dihydroxy-2-(4-hydroxyphenyl)-4-oxochroman-6-yl)methyl) piperazin-1-yl)benzoate (**23**)*

Naringenin (300 mg, 1.1 mmol) was dissolved in methanol followed by the addition of 37% formaldehyde solution (107 µl, 1.32 mmol) and the corresponding amine ethyl 4-(1-piperazinyl)benzoate (309 mg, 1.32 mmol). The mixture was then stirred at 65 °C 2 hours. After the reaction, the solvent was removed under reduced pressure and the residue was purified on silica column with 5% methanol in dichloromethane. Yellow white powder was achieved. Yield: 76%; white solid; mp > 120 °C (dec.); ^{1}H NMR (400 MHz, $CDCl_3$): δ 1.22 (3H, t, -CH_3), 2.62 (1H, dd, *J* = 3.0, 17.1 Hz, H-3), 2.92 (1H, dd, *J* = 12.8, 17.1 Hz, H-3), 2.60- 3.36 (8H, br, 2 × -N-CH_2-CH_2-N-) 3.69 (2H, s, -N-$\underline{CH_2}$-Ar), 4.20 (2H, q, -

$\underline{CH_2}$-CH_3), 5.20 (1H, dd, J = 3.0, 12.8 Hz, H-2), 5.83 (1H, s, H-8), 6.72 (4H, two doublets, J_1 = 8.5 Hz, J_2 = 8.8 Hz, -ArH), 7.17 (2H, d, J = 8.5 Hz, -ArH), 7.78 (2H, d, J = 8.8 Hz, -ArH); ^{13}C NMR (100 MHz, $CDCl_3$): 14.39 (-CH_3), 43.13 (C-3), 47.58 (C-1''), 52.12, 53.01 (-N-**CH_2**-**CH_2**-N-), 60.45 (-O-CH_2), 78.76 (C-2), 96.01 (C-8), 100.13 (C-10), 102.10 (C-6), 114.14 (-Ar), 115.65 (C-3', 5'), 121.05 (-$\underline{C}$-C=O), 127.89 (C-2', 6'), 131.20 (-Ar), 137.67 (-Ar-N-), 153.67 (C-4'), 156.12 (C-9), 161.34 (C-5), 166.57 (C-7), 168.17 (-O-C=O), 195.78 (-C=O).

*5,7-Dihydroxy-2-(4-hydroxyphenyl)-6-(morpholinomethyl)chroman-4-one (**24**)*

Naringenin (300 mg, 1.1 mmol) was dissolved in methanol followed by the addition of 37% formaldehyde solution (107 µl, 1.32 mmol) and the corresponding amine morpholine (115 µl, 1.32 mmol). The mixture was then stirred at 55 °C 1-2 hours. After the reaction, the solvent was removed under reduced pressure and the residue was purified on silica column with 5-10% methanol in dichloromethane. Yield: 76%; white solid; mp 115-116 °C; ^{1}H NMR (400 MHz, MeOD-d_4): δ 2.59-2.64 (1H, H-3, dd, J = 17.16, 3.1 Hz), 2.72 (4H, H-3'', 7'', m), 2.96- 3.04 (1H, H-3, dd, J = 12.68 17.16 Hz), 3.65-3.68 (4H, H-4'', 5'', m), 3.79 (2H, H-1'', s), 5.21-5.25 (1H, H-2, dd, J = 3.1, 12.68 Hz), 6.71 (2H, H-3', 5', d, J = 8.6 Hz), 7.19 (2H, H-2', 6', d, J = 8.6 Hz), ^{13}C NMR (100 MHz, MeOD-d_4): δ 43.86 (C-3), 52.71 (C-1''), 53.63 (C-3'', 7''), 66.90 (C-4'', 6''), 80.44 (C-2), 96.73 (C-8), 100.79 (C-10), 102.59 (C-6), 116.38, 116.47 (C-3', 5'), 129.02 (C-2' 6'), 131.04 (C-1'), 159.07 (C-4'), 163.43, 164.54 (C-5, 9), 170.07 (C-7), 197.59 (C-4).

*5,7-Dihydroxy-6-(morpholinomethyl)-2-phenyl-4H-chromen-4-one (**25**)*

Chrysin (150 mg, 0.59 mmol) was dissolved in methanol/tetrahydrofuran (1:1) followed by the addition of 37% formaldehyde solution (62 µl, 0.77 mmol) and the corresponding amine morpholine (77 µl, 0.89 mmol). The mixture was then stirred at 65 °C 2 hours. After the reaction, the solvent was removed under reduced pressure and the residue was purified on silica column with 20-50% ethyl acetate in hexane. Yield: 46%; yellow solid; mp 198-200 °C (dec.); ^{1}H NMR (400 MHz, DMSO-d_6): δ 2.68 (4H, br, H-4'', 6''), 3.80 (4H, br, H-3'', 7''), 4.01 (2H, s, H-1''), 6.31 (1H, s, H-8), 6.65 (1H, s, H-3), 7.56 (3H, m, H-3', 4' 5'), 7.83 (2H, dd, J = 1.5, 6.0 Hz, H-2', 6'); ^{13}C NMR (100 MHz, DMSO-d_6): δ 53.02 (C-1''), 54.17 (C-3'', 7''), 66.66 (C-4'', 6''), 98.00 (C-8), 100.31 (C-3), 104.89 (C-10), 105.97 (C-6), 126.11 (C-2'), 129.23 (C-3'), 131.58 (C-4'), 131.82 (C-1'), 154.89 (C-9), 161.80 (C-2), 163.17 (C-5), 165.35 (C-7), 182.40 (C-4).

6.5 References

2014. IDF Diabetes Atlas, 6th edn. 2014 update. Brussels, Belgium: International Diabetes Federation. International Diabetes Federation.

Brayer, G.D., Sidhu, G., Maurus, R., Rydberg, E.H., Braun, C., Wang, Y., Nguyen, N.T., Overall, C.M. and Withers, S.G., 2000. Subsite mapping of the human pancreatic α-amylase active site through structural, kinetic, and mutagenesis techniques. Biochemistry, 39(16), pp.4778-4791.Vancouver

Brindis, F., Rodríguez, R., Bye, R., González-Andrade, M.n., Mata, R., 2010. (Z)-3-Butylidenephthalide from *Ligusticum porteri*, an α-Glucosidase Inhibitor. J Nat Prod 74, 314-320.

Chen, L., Hu, T.S., Zhu, J., Wu, H.M., Yao, Z.J., 2006. Application of a regioselective Mannich reaction on naringenin and its use in fluorescent labeling. Synlett, 1225-1229.

Cornish-Bowden, A., 1974. A simple graphical method for determining the inhibition constants of mixed, uncompetitive and non-competitive inhibitors. Biochemical Journal 137, 143.

DeLano, W.L. The PyMOL User's Manual (2002) DeLano Scientific, San Carlos, CA, USA.

Guariguata, L., Whiting, D., Hambleton, I., Beagley, J., Linnenkamp, U., Shaw, J., 2014. Global estimates of diabetes prevalence for 2013 and projections for 2035. Diabetes research and clinical practice 103, 137-149.

He, L., 1998. Alpha-glucosidase inhibitors as agents in the treatment of diabetes. Diabetes review, 6, pp.132-145.

Helgren, T.R., Sciotti, R.J., Lee, P., Duffy, S., Avery, V.M., Igbinoba, O., Akoto, M., Hagen, T.J., 2015. The synthesis, antimalarial activity and CoMFA analysis of novel aminoalkylated quercetin analogs. Bioorg Med Chem Lett 25, 327-332.

Hollander, P., 1992. Safety profile of acarbose, an α-glucosidase inhibitor. Drugs 44, 47-53.

Iio, M., Yoshioka, A., Imayoshi, Y., Koriyama, C., Ayako, M., 1984. Effect of flavonoids on α-glucosidase and β-fructosidase from yeast. Agr Biol Chem Tokyo 48, 1559-1563.

Khadem, S., Marles, R.J., 2011. Chromone and flavonoid alkaloids: occurrence and bioactivity. Molecules 17, 191-206.

Li, H.T., Zhu, F., Chen, H.Y., Cheng, K.W., Zykova, T., Oi, N., Lubet, R.A., Bode, A.M., Wang, M.F., Dong, Z.G., 2014. 6-C-(E-phenylethenyl)-Naringenin Suppresses Colorectal Cancer Growth by Inhibiting Cyclooxygenase-1. Cancer research 74, 243-252.

Matsui, T., Kobayashi, M., Hayashida, S. and MATSUMOTO, K., 2002. Luteolin, a flavone, does not suppress postprandial glucose absorption through an inhibition of α-glucosidase action. Bioscience, biotechnology, and biochemistry, 66(3), pp.689-692. Vancouver

Nguyen, T.B., Wang, Q., Gueritte, F., 2011. An Efficient One-Step Synthesis of Piperidin-2-yl and Pyrrolidin-2-yl Flavonoid Alkaloids through Phenolic Mannich Reactions. Eur J Org Chem, 7076-7079.

Priscilla, D.H., Roy, D., Suresh, A., Kumar, V., Thirumurugan, K., 2014. Naringenin inhibits alpha-glucosidase activity: a promising strategy for the regulation of postprandial hyperglycemia in high fat diet fed streptozotocin induced diabetic rats. Chem Biol Interact 210, 77-85.

Rivera-Chávez, J., Figueroa, M., González, M.D.C., Glenn, A.E. and Mata, R., 2015. α-Glucosidase inhibitors from a *Xylaria feejeensis* associated with Hintonia latiflora. Journal of natural products, 78(4), pp.730-735.

Scheen, A.J., 2003. Is there a role for α-glucosidase inhibitors in the prevention of type 2 diabetes mellitus Drugs 63, 933-951.

Sedlacek, H.H., 2001. Mechanisms of action of flavopiridol. Critical reviews in oncology/hematology 38, 139-170.

Simon, J.E., Wu, Q. and Welch, C., 2014. Peperidine-flavan alkaloid compounds derived from African herb tea kinkeliba as anti-diabetic agents. U.S. Patent 8,642,769.

Trott, O., Olson, A.J., 2010. AutoDock Vina: improving the speed and accuracy of docking with a new scoring function, efficient optimization, and multithreading. Journal of computational chemistry 31, 455-461.

Tundis, R., Loizzo, M., Menichini, F., 2010. Natural products as α-amylase and α-glucosidase inhibitors and their hypoglycaemic potential in the treatment of diabetes: an update. Mini reviews in medicinal chemistry 10, 315-331.

Wang, G.G., Lu, X.H., Li, W., Zhao, X., Zhang, C., 2011. Protective effects of luteolin on diabetic nephropathy in STZ-induced diabetic rats. Evid-Based Compl Alt 2011.

Wang, T., Li, X., Zhou, B., Li, H., Zeng, J., Gao, W., 2015. Anti-diabetic activity in type 2 diabetic mice and α-glucosidase inhibitory, antioxidant and anti-inflammatory potential of chemically profiled pear peel and pulp extracts (Pyrus spp.). J Funct Foods 13, 276-288.

Welch, C.R., 2010. Chemistry and pharmacology of Kinkéliba (*Combretum micranthum*), a west African medicinal plant. Rutgers, The State University of New Jersey.

Yan, J.K., Zhang, G.W., Pan, J.H., Wang, Y.J., 2014. alpha-Glucosidase inhibition by luteolin: Kinetics, interaction and molecular docking. Int J Biol Macromol 64, 213-223.

CHAPTER SEVEN

Conclusions

7.1 Summary

This research study investigated the phytochemical contents from selected sub-Saharan African medicinal plants, with special focus on polyphenol compounds and other compounds with unique structures. In initial screening discoveries, we successfully discovered a number polyphenol compounds from the leaf extract from the African plants *Ximenia caffra* and *Hibiscus sabdariffa*, two well-known indigenous plants, each with some traditional pharmacological properties in Africa. Further phytochemical identifications were performed on LC/MS. These compounds include phenolic acids and flavonoids and their glycosides. The major compounds of special interests were quantitated using HPLC/UV. The *in vitro* anti-oxidant activities of both plants materials were demonstrated using Folin-Ciocalteu assay and ABTS free radical scavenging assays. The anti-inflammatory activities of *Ximenia caffra* were further demonstrated using cell-culture based assays through the observed decreased expressions of pro-inflammatory genes including iL-6, iNOS and TNF-α. Further investigation suggested that the *Ximenia caffra* would inhibit the activation of NF-κB, which would be a partial underlying mechanism for the observed anti-inflammation and anti-proliferation activities. For *Hibiscus sabdariffa,* we compared the polyphenol contents of leaves from 25 different populations from worldwide. As much of the focus on this species was on the calyx, ours

was the first complete examination of the leaves. We also found that the compound 5-HMF (5-(hydroxymethyl)furfural) was present in dried leaves. This is the first report that 5-HMF could be formed in this species and is associated with improper drying and storage as a postharvest concern. The formation of 5-HMF could potentially be used as a biomarker for the quality control during the drying of leaves. That is the absence of 5-HMF indicates the sample and postharvest handling was done properly. Anti-inflammatory activity from the leaves of *H. sabdariffa* was demonstrated on LPS-treated RAW 264.7 cell with the observed reduction of NO production after the treatment of leaf extract. The leaves were found to be a significant source of bioactive healthy secondary products and thus serve as an excellent indigenous leafy vegetable.

In previous research, groups of unique flavan alkaloids were discovered by our university laboratory from the leaves of African plant *Combretum micranthum* (Welch 2010; Simon et al 2014). Due to the limited amount of compounds that were purified from plant materials, the regio-isomers of these compounds were not fully determined. Here, in this study, we further developed the synthetic methods for these flavan alkaloids and successfully generated flavan alkaloids groups A and B artificially. The synthesized standards were then used for further confirmation of the identities of flavan alkaloids from the plant material. Sufficient amounts of synthesized flavan alkaloids were produced and contributed to the regio-isomers differentiation. For A and B group, the plant materials contain both 6 and 8 position substituted piperidine flavans. Considering the traditional uses of *Combretum micranthum* and previous *in vitro, in vivo* experiments conducted and reported by our lab, we further investigated the relationship between the

discovered flavan alkaloids and diabetes, especially on therapeutic target α-glucosidase, which would convert polysaccharides to single glucose molecule. We found that the discovered flavan alkaloids do not exhibit potent inhibition toward purified enzyme α-glucosidase. Further structure modification was performed with a number of flavonoids and nitrogen-containing functional groups. Some synthesized derivatives would increase the inhibition activity toward purified enzyme, with highest IC_{50} of 4.13 μM. But these achieved inhibitory activities are still much less the therapeutic reagents on the market such as acarbose, miglitol, voglibose, whose IC_{50} are in the nanomolar range. Further computational studies were performed to elucidate the binding between flavonoid alkaloids and α-glucosidase. We found the best binding site between most potent compounds 15, 23 is a location close to the catalytic center, which supports its non-competitive inhibition mechanism. The structure activity relationship (SAR) was also analyzed and suggested that the 4' position hydroxyl group and 4-position carbonyl may be required to maintain the inhibitory activity. The addition of hydrophobic groups at 6-position of flavonoids may increase the binding affinity with the enzyme. This study may help α-glucosidase inhibitors developments in the future.

7.2 Recommendations for Future Work

7.2.1 CDK Enzymes Inhibition Assay

Cyclin-dependent kinases (CDKs) are a family of very important protein kinases in the regulation of cell cycle (Harper and Adams, 2001). CDK enzymes can bind with corresponding protein cyclins to become active and subsequently phosphorylate various

protein substrates involved in cell cycle. Cancer is featured by uncontrolled growth or cell division. As most cancer cells have deranged the normal controls over the cell cycle. targeting cylcin-dependent kinases could yield therapeutic effects considering their function of promoting transitions through cell cycles (Asghar et al., 2015). In the past decades, large number of small molecules have been developed to interfere the activity of CDKs and some of them have been tested in clinical trials.

One of the most extensively studied CDKs inhibitors, flavopiridol, has been demonstrated to inhibit kinases CDK1, CDK2, CDK4, CDK6, CDK7(Sedlacek, 2001). This inhibition is in a competitive manner with its substrate ATP. Flavopiridol has been studied in over 60 clinical trials. Even if it has shown cell cycle arrest activities in G1 and G2 phases, it also has cytotoxic responses probably due to the lack of selectivity. A number of flavopiridol analogues have also been synthesized, some of which are nitrogen-containing flavonoids (Liu et al., 2007; Zhang et al., 2008). These nitrogen-containing flavonoids have shown potent CDK1/Cyclin B inhibitory activity and have shown growth inhibitory activity *in vitro* against a number of different cell lines (Nguyen et al., 2012).

In our preliminary study, we tested the anti-proliferation activity of the flavan alkaloids from kinkéliba and its synthesized flavonoid alkaloids on PC-3 cells. We found the kinkéloids A & B did not show strong anti-proliferation activity, but some analogues did have better and improved activities (Table 7). For example, compound **19** would research

IC_{50} up to 29 uM. This cell-culture based assay only serves as an initial screening process to evaluate kinkéloids and synthesized analogues. Detailed experimental procedures are described in Appendix IV. In the future, it would be productive to continue on this experimental path through the development of an assay experiment, which would directly quantify the inhibitory activity toward certain CDKs. Then, both the natural kinkéloids and synthesized analogues could be tested for their potential inhibitory activities toward certain CDKs. The binding mechanism would also be subsequently analyzed using computational docking; then structure activity relationship would be generalized. This work to be done in the future would benefit the design of inhibitors CDKs in the future for cancer treatment.

Table 10. Anti-proliferation activity of synthesized flavonoid alkaloids on PC-3 cells.

No.	Flavonoid Moiety*	Alkaloid Moiety	Position	Substituted Groups			IC_{50} in µM
				R_1	R_2	R_3	
1	I		6	OH	H	H	> 200
2			6	OCH_3	OH	H	> 200
3			6	OH	OH	OH	> 200
4	II		6	H	H	-	> 200
5			8				68.2
6			6	OH	H	H	83.9
7	IV		6	OH	-	-	>200
8			8	OH	-	-	>200
9			6	OH	OH	-	>200
10			8	OH	OH	-	>200
11	I		6	OH	H	H	41.2
12	II		6	H	H	-	>200
13	II		6	H	H	-	> 200
15	I	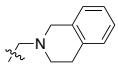	6	OH	H	H	61.1
16	II		6	H	H	-	NS
17	I	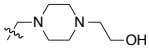	6	OH	H	H	66.9
18	II		6	H	H	-	112.1
19			8				29.0
20	I	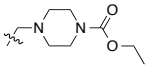	6	OH	H	H	52.5
21	II		6	H	H	-	>200
22			8	H	H	-	87.5
23	I	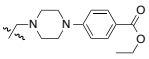	6	OH	H	H	38.3
24	I II		6	OH	H	H	68.6
25			Di	H	H	-	36.7

* The compounds structures and synthesis methods have been described in Chapter 6

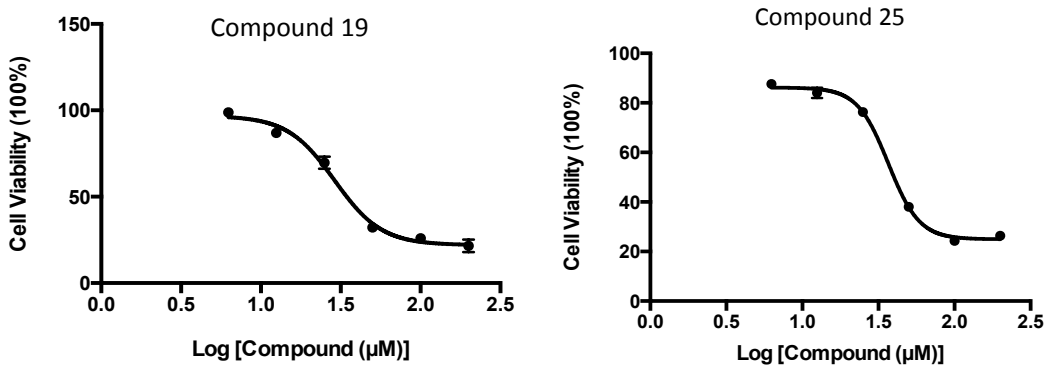

Figure 67. The anti-proliferation activities of representative synthesized flavonoids alkaloids

7.2.2 Chiral Separation Methods Development

In a previous research project, two flavan molecules 4', 5, 7- trihydroxyflavan, 3', 4', 5, 7-tetrahydroxyflavan were found by our laboratory (Welch 2010). Each of them has a chiral center at position 2, but the analytical methods for their enantiomers separation have not been reported yet. In our preliminary analysis we successfully developed methods to separate the enantiomers of each identified flavan, 4', 5, 7- trihydroxyflavan (A), 3', 4', 5, 7- tetrahydroxyflavan (B) from *Combretum micranthum* on amylose-based chiral stationary phase. The enantiomers of an artificially synthesized flavan molecule 3', 5, 7-trihydroxy-4'-methoxyflavan (C) was also separated for structure relationship study. Several different elution conditions were tried. As shown in Table 7, their separation effects on different molecules were compared and further analyzed. Detailed experimental conditions and parameters explanations are described in Appendix V.

Table 11. Chromatographic results for flavan enantiomers separation on Chiralpak AD-RH CSP

Flavans*	Eluent*	t_1 (min)	t_2 (min)	k_1	k_2	R_s	α
A	MeOH-H_2O, 95:5	9.60	14.01	1.34	2.42	1.66	1.80
B		6.30	7.36	0.54	0.80	0.77	1.48
C		10.95	13.84	1.67	2.38	1.06	1.42
A	MeOH-H_2O, 90:10	11.82	18.43	1.88	3.50	2.73	1.86
B		7.01	8.46	0.71	1.06	1.06	1.50
C		14.31	17.24	2.49	3.20	0.97	1.29
A	ACN-H_2O, 50:50	6.78	8.82	0.65	1.15	2.14	1.77
B		5.51	5.81	0.34	0.42	-	1.21
C		8.61	9.45	1.10	1.30	-	1.19
A	ACN-H_2O, 40:60	8.57	12.61	1.09	2.08	1.78	1.91
B		6.21	6.78	0.51	0.65	-	1.27
C		11.89	13.23	1.90	2.23	-	1.17
A	ACN-H_2O, 30:70	17.38	30.08	3.24	6.34	2.08	1.96
B		9.79	11.84	1.39	1.89	-	1.36
C		28.70	32.86	6.00	7.02	-	1.17

* A: 4', 5, 7- trihydroxyflavan; B: 3', 4', 5, 7- tetrahydroxyflavan; C: 3', 5, 7- trihydroxy-4'-methoxyflavan; H_2O contains 0.1% TFA

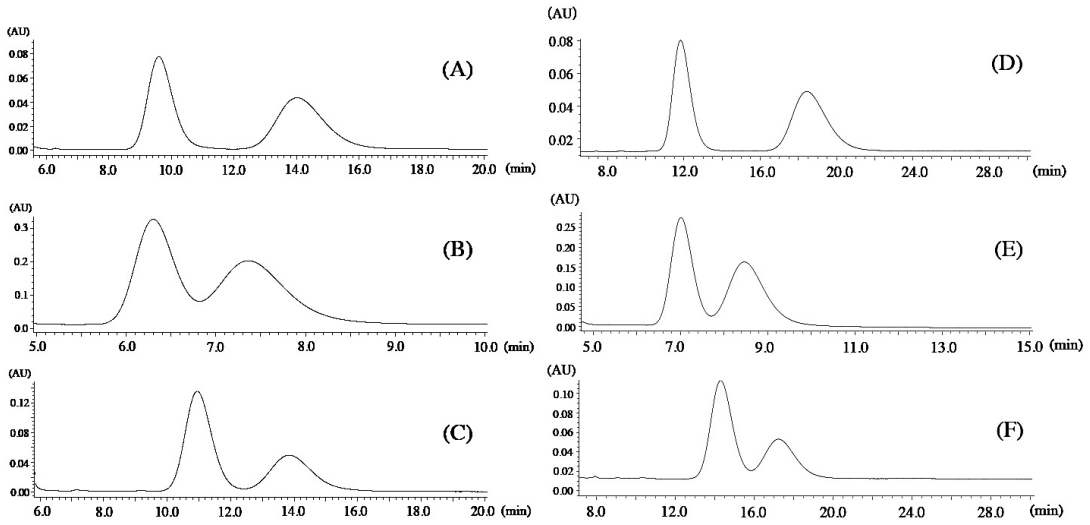

Figure 68. Representative chromatograms of flavan enantiomers separation of Chiralpak AD-RH; (A) 4', 5, 7- trihydroxyflavan; methanol-H_2O doped with 0.1% TFA, 95:5 (v/v) (B) 3', 4', 5, 7- tetrahydroxyflavan; methanol-H_2O doped with 0.1% TFA, 95:5; (C) 3', 5, 7- trihydroxy-4'-methoxyflavan; methanol-H_2O doped with 0.1% TFA, 95:5; (D) 4', 5, 7-trihydroxyflavan; methanol-H_2O doped with 0.1% TFA, 90:10 (v/v) (E) 3', 4', 5, 7-tetrahydroxyflavan; methanol-H_2O doped with 0.1% TFA, 90:10; (F) 3', 5, 7- trihydroxy-4'-methoxyflavan; methanol-H_2O doped with 0.1% TFA, 90:10

Another group of compounds, kinkéloids, discovered from *Combretum micranthum* contain two to three chiral bonds. For kinkéloids A and B, each has one chiral bond at position 2 of the flavan moiety and another one at the 1'' position of the piperidine moiety. Further chiral separation of flavan alkaloids were tried using a number of different chiral columns and different conditions, but still we were not able directly separated them in our experiments. The challenging part is contributed by the amphoteric properties of flavan alkaloids. In the reverse-phase chromatography, the addition of acid modifier in the elution solvents would increase the binding between stationary phase and phenol moieties, but it would also form salt with the amine moiety, which then drags the whole molecule which is more polar and water-soluble, resulting in very weak overall

binding with stationary phrase. The same situation applies for the addition of base modifier in the elution solvents, which would form salt with phenol groups. For normal-phase chromatography, several conditions were also tried but without success separations so far. In the future, it would be possible to selectively protect the amine groups while leaving the phenol groups unprotected and then separate the protected kinkéloids on chiral stationary phase in reverse-phase chromatography with the addition of acid modifier. Supercritical fluid chromatography (SFC) could also be tried to directly separate the kinkéloids in the future.

7.3 References

Asghar, U., Witkiewicz, A.K., Turner, N.C., Knudsen, E.S., 2015. The history and future of targeting cyclin-dependent kinases in cancer therapy. Nature reviews Drug discovery 14, 130-146.

Harper, J.W., Adams, P.D., 2001. Cyclin-dependent kinases. Chemical reviews 101, 2511-2526.

Liu, T., Xu, Z.M., He, Q.J., Chen, Y.H., Yang, B., Hu, Y.Z., 2007. Nitrogen-containing flavonoids as CDK1/Cyclin B inhibitors: Design, synthesis, and biological evaluation. Bioorg Med Chem Lett 17, 278-281.

Nguyen, T.B., Lozach, O., Surpateanu, G., Wang, Q., Retailleau, P., Iorga, B.I., Meijer, L., Gueritte, F., 2012. Synthesis, Biological Evaluation, and Molecular Modeling of Natural and Unnatural Flavonoidal Alkaloids, Inhibitors of Kinases. Journal of medicinal chemistry 55, 2811-2819.

Sedlacek, H.H., 2001. Mechanisms of action of flavopiridol. Critical reviews in oncology/hematology 38, 139-170.

Simon, J.E., Wu, Q. and Welch, C., 2014. Peperidine-flavan alkaloid compounds derived from African herb tea kinkeliba as anti-diabetic agents. U.S. Patent 8,642,769.

Welch, C.R., 2010. Chemistry and pharmacology of Kinkéliba (*Combretum micranthum*), a west African medicinal plant. Rutgers, The State University of New Jersey.

Zhang, S.X., Ma, J.G., Bao, Y.M., Yang, P.W., Zou, L., Li, K.J., Sun, X.D., 2008. Nitrogen-containing flavonoid analogues as CDK1/cyclin B inhibitors: Synthesis, SAR analysis, and biological activity. Bioorganic & medicinal chemistry 16, 7127-7132.

Appendices

Appendix I. The detailed sample information of each *Hibiscus sabdariffa* leaf accessions

#	Variety/Source	Accession label	Date Collected
1	Cuba-1	PI-207920 (Plant introduction from Cuba by USDA/ARS)	9/18/2009
2	Cuba-2	PL-265319 LaHabana (Plant introduction from Cuba by USDA	9/18/2009
3	Georgia, USA	PI-468413 (Plant introduction by USDA/ARS/national Clonal Germplasm repository)	9/21/2009
4	Ghana-1	PI-286319 (Plant introduction from Ghana by USDA/ARS/national Clonal Germplasm repository)	9/21/2009
5	Ghana-2	PI-286312 (Plant introduction from Ghana by USDA/ARS/national Clonal Germplasm repository)	9/21/2009
6	India (India accession by an Indian Professor)	SU Hort Farm plot 1	10/1/2009
7	Jamaica (Jamaica accession by a Baton Rouge local nursery)	SU Hort Farm plot 1	10/1/2009
8	Malaysia (Malaysia accession by Dr. Chin)	SU Hort Farm plot 1	10/1/2009
9	Nigeria-1 (Nigeria accession by a professor at Alcorn State University)	SU Hort Farm plot 1	10/1/2009
10	Nigeria-2	PI-268100 (Plant introduction from Ghana by USDA/ARS)	9/21/2009
11	Nigeria-3	SU Hort Farm plot 2	10/9/2009
12	Poland	PI-256041 (Plant introduction from Ghana by USDA/ARS)	9/18/2009
13	Senegal-1 (From Jim Simon)	SU Hort Farm plot 1	10/9/2009
14	Senegal-2 (From Jim Simon)	SU Hort Farm plot 2	10/1/2009
15	South Africa-1	PI-273459 Transvaal (Plant introduction from	9/21/2009

		Ghana by USDA/ARS/national Clonal Germplasm repository)	
16	South Africa-2	PI-638933 (Plant introduction from Ghana by USDA/ARS/national Clonal Germplasm repository)	9/21/2009
17	South Africa-3	SU Hort Farm plot 1	10/9/2009
18	South Africa-4	SU Hort Farm plot 2	10/1/2009
19	Sudan-1	PI-496717 (Plant introduction from Sudan by USDA/ARS/national Clonal Germplasm repository)	9/21/2009
20	Sudan-2	PI-267778 (Plant introduction from Sudan by USDA/ARS/national Clonal Germplasm repository)	9/21/2009
21	Sudan-3	PI-496938 (Plant introduction from Sudan by USDA/ARS/national Clonal Germplasm repository)	9/21/2009
22	Taiwan	PI-273389 (Plant introduction from Taiwan by USDA/ARS/national Clonal Germplasm repository)	9/21/2009
23	Thailand	PI-365477 (Plant introduction from Thailand by USDA/ARS/national Clonal Germplasm repository)	9/21/2009
24	Zambia-1	PI-500737 (Plant introduction from Zambia by USDA/ARS/national Clonal Germplasm repository)	9/21/2009
25	Zambia-2	PI-500725 (Plant introduction from Zambia by USDA/ARS/national Clonal Germplasm repository)	9/21/2009

*SU=Southern University

Appendix II.

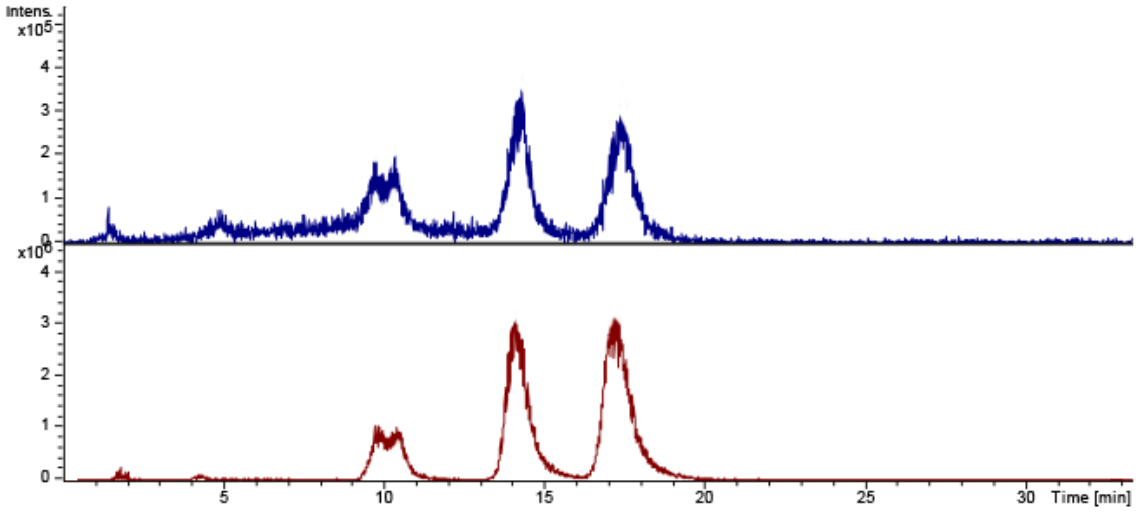

Appendix II. The extracted ion chromatogram of kinkéloids B. (A): The synthesized kinkéloids B, (B) The kinkéloids methanol extract

Appendix III.

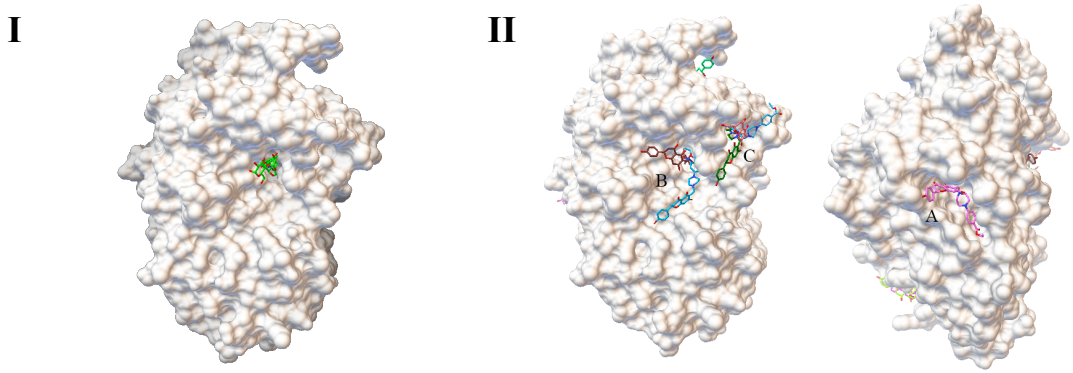

Appendix III. Binding sites predictions between α-glucosidase and compounds. (I) The binding site of acarbose predicted by the docking method developed. (II) The predicted potential binding sites of synthesized flavonoid alkaloid on the surface of α-glucosidase

Appendix IV.

Appendix IV. Experimental methods of anti-proliferation assay of synthesized flavonoid alkaloids

All synthetic materials including the solvents are all purchased from Sigma Aldrich (St. Louis, MO). The solvents used for silica gel chromatography were ACS grade and the one used for HPLC or LC/MS was HPLC grade. Column purification was performed using silica gel (230 - 400 mesh; Selecto Scientific, Suwanee, GA). Analytical HPLC-MS was performed on Hewlett-Packard Agilent 1100 series HPLC-MSD (Agilent Technologies, Waldbronn, Germany) equipped with a quaternary pump system, a degasser, an auto-sampler, a DAD detector, a MSD trap with electrospray ion source (ESI). ^{1}H and ^{13}C NMR spectra were conducted on Bruker Avance 400 MHz spectrometer (Billerica, MA).

The anti-proliferative effect of each compound was first tested in PC-3 cells using the MTS assay. MTS assay, usually called "one step" MTT assay, is used for assessing cell viability. NAD(P)H-dependent cellular oxidoreductase enzymes from live cells can reduce MTS reagent and form a formazan product with maximum absorption at 490-500 nm. The PC-3 cells were seeded in a 96-well tissue culture plate at an initial density of 10,000 cells/ml. After 24 hr, the cells were treated with various concentration of compound in DMSO for another 72 hr. The MTS assay was then performed using the CellTiter 96 aqueous nonradioactive cell proliferation assay kit [MTS: 3-(4,5-dimethylthiazol-2-yl)-5-(3-carboxymethoxyphenyl)-2-(4-sulfophenyl)-2H-tetrazolium, inner salt] (Promega, Madison, WI, USA) as previously described. The absorbance of the formazan product was measured at 490 nm using a µQuant Biomolecular Spectrophotometer (Bio-Tek Instruments, Inc., Winooski, VT, USA). The cell viability (%) was expressed as follows: (optical density of sample) / (optical density of DMSO) x 100%.

Appendix V.

Appendix V. Experimental methods for flavan enantiomers separation

The flavan molecules were artificially synthesized using methods at Chapter 4. The structures were further confirmed using LC/MS and NMR. ^{1}H and ^{13}C NMR spectra were performed on Bruker Avance 400 MHz spectrometer (Billerica, MA). Analytical LC-MS was performed on Hewlett-Packard Agilent 1100 series HPLC-MSD (Agilent Technologies, Waldbronn, Germany) equipped with a quaternary pump system, a degasser, an auto-sampler, a DAD detector, a MSD trap with electrospray ion source (ESI). Column chromatography was performed using silica gel (230 - 400 mesh; Selecto Scientific, Suwanee, GA). HPLC analysis was performed on Waters 2695 separation module equipped with a photodiode array detector (PDA). Polysaccharide CSP column was used in this study, Chiralcel® AD-RH. Column AD-RH is amylose tris (3,5-dimethylphenyl carbamate). The column was purchased from Daicel Corporation (Tokyo, Japan). Experiments were performed at room temperatures. All solvents used for chromatographic separations had been degassed in ultrasonic bath before the experiment. Before a new organic modifier was used, the column was regenerated vendor's instruction methods to remove some unexpected memory effects. The column was equilibrated for around one hour before the application of a new chromatographic condition. Each sample was diluted in methanol to a concentration of 0.1 mg/mL (1 mg/ml for flavanone and flavans, 0.1 mg/ml for nitrogen-containing flavanones) for HPLC-UV. The column void volume (t_0) was measured by the injection of non-retained marker. The retention factor (k) was calculated using equations $k_1 = (t_1 - t_0)/t0$ and $k_2 = (t_2 - t_0)$, where t_1 and t_2 are the retention time for each separated enantiomers on the HPLC chromatogram. The separation factor (α) was calculated through equation $\alpha = k_2/k_1$. The resolution factor was calculated using equation $Rs = 2\,(t_2 - t_1) / (w_1 + w_2)$.

Appendix VI

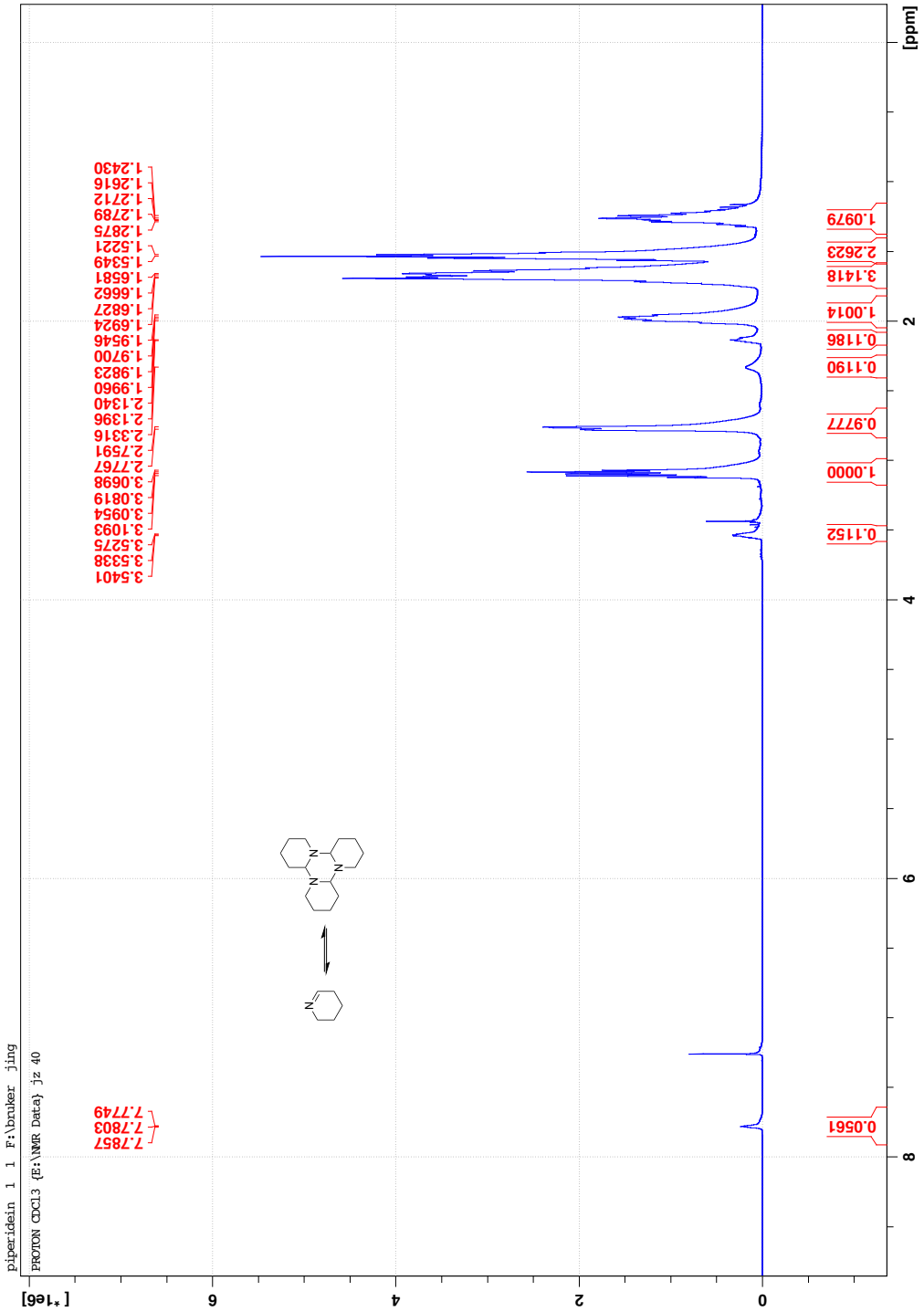

Appendix VI. ^{1}H spectrum of Δ^{1}-piperidein

Appendix VII

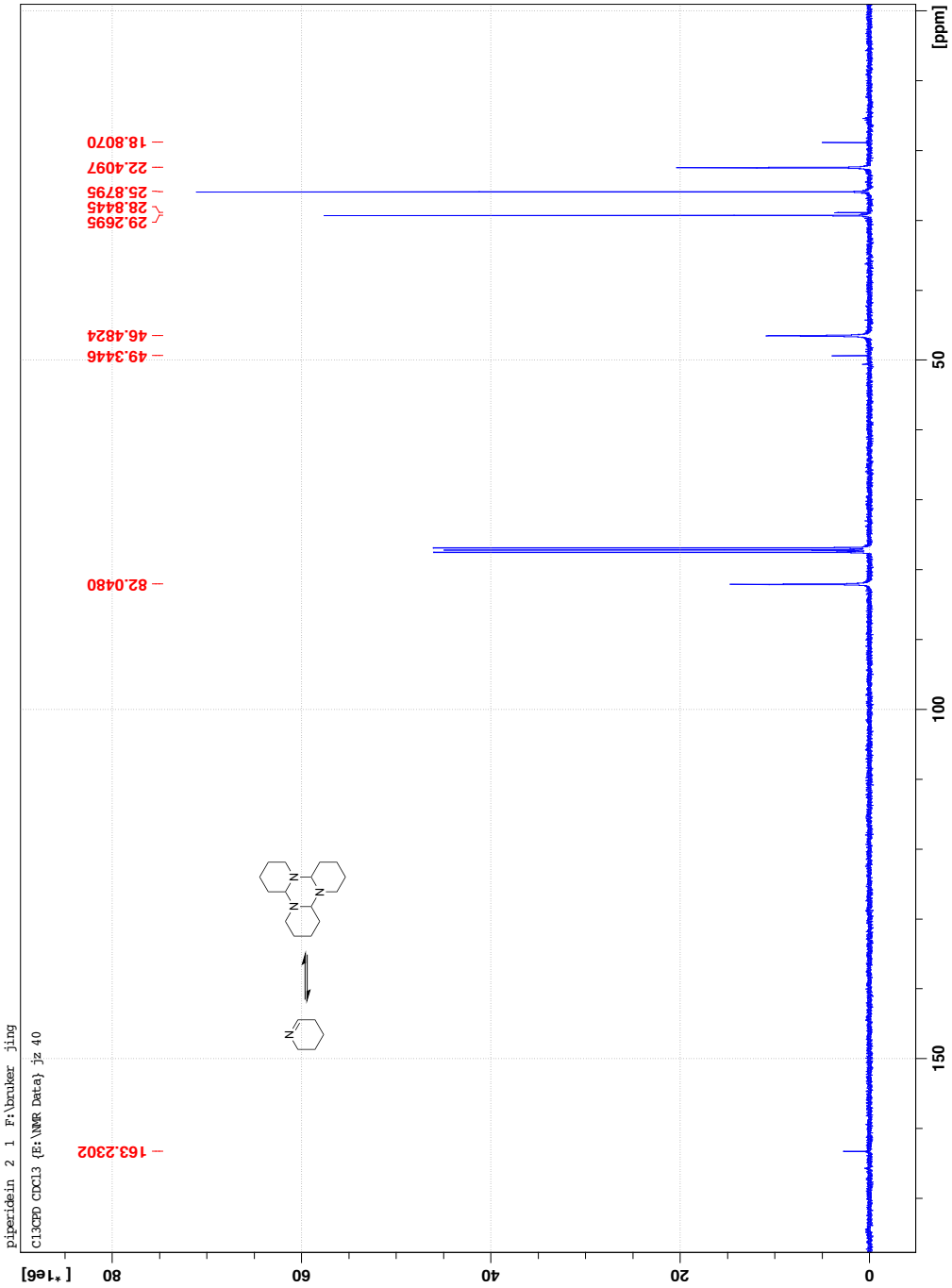

Appendix VII. ^{13}C spectrum of Δ^1-piperidein

Appendix VIII

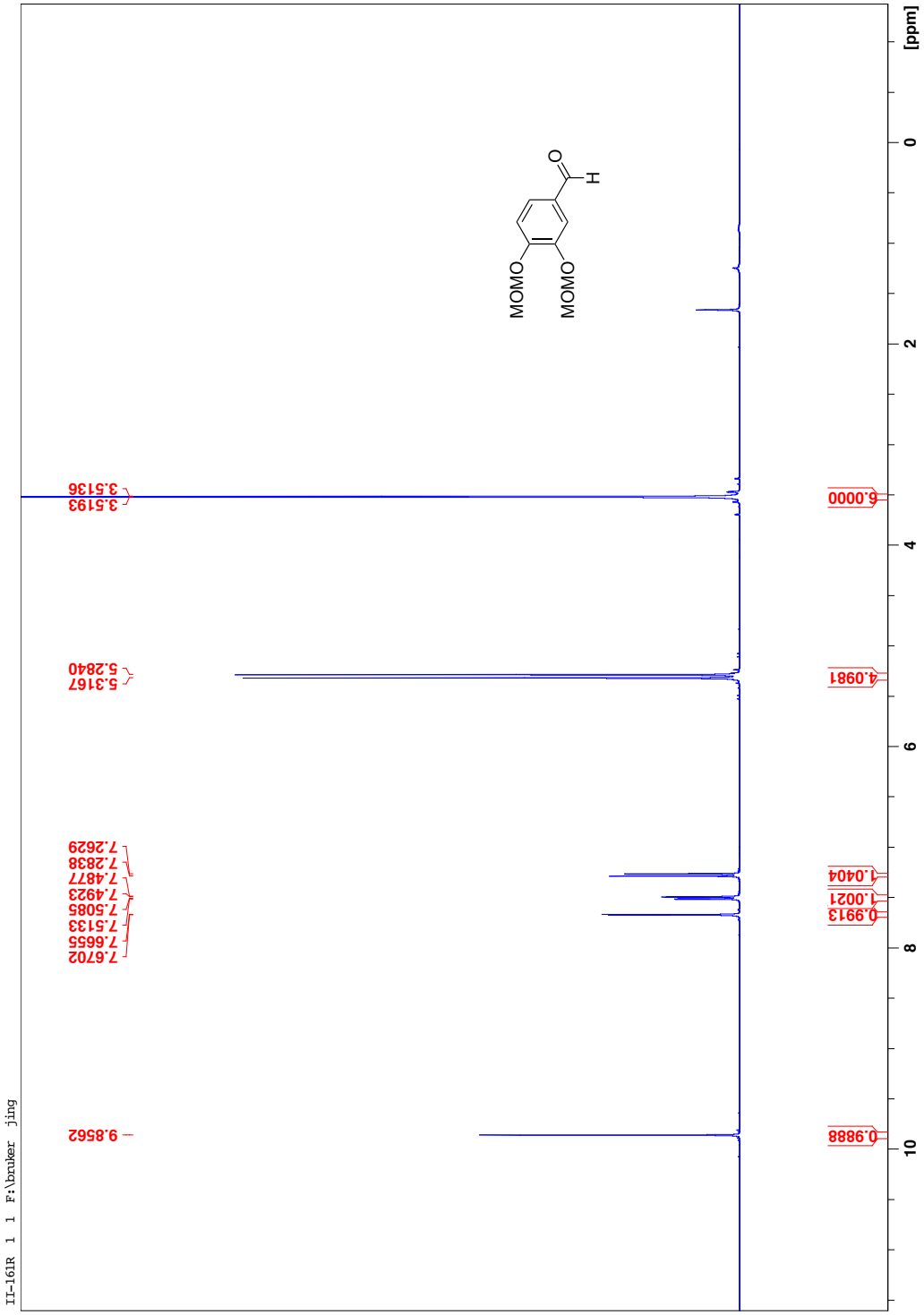

Appendix VIII. ^{1}H spectrum of 3,4-bis(methoxymethoxy)benzaldehyde

Appendix IX

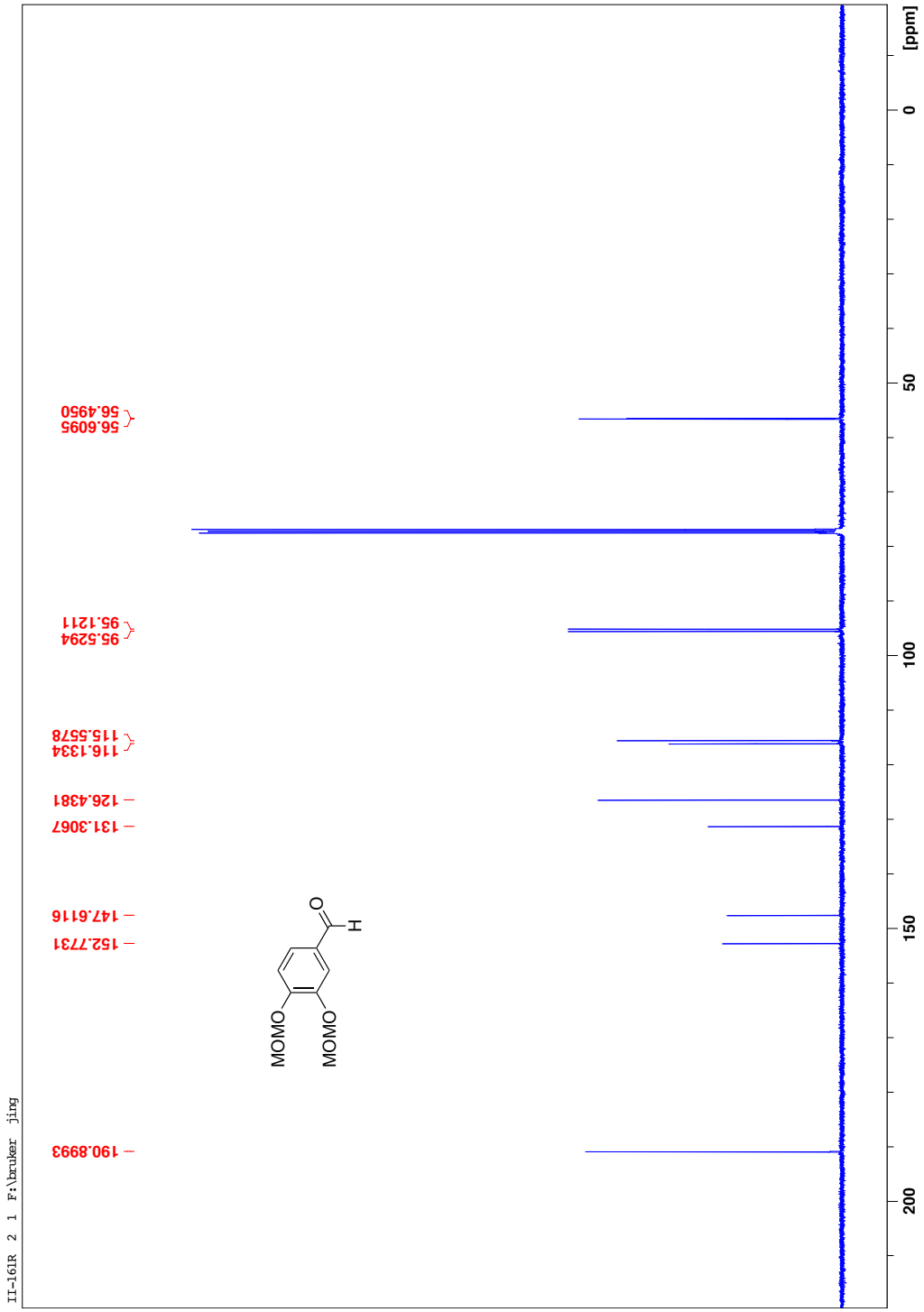

Appendix IX. ^{13}C spectrum of 3,4-bis(methoxymethoxy)benzaldehyde

Appendix X

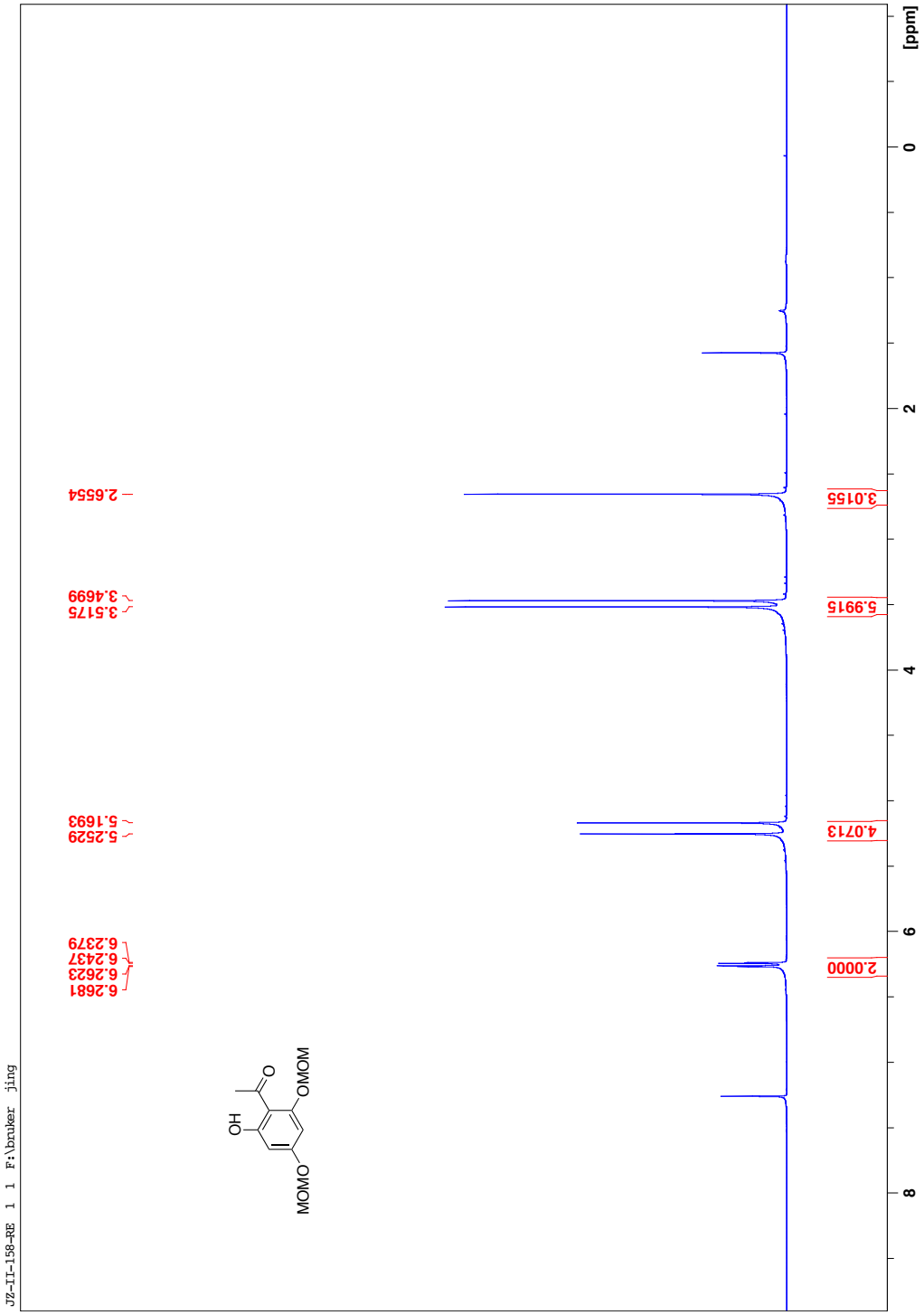

Appendix X. ^{1}H spectrum of 1-(2-hydroxy-4,6-bis(methoxymethoxy)phenyl)ethan-1-

Appendix XI

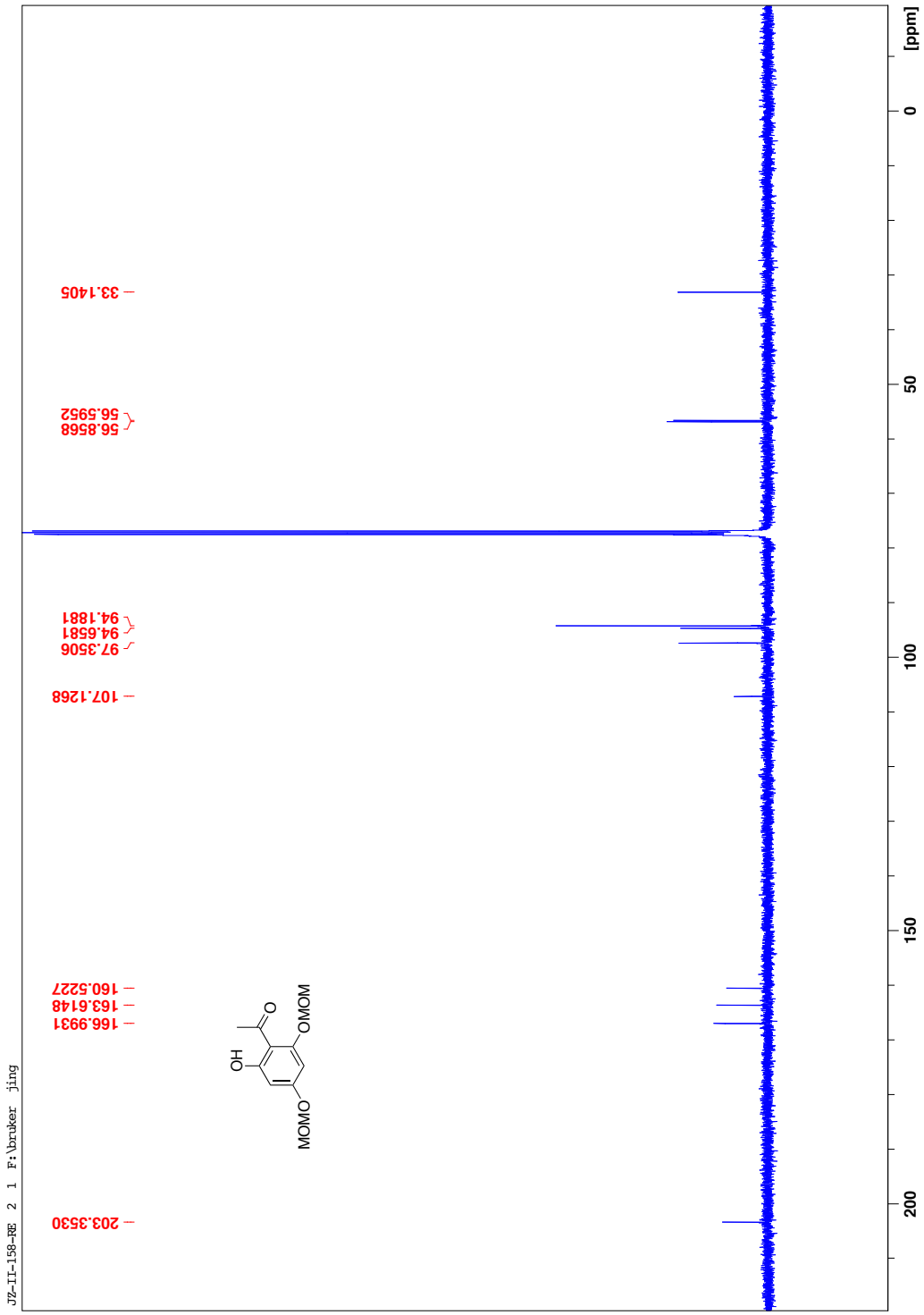

Appendix XI. ^{13}C spectrum of 1-(2-hydroxy-4,6-bis(methoxymethoxy)phenyl)ethan-1-

Appendix XII

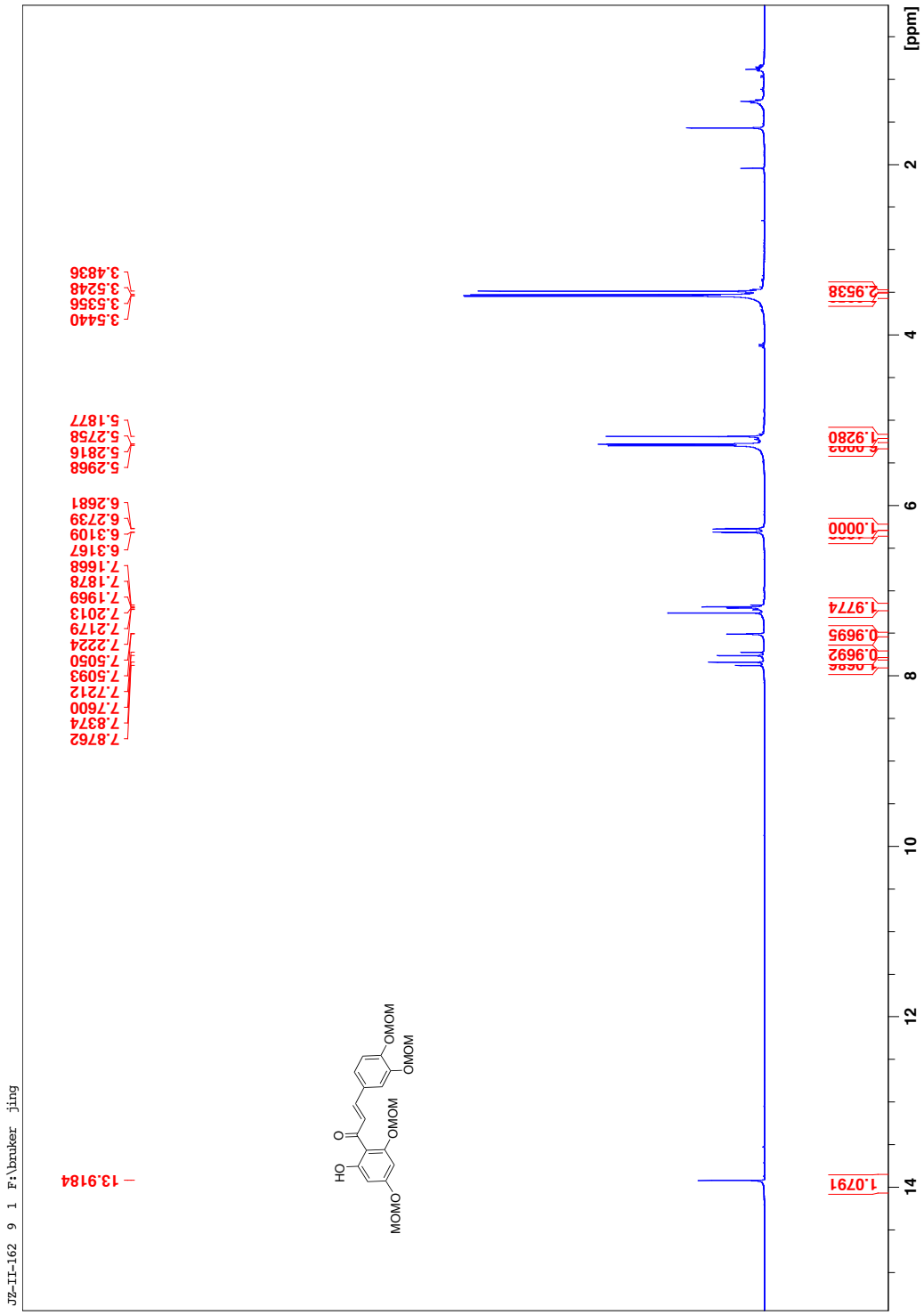

Appendix XII. ^{1}H spectrum of 3-(3,4-bis(methoxymethoxy)phenyl)-1-(2-hydroxy-4,6-bis(methoxymethoxy)phenyl)prop- 2-en-1-one

Appendix XIII

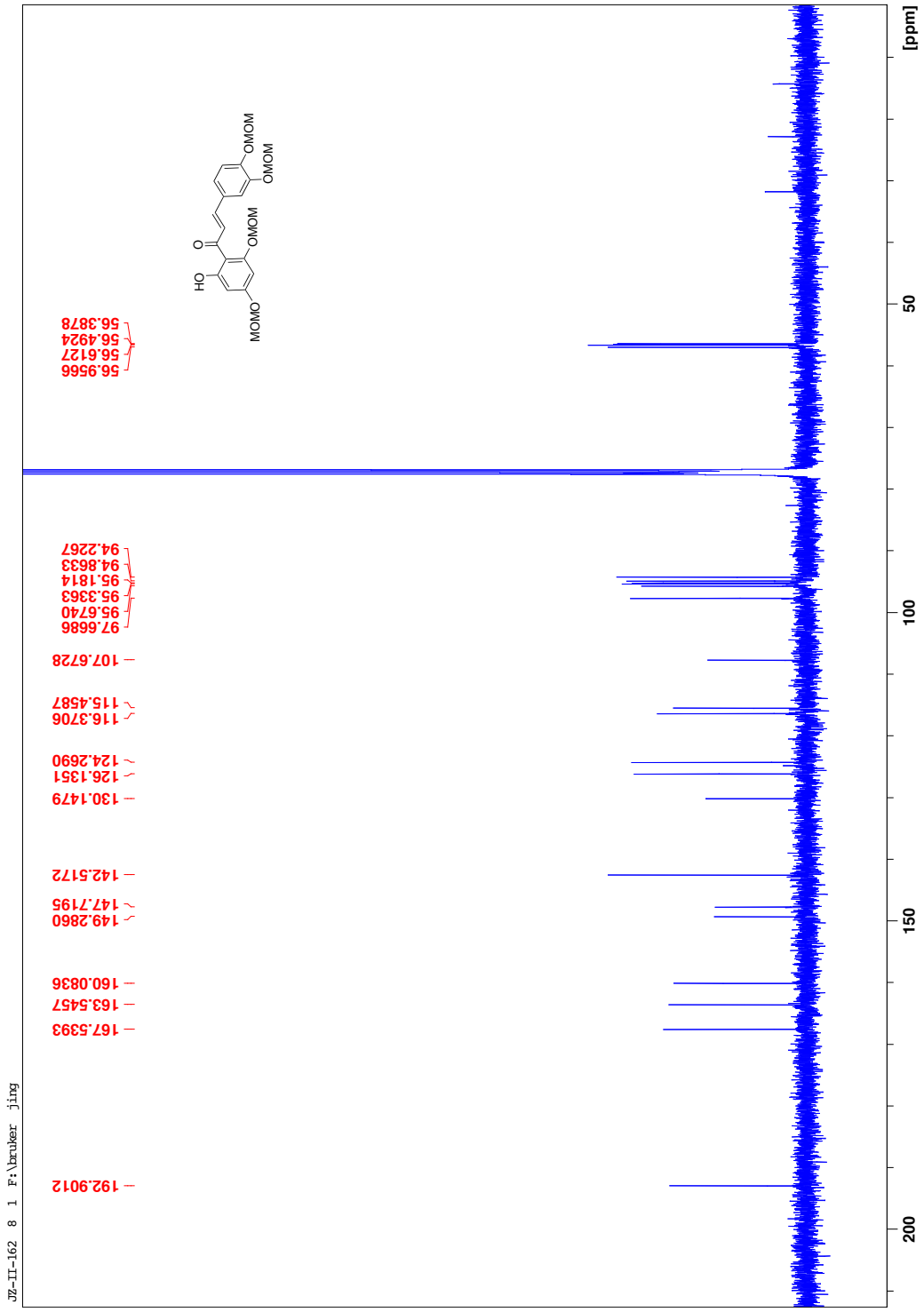

Appendix XIII. ^{13}C spectrum of 3-(3,4-bis(methoxymethoxy)phenyl)-1-(2-hydroxy-4,6-bis(methoxymethoxy)phenyl)prop- 2-en-1-one

Appendix XIV

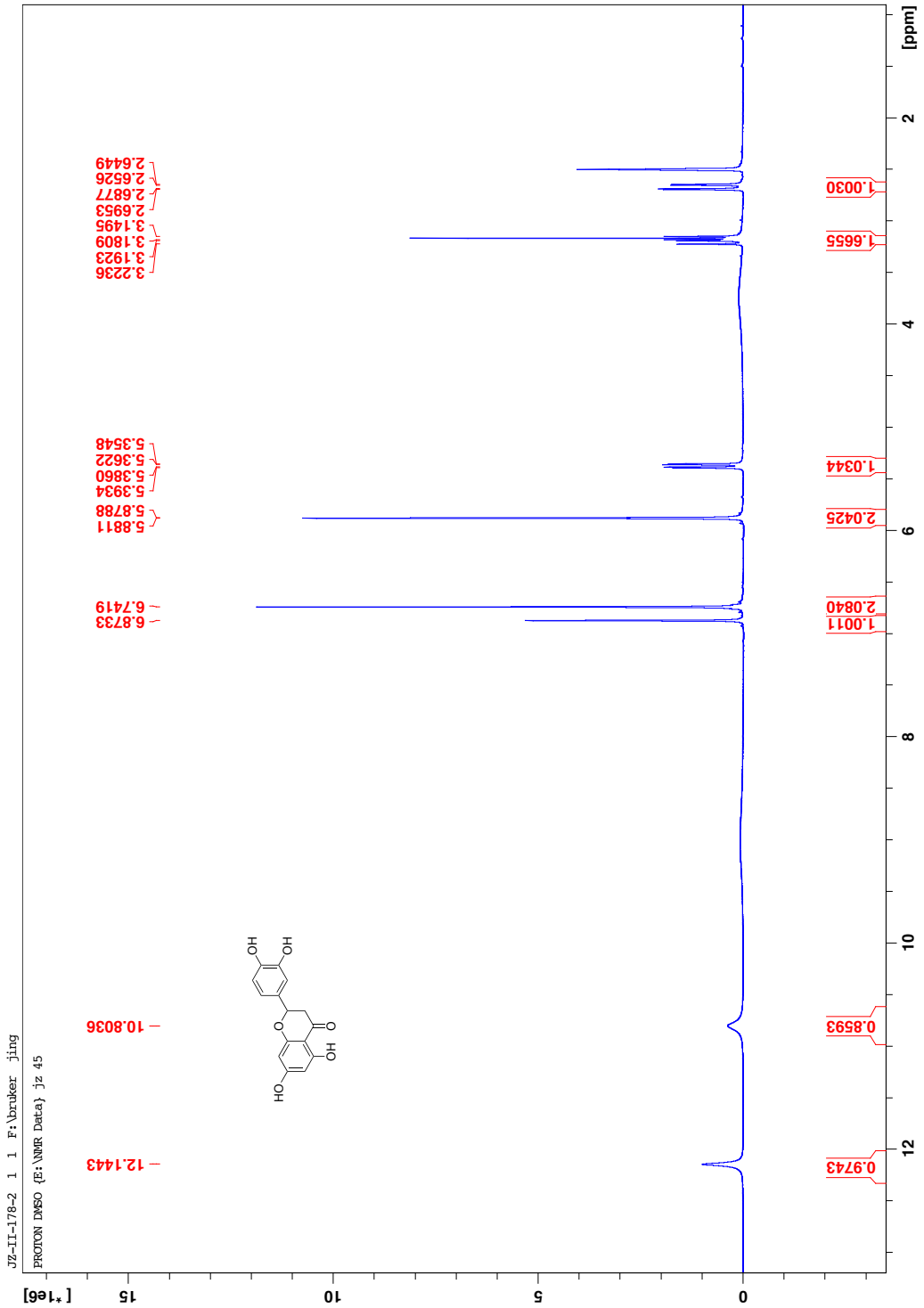

Appendix XIV. ^{1}H spectrum of 2-(3,4-dihydroxyphenyl)-5,7-dihydroxychroman-4-one

Appendix XV

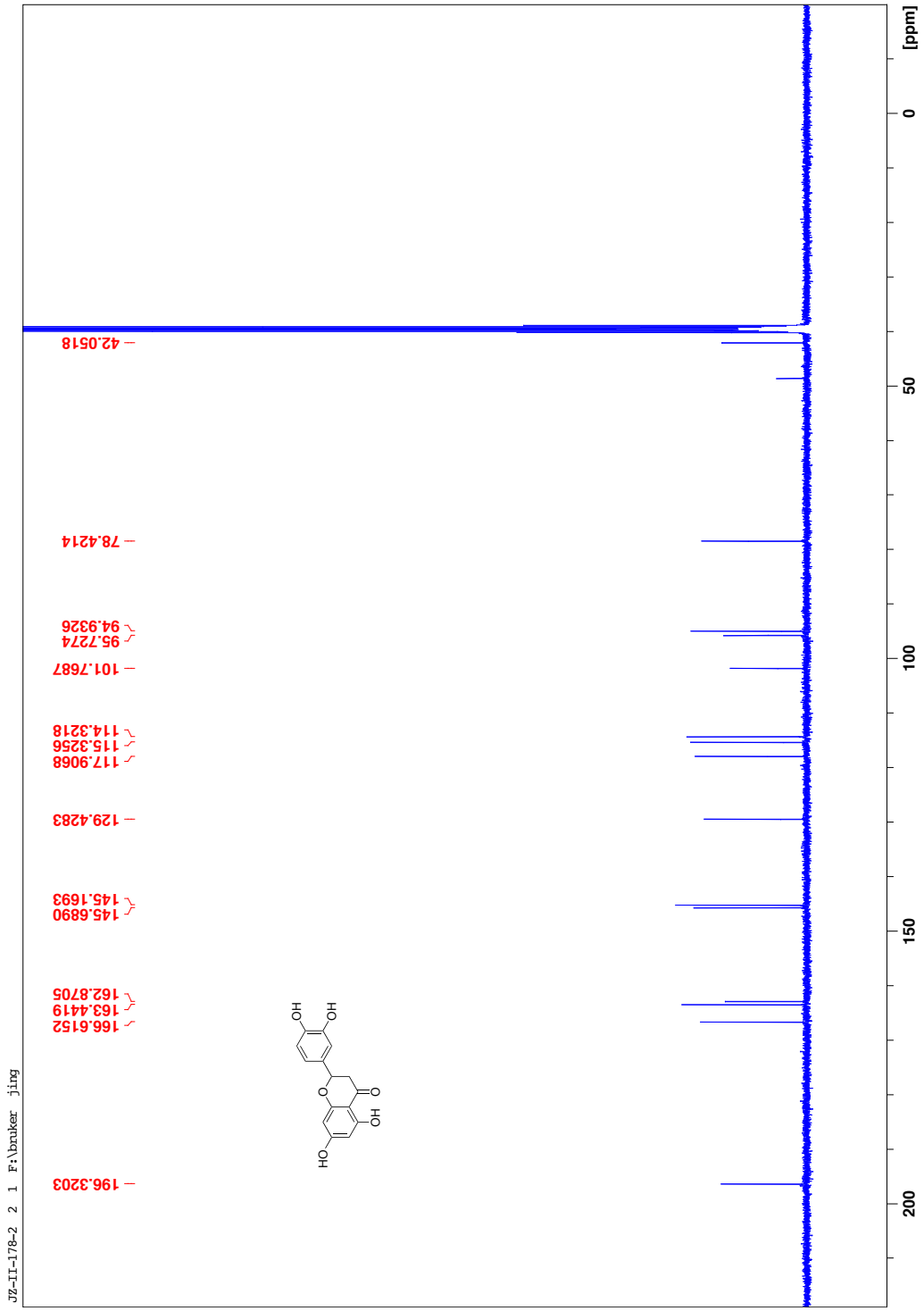

Appendix XV. ^{13}C spectrum of 2-(3,4-dihydroxyphenyl)-5,7-dihydroxychroman-4-one

Appendix XVI

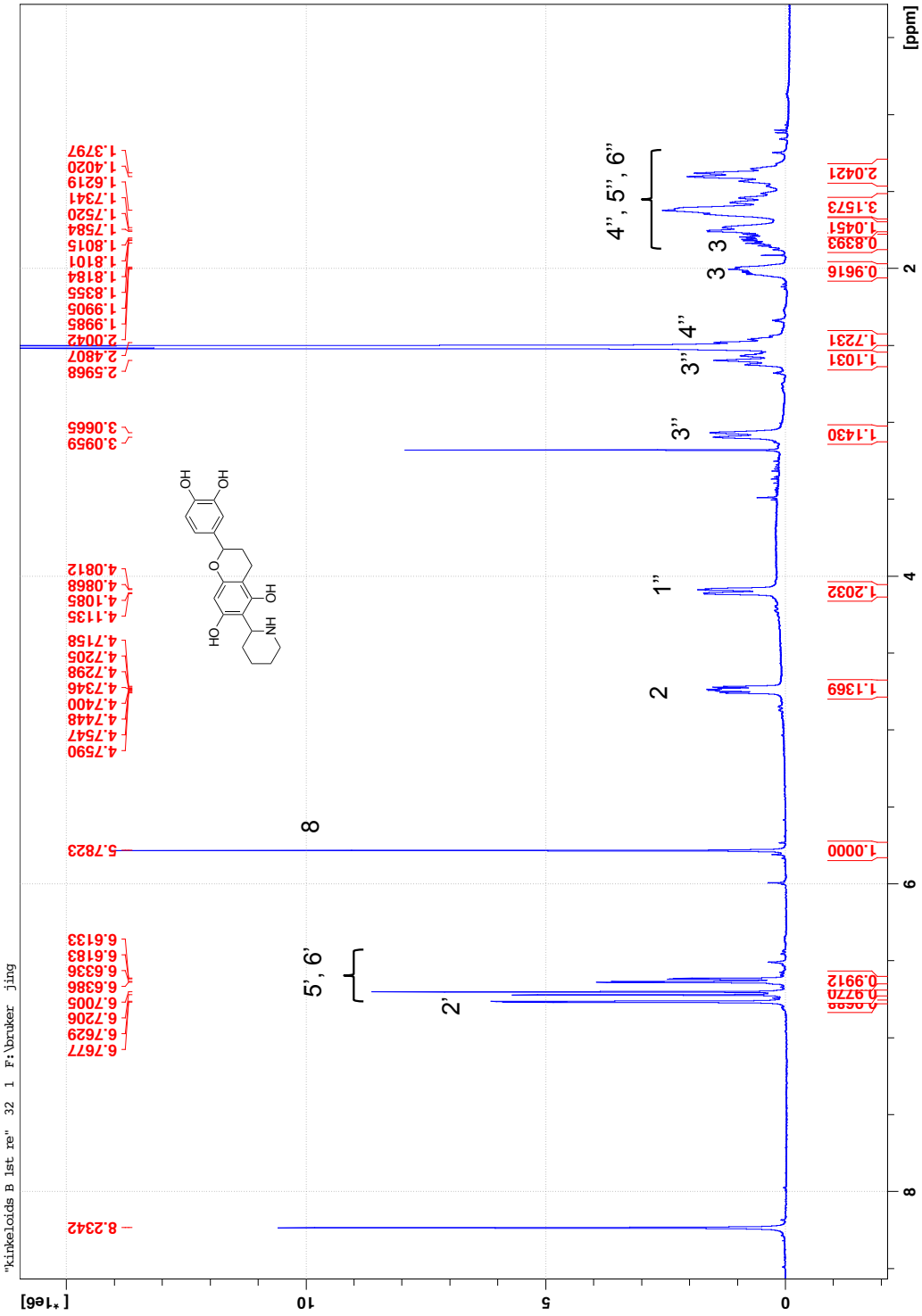

Appendix XVI. ^{1}H spectrum of 6-piperidyl kinkeloids B

Appendix XVII

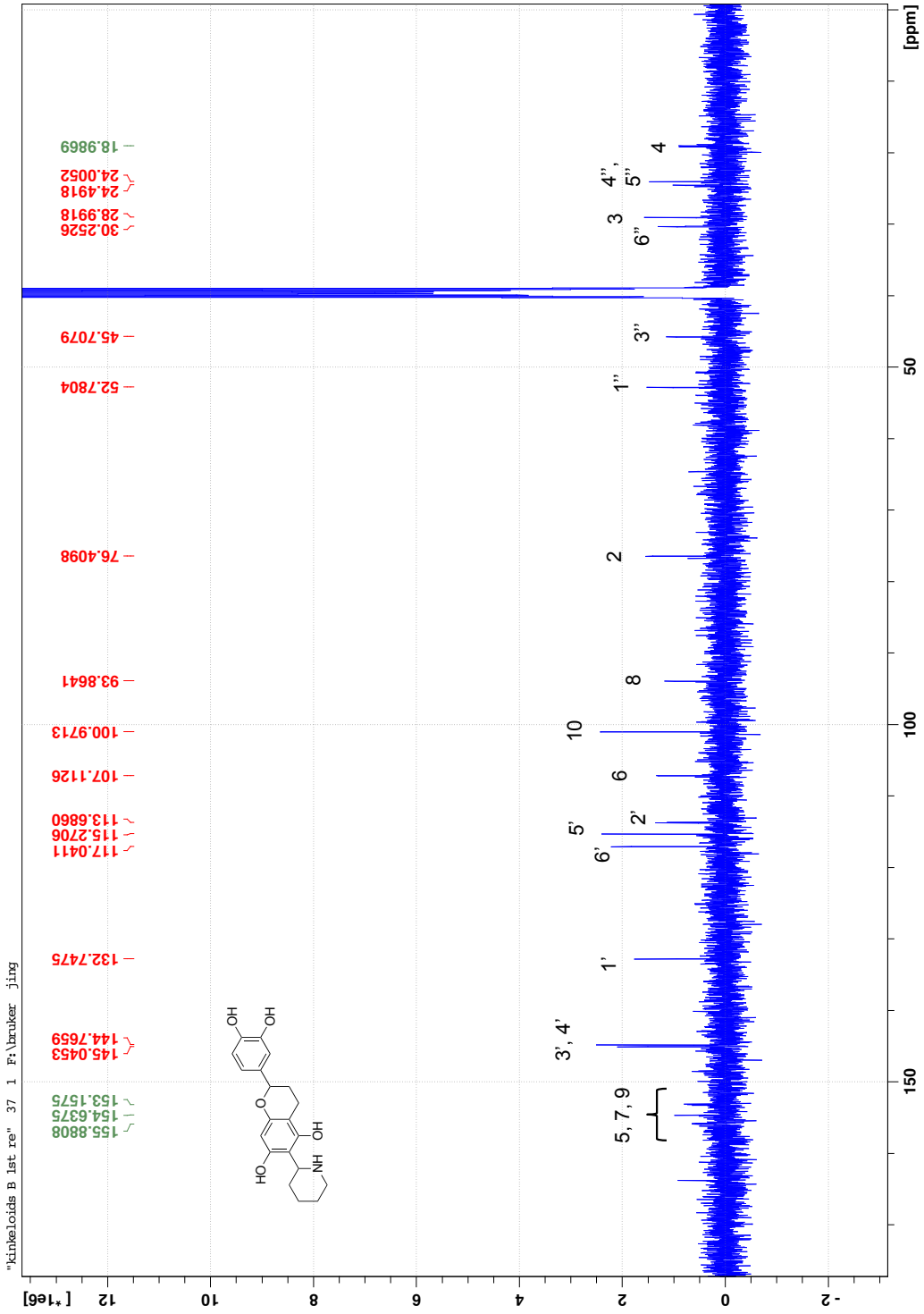

Appendix XVII. ^{13}C spectrum of 6-piperidyl kinkeloids B

Appendix XVIII

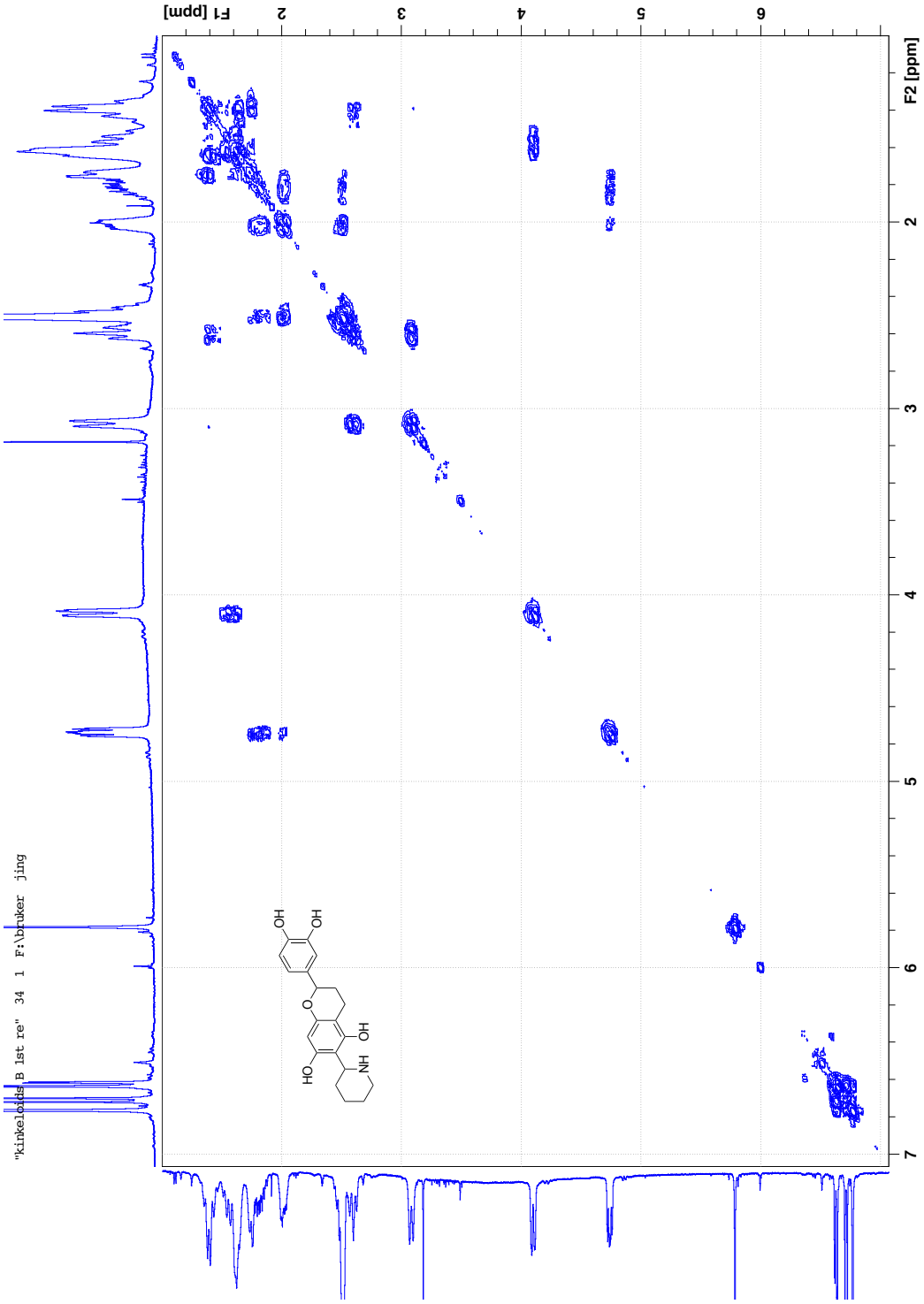

Appendix XVIII. COSY spectrum of 6-piperidyl kinkeloids B

Appendix XIX

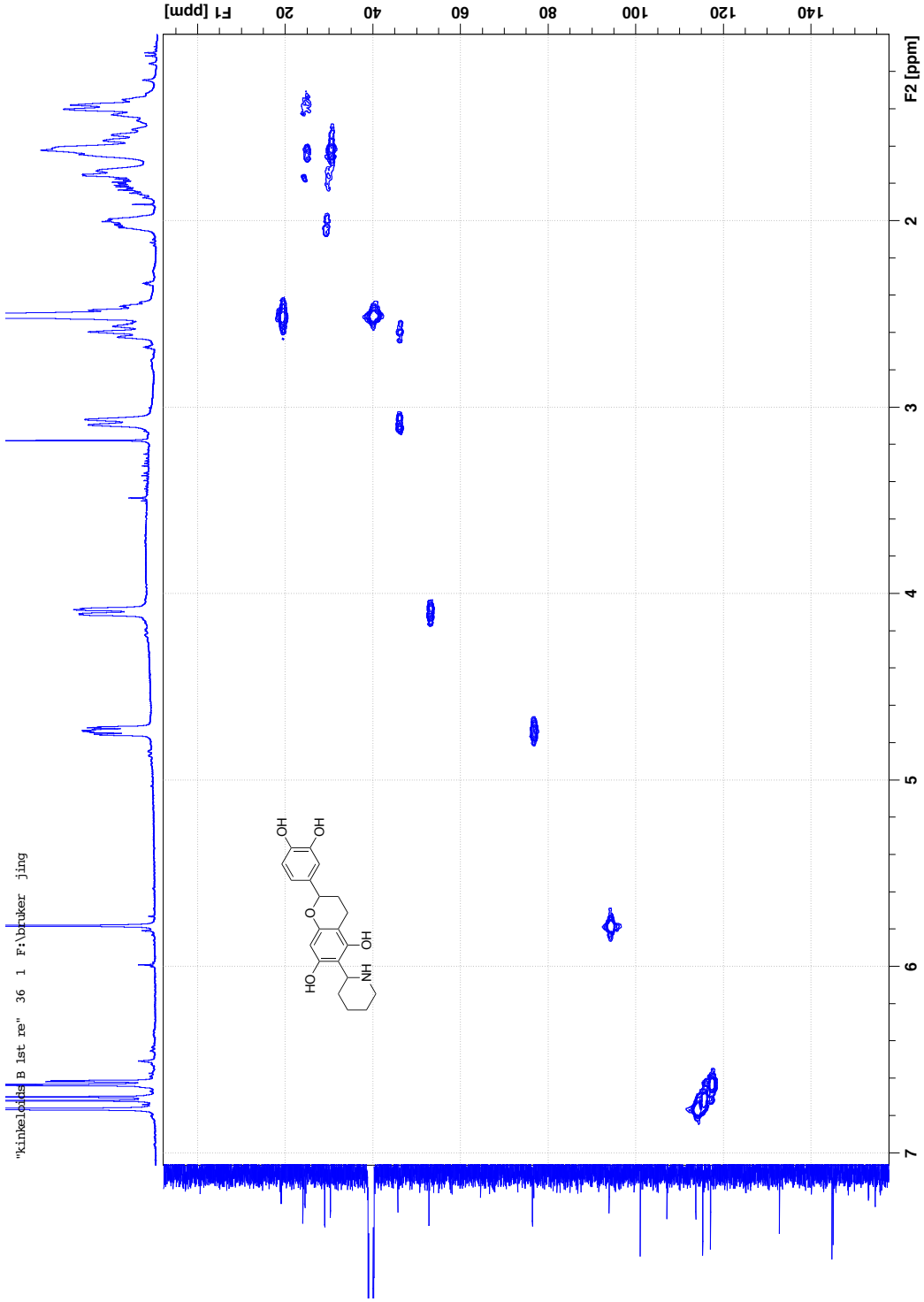

Appendix XIX. HMQC spectrum of 6-piperidyl kinkeloids B

Appendix XX

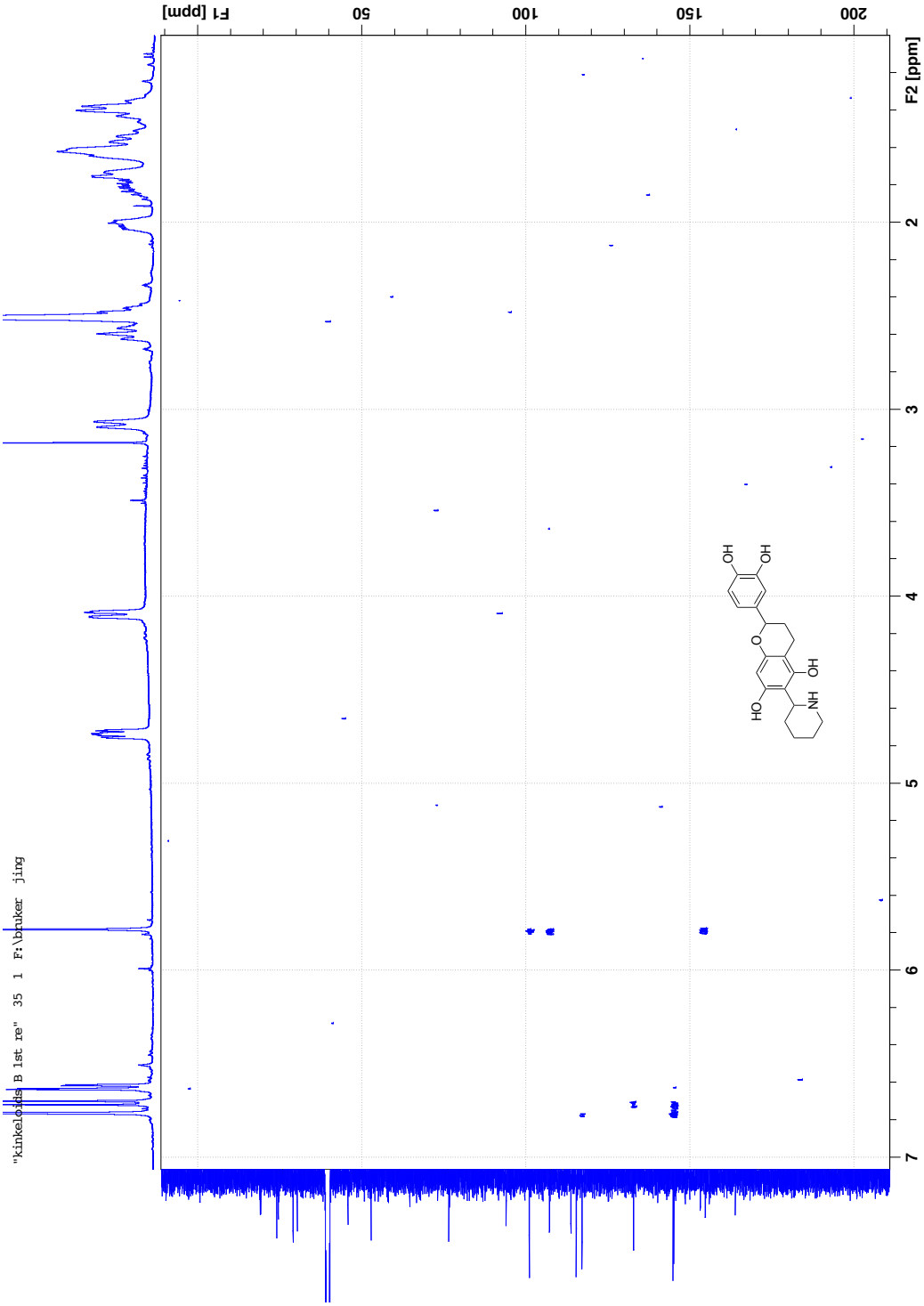

Appendix XX. HMBC spectrum of 6-piperidyl kinkeloids B

Appendix XXI

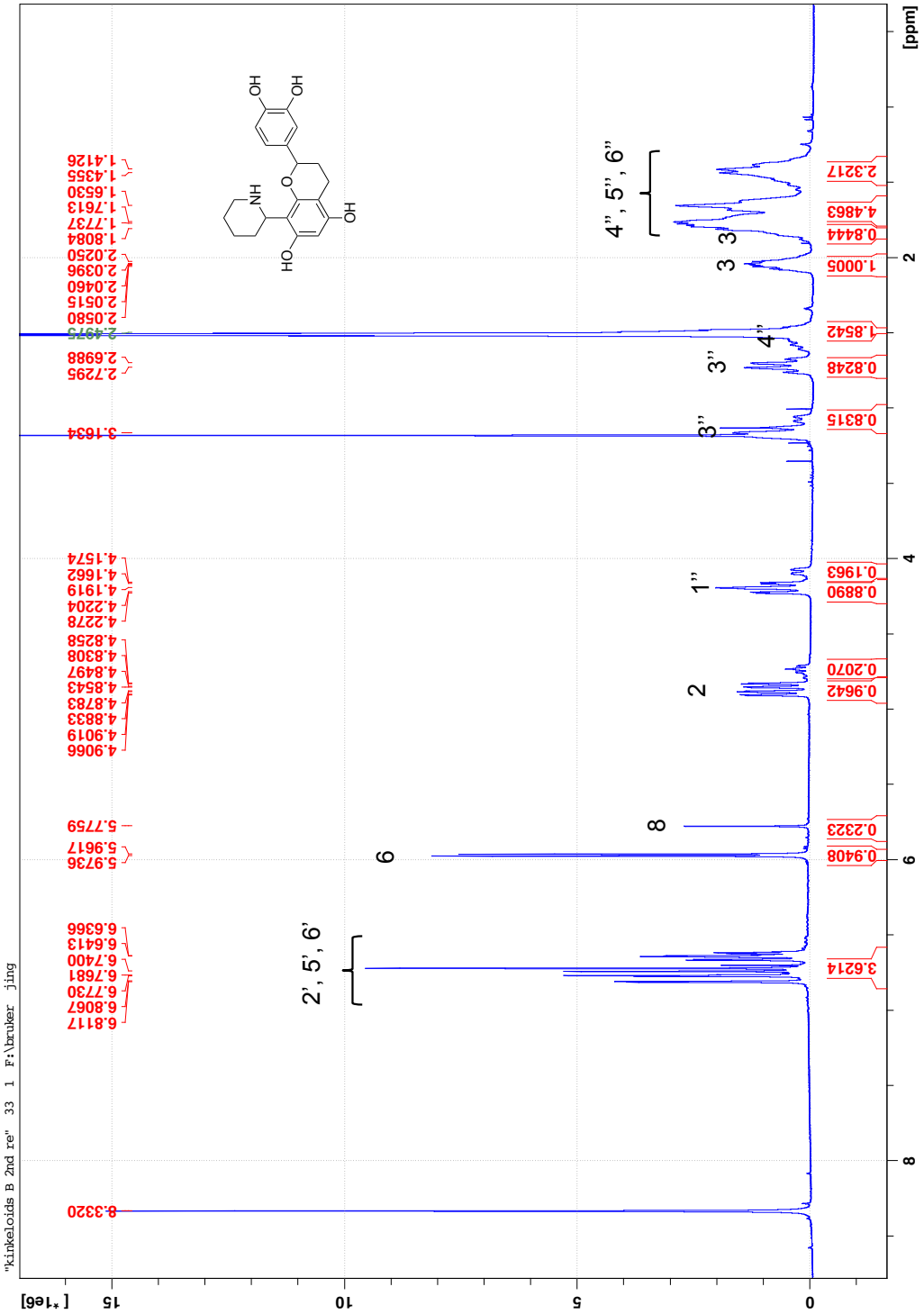

Appendix XXI. ^{1}H spectrum of 8-piperidyl kinkeloids B. (Partially mixed with regioisomers 6-piperidyl kinkeloids B

Appendix XXII

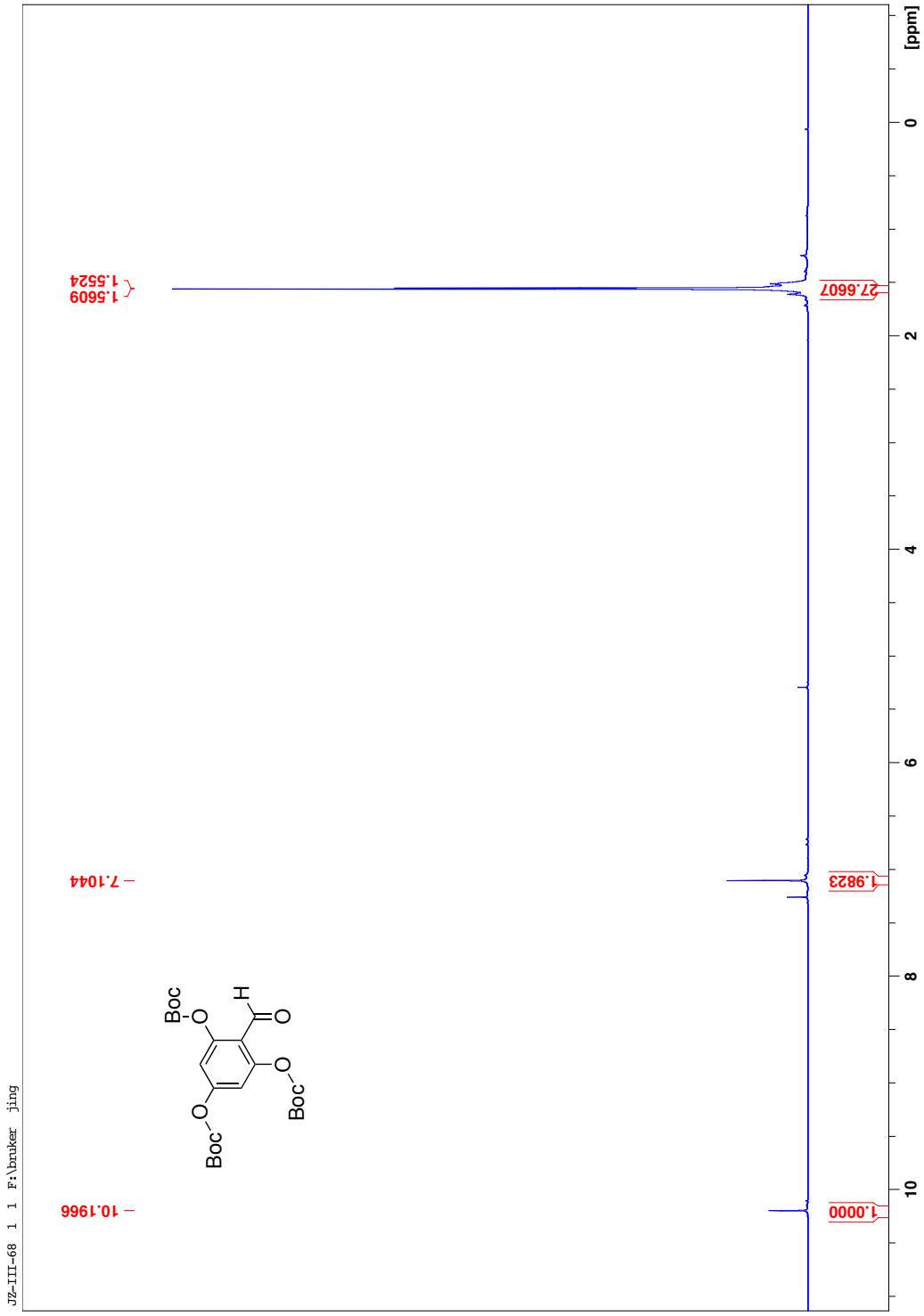

App XXII. ^{1}H spectrum of tri-tert-butyl (2-formylbenzene-1,3,5-triyl) tricarbonate

Appendix XXIII

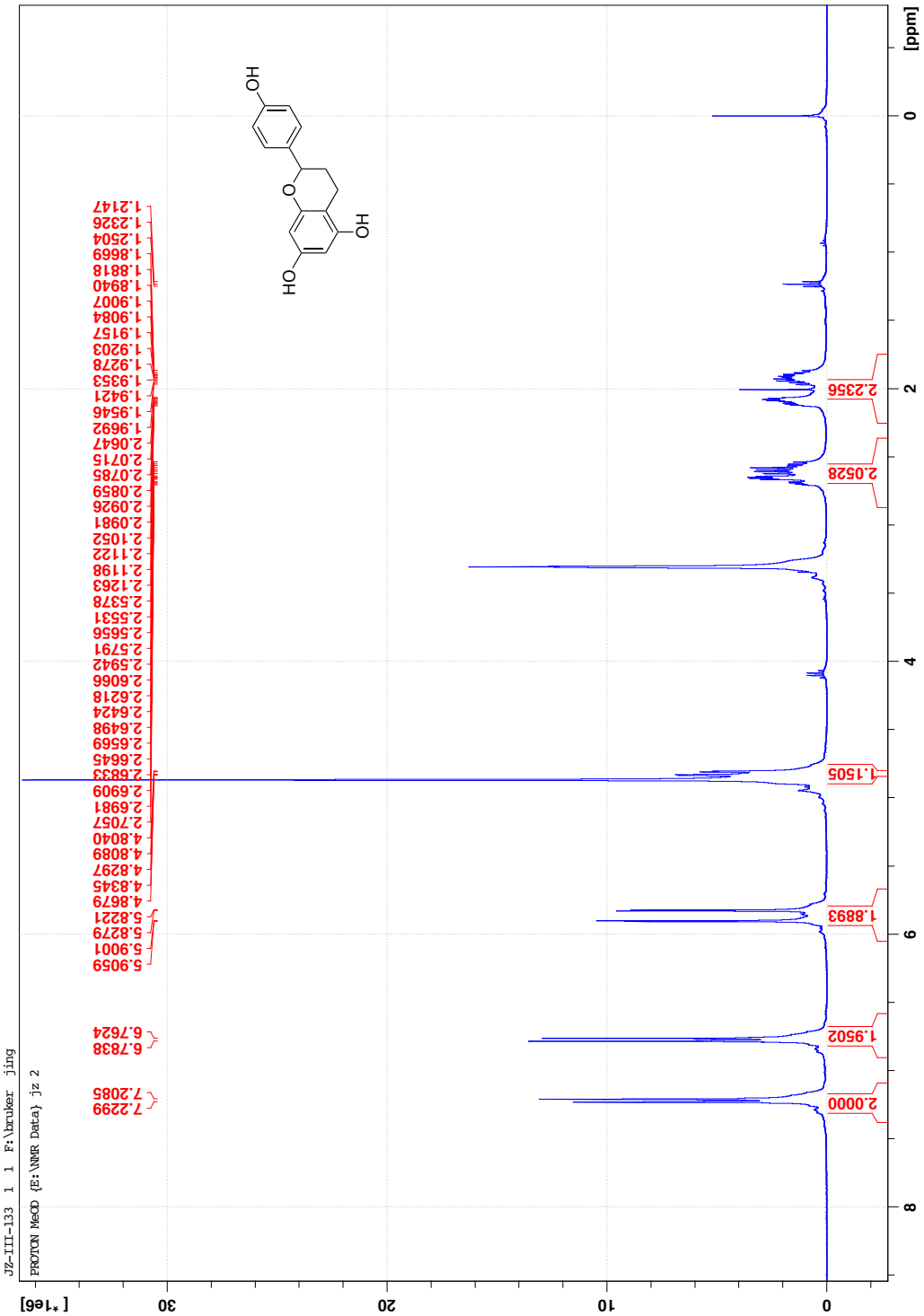

Appendix XXIII. ^{1}H spectrum of 2-(4-hydroxyphenyl)chromane-5,7-diol

Appendix XXIV

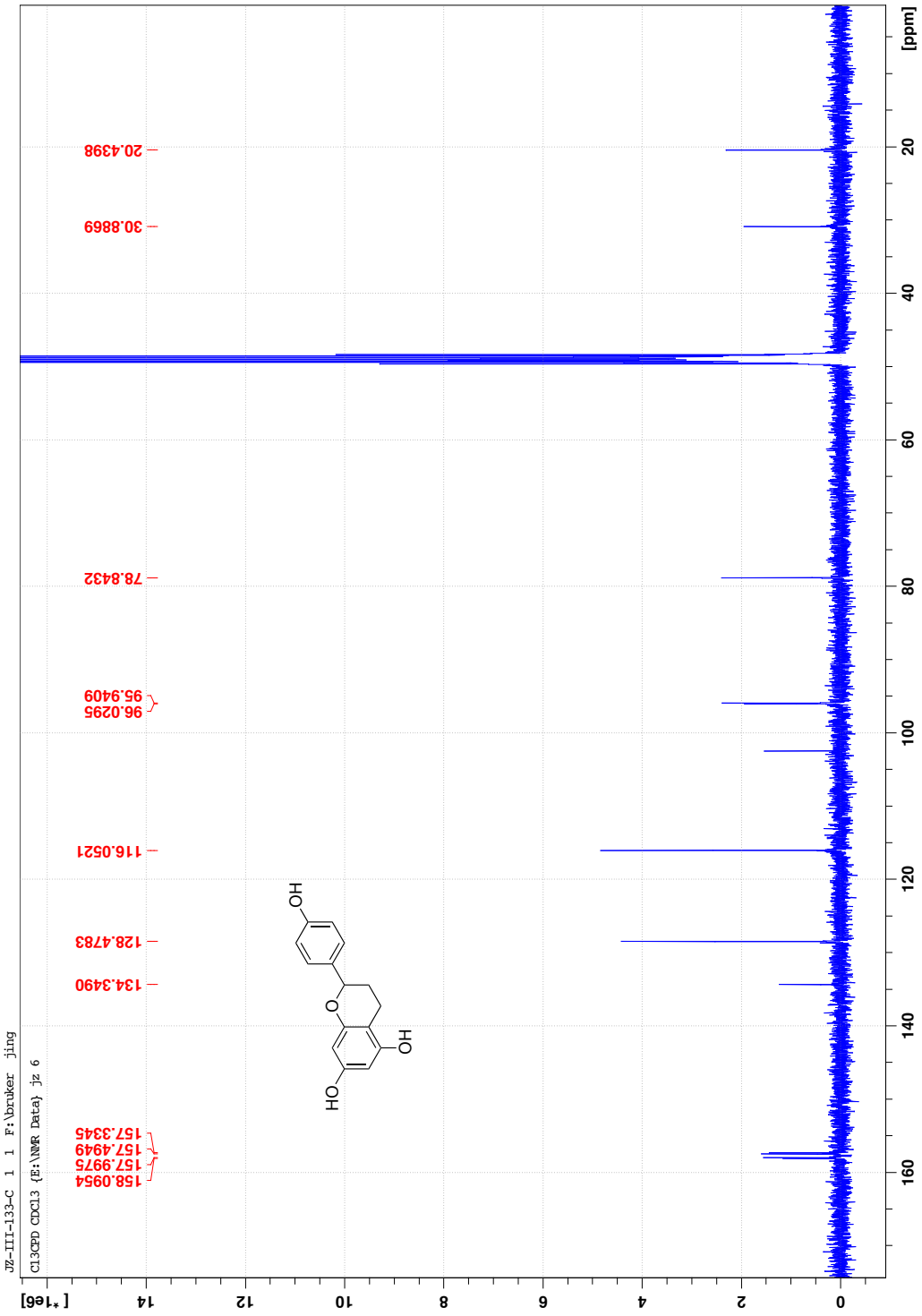

Appendix XXIV. ^{13}C spectrum of 2-(4-hydroxyphenyl)chromane-5,7-diol

Appendix XXV

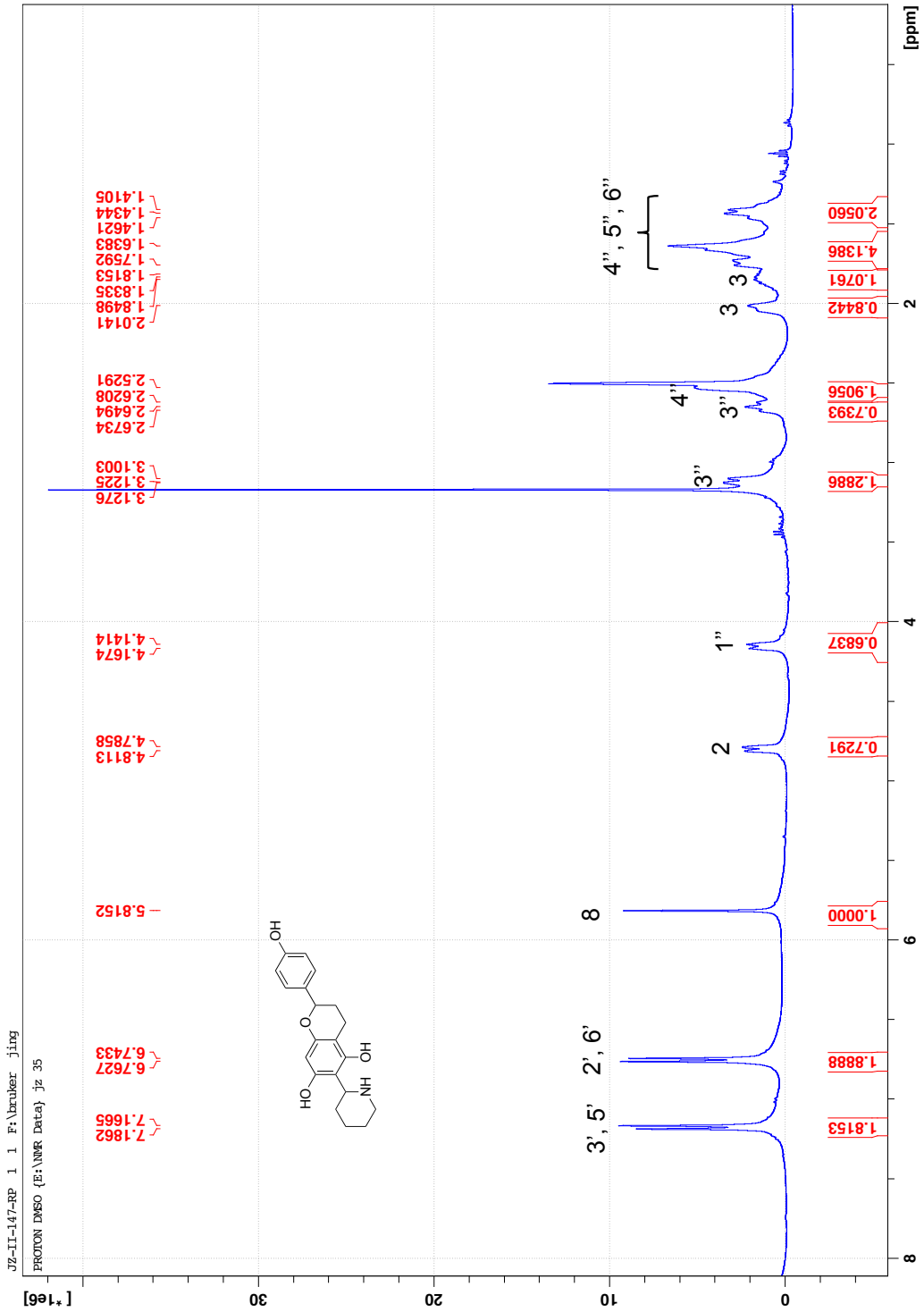

Appendix XXV. ^{1}H spectrum of 6-piperidyl kinkeloids A

Appendix XXVI

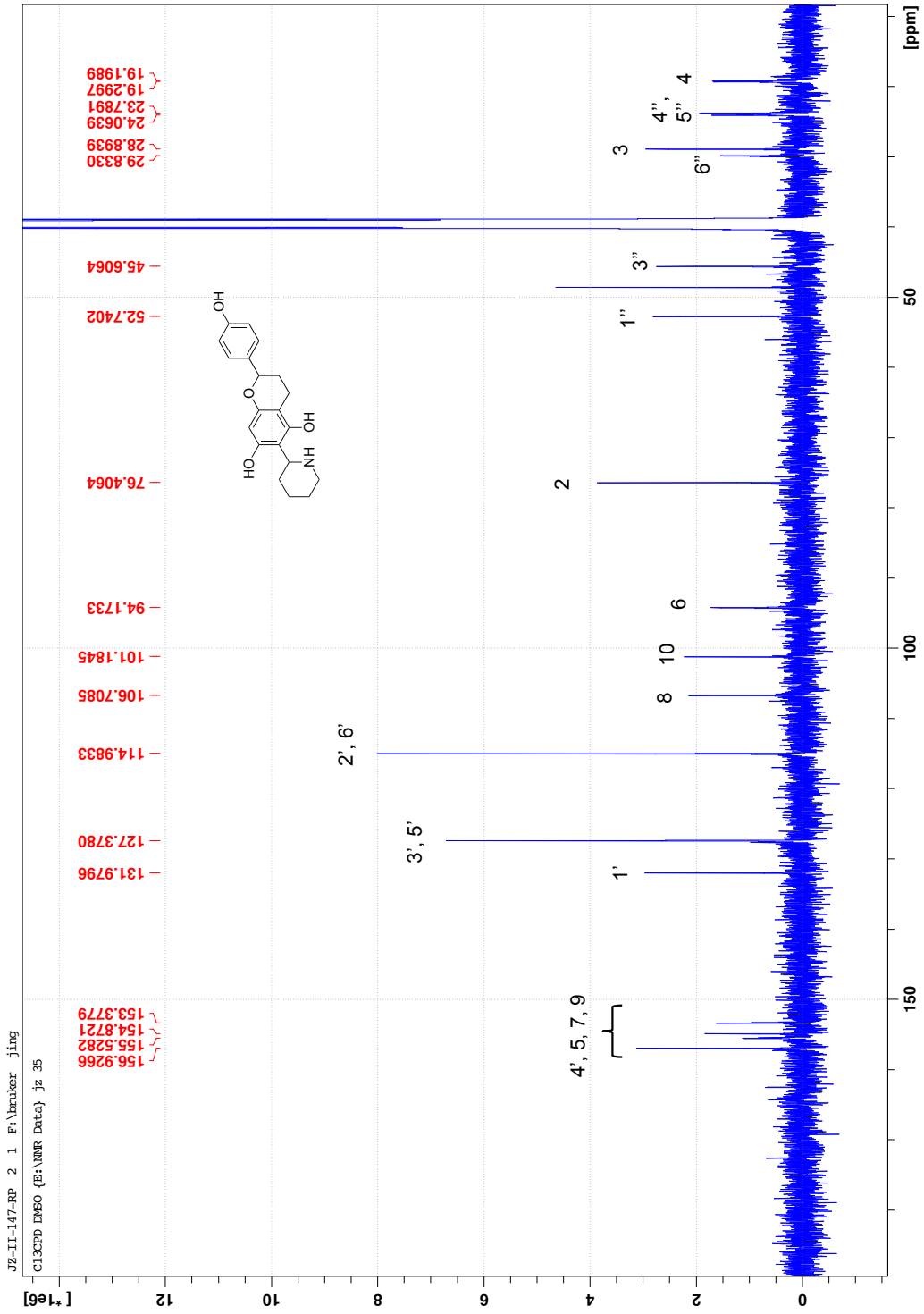

Appendix XXVI. ^{13}C spectrum of 6-piperidyl kinkeloids A

Appendix XXVII

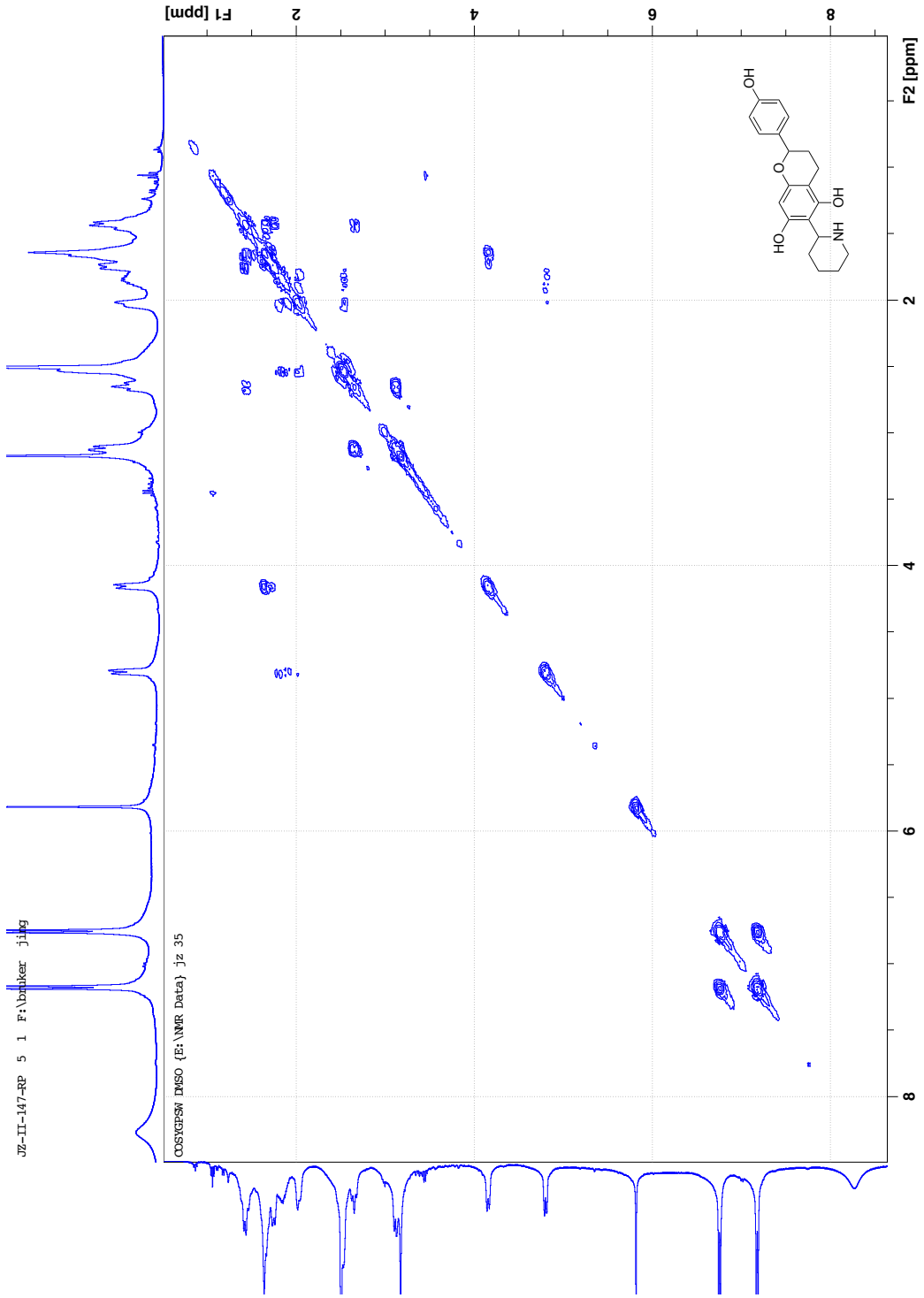

Appendix XXVII. COSY spectrum of 6-piperidyl kinkeloids A

Appendix XXVIII

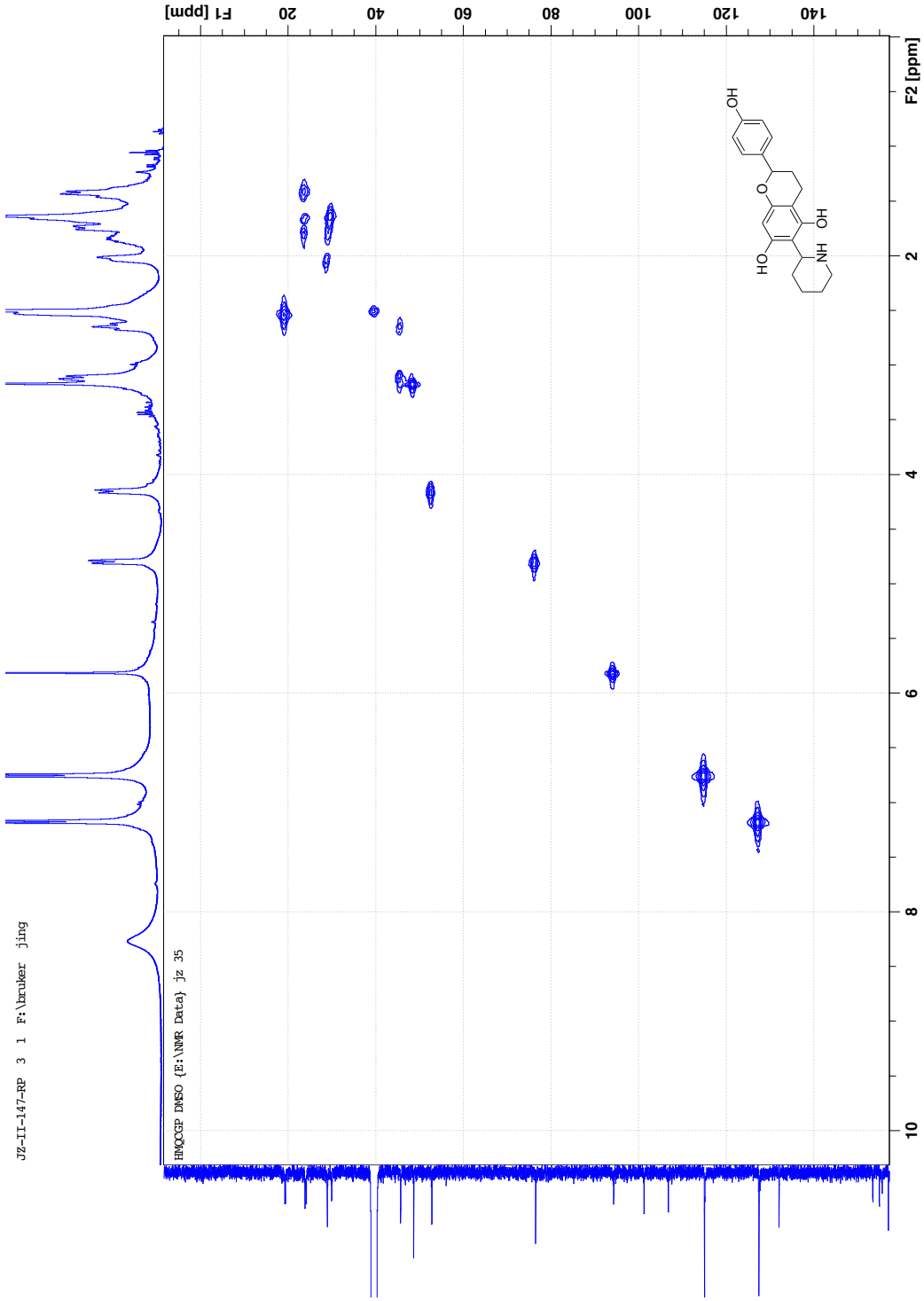

Appendix XXVIII. HMQC spectrum of 6-piperidyl kinkeloids A

Appendix XXIX

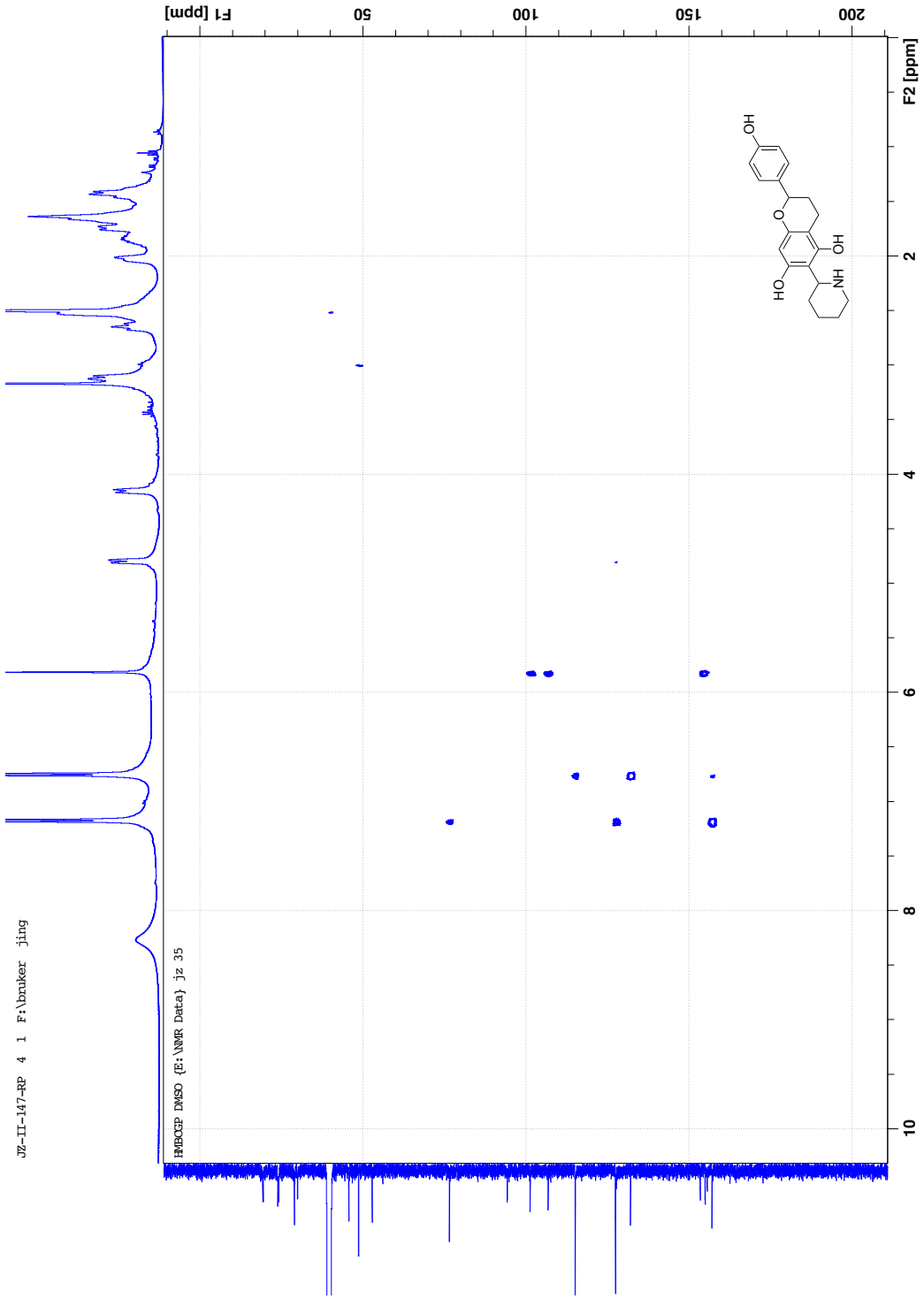

Appendix XXIX. HMBC spectrum of 6-piperidyl kinkeloids A

Appendix XXX

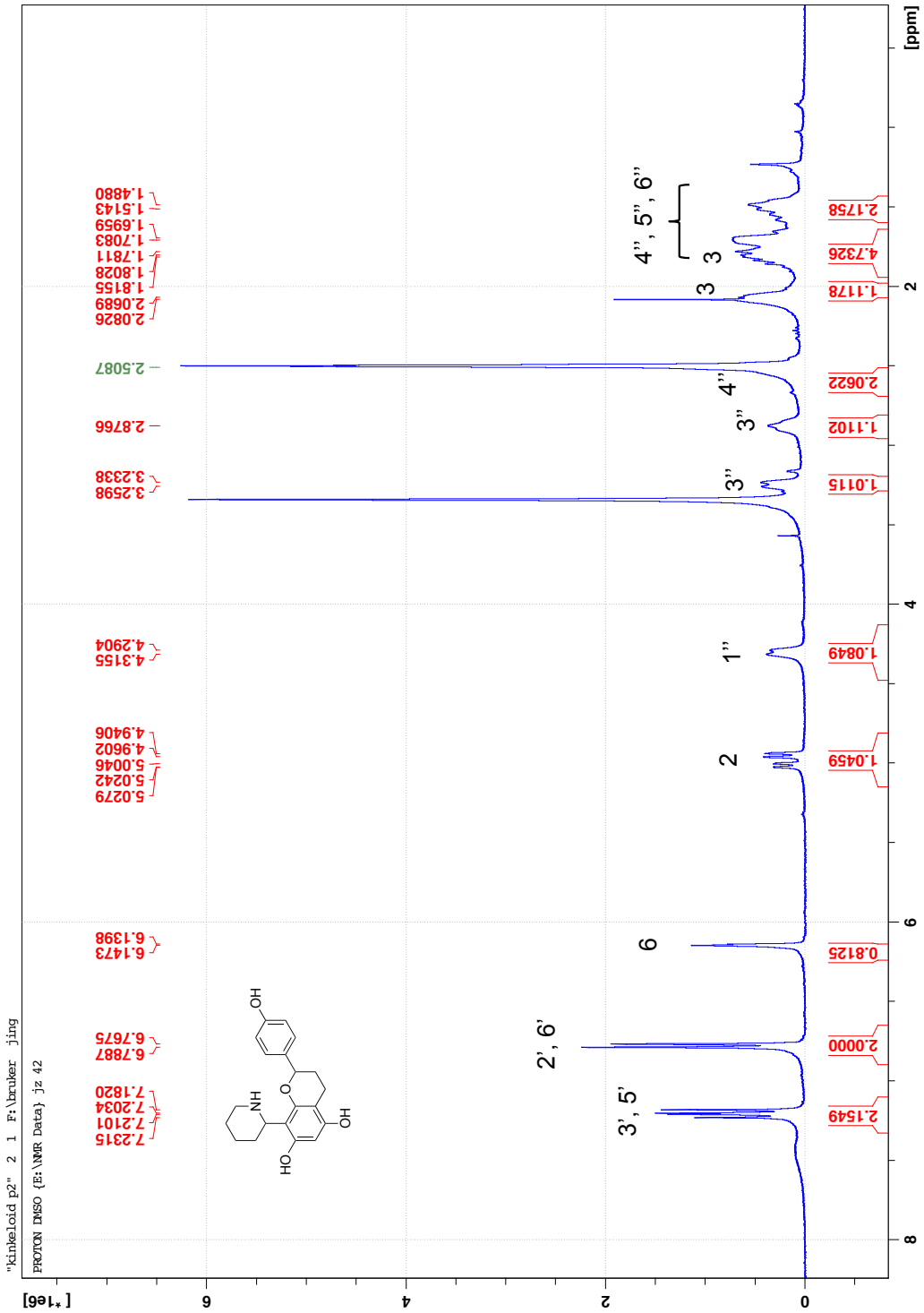

Appendix XXX. ^{1}H spectrum of 8-piperidyl kinkeloids A